Kinetische studie van de (trans)esterificatie gekatalyseerd met gel en macroporeuze harsen

Kinetic Study of the (Trans)Esterification Catalyzed by Gel and Macroporous Resins

Evelien Van de Steene

Promotoren: prof. dr. ir. J. W. Thybaut, prof. dr. ir. J. De Clercq
Proefschrift ingediend tot het behalen van de graad van
Doctor in de Ingenieurswetenschappen: Chemische Technologie

Vakgroep Chemische Proceskunde en Technische Chemie
Voorzitter: prof. dr. ir. G. B. Marin

Vakgroep Industriële Technologie en Constructie
Voorzitter: prof. dr. M. Vanhaelst

Faculteit Ingenieurswetenschappen en Architectuur
Academiejaar 2013 - 2014

UNIVERSITEIT GENT

ISBN 978-90-8578-684-9
NUR 913
Wettelijk depot: D/2014/10.500/30

Promotoren:

Prof. Dr. Ir. Joris Thybaut	Universiteit Gent
Prof. Dr. Ir. Jeriffa De Clercq	Universiteit Gent

Examencommissie:

Prof. Dr. Ir. Patrick De Baets, voorzitter	Universiteit Gent, EA04
Prof. Dr. Ir. An Verberckmoes*, secretaris	Universiteit Gent, EA20
Prof. Dr. Ir. Jeriffa De Clercq, promotor	Universiteit Gent, EA20
Prof. Dr. Ir. Dirk De Vos	Katholieke Universiteit Leuven
Prof. Dr. Peter Dubruel*	Universiteit Gent
Prof. Dr. Ir. Guy Marin	Universiteit Gent, EA12
Dr. Ir. Dirk Packet	Oleon, Ertvelde
Prof. Dr. Nikos Papayannakos*	National Technical University of Athens, Greece
Prof. Dr. Ir. Joris Thybaut*, promotor	Universiteit Gent, EA12
Dr. Rudolf Wagner	Lanxess Deutschland

* lees commissie

Universiteit Gent
Faculteit Ingenieurswetenschappen en Architectuur

Vakgroep Chemische Proceskunde en Technische Chemie
Laboratorium voor Chemische Techniek
Technologiepark 914, B-9052 Gent
België
http://www.lct.ugent.be

Vakgroep Industriële Technolgie en Constructie
Valentin Vaerwyckweg 1, B-9000 Gent
België
http://www.it-c.ugent.be

This work was supported by the Research Fund of the University College Ghent.

By three methods we may learn wisdom:
First, by reflection, which is noblest;
Second, by imitation, which is the easiest;
And third, by experience, which is the most bitter.

Confucius

Dankwoord

Het lijkt alsof het gisteren was, de eerste transesterificatie experimenten, een simulatie zonder foutmeldingen, het heuglijke nieuws dat je eerste paper aanvaard is, … en nu is het zover: mijn doctoraat is af! Als ik er nu op terugkijk op 6 jaar onderzoek, met twee onderbrekingen, ervaar ik mijn doctoraat als een boeiende en uitdagende maar zeker ook inspannende levensreis. Het was een reis waarin ik niet alleen op wetenschappelijk vlak maar ook op persoonlijk vlak mij heb kunnen ontplooien. Ik heb deze reis niet alleen gemaakt, heel wat mensen hebben me op uiteenlopende manieren bijgestaan en gemotiveerd. Ik wens dan ook graag van deze gelegenheid gebruik te maken om een aantal mensen speciaal te bedanken.

Als eerste wil ik mijn promotoren bedanken: Prof. dr. ir. Joris W. Thybaut en Prof. dr. ir. Jeriffa De Clercq. De gedreven academische opvolging van hun beiden en hun bijsturing was een onontbeerlijke motivatie om dit doctoraat te finaliseren. Hun beide deuren stonden voor mij steeds letterlijk en figuurlijk open.
Joris, bedankt voor de ondersteuning en het vertrouwen dat je me hebt gegeven. Ik apprecieer het enorm dat je ondanks je drukke agenda er toch in slaagde om snel en vakkundig feedback te geven op mijn werk en ook maandelijks tijd voor me vrijmaakte om allerhande onderzoeksideeën en –resultaten te bespreken. Dankjewel voor de aangename en collegiale samenwerking.
Jeriffa, dankzij jou ben ik dit doctoraat gestart. Bedankt om mij deze kans te geven. Je nauwgezette opvolging van mijn werk, boeiende en soms ook uitdagende discussies en onze goede samenwerking hebben uitermate bijgedragen tot dit resultaat.
Ik wil jullie beiden graag bedanken voor 1001 dingen!

Een bijzonder woordje van dank wens ik te richten tot ir. Jean Moriau. Jean, dankzij jouw expertise en enthousiasme heb ik me vol overgave in de wereld van de ionenwisselaars gestort. Dankzij jou kwam ik in contact met dr. Rudolf Wagner. Hij zorgde ervoor dat mijn doctoraatsonderzoek in een stroomversnelling kwam en ik op IEX2012 een prachtig verhaal kon brengen.

I would like to express my gratitude to the members of my examination committee. Thanks for your valuable comments and suggestions on this PhD dissertation.

Graag wil ik ook mijn collega's, vrienden van de twee onderzoeksgroepen INKAT en CaRE danken voor de leuke babbels, de aangename sfeer, de gezellige middagpauzes incl. saboteur, … kortom voor alle fijne momenten van de voorbije jaren. Bedankt voor jullie steun en hulp bij allerhande zaken, klein en groot. Een aantal collega's verdienen echter speciale aandacht in dit dankwoord. Kristof en Kenneth, bedankt om te zoeken naar antwoorden op mijn Aspen en Athena Visual Studio vragen. Pieter, we startten samen aan ons doctoraatsavontuur, jouw enthousiasme, jouw gedrevenheid werkten zeer inspirerend en motiverend en waren een stimulans om de laatste loodjes te dragen. An, Maarten en Wannes, bedankt voor de gezellige bureau-gesprekken: verbouwen, keukengeheimen of citytrips, … het waren aangename afleidingen tussen het simuleren door.
Peter, bedankt voor de gezellige babbels terwijl we wachtten op de chromatogrammen en tevens ook bedankt voor de raad, tips en kennis over de GC die je met mij deelde. Nicole, Nico, Hans en Michaël, bedankt voor jullie technische hulp als ik eventjes met mijn handen in het haar zat. Bedankt, thesisstudenten voor de bijdrage die jullie leverden aan dit werk: Tracy, Clara, Alberto, Aidé, Bram, Olivier, Robin, Jelle en Jannik.

Hoewel werk van groot belang is, is dit niet het enige dat telt. Ik wil dan ook van harte aan aantal vrienden bedanken voor de immer enthousiaste en opbeurende mails als ik het eventjes zwart zag, een ontspannende lunch, de kook-babbel-events, de goede raad en allerhande andere activiteiten: Griet, Sophie, Anneline en Stephanie. Bedankt hiervoor!

Bedankt Matthias & Sarah, Bram & Stefanie, Mama & Papa, Kris & Marieke, Daniël & Magda, Jolien & Bart voor de steun maar ook voor het babysitten als ik nog even wou verder werken. Memé & Pepé, bedankt voor jullie interesse en verwonderde, stimulerende woorden gedurende al deze jaren. Mama & Papa, bedankt voor jullie opofferingen en onvoorwaardelijke steun, zonder jullie zou ik niet zover geraakt zijn. Mama, bij deze wil ik me ook excuseren voor alle uren die je op me wachtte omdat ik nog net een staal moest nemen of toen ik nog in wetenschappelijke discussie was. Merci! Ik wil ook heel speciaal mijn zus bedanken omdat ze zoveel meer voor me betekent dan alleen maar mijn kleine zus. Stefanie, bedankt voor de vele ontspannende momenten, de opvang in nood, de bezoekjes op mijn bureau en de middagpauzes waarin we samen onze boterhammen opaten.

Last but not least, Karel, mijn zoetje, onmeetbaar en onmisbaar is de steun die ik van jou heb gekregen. Met jou kan ik alles delen, lachen, huilen, genieten, … met jou kan ik de wereld aan! Je hebt me leren trots zijn op wie ik ben en wat ik doe. Bedankt om er altijd te zijn voor mij. De laatste maanden waren niet gemakkelijk, jouw werk in combinatie met de full-time zorg voor onze kindjes, maar we zijn er samen geraakt! Mijn kleine kapoentjes, Henri en Alice, als ik naar jullie kijk besef ik dat chemie iets wonderlijks is. Dankzij jullie weet ik waar het leven om draait. Ik hoop dat mijn onderzoek, ook al is het maar een heel klein beetje, mag bijdragen tot een milieuvriendelijkere toekomst voor jullie.

Evelien,

Januari 2014

Table of Contents

List of tables

List of Figures

Nomenclature

Roman symbols

*	active site on catalyst surface
$a^{'}$	specific surface area particle ($m^{2}_{particle} m^{-3}_{particle}$)
a_i	activity of component *i* ($mol\ m^{-3}$)
$a_{l,s}$	external surface of catalyst per unit of liquid volume ($m_k^2 m_l^{-3}$)
a_v	external volumetric catalyst surface ($m^2 m^{-3}$)
A	pre-exponential factor ($m^3 kg^{-1}_{cat} mol^{-1} s^{-1}$)
$A_{peak,i}$	surface peak area of component *i* ($V\ s^{-1}$)
b	model parameter vector containing the estimated parameter values
c_b	bulk fluid concentration ($mol.m^{-3}_{gas}$)
c_s	concentration at external particle surface ($mol.m^{-3}_{gas}$)
C_a	Carberry number
CF_i	calibration factor of component *i* with regards to n-octane
C_i	observed concentration of component *i* ($mol\ m^{-3}$)
$\hat{C}_i$	predicted concentration of component *i* ($mol\ m^{-3}$)
d_k	diameter of the catalyst particle (m_p)
d_r	reactor diameter (m)
D_e	effective diffusion coefficient ($m^2\ s^{-1}$)
$D_{i,eff}$	effective diffusion coefficient of component *i* in the catalyst ($m^2\ s^{-1}$)
$D_{m,i}$	molecular diffusion coefficient of component *i* in the liquid phase ($m_l^3 m^{-1} s^{-1}$)
E_A	activation energy ($kJ\ mol^{-1}$)
F value	F value for the significance of the regression
$\Delta G^{\circ}_f(i)$	Standard Gibbs formation energy of component *i* ($kJ\ mol^{-1}$)
ΔG°_r	Standard Gibbs energy of the reaction ($kJ\ mol^{-1}$)
$\Delta H^{\circ}_f(i)$	Standard enthalpy of formation of component *i* ($kJ\ mol^{-1}$)
ΔH°_r	Standard enthalpy of the reaction ($kJ\ mol^{-1}$)

k	reaction rate coefficient ($m^3 kg_{cat}^{-1} mol^{-1} s^{-1}$)
k_g	mass transfer coefficient ($m\ s^{-1}$)
k_s	mass transfer coefficient between catalyst and bulk $\left(m_l^3 m_k^{-2} s^{-1}\right)$
k_{SR}	surface reaction rate coefficient ($mol\ kg_{cat}^{-1}\ s^{-1}$)
K_{eq}	equilibrium constant of the overall reaction
K_i	adsorption or exchange equilibrium constant of component *i*
L	characteristic particle size (m)
$L_{\max}$	likelihood function
m_i	mass of component *i* (kg)
M	molecular weight *(kg mol^{-1})*
n	order of the reaction
n_i	number of moles of component *i* (mol)
N	total number of experimental points or components
N_p	power number of the stirrer
N_i	stirrer speed *(s^{-1})*
p	number of parameters
r	reaction rate ($mol_{\,kg_{cat}^{-1} s^{-1}}$)
r_{obs}	observed volumetric reaction rate ($mol\ m^{-3} s^{-1}$)
R	universal gas constant (8.314 *J mol^{-1} K^{-1})*
R_i	net production rate of component i ($mol\, kg_{cat}^{-1} s^{-1}$ *)*
$R_{v,L}^{obs}$	observed volumetric production rate per unit of liquid volume ($mol\ m_l^{-3} s^{-1}$)
$R_{v,\mathrm{k}}^{obs}$	observed reaction rate per mass of catalyst ($mol\, kg_{cat}^{-1} s^{-1}$ *)*
Re_K	Reynolds number (Kolmogoroff theory)
S	objective function
Sc	Schmidt number
Sh	Sherwood number
t	time (s)
T	temperature (K)
t	Student t-value for the significance of an individual parameter

V_l	reaction mixture volume *(m^3)*
V_m	molar volume of solute at its boiling point *(m^3 $kmol^{-1}$)*
W	weight of catalyst (kg_{cat})
X_i	conversion of component *i*

Greek symbols

β	model parameter vector containing the estimated parameter values
γ_i	activity coefficient of component *i*
Δ	difference
ε	energy dissipation of the stirrer (W kg^{-1})
ε_b	void fraction in catalyst bed *(m_f^3 m_p^{-3})*
ε_k	the porosity of the catalyst *(m_{pore}^3 m_c^{-3})*
η	effectiveness factor
θ_i	fractional coverage of catalyst surface of component *i*
Λ	likelihood ratio
μ_l	viscosity of the liquid *(cP)*
ν_i	stoichiometric coefficient for component *i*
ρ_k	density of the catalyst *(kg m^{-3})*
ρ_l	density of the liquid (kg m_l^{-3})
τ	catalyst tortuosity
Φ	Weisz modulus

Superscripts

^	model calculated
o	initial conditions
o	standard conditions

Subscripts

cat	catalyst
b	bulk
eq	at equilibrium

i	component *i*
ref	reference
s	at catalyst surface

Abbreviations

BLT	Bundesanstalt für Landtechnik,
	the Austrian Federal Institute of Agricultural Engineering
EtOAc	ethyl acetate
EtOH	ethanol
FAEEs	fatty acid ethyl esters
FAMEs	fatty acid methyl esters
FFA	free fatty acid
IEX	ion exchange resin
HOAc	acetic acid
MeOAc	methyl acetate
MeOH	methanol
OAPEC	Organisation of Arab Petroleum Exporting Countries
REG	regression sum of squares
RDS	rate-determining step
RSSQ	residual sum of squares
TG	triglyceride
UNIFAC	UNIQUAC Functional-Group Activity Coefficients
UNIQUAC	Universal Quasi Chemical
WCO	waste cooking oil

Glossary of terms

Activation energy	For an elementary step, it is the difference in internal energy between the transition state and reactants. A measure for the temperature dependence of the rate coefficient $k = A\exp\left(-\frac{E_A}{RT}\right)$ with R the universal gas constant, T the temperature and A the pre-exponential factor.
Active site	Also called active centre. Groups at the surface of a solid, responsible for their catalytic activity
Activity	A measure of the "effective concentration" of a species in a mixture
Adsorbate	The adsorbed species.
Adsorption	Adhesion of the atoms, ions or molecules from a gas, liquid or dissolved solid to the surface of another substance.
Adsorption isotherm	The function, for a single gaseous species on a solid, which relates at constant temperature the amount of species adsorbed at equilibrium to the pressure (or concentration) of the species in the gas phase.
Arrhenius relation	Expresses the dependence of a reaction rate coefficient k on the temperature T and activation energy, E_A: $k = A\exp\left(-\frac{E_A}{RT}\right)$ with R the universal gas constant and A the pre-exponential factor.
Catalyst	A source of active sites, which augments the rate of a chemical reaction and is regenerated at the end of a closed reaction sequence.

Chemisorption	Also known as chemical adsorption. Adsorption in which the forces involved are valence forces of the same kind as those operating in the formation of chemical compounds. Chemisorption strongly depends on the surface and the adsorbing species, and only one layer of chemisorbed molecules is formed. Its energy of adsorption is the same order of magnitude as in chemical reactions, and the adsorption may be activated.
Conversion	Measure for the amount of a reactant that has been transformed into products as a result of a chemical reaction.
Deactivation	The decrease in conversion in a catalytic reaction with time under constant reaction conditions.
Effectiveness factor	Ratio of actual reaction rate for a porous catalyst to the reaction rate that would be observed if the total surface area throughout the catalyst interior was exposed to a fluid of the same composition and temperature as that found at the outside of the particle.
Eley Rideal (ER) mechanism	This mechanism assumes that one of the reactants must be adsorbed on the catalyst in order to react. The reaction occurs by the other reactant passing by and interacting with the one on the surface. The formed molecule desorbs. Usually adsorption-desorption steps are essentially at equilibrium and the surface reaction is rate determining. Adsorption steps can also be rate determining.
External diffusion	Also called interphase diffusion. Diffusion from the fluid phase to the external surface of catalyst.

Gas Chromatography (GC)	The process in which the components of a mixture are separated from one another by injecting the sample into a carrier gas which is passing through a column or over a bed of packing with different adsorption affinities for the components to be separated.
Group contribution method	A technique to estimate and predict thermodynamic and other properties from molecular structures, i.e., atoms, atomic groups, bond type etc.
Homogeneous catalysis	Is a sequence of reactions that involve a catalyst in the same phase as the reactants. Most commonly the homogeneous catalyst is codissolved in a solvent with the reactants.
Heterogeneous catalysis	It is a sequence of reactions that involve a catalyst in another phase of that of the reactants. Most commonly a solid catalyst is involved with the reactants in either the liquid or gas phase.
Intermediate	Is formed from a reactant and transforms into a product during a chemical reaction. The intermediate is often a short-living and unstable species that cannot directly be detected during a reaction.
Inhibition	Decrease in reaction rate due to a substance (inhibitor, poison) which may be produced during the reaction itself or may be a foreign substance.
Internal diffusion	Also called intraparticle diffusion. Motion of atoms within the particles of a solid phase that has a sufficiently large porosity to allow this motion.
Intraparticle diffusion	Motion of atoms or molecules in a porous particle

Ion exchange resin	Insoluble matrix containing labile ions susceptible to exchange with ions in the surrounding medium without major physical change in its structure
Langmuir adsorption	Mono-layer adsorption of a gas on a uniform surface in which there is no interaction between adsorbed species. Langmuir isotherm for non-dissociative adsorption has the form $\theta = \frac{kp}{1+kp}$ where θ = surface coverage, p = gas phase pressure of species, k = Langmuir adsorption equilibrium constant.
Langmuir-Hinshelwood (LH) mechanism	It is assumed that both reactants must be adsorbed on the catalyst in order to react. Usually adsorption-desorption steps are essentially at equilibrium and the surface reaction is rate-determining. Adsorption steps can also be rate-determining.
Mechanism	A sequence of elementary steps in which reactants are converted into products, through the formation of intermediates.
Objective function	Is a function used during optimization problems which has to be minimized or maximized by choosing the best set of variables which determines the values of this function.
Pseudo-homogeneous model	The model does not explicitly account for the presence of a heterogeneous catalyst in the reaction mixture.
Pseudo-steady state	Its mathematical expression is that the time rate of change of the concentration of all active centres in a reaction sequence is equal to zero
Parameter estimation	Process of estimating the parameters of a relation between independent and dependent variables as to describe a chemical reaction as good as possible.

Parity diagram	Diagram representing the model calculated values as a function of the experimentally observed values. The better the correspondence with the first bisector, the better the model.
Physisorption	Also known as physical adsorption. Adsorption in which the forces involved are intermolecular forces (van der Waals forces) of the same kind as those responsible for deviation from ideal gas behavior or real gases at the condensation of vapors, and which do not involve a significant change in the electronic orbital patterns of the species involved. Physisorption usually occurs at temperatures near the boiling point of the adsorbate, and multilayers can occur. The heat of adsorption is usually significantly less than 10 kcal/mol.
Porosity	A measure of the void spaces in a material, expressed as the ratio of the pore volume to the total volume of the material.
Pre-exponential factor	The temperature-independent factor of a rate coefficient $k = A\exp\left(-\frac{E_A}{RT}\right)$ also called the frequency factor.
Reaction rate	The number of moles of a component created by a chemical reaction per unit of time, volume or catalyst mass.
Rate-determining step	If, in a reaction sequence consisting of *n* steps, *(n-1)* steps are reversible and if the rate of each of these *(n-1)* steps is potentially larger in either direction than the rate of the *n*th step, the latter is said to be rate-determining.
Reversible	A process or reaction that can be reversed by an infinitesimally small change in conditions.
Residual plot	Plot showing the difference between model calculated and experimentally observed values as a function of an operating

	condition such as the temperature, pressure, inlet concentration.
Sorption	Assimilation of molecules of one substance by a material in a different phase. Adsorption (sorption on a surface) and absorption (sorption into bulk material) are two types of sorption phenomena.
Steady state	A system in steady-state has certain properties that are time-independent.
Support	Also called carrier. Material, usually of high specific surface area, on which the active catalytic material, present as the minor component, is dispersed. The support may be catalytically inert, but it may contribute to the overall catalytic activity.
Surface coverage	Ratio of the amount of adsorbed substance to the monolayer capacity
Steady state	A system in steady-state has certain properties that are time-independent.
Swelling	The increase in volume by uptake of a liquid species
Tortuosity	Tortuosity of a catalyst expresses that transport through a porous catalyst particle does not occur along the radius of the particle, but occurs through the pores of the solid material. For pores with a uniform diameter, the tortuosity is defined as the square of the ratio of the average distance between two points and the shortest distance between them.
Transition state	Also called activated complex. The configuration of highest potential energy along the path of lowest energy between reactants and products.

Summary

Introduction

(Trans)esterification reactions with typical production volumes ranging from a few hundred to thousand tonnes per year are commercially important and are used to make esters which serve as precursors or additives for a variety of perfumes and flavours, pharmaceuticals, agrochemicals and polymers [1-3]. The significant expansion of the biodiesel production capacity in the last decade has reinforced the interest in both reactions and the optimization of their industrial implementation. The homogeneous Lewis or Brønsted acids and bases that are commonly used for (trans)esterification purposes exhibit several well-known disadvantages, such as additional separation and neutralisation steps. A heterogeneously catalysed implementation of the reaction making use of acid ion exchange resins is promising as they are ecofriendly, noncorrosive and reusable [4-7]. The nature and the type of ion exchange resin will, in addition to the conventional reaction parameters, also strongly affect the time required to reach a target conversion. For this purpose, there is a need to compare the kinetic performance of different types of ion exchange resins as catalysts over a wide range of operating conditions. Moreover, the development of a kinetic model that is capable of reproducing the reaction kinetics behavior in such a wide range of reaction conditions, including different types of ion exchange resins as catalyst, would provide a useful tool for catalyst selection and design as well as reactor optimization.

Experimental results

The kinetics of ethyl acetate transesterification with methanol, and acetic acid esterification with methanol have been investigated on gel-type and macroporous resins. Intrinsic kinetics data were acquired in an isothermal perfectly mixed batch reactor equipped with a reflux condenser, a thermocouple and a sampling port. External or internal mass transfer limitations were assessed quantitatively and qualitatively and were found not to significantly affect the observations made. The reaction mixture was stirred with a magnetic stirrer at a constant speed of 500 rpm throughout the experiment. Samples of the reaction mixture were withdrawn through the sampling port every 1800 s. The samples were analysed by gas chromatography. *n*-Octane was used as internal standard for analytical purposes as well as for obtaining a constant reaction volume. Prior to the (trans)esterification reaction, the catalyst was dried under vacuum, to completely remove any moisture.

The investigated ion exchange resins Lewatit K1221, Lewatit K2640, Lewatit K2629 (Lanxess) and Amberlyst 15 (Rohm & Haas) are spherical polystyrene-based resins beads crosslinked with divinylbenzene, with sulfonic acid groups. The chemical and physical properties of the ion exchange resins are given in Table 1. The gel type resin, Lewatit K1221, consists of, on a microscopic scale, a homogenous matrix without discontinuities [8]. The macroporous resins, Lewatit K2629, Lewatit K2640 and Amberlyst 15, consist of agglomerates of very small microspheres interspersed with macropores [9, 10].

Table 1: Chemical and physical properties of ion-exchange resins

Property	K1221	K2629	K2640	Amberlyst 15
Appearance	dark brown, translucent	beige, opaque	beige, opaque	deep grey, beige opaque
Type	gel	macroporous	macroporous	macroporous
Acid site (eq/kg)	5.3	4.8	5.2	4.8
% divinylbenzene	4 %	18 %	18 %	20 %
Bead size (mm)	0.4 – 1.25	0.4 – 1.2	0.4 – 1.25	0.3 – 1.2
Sulfonation degree	stoichiometric	stoichiometric	poly	stoichiometric

Prior to the kinetic experiments, independent volumetric swelling experiments were performed to evaluate the swelling ratio of all resins in contact with different solvents. The swelling ratio is defined as the ratio between the volume of the swollen resin and the volume of the dry resin.

The swelling experiments showed that the resins swell when in contact with all pure reactants and products, but to a different extent. The swelling ratio is found to be proportional to the dielectric constant of the solvent. Hence, the more polar the solvent, the higher the swelling ratio. Gel type resins exhibit a higher swelling ratio than macroporous ones, which is a logic consequence of their lower crosslinking degree.

The kinetic data showed that Lewatit K1221 has a noticeably higher activity than the macroporous resins for both reactions, despite the comparable active site concentration, see Table 1. The catalytic activity for transesterification of Lewatit K2629 and Lewatit K2640 is quite similar. Amberlyst 15 exhibits the lowest catalytic activity for transesterification. For esterification, the catalytic activities of Amberlyst 15 and Lewatit K2629 were comparable. These observations show that reaction rate of resin-catalyzed (trans)esterification depends not only on the number of active sites but also on and their accessibility. As already evident from the swelling experiments, the latter is affected by the divinylbenzene (DVB) content, i.e., a higher DVB content reduces the resins' swelling, the accessibility of the active sites and, hence, the catalytic activity.

For the (trans)esterification the effect of temperature and initial molar methanol to ester/acid ratio was investigated for both gel and macroporous resins. In accordance with the Arrhenius law, a higher temperature resulted in a higher reaction rate and correspondingly higher conversions at the same batch time. Higher initial molar methanol to ester/acid ratios result in higher conversions, which corresponds to higher reaction rates, because the (ethyl acetate)acetic acid/catalyst amount ratio was kept constant. Thanks to the pronounced polarity of the reaction mixtures, the highest reaction rates were found with gel type resins.

Kinetic Modelling

In literature, several kinetic studies on the reactions catalyzed by ion exchange resins can be found. For transesterification, pseudo-homogeneous (PH) as well as adsorption-based mechanisms, such as Eley-Rideal (ER) and Langmuir-Hinselwood (LH) have been used [11-15]. The most commonly used model is the simpler, pseudo-homogeneous one which gave similar simulation results as the more complex Langmuir-Hinshelwood model [11, 14, 15].

The esterification catalyzed by ion exchange resins has also been conceptualized and quantified by a PH, ER or LH mechanisms [1, 16-20]. In contrast to transesterification, several authors found that the classic adsorption-based models, such as ER and LH, did not suffice to describe the reaction kinetics catalyzed by ion exchange resins. Therefore, more advanced models, accounting for resins' swelling, were developed [4, 18, 19].

The volumetric swelling and kinetic experiments showed the importance of swelling on the catalytic performance of ion exchange resins. Hence the swelling phenomena should be assessed, either via an adsorption or an exchange based model. The adsorption-based models are commonly used to describe the reaction kinetics on heterogeneous catalysts, but they do not account for the swelling behavior of the resins. The first step in an adsorption-based model is the adsorption of a component on the free active site of the resin, whereas in the exchange based model it is assumed that all active sites are always occupied and, hence, the first step is an equilibrium exchange between 2 components. Next is the surface reaction which is considered to be rate determining. In the exchange based model the surface reaction is assumed to be of the Eley-Rideal type and to occur between protonated (ethyl acetate)acetic acid with methanol from the bulk. The exchange based reaction mechanisms for (trans)esterification are given in Figures 1 and 2. The non-ideal behavior of the reaction mixture was assessed. Results showed that activity coefficients are quite different from 1, indicating non-ideality mixture. Therefore activities instead of concentrations were used in the kinetic models.

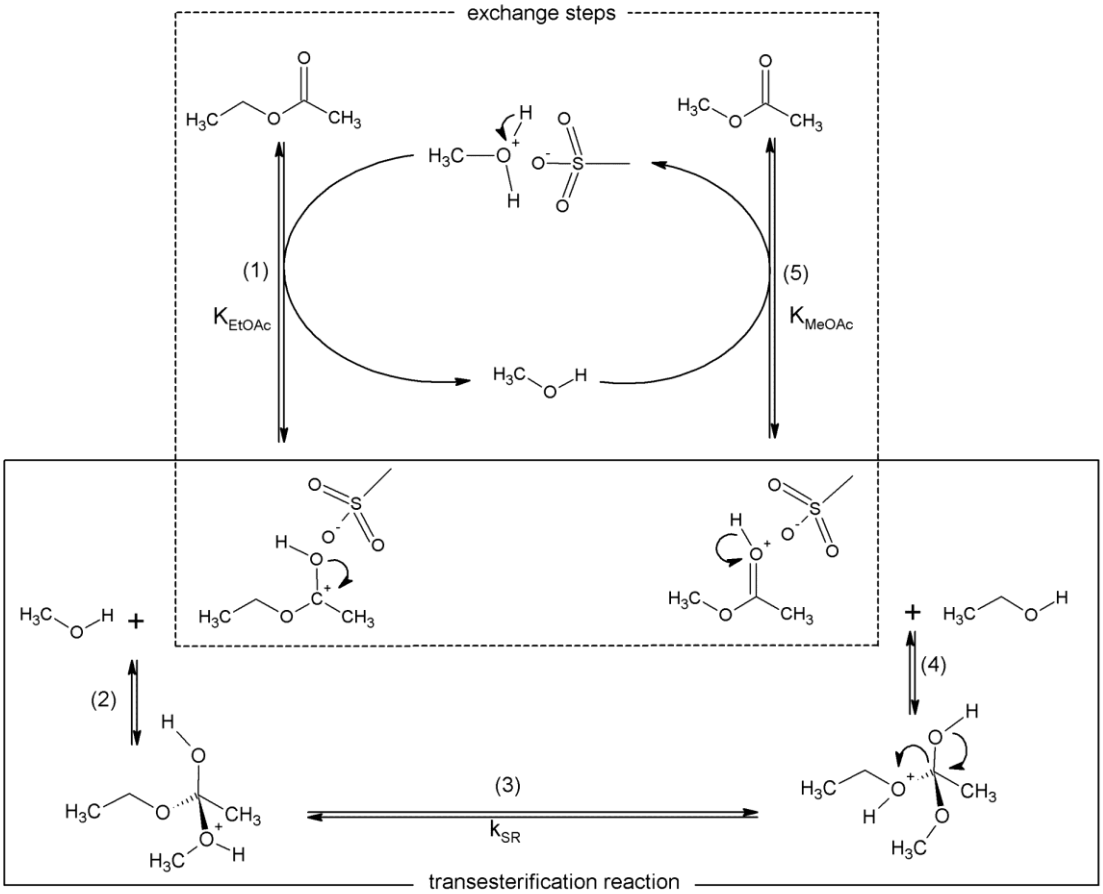

Figure 1: **Heterogeneous acid ion exchange resin catalyzed reaction mechanism for the transesterification of ethyl acetate with methanol.**

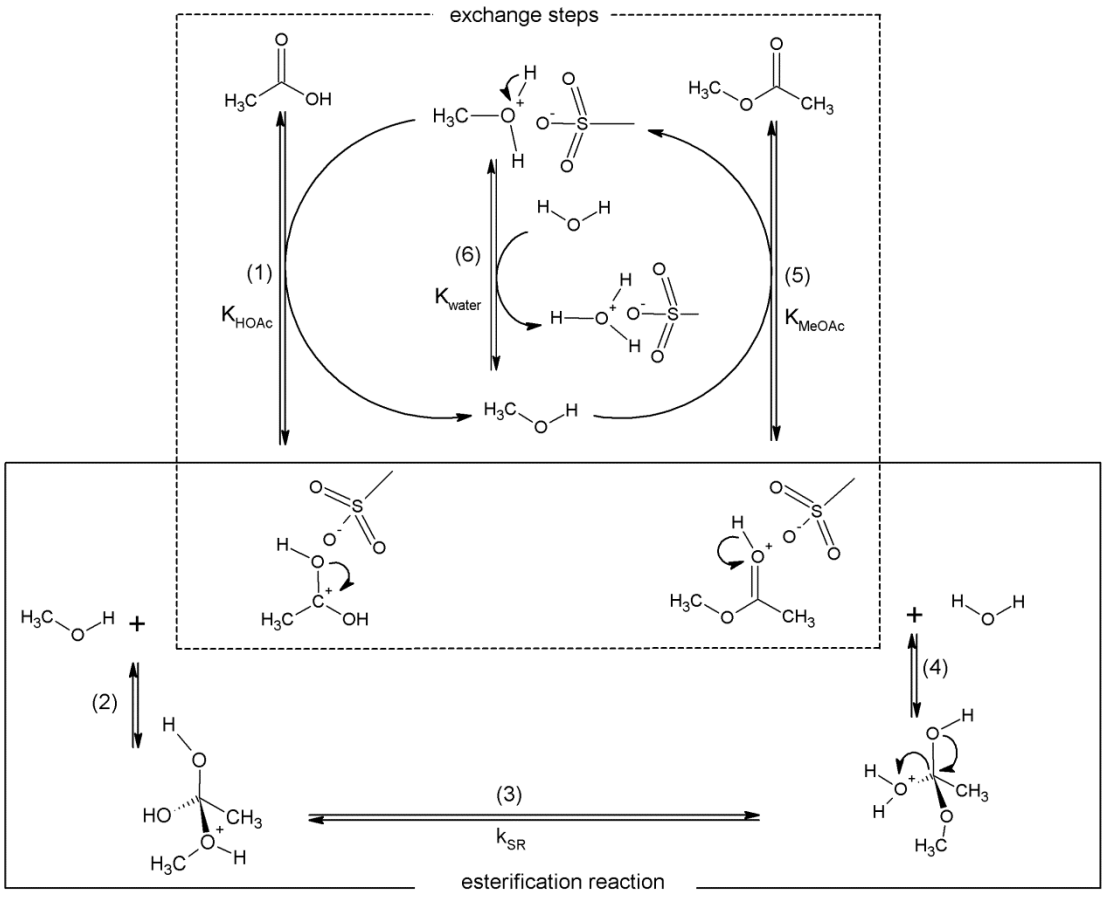

Figure 2: Heterogeneous acid ion exchange resin catalyzed reaction mechanism for the esterification of acetic acid with methanol.

First, a model discrimination between the adsorption-based models, has been performed for ethyl acetate transesterification reaction catalyzed by Lewatit K1221. The best performing model was that based on an Eley-Rideal mechanism, with the surface reaction of adsorbed methanol with ethyl acetate from the bulk as the rate-determining step. It indicates that pronounced sorption saturation effects occurred for methanol whereas, according to the homogeneous transesterification reaction mechanism, such effects would rather have been expected for ethyl acetate. This apparent contradiction, indicates that the heterogeneous reaction mechanism is more complex. To describe the reaction kinetics on gel and macroporous resins, which exhibit a distinct swelling behavior, a novel reaction mechanism, mathematically expressed as the exchange based model, is needed.

Second, model discrimination between the exchange and the adsorption-based model for the (trans)esterification catalyzed with the gel type resin is performed. The best performing model for simulating experimentally observed kinetics is the exchange based model which has the lowest residual sum of squares and the highest F value for the global significance of the regression. Although it does not outperform the adsorption-based model,

the good statistics combined with the physicochemical meaning of the model make the exchange based model the preferred one for further assessment of the (trans)esterification kinetics on the other resins.

The exchange based model describes all experimental (trans)esterification data accurately. Activation energies equal to 49 kJ mol^{-1} and 47 kJ mol^{-1}, for transesterification and esterification respectively, irrespective of the resin used, are estimated. For both reactions the product of the surface reaction rate coefficient and the ester/acid exchange coefficient at the reference temperature, are three to four times higher for the gel type catalyst compared to the macroporous catalyst. This could be expected from the experimental data and the similar activation energies. The reaction rate coefficient for the esterification reaction is about 4 to 6 times higher than that of transesterification.

For the (trans)esterification the exchange equilibrium coefficients have the same order of magnitude for all catalysts. For transesterification, the ratio between the methyl and ethyl acetate exchange coefficient is identical for all four resins, Lewatit K1221, Lewatit K2629, Lewatit K2640 and Amberlyst 15, and amounts to approximately 4 This reflects the similarity of the resins. The additional methylene group in ethyl acetate results in a lower exchange equilibrium coefficient. For esterification the exchange coefficients of acetic acid and the products exhibit some apparent discrepancies. The more pronounced variation of the polarity of the reaction mixture in esterification compared to in transesterification, in addition to the 20 to 60 times lower reactant to resin ratio in the literature reported data set on Amberlyst 15 compared to the data sets acquired on Lewatit K1221 and Lewatit K2629 acquired in the present work, apparently resulted in exchange behavior that can only be captured by an enhanced version of the model for describing the thermodynamics in the resin, e.g., by the Flory Huggins theory.

General conclusions

Acid ion exchange resins are promising catalysts for (trans)esterification. Thanks to their pronounced swelling when in contact with polar media, the highest conversions are obtained with a gel type resin, Lewatit K1221. The resins' swelling significantly affects the catalytic activity and, hence, should also be reflected in the kinetic model. A novel kinetic model, implicitly accounting for resin swelling, was developed based on the following assumptions: (1) all active sites are occupied, (2) the exchange reactions between reagents or products are quasi equilibrated and (3) an Eley-Rideal type surface reaction between protonated (ester)acid with methanol from the bulk occurs as the rate-determining step. This

kinetic model describes accurately the (trans)esterification reaction kinetics on different type of resins. Parameter estimates generally adopted physically meaningful values although the exchange coefficients obtained for acetic acid esterification indicated the need for further model refinement, in particular with respect to the description of the thermodynamics inside the resin. The kinetic model can be used as a helpful tool for resin selection. While resin selection and design frequently occurs on a trial and error base, the insight gained by the model, may provide clear guidelines about the desired resin properties. This knowledge may further lead to an enlargement of the use of ion exchange resins as catalysts, and, hence, also be exploited for industrial reactor design and optimization.

References

1. Ali, S.H., *Kinetics of Catalytic Esterification of Propionic Acid with Different Alcohols over Amberlyst 15.* International Journal of Chemical Kinetics, 2009. **41**(6): p. 432-448.
2. Dossin, T.F., M.F. Reyniers, R.J. Berger, and G.B. Marin, *Simulation of heterogeneously MgO-catalyzed transesterification for fine-chemical and biodiesel industrial production.* Applied Catalysis B-Environmental, 2006. **67**(1-2): p. 136-148.
3. Yadav, G.D. and M. Rahuman, *Cation-exchange resin-catalysed acylations and esterifications in fine chemical and perfumery industries.* Organic Process Research & Development, 2002. **6**(5): p. 706-713.
4. Tesser, R., L. Casale, D. Verde, M. Di Serio, and E. Santacesaria, *Kinetics and modeling of fatty acids esterification on acid exchange resins.* Chemical Engineering Journal, 2010. **157**(2-3): p. 539-550.
5. Russbueldt, B.M.E. and W.F. Hoelderich, *New sulfonic acid ion-exchange resins for the preesterification of different oils and fats with high content of free fatty acids.* Applied Catalysis a-General, 2009. **362**(1-2): p. 47-57.
6. Zielinska-Nadolska, I., K. Warmuzinski, and J. Richter, *Zeolite and other heterogeneous catalysts for the transesterification reaction of dimethyl carbonate with ethanol.* Catalysis Today, 2006. **114**(2-3): p. 226-230.
7. Ozbay, N., N. Oktar, and N.A. Tapan, *Esterification of free fatty acids in waste cooking oils (WCO): Role of ion-exchange resins.* Fuel, 2008. **87**(10-11): p. 1789-1798.
8. Chakrabarti, A. and M.M. Sharma, *Cationic Ion-Exchange Resins as Catalyst.* Reactive Polymers, 1993. **20**(1-2): p. 1-45.
9. Silva, V. and A.E. Rodrigues, *Kinetic studies in a batch reactor using ion exchange resin catalysts for oxygenates production: Role of mass transfer mechanisms.* Chemical Engineering Science, 2006. **61**(2): p. 316-331.
10. Ihm, S.K., J.H. Ahn, and Y.D. Jo, *Interaction of reaction and mass transfer in ion-exchange resin catalysts.* Industrial & Engineering Chemistry Research, 1996. **35**(9): p. 2946-2954.
11. Bozek-Winkler, E. and J. Gmehling, *Transesterification of methyl acetate and n-butanol catalyzed by Amberlyst 15.* Industrial & Engineering Chemistry Research, 2006. **45**(20): p. 6648-6654.
12. Saha, B. and M. Streat, *Transesterification of cyclohexyl acrylate with n-butanol and 2-ethylhexanol: acid-treated clay, ion exchange resins and tetrabutyl titanate as catalysts.* Reactive & Functional Polymers, 1999. **40**(1): p. 13-27.
13. Jimenez, L., A. Garvin, and J. Costa-Lopez, *The production of butyl acetate and methanol via reactive and extractive distillation. I. Chemical equilibrium, kinetics, and mass-transfer issues.* Industrial & Engineering Chemistry Research, 2002. **41**(26): p. 6663-6669.
14. Steinigeweg, S. and J. Gmehling, *Transesterification processes by combination of reactive distillation and pervaporation.* Chemical Engineering and Processing, 2004. **43**(3): p. 447-456.
15. Pappu, V.K.S., A.J. Yanez, L. Peereboom, E. Muller, C.T. Lira, and D.J. Miller, *A kinetic model of the Amberlyst-15 catalyzed transesterification of methyl stearate with n-butanol.* Bioresource Technology, 2011. **102**(5): p. 4270-4272.
16. Sanz, M.T., R. Murga, S. Beltran, J.L. Cabezas, and J. Coca, *Autocatalyzed and ion-exchange-resin-catalyzed esterification kinetics of lactic acid with methanol.* Industrial & Engineering Chemistry Research, 2002. **41**(3): p. 512-517.

17. Ali, S.H. and S.Q. Merchant, *Kinetics of the esterification of acetic acid with 2-propanol: Impact of different acidic cation exchange resins on reaction mechanism.* International Journal of Chemical Kinetics, 2006. **38**(10): p. 593-612.
18. Mazzotti, M., B. Neri, D. Gelosa, A. Kruglov, and M. Morbidelli, *Kinetics of liquid-phase esterification catalyzed by acidic resins.* Industrial & Engineering Chemistry Research, 1997. **36**(1): p. 3-10.
19. Popken, T., L. Gotze, and J. Gmehling, *Reaction kinetics and chemical equilibrium of homogeneously and heterogeneously catalyzed acetic acid esterification with methanol and methyl acetate hydrolysis.* Industrial & Engineering Chemistry Research, 2000. **39**(7): p. 2601-2611.
20. Song, W., G. Venimadhavan, J.M. Manning, M.F. Malone, and M.F. Doherty, *Measurement of residue curve maps and heterogeneous kinetics in methyl acetate synthesis.* Industrial & Engineering Chemistry Research, 1998. **37**(5): p. 1917-1928.

Samenvatting

Inleiding

Jaarlijks worden typisch enkele honderden tot duizenden tonnen esters geproduceerd door (trans)esterificatie reacties. Het industrieel belang van deze reacties is hierdoor groot. De geproduceerde esters worden gebruikt als tussenproduct in de bereiding van parfums en geuren, maar ook in de farmaceutische sector, de agrochemie en in de productie van kunststoffen worden ze ook frequent gebruikt [1-3]. De toename in de biodiesel productie zorgde ervoor dat onderzoek naar de optimalisatie van beide reacties terug in de spotlights werd geplaatst. De frequent gebruikte katalysatoren voor de (trans)esterificatie zijn homogeen met Lewis of Brønsted zure en basische actieve plaatsen. Het gebruik van deze katalysatoren in de industrie leidt tot een aantal gekende nadelen, zoals o.a. de moeilijke scheiding tussen katalysator enerzijds en producten anderzijds. Binnen de grote groep van heterogene katalysatoren, staan zure ionen uitwisselingsharsen bekend als veelbelovende katalysatoren, omdat ze ecologisch, niet corrosief en herbruikbaar zijn [4-7]. De chemische samenstelling en ook de morfologie van het uitwisselingshars zal, samen met de procesparameters, een sterke invloed hebben op de reactietijd die nodig is om de beoogde conversie te bereiken. Er is dus nood aan een vergelijkende studie tussen verschillende ionen uitwisselingsharsen als katalysator. Meer nog, de ontwikkeling van een kinetisch model dat het kinetisch gedrag van het systeem in een wijd bereik van reactieomstandigheden, inclusief de morfologisch verschillen in ionen uitwisselingsharsen, kan beschrijven, zou een zeer bruikbaar instrument zijn voor zowel katalysator selectie als reactor optimalisatie.

Experimentele resultaten

De kinetiek van de transesterificatie van ethylacetaat met methanol en van de esterificatie van azijnzuur met methanol werden onderzocht zowel voor een gel type als voor macroporeuze katalysator. Intrinsieke kinetische data werden verworven in een isotherme, perfect gemengde batch reactor, welke uitgerust is met een reflux koeler, een thermokoppel en een staalname-eenheid. De afwezigheid van interne en externe massa transfer limitatie werd kwantitatief en kwalitatief geëvalueerd. Tijdens de reactie werd constant geroerd met een magnetische roervlo met een snelheid van 500 rpm. Elke 30 minuten werden er stalen genomen. Met gas chromatografie werd de concentratie van de reagentia en producten in de stalen bepaald. *n*-Octaan werd toegevoegd als interne standaard en om een constant reactie

volume te bekomen. Als voorbehandeling werd de katalysator gedurende 24 u gevriesdroogd om alle vocht te verwijderen.

De onderzochte ionen uitwisselingsharsen zijn Lewatit K1221, Lewatit K2640, Lewatit K2629 (Lanxess) en Amberlyst 15 (Rohm & Haas). De harsen zijn bolletjes die bestaan uit met divinylbenzeen gecrosslinkte polystyreen ketens, waarop op de benzeen groepen sulfonzure groepen gesubstitueerd zijn. De chemisch en fysische eigenschappen van de verschillende harsen zijn gegeven in Tabel 1. Het gel type hars, Lewatit K1221, is microscopisch gezien een glad mooi rond homogeen bolletje zonder gebreken [8]. Een macroporeus hars, zoals Lewatit K2629, Lewatit K2640 en Amberlyst 15, daarvan lijkt het bolletje microscopisch gezien op bloemkoolroosjes die heel dicht bij elkaar zitten. Het zijn, de facto, heel kleine gel bolletjes afgewisseld met macroporiën [9, 10].

Tabel 1: Chemische en fysische eigenschappen van de gebruikte ionen uitwisselingsharsen

Eigenschap	K1221	K2629	K2640	Amberlyst 15
Voorkomen	donker bruin, doorzichtig	beige, ondoorzichtig	beige, ondoorzichtig	donker grijs, ondoorzichtig
Type	gel	macroporeus	macroporeus	macroporeus
Zure sites (eq/kg)	5.3	4.8	5.2	4.8
% divinylbenzene	4 %	18 %	18 %	20 %
Grootte (mm)	0.4 – 1.25	0.4 – 1.2	0.4 – 1.25	0.3 – 1.2
Sulfoneringsgraad	stoichiometrisch	stoichiometrisch	meervoudig	stoichiometrisch

Voordat de kinetiek van de harsen geëvalueerd werd, werden er onafhankelijke zwellingsexperimenten uitgevoerd. Deze, op volume gebaseerde, zwellingsexperimenten hadden als doel de zwellingsgraad van al de harsen te bepalen in de verschillende componenten. De zwellingsratio is bepaald als de verhouding tussen het volume nat, c.q. gezwollen, en het volume droog hars.

Deze zwellingsexperimenten toonden aan dat alle harsen zwellen wanneer deze in contact komen met de pure reagentia en componenten. Er kon besloten worden dat de zwellingsgraad evenredig is met de diëlektrische constante van het medium, en tevens hoe meer polair het medium is, hoe meer het hars zal zwellen. Gel type harsen zullen meer zwellen dan macroporeuze harsen, wat een logisch gevolg is omwille van hun lagere graad van crosslinking met divinylbenzeen.

De kinetische experimenten toonden dat, voor de beide reacties, Lewatit K1221 duidelijk een hogere activiteit had dan de macroporeuze harsen en dit ondanks hun vergelijkbare concentratie aan zure sites, zie Tabel 1. De katalytische activiteit van Lewatit K2629 en Lewatit K2640 is vergelijkbaar voor de transesterificatie. Amberlyst 15 geeft de

laagste katalytische activiteit voor deze reactie. Voor de esterificatie is de katalytische activiteit van Amberlyst 15 en Lewatit K2629 vergelijkbaar.

Uit deze kinetische experimenten kon besloten worden dat de reactiesnelheid van de door harsen gekatalyseerde (trans)esterificatie reacties niet enkel afhankelijk is van de concentratie aan zure plaatsen, maar vooral van hun beschikbaarheid voor reactie. Zoals reeds duidelijk uit de zwellingsexperimenten wordt dit laatste beïnvloed door het gehalte divinylbenzeen. Zo zal een hoger gehalte divinylbenzeen (DVB) de zwelling van het hars tegengaan, en daardoor zal slechts een beperkt aantal actieve plaatsen beschikbaar zijn voor reactie, wat resulteert in een lagere katalytische activiteit.

De invloed van de temperatuur en de initiële molaire methanol t.o.v. ester/zuur verhouding werd zowel voor gel als voor macroporeuze harsen, op de (trans)esterificatie geëvalueerd. In overeenstemming met het Arrhenius verband, zal een hogere reactietemperatuur resulteren in een hogere reactiesnelheid en dus hogere conversies na dezelfde batch tijd. Hogere initiële molaire verhoudingen resulteren in hogere conversies, welke overeenkomen met hogere reactiesnelheden daar de verhouding (ethylacetaat)azijnzuur t.o.v. katalysator constant gehouden werd. De hoogste reactie snelheid werd waargenomen als de reactie doorging in een polair reactiemedium, bv. bij een initiële verhouding van 1:10, waarbij de reactie gekatalyseerd werd door een gel type hars.

Kinetische modelering

Voor de beide reacties gekatalyseerd met harsen zijn reeds verschillende kinetische studies gepubliceerd. Voor de transesterificatie wordt het pseudo-homogeen (PH) model alsook de op adsorptie gebaseerde modellen, zoals Eley-Rideal (ER) en Langmuir-Hinshelwood (LH) gebruikt om de experimentele data te beschrijven en te voorspellen [11-15]. Meestal werd er geopteerd voor het PH model, omdat dit het meest eenvoudige model is en in vergelijking met het meer complexe LH model vergelijkbare resultaten gaf [11, 14, 15].

De esterificatie gekatalyseerd door ionen uitwisselingsharsen wordt gekwantificeerd aan de hand van het PH, ER of LH model [1, 16-20]. In tegenstelling tot de transesterificatie, stelden verschillende auteurs vast dat de klassieke adsorptie gebaseerde modellen, zoals ER en LH, niet in staat waren om de kinetiek van de esterificatie reactie gekatalyseerd met ionen uitwisselingsharsen te beschrijven. Hiervoor werden dan ook meer complexe modellen ontwikkeld, welke het zwellingsgedrag wel in hun berekening opnemen [4, 18, 19].

De zwellingsexperimenten in combinatie met de kinetische experimenten toonden aan dat zwelling een belangrijk aspect is voor de bespreking en vergelijking van de katalytische

activiteit van verschillende types harsen. Deze zwellingsfenomenen moeten dan ook opgenomen worden in het kinetisch model, hetzij in een adsorptie gebaseerd model of in een uitwisseling gebaseerd model. De adsorptie gebaseerde modellen worden frequent gebruikt om de reactie kinetiek van heterogene katalytische reacties te beschrijven. Deze zullen niet expliciet rekening houden met het zwellingsgedrag van de harsen. De eerste stap in een adsorptie gebaseerd model is steeds de adsorptie van een reagens op een vrije actieve plaats van het hars. In een uitwisseling gebaseerd model is de eerste stap steeds een uitwisselingsreactie tussen twee componenten. Nadien volgt, in beide modellen de oppervlakte reactie, welke snelheidsbepalend is. Voor het uitwisseling gebaseerd model, zal vervolgens een oppervlakte reactie gebeuren via een Eley-Rideal reactie mechanisme tussen een geprotoneerd (ethylacetaat) azijnzuur met methanol uit de bulk. Het reactiemechanisme van dit uitwisseling gebaseerde model voor de (trans)esterificatie is gegeven in Figuren 1 en 2. Het niet ideaal gedrag van het reactie mengsel werd onderzocht en de resultaten toonden activiteitscoëfficiënten met waarden sterk verschillend van 1. Er werden dus activiteiten in plaats van concentraties gebruikt in de kinetische modellen.

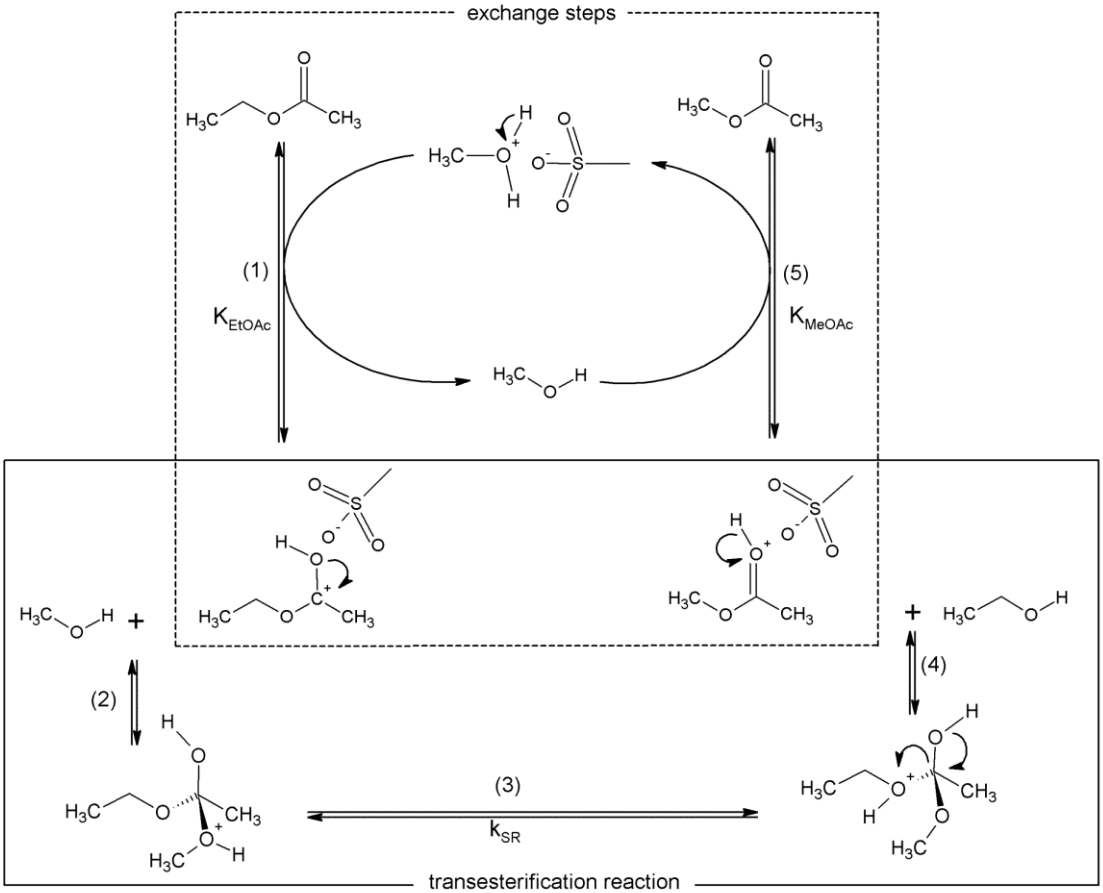

Figuur 1: Mechanisme voor de heterogeen zuur met ionen uitwisselingshars gekatalyseerde transesterificatie van ethylacetaat met methanol.

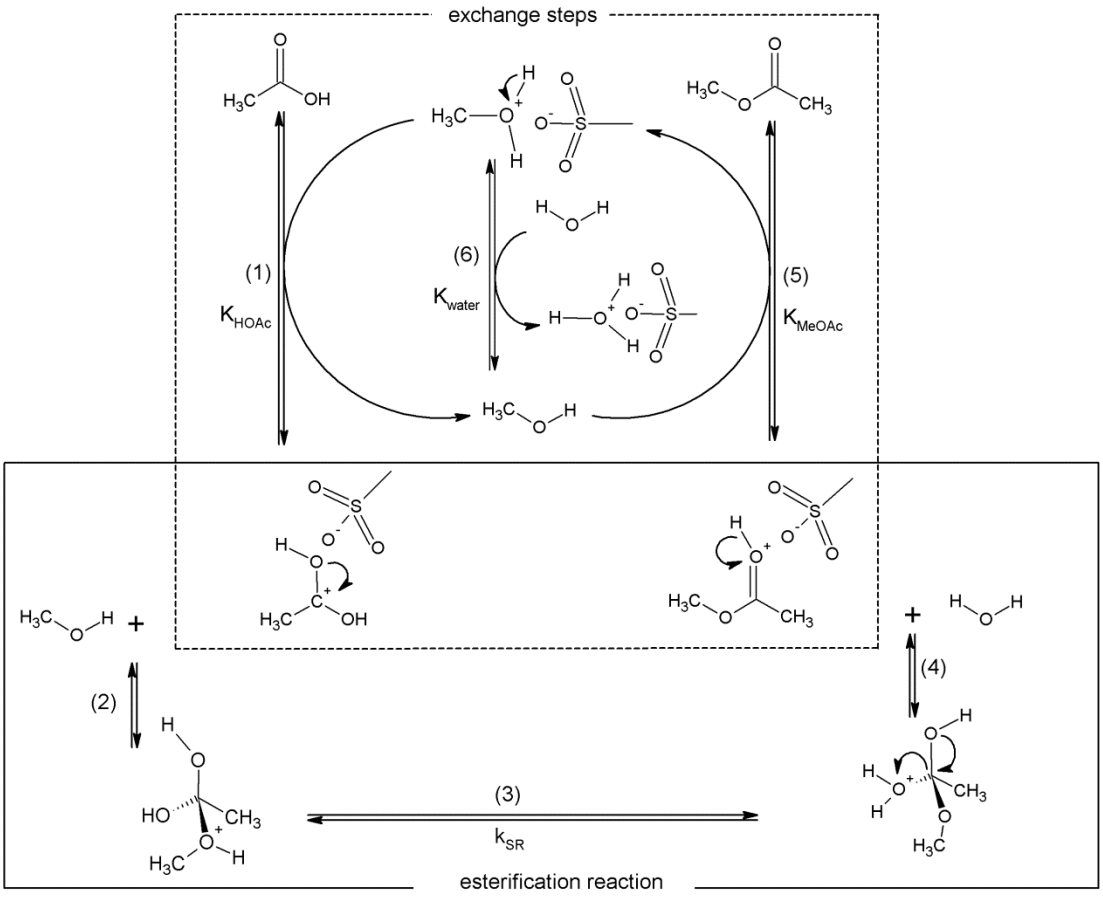

Figuur 2: **Mechanisme voor de heterogeen zuur met ionen uitwisselingshars gekatalyseerde esterificatie van azijnzuur met methanol.**

Allereerst is een model discriminatie tussen de adsorptie gebaseerde modellen gebeurd voor de ethylacetaat transesterificatie gekatalyseerd met de referentie katalysator, Lewatit K1221. Het beste model is het kinetisch model dat overeenkomt met een Eley-Rideal mechanisme, waarbij de oppervlakte reactie tussen geadsorbeerd methanol met ethylacetaat uit de bulk, de snelheidsbepalende stap is. Dit model wijst op de meer uitgesproken sorptie effecten voor methanol, welke volgens het homogene reactiemechanisme verwacht worden van geprotoneerd ethylacetaat. Deze aanwezige tegenstelling duidt aan dat het heterogeen reactiemechanisme meer complex is. In combinatie met de uitdaging om de reactie kinetiek van zowel gel als macroporeuze harsen te beschrijven, welke een totaal verschillend zwellingsgedrag hebben, zal een ander reactie mechanisme nodig zijn. Dit nieuw reactiemechanisme, voorgesteld in Figuur 1 en 2, wordt wiskundig beschreven a.d.h.v. het uitwisselingsmodel.

Vervolgens is er een model discriminatie gebeurd tussen het adsorptie gebaseerd model en het uitwisselingsmodel voor de (trans)esterificatie gekatalyseerd door Lewatit K1221. Het uitwisselingsmodel beschrijft de experimenteel waargenomen data met de laagste

residuele kwadratensom en de hoogste F waarde voor de globale significantie van de regressie. Deze goede statistische evaluatie in combinatie met de fysicochemische betekenis van het uitwisselingsmodel, zullen ervoor zorgen dat dit model de voorkeur krijgt ten opzichte van de adsorptie gebaseerde modellen voor de beschrijving van de (trans)esterificatie kinetiek met andere type harsen.

Het uitwisselingsmodel beschrijft alle experimentele (trans)esterificatie data accuraat. Activeringsenergie van 49 en 47 kJ mol^{-1} werden voor respectievelijk de transesterificatie en esterificatie geschat, onafhankelijk van het gebruikte hars. Voor beide reacties is de snelheidscoëfficiënt bij referentie temperatuur drie tot vier keer hoger voor de gel type katalysator in vergelijking met de macroporeuze katalysator. Dit kon verwacht worden uitgaande van de experimentele data en de vergelijkbare activeringsenergie. De reactie snelheid voor de esterificatie is 4 tot 6 keer sneller in vergelijking met de transesterificatie.

Voor zowel de trans- als esterificatie reactie hebben de uitwisselingscoëfficiënten dezelfde grootteorde voor alle onderzochte katalysatoren. Voor de transesterificatie is de verhouding tussen de uitwisselingscoëfficiënten van methylacetaat en ethylacetaat tussen drie en vier en identiek voor alle onderzochte harsen, Lewatit K1221, Lewatit K2629, Lewatit K2640 en Amberlyst 15. Deze waarde is een weerspiegeling van de chemische gelijkenis tussen de katalysatoren. De extra methyleen groep in ethylacetaat, t.o.v. methylacetaat, zorgt voor een lagere waarde voor de uitwisselingscoëfficiënt van ethylacetaat.

De uitwisselingscoëfficiënten van azijnzuur en de producten voor de esterificatie daarentegen vertonen een aantal duidelijke verschillen. De uitgesproken sterke verschillen in de polarisatie van het reactiemengsel voor de esterificatie t.o.v. de transesterificatie, tezamen met de 20 tot 60 keer lagere reagentia katalysator verhouding voor de in de literatuur gepubliceerde dataset aan experimenten, met Amberlyst 15, in vergelijking met de datasets van Lewatit K1221 en Lewatit K2629, leiden tot schijnbare verschillen in het katalytisch gedrag van de harsen. Deze kunnen opgevangen worden door het kinetisch model uit te breiden met een model welke ook de thermodynamica in het hars beschrijft, bijvoorbeeld a.d.h.v. het Flory-Huggins model.

Algemeen besluit

Zure ionen uitwisselingsharsen zijn veelbelovende heterogene katalysatoren voor de (trans)esterificatie reacties. Door hun sterk uitgesproken zwellingsgedrag, vooral als deze in een polair medium gebracht worden, zal de hoogste conversie voor beide reacties bekomen worden met een gel type hars, Lewatit K1221. Het zwellen van het hars beïnvloedt sterk de

katalytische activiteit van het hars, en dus ook het kinetisch model. Een nieuw kinetisch model, dat impliciet rekening houdt met het zwellingsgedrag van de harsen, werd ontwikkeld gebaseerd op de volgende veronderstellingen: (1) al de actieve plaatsen in het hars zijn bezet, (2) de uitwisselingsharsen tussen reagentia en producten zijn bijna in evenwicht en (3) de oppervlakte reactie, als snelheidsbepalende stap, wordt beschreven met een Eley-Rideal reactie mechanisme tussen geprotoneerd (ester)zuur met methanol uit de bulk. Dit kinetisch model beschrijft de (trans)esterificatie kinetiek accuraat voor verschillende harsen. De geschatte parameters kunnen toegewezen worden aan verschillen in katalytische activiteit. De parameterschattingen geven in het algemeen fysisch zinvolle waarden, alhoewel de uitwisselingscoëfficiënten voor de esterificatie van azijnzuur wijzen op een noodzakelijke verdere verfijning, in het bijzonder voor de beschrijving van de thermodynamica in het hars.

Dit kinetisch model kan gebruikt worden als een bruikbaar instrument voor de selectie van harsen, welke tegenwoordig vaak gebeurt a.d.h.v. try en error. Het inzicht dat verworven is met dit kinetisch model, kan een duidelijke handleiding zijn inzake de gewenste katalysator eigenschappen. Deze kennis kan leiden tot een breder gebruik van ionenwisselaars als katalysator en kan tevens gebruikt worden voor de ontwikkeling en optimalisatie van industriële reactoren.

References

1. Ali, S.H., *Kinetics of Catalytic Esterification of Propionic Acid with Different Alcohols over Amberlyst 15.* International Journal of Chemical Kinetics, 2009. **41**(6): p. 432-448.
2. Dossin, T.F., M.F. Reyniers, R.J. Berger, and G.B. Marin, *Simulation of heterogeneously MgO-catalyzed transesterification for fine-chemical and biodiesel industrial production.* Applied Catalysis B-Environmental, 2006. **67**(1-2): p. 136-148.
3. Yadav, G.D. and M. Rahuman, *Cation-exchange resin-catalysed acylations and esterifications in fine chemical and perfumery industries.* Organic Process Research & Development, 2002. **6**(5): p. 706-713.
4. Tesser, R., L. Casale, D. Verde, M. Di Serio, and E. Santacesaria, *Kinetics and modeling of fatty acids esterification on acid exchange resins.* Chemical Engineering Journal, 2010. **157**(2-3): p. 539-550.
5. Russbueldt, B.M.E. and W.F. Hoelderich, *New sulfonic acid ion-exchange resins for the preesterification of different oils and fats with high content of free fatty acids.* Applied Catalysis a-General, 2009. **362**(1-2): p. 47-57.
6. Zielinska-Nadolska, I., K. Warmuzinski, and J. Richter, *Zeolite and other heterogeneous catalysts for the transesterification reaction of dimethyl carbonate with ethanol.* Catalysis Today, 2006. **114**(2-3): p. 226-230.
7. Ozbay, N., N. Oktar, and N.A. Tapan, *Esterification of free fatty acids in waste cooking oils (WCO): Role of ion-exchange resins.* Fuel, 2008. **87**(10-11): p. 1789-1798.
8. Chakrabarti, A. and M.M. Sharma, *Cationic Ion-Exchange Resins as Catalyst.* Reactive Polymers, 1993. **20**(1-2): p. 1-45.
9. Silva, V. and A.E. Rodrigues, *Kinetic studies in a batch reactor using ion exchange resin catalysts for oxygenates production: Role of mass transfer mechanisms.* Chemical Engineering Science, 2006. **61**(2): p. 316-331.
10. Ihm, S.K., J.H. Ahn, and Y.D. Jo, *Interaction of reaction and mass transfer in ion-exchange resin catalysts.* Industrial & Engineering Chemistry Research, 1996. **35**(9): p. 2946-2954.
11. Bozek-Winkler, E. and J. Gmehling, *Transesterification of methyl acetate and n-butanol catalyzed by Amberlyst 15.* Industrial & Engineering Chemistry Research, 2006. **45**(20): p. 6648-6654.
12. Saha, B. and M. Streat, *Transesterification of cyclohexyl acrylate with n-butanol and 2-ethylhexanol: acid-treated clay, ion exchange resins and tetrabutyl titanate as catalysts.* Reactive & Functional Polymers, 1999. **40**(1): p. 13-27.
13. Jimenez, L., A. Garvin, and J. Costa-Lopez, *The production of butyl acetate and methanol via reactive and extractive distillation. I. Chemical equilibrium, kinetics, and mass-transfer issues.* Industrial & Engineering Chemistry Research, 2002. **41**(26): p. 6663-6669.
14. Steinigeweg, S. and J. Gmehling, *Transesterification processes by combination of reactive distillation and pervaporation.* Chemical Engineering and Processing, 2004. **43**(3): p. 447-456.
15. Pappu, V.K.S., A.J. Yanez, L. Peereboom, E. Muller, C.T. Lira, and D.J. Miller, *A kinetic model of the Amberlyst-15 catalyzed transesterification of methyl stearate with n-butanol.* Bioresource Technology, 2011. **102**(5): p. 4270-4272.
16. Sanz, M.T., R. Murga, S. Beltran, J.L. Cabezas, and J. Coca, *Autocatalyzed and ion-exchange-resin-catalyzed esterification kinetics of lactic acid with methanol.* Industrial & Engineering Chemistry Research, 2002. **41**(3): p. 512-517.

17. Ali, S.H. and S.Q. Merchant, *Kinetics of the esterification of acetic acid with 2-propanol: Impact of different acidic cation exchange resins on reaction mechanism.* International Journal of Chemical Kinetics, 2006. **38**(10): p. 593-612.
18. Mazzotti, M., B. Neri, D. Gelosa, A. Kruglov, and M. Morbidelli, *Kinetics of liquid-phase esterification catalyzed by acidic resins.* Industrial & Engineering Chemistry Research, 1997. **36**(1): p. 3-10.
19. Popken, T., L. Gotze, and J. Gmehling, *Reaction kinetics and chemical equilibrium of homogeneously and heterogeneously catalyzed acetic acid esterification with methanol and methyl acetate hydrolysis.* Industrial & Engineering Chemistry Research, 2000. **39**(7): p. 2601-2611.
20. Song, W., G. Venimadhavan, J.M. Manning, M.F. Malone, and M.F. Doherty, *Measurement of residue curve maps and heterogeneous kinetics in methyl acetate synthesis.* Industrial & Engineering Chemistry Research, 1998. **37**(5): p. 1917-1928.

OUTLINE

With the exception of hydroelectricity and nuclear energy, the majority of the world's energy needs are supplied via fossil resources, such as coal, oil and natural gas. All these sources are inherently finite and at current usage rates will be consumed by the end of the this century [1]. The depletion of world petroleum reserves and increased environmental concern have stimulated recent interest in alternative sources for petroleum derivates.

Vegetable and animal oils and fats essentially consist of triglycerides from which the chains can be eliminated by transesterification with a light alcohol such as methanol. The resulting pool of fatty acid methyl esters potentially exhibits a wide variety of chain lengths, see Table 1, and saturation degrees and can, among other applications, be used as a fuel, i.e., biodiesel.

Table 1 **Chemical compositions of vegetable oil samples [2, 3]**

Vegetable oil	Fatty acid composition, wt%									Acid value[a]
	16:0	18:0	18:1	18:2	18:3	20:0	22:0	22:1	24:0	
Corn	11.7	1.9	25.2	60.6	0.48	0.2	0.0	0.0	0.0	0.11
Crambe	2.1	0.7	18.7	9.0	6.9	2.1	0.8	58.5	1.1	0.07
Rapeseed	3.5	0.9	64.1	22.3	8.2	0.0	0.0	0.0	0.0	1.14
Sunflower	6.4	2.9	17.7	72.9	0	0.0	0.0	0.0	0.0	0.15
Soybean	11.8	3.2	23.2	56.2	6.31	0.0	0.0	0.0	0.0	0.20

[a] Acid values are miligrams of KOH necessary to neutralize the free fatty acids in 1 g of oil

While conventional, petroleum derived diesel is composed of saturated and aromatic hydrocarbons, as a fuel, biodiesel has very similar physical properties with a few notable exceptions: biodiesel exhibits higher viscosity, higher lubricity and it does not contain sulfur or aromatic hydrocarbons. The advantages of biodiesel compared to other renewable products are numerous: it is a liquid fuel, it is readily available from vegetable and animal oil feedstocks, it is renewable and it is energy dense. As already indicated above, biodiesel is produced from triglycerides of vegetable or animal origin via a transesterification reaction. This chemical reaction is catalyzed by both acids and bases in a homogeneous or heterogeneous configuration. The use of heterogeneous catalysts instead of homogeneous ones potentially leads to lower production costs because catalyst separation and neutralization issues from the product are avoided and limited catalysts losses. Besides triglycerides, the

feedstock also contains free fatty acids that may lead to saponification of the base catalysts that are typically used. An acid catalyzed esterification of these free fatty acids prior to the base catalyzed transesterification of the triglycerides may help overcoming this potential limitation. Ion exchange resins can, due to their simple separation from the reaction products, the correspondingly easy reuse and their noncorrosive character, be effective catalysts for these (trans)esterification reactions.

The present work fits in an overall strategy for the adequate simulation of a two-stage, namely, (pre)esterification followed by a transesterification, fatty acid methyl ester manufacturing process, catalyzed by ion exchange resins. Additionally, the results of this work could be used for the improvement of the ethyl acetate process or the alternative Davy Process Technology (DPT) used for the conversion of esters to alcohols and vice versa [4]. Hence, in this work, an intensive study was performed to:

- determine the experimental effects, e.g. initial molar methanol to ethyl acetate ratio, temperature, on the transesterification catalyzed with the reference catalyst, c.q. a gel type resin, Lewatit K1221 (Chapter 3)
- determine the most adequate kinetic model to simulate the transesterification kinetics catalyzed by Lewatit K1221 (Chapter 3) and by Lewatit K2629, Lewatit K2640 and Amberlyst 15 (Chapter 4) and, correspondingly, to elucidate the reaction mechanism.
- evaluate the catalytic activity of macroporous resins, c.q. Lewatit K2629, Lewatit K2640 and Amberlyst 15, against the reference catalyst K1221 (Chapter 4)
- determine the experimental effects, e.g., initial molar methanol to acetic acid ratio, temperature, on the esterification catalyzed by the reference catalyst, c.q. Lewatit K1221 (Chapter 5).
- verify if the reaction mechanism for the transesterification can be extended to the esterification (Chapter 5).
- describe the reaction kinetics of the esterification catalyzed by Lewatit K1221 (Chapter 5) and by Lewatit K2629 and Amberlyst 15 (Chapter 6)

Prior to describing the procedures that were followed in this work (Chapter 2) as well as the experimental and modeling kinetics results (Chapter 3-6), the industrial and the alternative production processes of biodiesel, the structure and use of ion exchange resins as catalyst in general and in particular the experimental and kinetic studies of (trans)esterification catalyzed by ion exchange resins, are reviewed in the introduction (Chapter 1).

1. Aksoy, H.A., I. Becerik, F. Karaosmanoglu, H.C. Yatmaz, and H. Civelekoglu, *Utillzation prospects of Turkish raisin seed oil as an alternative engine fuel.* Fuel, 1990. **69**(5): p. 600-603.
2. Demirbas, A., *Biodiesel production from vegetable oils via catalytic and non-catalytic supercritical methanol transesterification methods.* Progress in Energy and Combustion Science, 2005. **31**(5-6): p. 466-487.
3. Ma, F. and M.A. Hanna, *Biodiesel production: a review.* Bioresource Technology, 1999. **70**(1): p. 1-15.
4. Miller, B., *Forestry to fuels: Biodiesel via Fischer Tropsch.* Appita Journal, 2013. **66**(2): p. 132-136.

1

INTRODUCTION

(Trans)esterification reactions with industrial production volumes ranging from a few hundred to thousand tonnes per year are commercially important. The significant expansion of the biodiesel production capacity in the last decade has reinforced the research interest in both reactions. The industrially employed biodiesel production process starting from vegetable oils/fats essentially comprises a base catalyzed transesterification using KOH or NaOH as homogeneous catalyst and methanol as the alcohol. The use of homogeneous catalysts leads to several well-known disadvantages. When the vegetable oil contains more than 2.5 % free fatty acids, soap is formed as undesired side reaction on the base catalyst. The use of waste oils, which typically exhibit a higher free fatty acids content, forces to investigate alternative biodiesel processes or additional pretreatment steps. The replacement of a homogeneous base catalyst by a solid acid one allows addressing these issues. Within the wide range of solid acid catalysts, acid ion exchange resins are promising as they are ecofriendly, noncorrosive and reusable [1-4]. Two different resin morphology types exist, i.e., gel and macroporous ones. The nature and type of the ion exchange resin, in addition to the conventional reaction conditions, strongly affect the time required to establish a targeted reactant conversion or product yield. The effectiveness of ion exchange resins as catalysts for (trans)esterification is proven in literature [5, 6]. The corresponding kinetics have been conceptualized and quantified by several authors [1, 7-20]. Nevertheless, the actual reaction mechanism is still under debate. Hence, the development of a physically realistic mechanism corresponding with a statistically significant kinetic model that is capable of reproducing the experimentally observed (trans)esterification behavior on acid ion exchange resins would be a useful tool aiming at an enhanced understanding of the reaction mechanism, resin selection and design as well as industrial reactor optimization [21-23].

1.1 Esters and (Trans)Esterification

Esters are of great significance for various industrial products. Fatty acid esters of glycerol, also known as triglycerides, are present in large quantities in fats and fatty oils. They are used predominantly in foods, but also as raw material especially in the production of

surfactants and biodiesel. Synthetic esters are of increasing importance in many applications, e.g., fibers, films, adhesives, and plastics or for specific uses such as solvents, extractants, plasticizers, lubricants additives, and lacquer bases. A variety of volatile esters are used as aromatic materials in perfumes, cosmetics and foods [9, 24].

Synthetic esters can be produced via esterification and transesterification [25].

Esterification is the chemical reaction between an acid and an alcohol, which results in the formation of the desired ester and water as condensation product, see Figure 1-1. The reaction is slow and must be catalyzed, typically by acids. Since esterification is a reversible reaction, ester yields can be enhanced, according to Le Chatelier's principle, by using a large excess of alcohol or by removing the water formed. The latter may be achieved via distillation or by chemical or adsorptive binding.

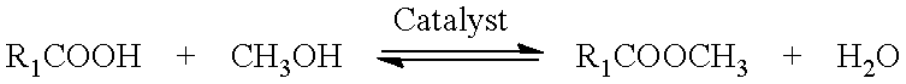

Figure 1-1 Esterification of free fatty acid (with R_1 = hydrocarbon chain ranging from 15 to 21 carbon atoms)

Transesterification comprises the displacement of the alcohol from an ester by another alcohol in a process similar to hydrolysis, except that an alcohol is used rather than water [26]. Transesterification reactions are also slow and need to be catalyzed by a strong acid or base [24, 26, 27]. Base catalyzed transesterification is reported to exhibit higher reaction rates than acid-catalyzed transesterification [28]. Transesterification is often used to tune the esters' boiling point or other physical properties by exchanging a long-chain alcohol group for a shorter one such as methanol. Transesterification can also be useful if direct esterification with the desired alcohol is technically difficult because of physical reasons e.g., high boiling point, low solubility or high viscosity. Polyester synthesis represents the largest scale implementation of transesterification reactions. Diesters react with diols to form macromolecules. E.g., poly-ethylene terephthalate is mainly produced via dimethyl terephthalate transesterification with ethylene glycol. The reverse reaction has already been used to recycle polyesters into their individual monomers. Another application of the transesterification is the conversion of triglycerides into biodiesel, see Figure 1-2. [24, 26, 27]

Methyl ester production from fatty acids and triglycerides out of waste cooking oil requires a two-step reaction process including both esterification as well as transesterification [29]. These fatty acid methyl esters are the main constituents of biodiesel.

The biodiesel history including the present-day status as well as an overview of the corresponding biodiesel production processes are given below.

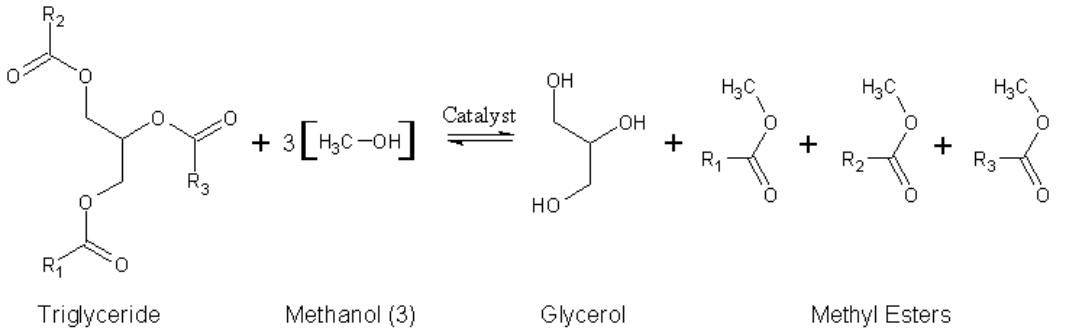

Figure 1-2 Transesterification of triglyceride (with R_1, R_2, R_3 = hydrocarbon chain ranging from 15 to 21 carbon atoms)

1.1.1 Biodiesel history and current situation

The diesel engine was invented by Otto Diesel in 1892. It was designed to run on a wide variety of fuels. Although Diesel demonstrated an engine running on peanut oil at the Paris Exhibition of 1900, the first commercially available diesel engines ran on kerosene. Due to their large size, diesel engines were first used in stationary applications such as general manufacturing or power generation. The first transportation vehicles making use of this new engine were ships in the 1900's. Diesel engines later appeared in trains in 1914 as a replacement of steam engines, but did not systematically replace the latter until World War II was finished. Diesel engines were first used in automobiles in 1924.

Otto Diesel was unquestionably a strong advocate for the use of renewable fuels such as seed oils. In 1912 he pronounced the prophetic words: "The use of vegetable oils for engine fuels may seem insignificant today, but such oils may become, in the course of time, as important as petroleum and the coal-tar products of the present times, … . Motive power can still be produced from the heat of the sun, always available, even when the natural stores of solid and liquid fuels are completely exhausted."

Despite the development of an almost total dependence on petroleum-derived diesel, the idea of using vegetable oil as an alternative source of diesel fuel was never abandoned. In 1937, a Belgian patent was granted to the University of Brussels for the use of palm oil ethyl esters, which would be described as a type of biodiesel today. The subsequent year, a commercial passenger bus operated between Brussels and Leuven running on palm-oil ethyl esters. The test was reported as a success. During World War II, vegetable oils were used as emergency fuels by various nations when normal supplies of petroleum-based fuels were

disrupted. But after the war, with the return of steady supplies of cheap petroleum oil, virtually all research on vegetable-oil fuels ceased [30].

The next resurgence of renewable fuels in history came during the oil crisis in 1973, when the members of Organization of Arab Petroleum Exporting Countries (OAPEC) announced a decision to raise the posted price of oil by 70% as well as a cut in production by five % and to continue to cut production over time with five % reductions until their economic and political objectives were met. In 1979, the revolution in Iran resulted in another global energy crisis. Oil prices again doubled, sending the industrial world into an economic tailspin. The price increases and the fuel shortages of the 1970s and early 1980s, spurred the interest in the development of alternate fuels around the world, which still continues today [31, 32]. Simultaneously the use of alternate fuels, such as biodiesel increases. Biodiesel is meant to be used in standard diesel engines in contrast to vegetable and waste oils that require tailor-made engines [33]. Biodiesel can be used in pure form, or blended with petroleum diesel in any ratio. Compared to conventional fossil fuels, biodiesel has many advantages such as high flash point, high cetane number, low viscosity, high lubricity, biodegradability, environmentally friendly due to less carbon monoxide emissions, as well as better emission profiles [34, 35]. The United States Environmental Protection Agency (EPA) published in February 2010 that biodiesel from soy oil results, on average, in a 57 % reduction of greenhouse gas emissions compared to petroleum diesel, and the biodiesel produced from waste grease even results in a 86 % reduction. Nevertheless, environmental organizations criticize the cultivation of plants, such as soy bean or sugar cane, for biodiesel production because of the (potential) competition with grounds for food production. It is, hence, clear that a meticulous balance needs to be pursued between agriculture, economic development, environment and general societal needs [26].

The European Union (EU-27) produced over 22 million tonnes of biodiesel in 2011 compared to 9.5 million tonnes in 2010, while the US approximately reached 3.7 million tonnes of biodiesel in 2011. Notwithstanding these differences, it is certain that the production volume of biodiesel shows an increasing trend in both the EU as well as the US [36]. This trend is only partially due to environmental and technological advantages of biodiesel. The greatest driving force originates from government legislation which forces or provides strong incentives for the use of biodiesel through tax reductions. These incentives are necessary because of the higher biodiesel cost with respect to petroleum diesel even at current petroleum prices. As a consequence, many research groups are spending significant efforts to reduce the biodiesel cost by improving the corresponding production processes

[37]. The steadily increasing interest in biodiesel may be testified by the increasing number of scientific articles and patents in the last five years [35]. By the end of 2005 563 articles were found on the topic "biodiesel" on Web of Science, at the end of 2010 there were 4 442 results, up to now the number increased to 10 505 (Figure 1-3).

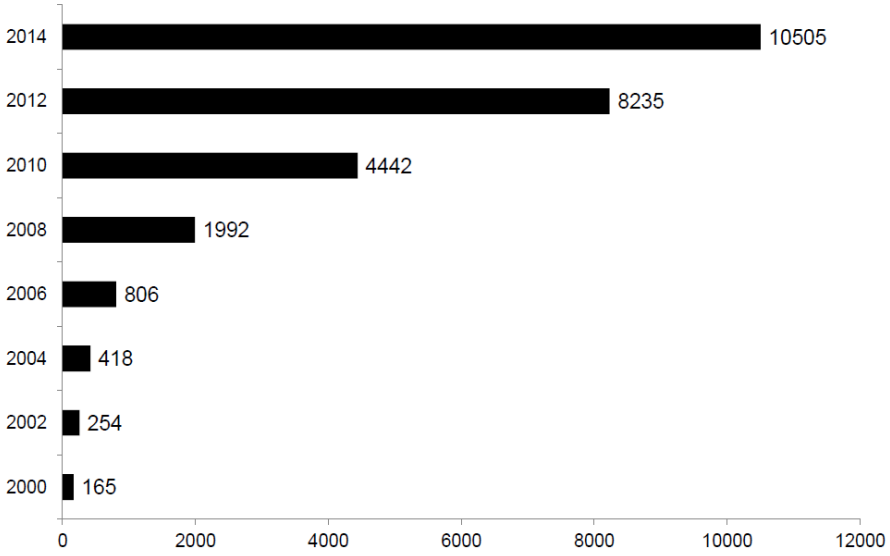

Figure 1-3 Number of articles on biodiesel since 2000 (Source: Web of Science)

1.2 Commercial biodiesel production

The most widely used industrial biodiesel production process from vegetable oils/fats is a base catalyzed transesterification using KOH or NaOH as homogeneous catalyst and methanol as the alcohol, see Figure 1-4 [28, 29, 38]. Besides methanol, other alcohols such as ethanol, propanol and butanol can be used. Nevertheless, methanol is commonly used because of its low price and availability [33]. Sodium or potassium hydroxide are commonly used as industrial catalysts, since they are relatively cheap and also very active.

As commented above, feeds such as vegetable oils or animal fats, chemically consist of triglycerides. These vegetable oils or fats usually also contain free fatty acids, phospholipids, sterols, water, odorants and other impurities. When present in too large quantities, e.g., a free fatty acid content exceeding 2.5 wt%, an adequate pretreatment, see Figure 1-4, such as degumming, pyrolysis and emulsification, is required [28, 39] prior to the actual transesterification. The substituents on the glycerol backbone in triglycerides typically differ, depending on the type of oil, with respect to the carbon chain length and the number, orientation and position of double bounds in these chains [26]. Different varieties of vegetable oils such as canola, corn, cramble, jatropha, palm kernel, sunflower, soybean and

coconut have been studied for biodiesel production [33]. In Europe and US, edible oils such as those obtained from rapeseed, sunflower and soybean are typically used for biodiesel production [38]. The chemical composition of these oils is given in Table 1.

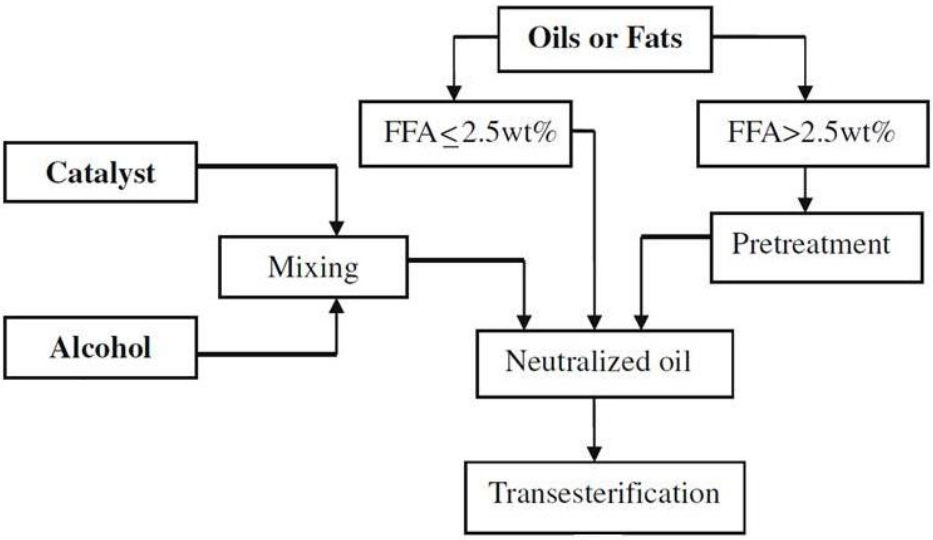

Figure 1-4 Simplified process flow chart of alkali-catalyzed biodiesel production [29]

A review by Ma and Hanna [31] summarized the dominant parameters in transesterification, c.q., the reaction temperature, the inlet alcohol to oil molar ratio, the catalyst type and concentration. The methyl ester yield increases with the reaction temperature. A yield of 98 % can be achieved with a homogeneous base catalyst at mild conditions, i.e., atmospheric pressure and 338 K [26]. However, if the temperature reaches the boiling point of methanol, a lack of methanol may develop in the liquid phase resulting in reduced reaction rates. The stoichiometrically required alcohol to oil ratio amounts to three moles of alcohol for one mole of oil. By using an alcohol excess, the methyl ester formation is favored. The optimal initial alcohol oil molar ratio is experimentally determined for several different catalysts, e.g. for KOH an initial molar ratio of 6:1 is required [33]. High free fatty acid feedstocks will react with the base catalyst to form soap, see Figure 1-5. As mentioned above, the soap formation is an undesirable side-reaction because it partially consumes the catalyst, decreases the biodiesel yield and complicates the separation and purification steps [28, 35]. The maximum amount of free fatty acids acceptable in a base catalyzed system is less than 2.5 %, and preferably less than 0.5 %, Figure 1-4 [29].

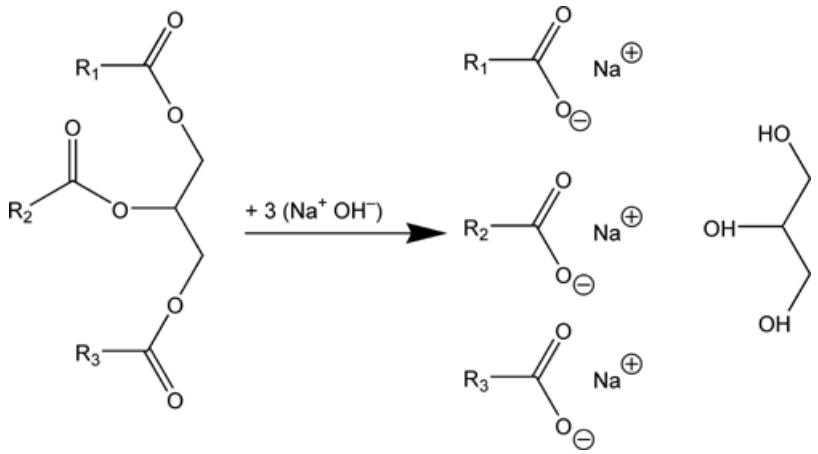

Figure 1-5 Saponification of a triglyceride with sodium hydroxide

The most elegant way to treat the free fatty acids (FFA) in a high FFA feedstock, is by esterifying them with methanol or ethanol and, hence, producing some additional fatty acid methyl esters. This acid catalyzed process can be used as pretreatment (two-step production) (Figure 1-4) or as direct method (one-step production). The acid catalyst can be sulfuric acid or acid ion exchange resins [39]. In the direct method, FFA can undergo an esterification simultaneously with the transesterification of triglycerides. In the two-step production process, the FFA esterification is followed by the base catalyzed transesterification [28, 29, 40]. Both processes and other alternative biodiesel production methods are discussed now.

1.3 Alternative biodiesel production methods

The advantages of the conventional biodiesel process is that a fast methyl ester production with yields exceeding 98 % can be achieved at mild conditions, i.e., atmospheric pressure and 338 K (Table 1-1) [26]. Some major disadvantages potentially jeopardize the widespread economical implementation of the conventional biodiesel production process:

(1) Operating problems related to the use of alkali hydroxides as a catalyst because they are hazardous.

(2) A significant number of washing and purification steps is required and produce a large amount of wastewater, which is environmentally unfavorable and requires appropriate treatment [31, 40].

(3) Difficult removal of the K/Na/Cl traces, mainly in the polar phase containing the glycerin.

(4) The price of the vegetable, edible oil feedstock, which accounts for 70 – 95 % of the total estimated production cost [40, 41].

Therefore, great economic advantage could be achieved if the commercial biodiesel plant has the inbuilt capacity to handle a variety of feedstocks with different qualities. The vegetable oils may originate from edible sources, non-edible sources, waste cooking oils, animal fats, algae, fungi etc. [40, 42-45]. For these reasons alternative methods or new catalysts for biodiesel production, are (being) developed [35, 40].

Table 1-1 Comparison of reaction conditions and performance of various types of catalysts to (trans)esterify various feedstocks into biodiesel [36, 40, 51]

Feedstock	Catalyst	Reaction conditions				Yield	Ref.
		T (°C)	MeOH:Oil (mol:mol)	Cat (wt.%)	t (h)	(%)	
Jatropa oil	KOH	50	6:1	1	2	97.1	[52]
Waste cooking oil	H_2SO_4	80	162:1	1.9	4	98.9	[53]
Castor oil	Li-CaO	65	12:1	1.5	0.75	> 99	[54]
Waste cooking oil	zinc stearate immobilized on silica gel	200	18:1	5.35	0.5	98.0	[55]
Yellow horn seed oil	Amberlite IR-900	60	8:1	5	1.5	96.3	[56]
Cottonseeed oil	*Candida antractica* lipase on macroporous resin	50	6:1	1.7	24	97.0	[57]
Jatropa oil	supercritical (pressure: 7 MPa)	250	24:1	0.8	0.5	90.5	[58]

1.3.1 Heterogeneously catalyzed processes

Biodiesel synthesis using solid catalysts instead of homogenous ones potentially leads to lower production costs because catalyst separation issues from the product are avoided [46], catalyst losses are limited [38, 47] and high grade glycerol is produced, a simple product separation and purification reduce the waste water amount [40]. Compared to homogeneously catalyzed transesterification, a higher initial methanol:oil ratio, catalyst loading and reaction temperature as well as longer reaction times are required to achieve comparable ester yields, see Table 1-1 [40]. However, the major disadvantages of heterogeneous compared to homogeneous catalysis are the lower reaction rates resulting from less effective catalysts and potential diffusion limitations in the three-phase (oil-alcohol-catalyst) reaction mixture [38, 47, 48]. Mass transfer issues in three-phase mixtures may be overcome by using a co-solvent such as tetrahydrofuran (THF), dimethyl sulfoxide (DMSO), n-hexane or ethanol, which enhance the miscibility of oil and methanol [29, 38].

Various heterogeneous catalysts for (non-)edible vegetable oils and fats transesterification have already been studied. The catalytic activity of a heterogeneous catalyst depends on its nature, specific surface area, pore size and volume, and active site concentration. Apart from recyclability and reusability, an ideal solid catalyst should exhibit a high stability, numerous strong, active sites, large pores, a hydrophobic surface and a low production cost [40, 49]. The catalytic performance could be improved by using catalyst supports with a higher specific surface area or by applying appropriate pretreatments to increase the catalyst acidity or basicity [40].

Generally, base catalysis is a better choice than acid catalysis in terms of reaction rate and biodiesel yield for oils with a lower FFA content. However, for oils with a higher FFA content, the solid acid catalyst's ability to simultaneously catalyze esterification and transesterification, represents an interesting alternative despite her/his lower transesterification activity [28, 33, 40, 50, 51]. However, in the acid catalyzed transesterification reaction the is the potential formation of acrolein out of glycerol deserves the necessary attention with respect to the glycerol quality.

An additional benefit of heterogeneous compared to homogeneous catalysis is the limited catalyst consumption. It has been reported that the production of 8000 tonnes of biodiesel, 88 tonnes of sodium hydroxide may be required [48], while 5.7 tonnes of solid supported MgO would be sufficient for the production of 100,000 tonnes of biodiesel [47].

Solid base catalysts

Conventional heterogeneous base catalysts, comprising either Lewis or Brønsted base sites, are the most extensively evaluated solid catalysts for the transesterification reactions of triglycerides. However, their industrial use is rather limited due to their high sensitivity to carbon dioxide, water and oxygen. In contrast with homogeneous catalysts, heterogeneous ones must be pretreated, e.g., washed with methanol and dried, washed with methanol and hexane followed by drying and calcination to activate the catalytic sites and remove adsorbed molecules [25, 39, 40].

Solid base catalysts can be classified into six categories according to Hattori:

(1) single metal oxides, e.g. MgO, CaO, La_2O_3, ZnO, BaO, SrO, …,

(2) mixed metal oxides, e.g. Al_2O_3-SnO, Al_2O_3-ZnO, $Ca_2Fe_2O_5$, $CaMgO_3$, …,

(3) zeolites, e.g. ETS-10, ETS-4, Zeolite X, …,

(4) supported alkali/alkaline earth metals, e.g. KF/Al_2O_3, KI/Al_2O_3, KNO_3/Al_2O_3, Li/CaO, …,

(5) hydrotalcites, e.g. Mg-Al hydrotalcites, Li-Al hydrotalcites, … and

(6) organic solid bases, e.g., guanidine-containing catalysts, PA306 as anion exchange resin with quaternary ammonium groups, … [59].

High oil conversion (>95%) and biodiesel yield, at optimal conditions have been reported when using solid base catalysts (Table 1-1) [36, 37, 40]. However their adverse effects on the activity in the presence of FFA, make it interesting to study the performance of solid acid catalysts for transesterification as well [37, 51, 59, 60].

Solid acid catalysts

Solid acid catalysts have been largely ignored for biodiesel synthesis due to pessimistic expectations in terms of reaction rates. However, solid acids, indeed, potentially deserve a place in the biodiesel synthesis [39]. Solid acid catalysts, such as acid ion exchange resins, superacid catalysts (tungstated and sulfated zirconia), polyaniline sulfate, heteropolyacid, pyrone complexes with metals, metal oxides (e.g. V_2O_5, Nb_2O_5, MoO_3, WO_3, Re_2O_7), zeolite, acid ionic liquid [60], differ in acidity, specific surface area, mechanical resistance, thermal and hydrothermal stability and production cost. Inorganic-oxide solid acids such as zeolites and niobic acid exhibit low acid site densities and readily lose their activities under harsh conditions, e.g., at temperatures above 373 K. Sulphated zirconia and tungstated zirconia, are efficient solid acid catalysts [61], but are expensive because zirconium is a rare and costly metal and high temperatures are required for the calcination and reactivation of the catalyst [60]. Strong acid ion exchange resins such as Amberlyst-15 and Nafion-NR50 have abundant sulfonic acid groups and show good catalytic activities [33, 50]. Nevertheless, compared to homogeneous acid catalysis, the initial methanol:oil molar ratio, the catalyst loading and the reaction time are much higher/longer to achieve comparable ester yields (Table 1-1) [40, 62, 63].

1.3.2 Enzyme-catalyzed processes

Although the enzyme based transesterification process is still not commercially developed, a number of studies have shown that enzyme catalysis is another option for biodiesel production. Lipase enzymes, e.g. *Candida antrctica* lipase, *Crypococcus* lipase, *Rhizopus oryzae* lipase, *Chromobacterium viscosum* lipase, *Rhizomucor miehei* lipase, immobilized or encapsulated are used as catalysts for both transesterification and esterification reactions with a high catalytic activity [35, 38, 64]. The reaction is generally carried out at more moderate conditions, i.e., 303 – 323 K, 4 – 30 % wt catalyst, and gives

high yields ranging from 74 to 99 % after 3.5 to 48 h (Table 1-1) [35, 65]. This simultaneously catalyzed (trans)esterification process can tolerate free fatty acids water without soap formation. Nevertheless, enzyme cost, immobilization, very slow reaction rates compared to base-catalyzed reaction systems and deactivation due to feed impurities currently compromise its commercial viability [33, 38, 40, 64, 66].

1.3.3 Supercritical processes

Supercritical transesterification is one of the most promising methods for biodiesel production from non-edible oils, as this process is very fast and does not require any catalyst [67]. Hence, there is no waste production from catalyst separation as well as an easier glycerol recovery [40]. The main disadvantages of supercritical conditions are the degradation of the esters at temperatures above 623 K and pressures exceeding 10 MPa, the high initial molar alcohol to oil ratio that is required, i.e., 42:1, and the high investment costs (Table 1-1). Some European production plants rely on this technology, but due to the high temperature and pressure requirements, it is equivalent with higher capital costs which inhibit its more widespread commercial implementation [29, 33, 38].

Recently, a novel two-step process has been proposed as a promising alternative to the one-step supercritical method. It consists of the hydrolysis of triglycerides in subcritical water, at 543 K, and the subsequent supercritical esterification of the produced and separated fatty acids in supercritical methanol or dimethyl carbonate. This allowed enhancing the fatty acid methyl ester (FAME) yield by 24 %, compared to the one-step supercritical methanol process. Also, a more valuable by-product, glyoxal, is produced instead of glycerol, which is not affected by the high FFA content [40, 68].

1.4 Catalysis by ion exchange resins

A large number of liquid reactions rely on homogeneous acid or base catalysis. In section 1.3.1, the use of acid ion exchange resins, as alternative catalysts for liquid phase (trans)esterification is proposed because they can be easily removed from the reaction medium, are noncorrosive, ecofriendly and they have good stability and reusability [5, 69, 70].

1.4.1 Ion exchange resins

An ion exchange material may be broadly defined as an insoluble matrix containing labile ions susceptible to exchange with ions in the surrounding medium without undergoing major structural changes [5, 69]. Ions can be exchanged for a stoichiometrically equivalent number of other ions of the same charge when the ion exchanger is in contact with an electrolyte solution. This ion exchange process is usually a reversible process. Ion exchange resembles sorption because in both cases, a dissolved species is taken up by a solid. The characteristic difference between the two phenomena is that ion exchange, in contrast to sorption, is a stoichiometric process in the sense that in sorption a solute is taken up without necessarily being replaced by another species [69].

In 1935 Adams and Holmes discovered the ion exchange properties of the condensation product of phenol and formaldehyde. This led to the synthesis of the first high-performance ion exchange resins [69]. Subsequently, numerous strong acid cation exchangers and weak base anion exchangers appeared in both Europe and the United States [71]. Finally, around 1969 – 1975, the use of ion exchange resins as catalysts has led to numerous examples that demonstrated their advantages as catalysts for chemical reactions involving organic substances. The reaction occurs in the pores of the ion exchange resin where the active sites are located [69]. The accessibility of the catalytically active sites depends on the porosity and the sorption properties of the resin [6].

Nowadays, there are strong and weak acid cation and strong and weak base anion exchangers commercially available that can be classified into two morphology types, gel and macroporous ones. The strong acid ion exchange resins, gel as well as macroporous, are the subject of this study. These resins are composed of styrene-polymers, crosslinked with divinylbenzene and sulfonic acid groups as functional groups or active sites, grafted on the benzene ring [4, 72], see Figure 1-6. The chemical, thermal and mechanical stability depend mainly on the structure and crosslinking degree of the polymer matrix and on the nature and number of the functional groups. Resins with a higher crosslinking degree are harder and more resistant to mechanical breakdown and attrition. The chemical and thermal stability of the resins is not unlimited. At temperatures slightly above 373 K, thermal hydrolysis takes place [69, 71]. Their thermal instability prohibits application to reactions that require higher temperatures [49, 71].

Although the chemical and thermal stability of gel and macroporous resins is comparable, their structure is different and will be discussed underneath.

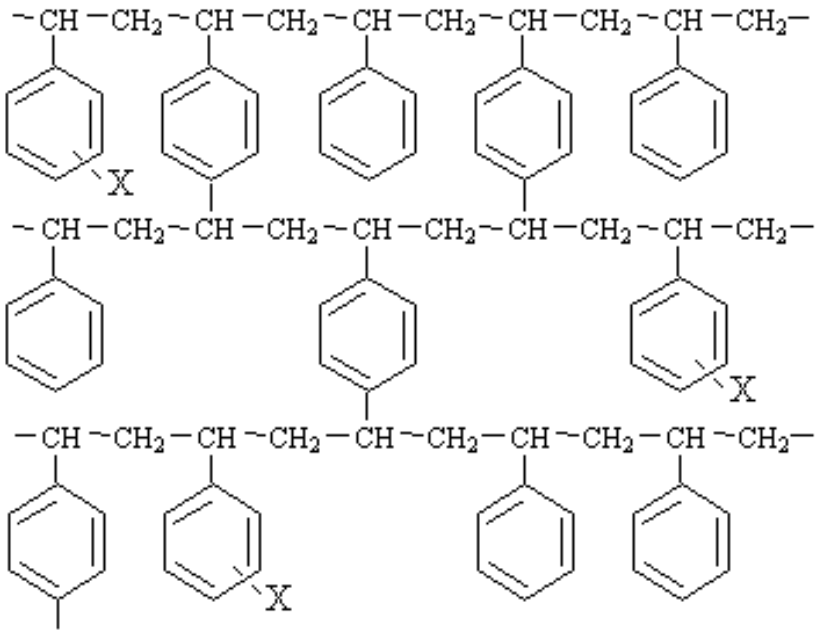

Figure 1-6 **Chemical structure of a polystyrene resin crosslinked by divinylbenzene. X represent possible active groups, for strong acid ion exchange resins X = SO_3H.**

Gel type resins

Gel type resins are hard glassy transparent resin beads which consist of a homogeneous matrix on a microscopic scale without discontinuities [5, 6], see Figure 1-7 (left). The matrix of a gel type resin can be seen as a network of elastic springs of polystyrene chains which are crosslinked with divinylbenzene. The crosslinker is more or less evenly distributed throughout the matrix. Because the polystyrene chains can perfectly align with each other, the 'pores' of such a resin in a dry state are extremely small with diameters below 0.1 nm. As a result, in dry state, a gel type resin has a very low specific surface area: typically below 10 $m^2\ g^{-1}$ as measured by BET. When the resin is placed in a polar solvent, the resin swells and the network is/polystyrene chains are stretched such that a pressure is exerted on the liquid contained in the pores. Hence, only in this swollen state, gel type resins exhibit pores with sizes in the micro- and small mesoporous range (up to 4 nm) [69, 73]. If the gel beads are dry, the polymer matrix collapses and the polymer chains are 'as close as atomic forces allow'. In this condition, unless the reactant is capable of swelling the matrix, the collapsed gel beads exhibit almost no catalytic activity because only the sites on the bead's external surface, which are insignificant in number compared to the total active sites within the body of the bead, are accessible to the reactants [5, 6, 69]. Therefore, the swelling ability by the reactants is a prerequisite for catalysis by gel resins.

The actual pore size decreases with the amount of divinylbenzene (DVB) because the swelling of the polymer structure gradually becomes more restricted. 12% DVB has been identified as the upper that can be used in gel type resins (<12%): too much DVB creates a structure with very small pores, which are no longer accessible for larger ions or molecules. To overcome this problem, macroporous resins, with a double porosity, the small pores of the matrix itself and the large macropores (several hundred nm) have been invented.

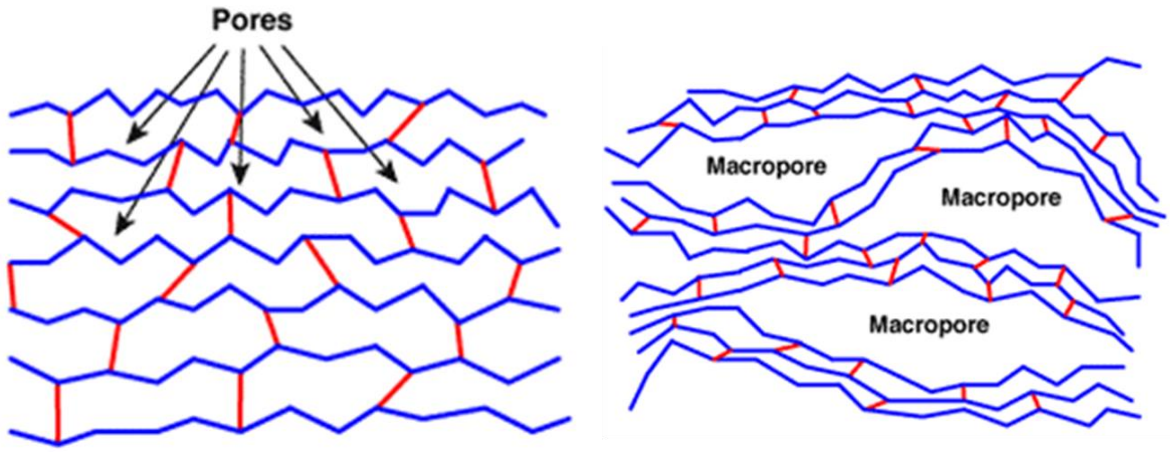

Figure 1-7 Macroscopic view of gel type resin (left) and macroporous resin (right).

Macroporous resin

Macroporous resins are hard opaque beads. These beads have a permanent macropore structure wherein small spherical gel particles are clustered, see Figure 1-7, right. This specific structure is obtained by incorporation, during the polymerisation, of a third component, called phase extender, in the reaction mixture. This phase extender, is an organic solvent, which is a good solvent for the monomers, but a poor solvent for the polymer. As polymerization progresses, the phase extender is squeezed out by the growing copolymer regions, and leaves macropores in the polymer structure [69]. Hence, the polymer matrix can be regarded as a conglomerate of permanent macropores and small gel particles. As a result, these macroporous resins have much higher specific surface areas in the dry state, typically ranging from ~50 to ~1000 $m^2\ g^{-1}$, and allow reactants to move more easily into the interior of the bead through these permanent macropores. Still, these small spherical gel particles are subjected to swelling when the resin is brought into a solvent This implies that, whereas gel resins can only function effectively as catalysts in a polar medium, macroporous resins are already quite effective in non-polar solvents, and, hence, are significantly expanding the application potential of resins as catalysts [5, 6, 69, 74, 75].

1.4.2 Swelling and catalytic properties of strong acid ion exchange resins

Swelling is of particular importance when using ion exchange resins. When a dry gel or macroporous resin is brought into contact with a solvent, the resin volume increases. This swelling due to solvent uptake exhibits features that can be referred to as adsorption or absorption and, hence, it will be described as 'sorption' [76]. The solvent is sorbed by the resin until equilibrium is reached with the liquid bulk phase. When, e.g., water diffuses into the resin, it interacts with its sulfonic acid sites, forms protonated water molecules and primary solvation shells. This solvation attracts additional water molecules into the gel phase and further extends the solvation shell. This phenomenon is observed at the macroscale as resin swelling, leading to e.g. a 55% volume increase of the macroporous Amberlyst 15 in methanol. [1, 7, 76, 77]. When dry resins are contacted with multicomponent mixtures, different components tend to sorb in a resin to a different extent [8, 77-80]. Sorption results in significant partitioning of the components between the bulk and the resin phase. This partitioning, like the resins' swelling, depends on the physicochemical characteristics of the components and the resin involved. These include not only the liquid phase composition and temperature but also the functional groups and the degree of crosslinking [5, 6, 8, 69].

The catalytic activity exhibited by ion exchange resins strongly depends on their swelling properties because the swelling capacity controls reactants accessibility to the acid sites and, therefore, affects their overall reactivity [49]. Theoretical models exist to calculate and describe the sorption and swelling behavior [76, 78].

1.4.3 Ion exchange resins as catalyst for (trans)esterification

As already mentioned, sulfonic acid ion exchange resins can be used as solid acid alternative for homogeneous catalysts. The use of ion exchange resins as catalysts for (trans)esterification, already reported in literature since 1995 [49, 81], is reviewed here.

Transesterification

The effectiveness of ion exchange resins as catalyst for transesterification was evidenced by a review of Chakrabarti and Sharma [5]. Several authors used ion exchange resins to catalyze the transesterification of triglycerides in vegetable oils and fats to fatty acid methyl esters (FAMEs). Vicente et al. [82] tested different types of catalysts, comprising

acids as well as bases, and homogeneous as well as heterogeneous ones, including Amberlyst 15 as sulfonic acid macroporous ion exchange resin, for the methyl ester synthesis from sunflower oil. The catalyst that showed the largest activity was NaOH, followed by MgO. The activity of the acid catalysts was negligible compared to the base ones. Nevertheless, Amberlyst 15, gave the highest activity of the studied heterogeneous acid catalysts [82]. López et al. [83] used perfluorinated-based Nafion®, gel and macroporous, ion exchange resins for the transesterification of triacetin with methanol. They concluded that the activity of the gel type resin strongly depends on the reactants' accessibility to the acid sites, and, hence, on the degree of swelling. The macroporous resin is less dependent of the swelling, and also more efficient use of the resin's active sites, i.e. unrestricted accessibility of the macropore active sites of the reacting molecules to the active sites [83]. Shibasaki-Kitakawa et al. [84] studied the transesterification of triolein with ethanol with one strong acid and various base ion exchange resins. The acid ion exchange resin scarcely consumed the reagent to the desired product, i.e. ethyl oleate, while the base ion exchange resins successfully catalyzed the transesterification reaction (conversions up to 80 % after 15 hours). They also concluded that the crosslinking degree of the resin, has a great effect on the catalytic activity [84].

Dos Reis et al. [85] compared three strong acid ion exchange resins, Amberlyst 15, Amberlyst 35 and Amberlyst 36, with sulfuric acid as catalysts for the transesterification of babassu oil and soybean vegetable oil. After 8 hours of reaction, the resins gave higher conversions than the sulfuric acid. This is, to our knowledge, the first study on the transesterification where the strong acid ion exchange resins outperform the homogenous catalysts.

Ion exchange resins were also studied in the transesterification of smaller esters. Zielinska-Nadolska et al. [3] proved that modified potassium carbonate, the strong acid gel type resin Lewatit K1221, and the superacidic Nafion SAC-13, gave the highest ethyl methyl carbonate yield in the transesterification of dimethyl carbonate with ethanol. Pappu et al. [20] used Amberlyst 15 as successful catalyst for the transesterification of methyl stearate with n-butanol. 90 % conversion was reached after 50 h with 4.8 wt% Amberlyst 15 at 363 K and an initial alcohol to ester molar ratio of 20:1. For the transesterification of methyl acetate with n-butanol, Bożek-Winkler and Gmehling [18] obtained a conversion of 62 % with 11.9 wt% Amberlyst 15 at 319.15 K and an initial molar ratio of 1:1.

Esterification

In literature a lot of ion exchange resin catalyzed esterification reactions can be found. In particular acetic acid esterification with methanol catalyzed by ion exchange resins was frequently investigated [7, 11, 19, 80, 86-88]. Acetic acid esterification was also performed with other alcohols with increasing the chain length. For ethanol, equilibrium was reached after 4 h with Amberlyst 15 [8]. For 2-propanol, a conversion of 57% with the gel type Dowex 50W8x-400 after 4 hours reaction at 343 K was observed [12]. Similar results were reported for dowex monosphere 650 C [89]. For butanol, ion exchange resins Smopex-101 and Amberlyst 15, gave conversions of 65 % after 6 h reaction at 348 K and were more effective than zeolites, sulphated zirconia and niobium acid [90]. For amyl alcohol, the gel type resin showed a higher activity than the macroporous one [91].

Also esterification with longer chain acids was studied extensively [13-15, 92, 93]. The esterification of free fatty acids (FFA) from several oils, is investigated by several research groups. Marchetti and Errazu [94] used a Dowex monosphere 550 resin for a successful FFA esterification of sunflower oil. Özbay et al. [4] investigated various strong acid ion exchange resins for the esterification of waste cooking oil and methanol, but the conversion of FFA was less than 50% for all resins after 3 h reaction at 333 K. Feng et al. [72] found a FFA conversion of ~90 % in an oil feedstock, which was generated from waste fried oil, with the strong acid ion exchange resin NKC-9. Russbueldt and Hoelderich [2] compared the catalytic activity of self-developed gel type strong acidic ion exchange resins with Amberlyst 15, for the esterification of free fatty acids. The catalytic performance of the gel type resin was superior over Amberlyst 15. They attributed this effect to the higher acid sites accessibility of the swollen gel type catalyst, while for the macroporous resins the reaction mainly occurs on the sulfonic acid groups on the outer surface of the small gel particles in the macropores. Nevertheless, several authors have reported that a non-negligible contribution to the esterification reactions, catalyzed by macroporous ion exchange resins, is made by the sulfonic acid groups in the swollen part of the small gel particles of the resin [8, 74, 78, 95].

In spite of the vast literature on esterification catalyzed by acid ion exchange resins, there is still no general agreement about the actual reaction mechanism and, more particularly about the resins' swelling, optimal reaction conditions selection, etc.

1.5 Kinetic modeling

Simulation models are essential tools for process design, optimization, control and trouble shooting. A general simulation model consists of a reactor model and a kinetic model. The reactor model accounts for the reactor type used, while the reaction or kinetic model describes the kinetics of the occurring chemical reactions. Commonly applied models to describe the kinetics of the (trans)esterification reaction catalyzed by ion exchange resins are the pseudo-homogeneous one (PH) and those based on Langmuir-Hinshelwood (LH) and Eley-Rideal (ER) type reaction mechanisms [96, 97]. The PH model considers the heterogeneous (trans)esterification as (quasi)-homogeneous and, hence, is similar to the power-law model for homogeneous reactions without adsorption terms for any of the species. In an Eley-Rideal mechanism one of the reactants is adsorbed and reacts with the other reactant from the bulk, to form an adsorbed product and a product in the bulk. A Langmuir Hinshelwood mechanism is applicable when both reactants and products are adsorbed on a catalytically active site. After the reaction step both products are desorbed from the active site of the catalyst.

The models used in the literature to describe the (trans)esterification kinetics, catalyzed by ion exchange resins, are discussed in next sections.

1.5.1 Transesterification

Pseudo-homogeneous (PH) and adsorption-based mechanisms, which include Eley-Rideal (ER) and Langmuir-Hinshelwood (LH) mechanisms, have been used to describe the heterogeneously catalyzed transesterification. Saha and Streat [16] have evaluated different heterogeneous acid catalysts, including gel and macroporous ion exchange resins, for cyclohexyl acrylate transesterification with n-butanol and 2-ethylhexanol. The experimental results were best described by a kinetic model based on a Langmuir-Hinshelwood mechanism. Jimenez et al. [17] studied the transesterification of n-butyl acetate and methanol catalyzed by the macroporous ion exchange resin Amberlyst 15 and found the pseudo-homogeneous model as the best description for the experimental data. Pappu et al. [20] assumed the pseudo-homogeneous system to describe successfully the experimental data of the Amberlyst 15 catalyzed transesterification of methyl stearate with n-butanol. Bożek-Winkler and Gmehling [18] and Steinigeweg and Gmehling [19] studied the kinetic behavior of the reaction of methyl acetate and butanol catalyzed by the ion exchange resin Amberlyst

15. Two different kinetic models, pseudo-homogeneous and Langmuir-Hinshelwood, were used to describe the reaction rate. The simpler pseudo-homogeneous model provided similar results as the Langmuir-Hinshelwood model [18].

In general the simpler pseudo-homogeneous model seems to be mostly preferred over the adsorption based models, c.q. LH and ER, to describe the experimental data for the transesterification catalyzed by gel and macroporous resins. Nevertheless, a pseudo-homogeneous model does not give insight into the actual reaction mechanism for the heterogeneously catalyzed transesterification reaction, because it lacks any adsorption effects or does not take swelling phenomena into account. Hence more advanced models are required when assessing the kinetics on a series of ion exchange resins with varying properties as (trans)esterification catalysts. This will be discussed in detail in Chapter 4. To our knowledge, an actual reaction mechanism for the ion exchange resin catalyzed transesterification is not known yet.

1.5.2 Esterification

Esterification catalyzed by ion exchange resins has also been conceptualized and quantified by a pseudo-homogeneous model (PH), as well as by models including adsorption phenomena via an Eley-Rideal (ER) or a Langmuir-Hinshelwood (LH) mechanisms [7-9, 11-13]. Also more advanced models have already been developed where resin swelling is accounted for [1, 7, 8]. The pseudo-homogeneous model is due to its simple mathematical expression frequently used especially for the free fatty acid esterification reactions [2, 13-15, 92].

For smaller molecules, adsorption based models, such as ER and LH are frequently discussed. The Eley-Rideal reaction mechanism where a protonated acid reacts with alcohol from the bulk, is proposed by Liu et al. [86] and by Bart et al. [89] to describe the acetic acid esterification with methanol and propanol respectively. Water, formed in the esterification, has a strong affinity for the sulfonic acid groups of the resin. This is also observed by the strong swelling of the resins in water, as mentioned in section 1.4.2. Because of this high affinity, several researchers [12, 91, 98] mathematically optimized the Langmuir-Hinshelwood reaction rate equation, by introducing an empirical correction factor α. To describe the propionic acid esterification with different alcohols such as methanol, ethanol and 1-butanol, using the macroporous acid exchange resin Amberlyst 15 in a fixed-bed plug

flow reactor. Ali et al. [9] used a modified Langmuir-Hinshelwood based model, developed by Pöpken et al. [53], with each adsorption term of the denominator divided by the molar mass of the component *i*. Moreover, Ali et al. described the esterification kinetics catalyzed by gel type resins [12] with the modified LH model with the correction factor α, while for the macroporous resin, they proposed the model derived from the LH model and published by Pöpken et al. [7]. No physicochemical meaning was given for these differences. Nevertheless, within a relative error, the LH or the by Pöpken et al.[7] published modified LH model, could also be used to describe the reaction kinetics the gel and macroporous resins.

In contrast to the transesterification, several authors found that the classic adsorption-based models, such as ER and LH, were not sufficient to describe the reaction kinetics catalyzed by ion exchange resins [1, 8]. Therefore, advanced models, which take into account the swelling, were developed. Sainio et al. [78] calculated the thermodynamic equilibrium between solvent mixtures and ion exchange resins based on the original Flory-Huggins theory. Mazzotti et al. [8] showed that this Flory-Huggins model successfully described the acetic acid esterification with ethanol catalyzed by Amberlyst 15. Tesser et al. [1] accounted for swelling in their ER model, by the use of a physical phase equilibrium, c.q. partitioning, for each component between the bulk liquid and the resin phase. Nevertheless, they suppose an ideal behavior of the components in the bulk liquid and in the resin phase This model successfully described the FFA esterification catalyzed by the macroporous resin Amberlyst 15. Ihm et al. [99] found that for the macroporous resin catalyzed esterification of phenol and acetic acid, the conversion increased with the resins' swelling capability. It was, hence, concluded that the reactant molecules can move more easily into the swollen gel particle, and that the reaction occurs also on the internal functional groups.

The literature is not clear about the best kinetic model to describe the esterification kinetics. Several authors investigated the same reaction and published different kinetic models. Moreover, the differences between the catalytic performance of gel and macroporous resins for esterification, although both are sulfonic acid catalysts, are, to our knowledge, not thoroughly investigated yet.

1.6 Scope of the thesis

The goal of this PhD thesis is to explore the potential of ion exchange resins as catalysts for (trans)esterification reactions. To this purpose the (trans)esterification has been performed on a selection of gel and macroporous resins. In order to gain an adequate insight in the corresponding reaction mechanisms, both for gel and macroporous resins, model components have been investigated rather than real feeds. E.g., for transesterification, ethyl acetate and methanol have been selected whereas for esterification, acetic acid was used together with methanol. These low-molecular-weight carboxylic reagents have been chosen because of their simplicity, availability and ease of product analysis. This fundamental approach will provide more easy access to the dominant factors and phenomena in (trans)esterification kinetics. A better understanding with respect to the use and the selection of ion exchange resins as catalysts for the (trans)esterification is pursued. Extrapolations from model molecules to longer chains have been published by Srilatha et al. [100] and Alonso et al. [101]. Hence, this research can also form a sound basis for the improvement of the industrial ethyl acetate and biodiesel production processes using ion exchange resins as catalyst.

After having introduced the procedures in Chapter 2, Chapter 3 discusses the development of a reaction mechanism for the transesterification catalyzed by the gel type resin Lewatit K1221, which was selected as benchmark resin. Several reaction mechanisms, based on the pseudo-homogeneous, the Eley-Rideal and the Langmuir-Hinshelwood model were discriminated against each other. The reaction mechanism as developed for the gel type resin, Lewatit K1221, catalyzed transesterification reaction in Chapter 3 is further extended towards various macroporous ion exchange resins in Chapter 4, where, in particular, swelling related effects were assessed. Subsequently the esterification kinetics are explored on the benchmark Lewatit K1221 in Chapter 5. Due to the chemical similarity between the transesterification and the esterification, we assume that the esterification kinetics modeling could build upon the experience gained from the transesterification kinetics modeling. Also for esterification the kinetics have been investigated on an alternative series of resins in Chapter 6. The general conclusions are given in Chapter 7.

1.7 References

1. Tesser, R., L. Casale, D. Verde, M. Di Serio, and E. Santacesaria, *Kinetics and modeling of fatty acids esterification on acid exchange resins.* Chemical Engineering Journal, 2010. **157**(2-3): p. 539-550.
2. Russbueldt, B.M.E. and W.F. Hoelderich, *New sulfonic acid ion-exchange resins for the preesterification of different oils and fats with high content of free fatty acids.* Applied Catalysis a-General, 2009. **362**(1-2): p. 47-57.
3. Zielinska-Nadolska, I., K. Warmuzinski, and J. Richter, *Zeolite and other heterogeneous catalysts for the transesterification reaction of dimethyl carbonate with ethanol.* Catalysis Today, 2006. **114**(2-3): p. 226-230.
4. Ozbay, N., N. Oktar, and N.A. Tapan, *Esterification of free fatty acids in waste cooking oils (WCO): Role of ion-exchange resins.* Fuel, 2008. **87**(10-11): p. 1789-1798.
5. Chakrabarti, A. and M.M. Sharma, *Cationic Ion-Exchange Resins as Catalyst.* Reactive Polymers, 1993. **20**(1-2): p. 1-45.
6. Coutinho, F.M.B., S.M. Rezende, and B.G. Soares, *Characterization of sulfonated poly(styrene-divinylbenzene) and poly(divinylbenzene) and its application as catalysts in esterification reaction.* Journal of Applied Polymer Science, 2006. **102**(4): p. 3616-3627.
7. Popken, T., L. Gotze, and J. Gmehling, *Reaction kinetics and chemical equilibrium of homogeneously and heterogeneously catalyzed acetic acid esterification with methanol and methyl acetate hydrolysis.* Industrial & Engineering Chemistry Research, 2000. **39**(7): p. 2601-2611.
8. Mazzotti, M., B. Neri, D. Gelosa, A. Kruglov, and M. Morbidelli, *Kinetics of liquid-phase esterification catalyzed by acidic resins.* Industrial & Engineering Chemistry Research, 1997. **36**(1): p. 3-10.
9. Ali, S.H., *Kinetics of Catalytic Esterification of Propionic Acid with Different Alcohols over Amberlyst 15.* International Journal of Chemical Kinetics, 2009. **41**(6): p. 432-448.
10. Ali, S.H. and S.Q. Merchant, *Kinetic Study of Dowex 50 Wx8-Catalyzed Esterification and Hydrolysis of Benzyl Acetate.* Industrial & Engineering Chemistry Research, 2009. **48**(5): p. 2519-2532.
11. Song, W., G. Venimadhavan, J.M. Manning, M.F. Malone, and M.F. Doherty, *Measurement of residue curve maps and heterogeneous kinetics in methyl acetate synthesis.* Industrial & Engineering Chemistry Research, 1998. **37**(5): p. 1917-1928.
12. Ali, S.H. and S.Q. Merchant, *Kinetics of the esterification of acetic acid with 2-propanol: Impact of different acidic cation exchange resins on reaction mechanism.* International Journal of Chemical Kinetics, 2006. **38**(10): p. 593-612.
13. Sanz, M.T., R. Murga, S. Beltran, J.L. Cabezas, and J. Coca, *Autocatalyzed and ion-exchange-resin-catalyzed esterification kinetics of lactic acid with methanol.* Industrial & Engineering Chemistry Research, 2002. **41**(3): p. 512-517.
14. Sanz, M.T., R. Murga, S. Beltran, J.L. Cabezas, and J. Coca, *Kinetic study for the reactive system of lactic acid esterification with methanol: Methyl lactate hydrolysis reaction.* Industrial & Engineering Chemistry Research, 2004. **43**(9): p. 2049-2053.
15. Delgado, P., M.T. Sanz, and S. Beltran, *Kinetic study for esterification of lactic acid with ethanol and hydrolysis of ethyl lactate using an ion-exchange resin catalyst.* Chemical Engineering Journal, 2007. **126**(2-3): p. 111-118.

16. Saha, B. and M. Streat, *Transesterification of cyclohexyl acrylate with n-butanol and 2-ethylhexanol: acid-treated clay, ion exchange resins and tetrabutyl titanate as catalysts.* Reactive & Functional Polymers, 1999. **40**(1): p. 13-27.
17. Jimenez, L., A. Garvin, and J. Costa-Lopez, *The production of butyl acetate and methanol via reactive and extractive distillation. I. Chemical equilibrium, kinetics, and mass-transfer issues.* Industrial & Engineering Chemistry Research, 2002. **41**(26): p. 6663-6669.
18. Bozek-Winkler, E. and J. Gmehling, *Transesterification of methyl acetate and n-butanol catalyzed by Amberlyst 15.* Industrial & Engineering Chemistry Research, 2006. **45**(20): p. 6648-6654.
19. Steinigeweg, S. and J. Gmehling, *Transesterification processes by combination of reactive distillation and pervaporation.* Chemical Engineering and Processing, 2004. **43**(3): p. 447-456.
20. Pappu, V.K.S., A.J. Yanez, L. Peereboom, E. Muller, C.T. Lira, and D.J. Miller, *A kinetic model of the Amberlyst-15 catalyzed transesterification of methyl stearate with n-butanol.* Bioresource Technology, 2011. **102**(5): p. 4270-4272.
21. Choudhury, I.R., K. Hayasaka, J.W. Thybaut, C.S.L. Narasimhan, J.F. Denayer, J.A. Martens, and G.B. Marin, *Pt/H-ZSM-22 hydroisomerization catalysts optimization guided by Single-Event MicroKinetic modeling.* Journal of Catalysis, 2012. **290**: p. 165-176.
22. Caruthers, J.M., J.A. Lauterbach, K.T. Thomson, V. Venkatasubramanian, C.M. Snively, A. Bhan, S. Katare, and G. Oskarsdottir, *Catalyst design: knowledge extraction from high-throughput experimentation.* Journal of Catalysis, 2003. **216**(1-2): p. 98-109.
23. Katare, S., J.M. Caruthers, W.N. Delgass, and V. Venkatasubramanian, *An intelligent system for reaction kinetic modeling and catalyst design.* Industrial & Engineering Chemistry Research, 2004. **43**(14): p. 3484-3512.
24. Riemenschneider, W. and H.M. Bolt, *Esters, Organic*, in *Ullmann's Encyclopedia of Industrial Chemistry*. 2000, Wiley-VCH Verlag GmbH & Co. KGaA.
25. Dossin, T.F., M.F. Reyniers, and G.B. Marin, *Kinetics of heterogeneously MgO-catalyzed transesterification.* Applied Catalysis B-Environmental, 2006. **62**(1-2): p. 35-45.
26. Meher, L.C., D. Vidya Sagar, and S.N. Naik, *Technical aspects of biodiesel production by transesterification—a review.* Renewable and Sustainable Energy Reviews, 2006. **10**(3): p. 248-268.
27. Ali, S.H., O. Al-Rashed, F.A. Azeez, and S.Q. Merchant, *Potential biofuel additive from renewable sources - Kinetic study of formation of butyl acetate by heterogeneously catalyzed transesterification of ethyl acetate with butanol.* Bioresource Technology, 2011. **102**(21): p. 10094-10103.
28. Leung, D.Y.C., X. Wu, and M.K.H. Leung, *A review on biodiesel production using catalyzed transesterification.* Applied Energy, 2010. **87**(4): p. 1083-1095.
29. Van Gerpen, J., B. Shanks, R. Pruszko, D. Clements, and G. Knothe, *Biodiesel Production Technology.* National Renewable Energy Laboratory, 1617 Cole Boulevard, Golden, CO, 2004.
30. Pahl, G., *Biodiesel: Growing a New Energy Economy*. 2008: Chelsea Green Publishing Company.
31. Ma, F. and M.A. Hanna, *Biodiesel production: a review.* Bioresource Technology, 1999. **70**(1): p. 1-15.

32. Vicente, G., M. Martínez, and J. Aracil, *Integrated biodiesel production: a comparison of different homogeneous catalysts systems.* Bioresource Technology, 2004. **92**(3): p. 297-305.
33. Zabeti, M., W.M.A. Wan Daud, and M.K. Aroua, *Activity of solid catalysts for biodiesel production: A review.* Fuel Processing Technology, 2009. **90**(6): p. 770-777.
34. Dorado, M.P., E. Ballesteros, J.M. Arnal, J. Gomez, and F.J. Lopez, *Exhaust emissions from a Diesel engine fueled with transesterified waste olive oil.* Fuel, 2003. **82**(11): p. 1311-1315.
35. Pinto, A.C., L.L.N. Guarieiro, M.J.C. Rezende, N.M. Ribeiro, E.A. Torres, W.A. Lopes, P.A.D. Pereira, and J.B. de Andrade, *Biodiesel: An overview.* Journal of the Brazilian Chemical Society, 2005. **16**(6B): p. 1313-1330.
36. Nurfitri, I., G.P. Maniam, N. Hindryawati, M.M. Yusoff, and S. Ganesan, *Potential of feedstock and catalysts from waste in biodiesel preparation: A review.* Energy Conversion and Management, 2013. **74**: p. 395-402.
37. Di Serio, M., R. Tesser, L. Pengmei, and E. Santacesaria, *Heterogeneous catalysts for biodiesel production.* Energy & Fuels, 2008. **22**(1): p. 207-217.
38. Semwal, S., A.K. Arora, R.P. Badoni, and D.K. Tuli, *Biodiesel production using heterogeneous catalysts.* Bioresource Technology, 2011. **102**(3): p. 2151-2161.
39. Lotero, E., J.G. Goodwin, D.A. Bruce, K. Suwannakarn, Y.J. Liu, and D.E. Lopez, *The Catalysis of Biodiesel Synthesis*, in *Catalysis, Vol 19*, J.J. Spivey and K.M. Dooley, Editors. 2006, Royal Soc Chemistry: Cambridge. p. 41-83.
40. Bankovic-Ilic, I.B., O.S. Starnenkovic, and V.B. Veljkovic, *Biodiesel production from non-edible plant oils.* Renewable & Sustainable Energy Reviews, 2012. **16**(6): p. 3621-3647.
41. Haas, M.J., A.J. McAloon, W.C. Yee, and T.A. Foglia, *A process model to estimate biodiesel production costs.* Bioresource Technology, 2006. **97**(4): p. 671-678.
42. Canakci, M., *The potential of restaurant waste lipids as biodiesel feedstocks.* Bioresource Technology, 2007. **98**(1): p. 183-190.
43. Karmee, S.K. and A. Chadha, *Preparation of biodiesel from crude oil of Pongamia pinnata.* Bioresource Technology, 2005. **96**(13): p. 1425-1429.
44. Granados, M.L., M.D.Z. Poves, D.M. Alonso, R. Mariscal, F.C. Galisteo, R. Moreno-Tost, J. Santamaria, and J.L.G. Fierro, *Biodiesel from sunflower oil by using activated calcium oxide.* Applied Catalysis B-Environmental, 2007. **73**(3-4): p. 317-326.
45. Ji, J.B., J.L. Wang, Y.C. Li, Y.L. Yu, and Z.C. Xu, *Preparation of biodiesel with the help of ultrasonic and hydrodynamic cavitation.* Ultrasonics, 2006. **44**: p. E411-E414.
46. Suppes, G.J., M.A. Dasari, E.J. Doskocil, P.J. Mankidy, and M.J. Goff, *Transesterification of soybean oil with zeolite and metal catalysts.* Applied Catalysis a-General, 2004. **257**(2): p. 213-223.
47. Dossin, T.F., M.F. Reyniers, R.J. Berger, and G.B. Marin, *Simulation of heterogeneously MgO-catalyzed transesterification for fine-chemical and biodiesel industrial production.* Applied Catalysis B-Environmental, 2006. **67**(1-2): p. 136-148.
48. Mbaraka, I.K., K.J. McGuire, and B.H. Shanks, *Acidic mesoporous silica for the catalytic conversion of fatty acids in beef tallow.* Industrial & Engineering Chemistry Research, 2006. **45**(9): p. 3022-3028.
49. Lotero, E., Y.J. Liu, D.E. Lopez, K. Suwannakarn, D.A. Bruce, and J.G. Goodwin, *Synthesis of biodiesel via acid catalysis.* Industrial & Engineering Chemistry Research, 2005. **44**(14): p. 5353-5363.
50. Furuta, S., H. Matsuhashi, and K. Arata, *Biodiesel fuel production with solid superacid catalysis in fixed bed reactor under atmospheric pressure.* Catalysis Communications, 2004. **5**(12): p. 721-723.

51. Atadashi, I.M., M.K. Aroua, A.R.A. Aziz, and N.M.N. Sulaiman, *The effects of catalysts in biodiesel production: A review.* Journal of Industrial and Engineering Chemistry, 2013. **19**(1): p. 14-26.
52. Berchmans, H.J., K. Morishita, and T. Takarada, *Kinetic Study of Methanolysis of Jatropha Curcas-Waste Food Oil Mixture.* Journal of Chemical Engineering of Japan, 2010. **43**(8): p. 661-670.
53. Wang, Y., S.Y. Ou, P.Z. Liu, F. Xue, and S.Z. Tang, *Comparison of two different processes to synthesize biodiesel by waste cooking oil.* Journal of Molecular Catalysis a-Chemical, 2006. **252**(1-2): p. 107-112.
54. Kumar, D. and A. Ali, *Nanocrystalline Lithium Ion Impregnated Calcium Oxide As Heterogeneous Catalyst for Transesterification of High Moisture Containing Cotton Seed Oil.* Energy & Fuels, 2010. **24**: p. 2091-2097.
55. Jacobson, K., R. Gopinath, L.C. Meher, and A.K. Dalai, *Solid acid catalyzed biodiesel production from waste cooking oil.* Applied Catalysis B-Environmental, 2008. **85**(1-2): p. 86-91.
56. Li, J., Y.J. Fu, X.J. Qu, W. Wang, M. Luo, C.J. Zhao, and Y.G. Zu, *Biodiesel production from yellow horn (Xanthoceras sorbifolia Bunge.) seed oil using ion exchange resin as heterogeneous catalyst.* Bioresource Technology, 2012. **108**: p. 112-118.
57. Royon, D., M. Daz, G. Ellenrieder, and S. Locatelli, *Enzymatic production of biodiesel from cotton seed oil using t-butanol as a solvent.* Bioresource Technology, 2007. **98**(3): p. 648-653.
58. Tang, Z.Y., L.Y. Wang, and J.C. Yang, *Transesterification of the crude Jatropha curcas L. oil catalyzed by micro-NaOH in supercritical and subcritical methanol.* European Journal of Lipid Science and Technology, 2007. **109**(6): p. 585-590.
59. Lee, D.W., Y.M. Park, and K.Y. Lee, *Heterogeneous Base Catalysts for Transesterification in Biodiesel Synthesis.* Catalysis Surveys from Asia, 2009. **13**(2): p. 63-77.
60. Sharma, Y.C., B. Singh, and J. Korstad, *Advancements in solid acid catalysts for ecofriendly and economically viable synthesis of biodiesel.* Biofuels Bioproducts & Biorefining-Biofpr, 2011. **5**(1): p. 69-92.
61. Kiss, A.A., A.C. Dimian, and G. Rothenberg, *Solid acid catalysts for biodiesel production - Towards sustainable energy.* Advanced Synthesis & Catalysis, 2006. **348**(1-2): p. 75-81.
62. Canakci, M. and J. Van Gerpen, *Biodiesel production via acid catalysis.* Transactions of the Asae, 1999. **42**(5): p. 1203-1210.
63. Freedman, B., E.H. Pryde, and T.L. Mounts, *Variables affecting the yields of Fatty Esters from transesterified vegetable-oils.* Journal of the American Oil Chemists Society, 1984. **61**(10): p. 1638-1643.
64. Fjerbaek, L., K.V. Christensen, and B. Norddahl, *A Review of the Current State of Biodiesel Production Using Enzymatic Transesterification.* Biotechnology and Bioengineering, 2009. **102**(5): p. 1298-1315.
65. Shimada, Y., Y. Watanabe, A. Sugihara, and Y. Tominaga, *Enzymatic alcoholysis for biodiesel fuel production and application of the reaction to oil processing.* Journal of Molecular Catalysis B-Enzymatic, 2002. **17**(3-5): p. 133-142.
66. Demirbas, A., *Biodiesel production from vegetable oils via catalytic and non-catalytic supercritical methanol transesterification methods.* Progress in Energy and Combustion Science, 2005. **31**(5-6): p. 466-487.

67. Minami, E. and S. Saka, *Kinetics of hydrolysis and methyl esterification for biodiesel production in two-step supercritical methanol process.* Fuel, 2006. **85**(17-18): p. 2479-2483.
68. Kusdiana, D. and S. Saka, *Two-step preparation for catalyst-free biodiesel fuel production - Hydrolysis and methyl esterification.* Applied Biochemistry and Biotechnology, 2004. **113**: p. 781-791.
69. Helfferich, F.G., *Ion Exchange*. 1995: Dover Publications.
70. Van de Steene, E., J. De Clercq, and J.W. Thybaut, *Adsorption and reaction in the transesterification of ethyl acetate with methanol on Lewatit K1221.* Journal of Molecular Catalysis A: Chemical, 2012. **359**(0): p. 57-68.
71. Abrams, I.M. and J.R. Millar, *A history of the origin and development of macroporous ion-exchange resins.* Reactive & Functional Polymers, 1997. **35**(1-2): p. 7-22.
72. Feng, Y.H., B.Q. He, Y.H. Cao, J.X. Li, M. Liu, F. Yan, and X.P. Liang, *Biodiesel production using cation-exchange resin as heterogeneous catalyst.* Bioresource Technology, 2010. **101**(5): p. 1518-1521.
73. Oancea, A.M.S., C. Drinkal, and W. Hoell, *Evaluation of exchange equilibria on strongly acidic ion exchangers with gel-type, macroporous and macronet structure.* Reactive & Functional Polymers, 2008. **68**(2): p. 492-506.
74. Martinec, A., K. Setinek, and L. Beranek, *Effect of cross-linking on catalytic properties of macroporous styrene-divinylbenzene ion-exchangers.* Journal of Catalysis, 1978. **51**(1): p. 86-95.
75. Ihm, S.K., J.H. Ahn, and Y.D. Jo, *Interaction of reaction and mass transfer in ion-exchange resin catalysts.* Industrial & Engineering Chemistry Research, 1996. **35**(9): p. 2946-2954.
76. Gusler, G.M., T.E. Browne, and Y. Cohen, *Sorption of Organics from Aqueous-solution onto Polymeric Resins.* Industrial & Engineering Chemistry Research, 1993. **32**(11): p. 2727-2735.
77. Polyanskii, N.G. and V.K. Sapozhnikov, *New Advances in Catalysis by Ion-exchange Resins.* Russian Chemical Reviews, 1977. **46**(3): p. 445-476.
78. Sainio, T., M. Laatikainen, and E. Paatero, *Phase equilibria in solvent mixture-ion exchange resin catalyst systems.* Fluid Phase Equilibria, 2004. **218**(2): p. 269-283.
79. Horstmann, S., T. Popken, and J. Gmehling, *Phase equilibria and excess properties for binary systems in reactive distillation processes Part I. Methyl acetate synthesis.* Fluid Phase Equilibria, 2001. **180**(1-2): p. 221-234.
80. Tesser, R., M. Di Serio, L. Casale, G. Carotenuto, and E. Santacesaria, *Absorption of water/methanol binary system on ion-exchange resins.* Canadian Journal of Chemical Engineering, 2010. **88**(6): p. 1044-1053.
81. Harmer, M.A. and Q. Sun, *Solid acid catalysis using ion-exchange resins.* Applied Catalysis a-General, 2001. **221**(1-2): p. 45-62.
82. Vicente, G., A. Coteron, M. Martinez, and J. Aracil, *Application of the factorial design of experiments and response surface methodology to optimize biodiesel production.* Industrial Crops and Products, 1998. **8**(1): p. 29-35.
83. Lopez, D.E., J.G. Goodwin, and D.A. Bruce, *Transesterification of triacetin with methanol on Nafion (R) acid resins.* Journal of Catalysis, 2007. **245**(2): p. 381-391.
84. Shibasaki-Kitakawa, N., H. Honda, H. Kuribayashi, T. Toda, T. Fukumura, and T. Yonemoto, *Biodiesel production using anionic ion-exchange resin as heterogeneous catalyst.* Bioresource Technology, 2007. **98**(2): p. 416-421.

85. dos Reis, S.C.M., E.R. Lachter, R.S.V. Nascimento, J.A. Rodrigues, and M.G. Reid, *Transesterification of Brazilian vegetable oils with methanol over ion-exchange resins.* Journal of the American Oil Chemists Society, 2005. **82**(9): p. 661-665.
86. Liu, Y.J., E. Lotero, and J.G. Goodwin, *Effect of carbon chain length on esterification of carboxylic acids with methanol using acid catalysis.* Journal of Catalysis, 2006. **243**(2): p. 221-228.
87. JagadeeshBabu, P.E., K. Sandesh, and M.B. Saidutta, *Kinetics of Esterification of Acetic Acid with Methanol in the Presence of Ion Exchange Resin Catalysts.* Industrial & Engineering Chemistry Research, 2011. **50**(12): p. 7155-7160.
88. Tsai, Y.T., H.M. Lin, and M.J. Lee, *Kinetics behavior of esterification of acetic acid with methanol over Amberlyst 36.* Chemical Engineering Journal, 2011. **171**(3): p. 1367-1372.
89. Bart, H.J., W. Kaltenbrunner, and H. Landschutzer, *Kinetics of esterification of acetic acid with propyl alcohol by heterogeneous catalysis.* International Journal of Chemical Kinetics, 1996. **28**(9): p. 649-656.
90. Peters, T.A., N.E. Benes, A. Holmen, and J.T.F. Keurentjes, *Comparison of commercial solid acid catalysts for the esterification of acetic acid with butanol.* Applied Catalysis a-General, 2006. **297**(2): p. 182-188.
91. Lee, M.J., H.T. Wu, and H.M. Lin, *Kinetics of catalytic esterification of acetic acid and amyl alcohol over Dowex.* Industrial & Engineering Chemistry Research, 2000. **39**(11): p. 4094-4099.
92. Qu, Y.X., S.J. Peng, S. Wang, Z.Q. Zhang, and J.D. Wang, *Kinetic Study of Esterification of Lactic Acid with Isobutanol and n-Butanol Catalyzed by Ion-exchange Resins.* Chinese Journal of Chemical Engineering, 2009. **17**(5): p. 773-780.
93. Lilja, J., D.Y. Murzin, T. Salmi, J. Aumo, P.M. Arvela, and M. Sundell, *Esterification of different acids over heterogeneous and homogeneous catalysts and correlation with the Taft equation.* Journal of Molecular Catalysis a-Chemical, 2002. **182**(1): p. 555-563.
94. Marchetti, J.M., V.U. Miguel, and A.F. Errazu, *Heterogeneous esterification of oil with high amount of free fatty acids.* Fuel, 2007. **86**(5-6): p. 906-910.
95. Lode, F., S. Freitas, M. Mazzotti, and M. Morbidelli, *Sorptive and catalytic properties of partially sulfonated resins.* Industrial & Engineering Chemistry Research, 2004. **43**(11): p. 2658-2668.
96. Froment, G.F. and K.B. Bischoff, *Chemical Reactor Analysis and Design*. second edition ed. 1990: Wiley. 664.
97. Saha, B. and M.M. Sharma, *Reaction of dicyclopentadiene with formic acid and chloroacetic acid with and without cation-exchange resins as catalysts.* Reactive & Functional Polymers, 1997. **34**(2-3): p. 161-173.
98. Gangadwala, J., S. Mankar, S. Mahajani, A. Kienle, and E. Stein, *Esterification of acetic acid with butanol in the presence of ion-exchange resins as catalysts.* Industrial & Engineering Chemistry Research, 2003. **42**(10): p. 2146-2155.
99. Ihm, S.K., M.J. Chung, and K.Y. Park, *Activity difference between the internal and external sulfonic groups of macroreticular ion-exchange resin catalysts in isobutylen hydration. .* Industrial & Engineering Chemistry Research, 1988. **27**(1): p. 41-45.
100. Srilatha, K., N. Lingaiah, P.S.S. Prasad, B. Devi, R.B.N. Prasad, and S. Venkateswar, *Influence of Carbon Chain Length and Unsaturation on the Esterification Activity of Fatty Acids on Nb2O5 Catalyst.* Industrial & Engineering Chemistry Research, 2009. **48**(24): p. 10816-10819.

101. Alonso, D.M., M.L. Granados, R. Mariscal, and A. Douhal, *Polarity of the acid chain of esters and transesterification activity of acid catalysts.* Journal of Catalysis, 2009. **262**(1): p. 18-26.

2

PROCEDURES

This chapter explains the procedures adopted in the present work to obtain the experimental data as well as the methodology applied for parameter estimation and reactor model construction. Various ion exchange resins such as Lewatit K1221, Lewatit K2640, Lewatit K2629 and Amberlyst 15, have been used. The liquid phase (trans)esterification was performed in an isothermal batch reactor at atmospheric pressure, at the research laboratory of Industrial Chemistry at Ghent University. An in-depth interpretation of the experimental results, as well as a critical evaluation of literature reported kinetic models together with an assessment of their physicochemical meaning lead to guidelines for the construction of a set of rival kinetic models for the (trans)esterification catalyzed by ion exchange resins. Via model regression to the experimental data, kinetic parameter estimates have been obtained that provide a basis for the identification of the most likely reaction mechanism.

2.1 Materials

The reagents, methanol (Fiers, purity > 99.85 %), ethyl acetate (Fiers, purity $\geq$ 99.5 %) and acetic acid (Fiers, purity $\geq$ 99.5 %) were used as received. *n*-Octane (Acros Organics, purity > 99%) was used as internal standard. Methyl acetate (Acros, purity > 99%) and ethanol (Fiers, purity > 99.8) are used for calibration purposes.

For the determination of the total active sites concentration a 2.0 mol m^{-3} sodium hydroxide solution was prepared from NaOH pellets (Acros, purity > 98%). The exact NaOH concentration was determined by titration with oxalic acid (Acros, purity > 98%) as primary standard. A 0.1 mol m^{-3} HCl solution was diluted from a concentrated 37 % HCl solution (VWR BDH Prolabo, purity > 99%) for back titration purposes, see Section 2.2.1.

The ion-exchange resins Lewatit K1221, Lewatit K2640, Lewatit K2629 (Lanxess) and Amberlyst 15 (Rohm & Haas) are spherical polystyrene-based resin beads that are cross-linked with divinylbenzene, with sulfonic acid groups as active centres. The resins' properties

are reported in Table 2-1. These resins are heat-sensitive and experience an activity loss above 398 K. Prior to (trans)esterification, the resins were freeze dried under vacuum at 233 K for 24 h to completely remove any moisture, as advised by the suppliers.

Table 2-1 Chemical and physical properties of ion-exchange resins

Property	K1221	K2629	K2640	Amberlyst 15
Appearance	dark brown, translucent	beige, opaque	beige, opaque	deep grey, beige opaque
Type	gel	macroporous	macroporous	macroporous
Acid site (eq/kg)	5.3	4.8	5.2	4.8
% DVB	4 %	18 %	18 %	20 %
Bead size (mm)	0.4 – 1.25	0.4 – 1.2	0.4 – 1.25	0.3 – 1.2
Sulfonation degree	stoichiometric	stoichiometric	poly	stoichiometric

2.2 Characterization

2.2.1 Total concentration of acid sites

The total acid sites concentration of the resin (eq/kg) was determined by a back titration. 1.0 g of dry resin was put in a closed recipient with 50 mL 2.0 M NaOH solution. After 24 hours of shaking at room temperature, 3 times 10 mL of the supernatant was titrated with 0.1 M HCl solution to quantify the remaining NaOH concentration. The difference between the original and the final NaOH concentration allows determining the number of active sites as follows:

$$C_{H^+} = \frac{\left(C_{NaOH} - \frac{V_{HCl} C_{HCl}}{V_{NaOH}} \right) V}{W_{catalyst}} \tag{2-1}$$

with $W_{catalyst}$, the mass of catalyst, C_i, and V_i respectively the concentration of component *i*, the volume of solution *i* and *V* the initial NaOH solution volume.

2.2.2 Volumetric swelling experiments

As mentioned in Chapter 1, swelling in polar liquid media is a special feature of ion exchange resins. The swelling is quantified by measuring the swelling ratio *S*. The latter is defined as the ratio of the volume of the swollen resin, in the presence of a solvent, to the volume of the dry resin. A graduated cylinder of 25 mL was filled with 10 mL of dry resin and subsequently 25 mL of solvent was added. A steady (resin) level was obtained in less than 1 minute. From

the volume of the wet resin V_{wet} and the initial volume of dry resin V_{dry} used, the swelling ratio S is calculated:

$$S = \frac{V_{wet}}{V_{dry}} \quad (2\text{-}2)$$

No effect of compressibility was observed when using graduated cylinders of different diameters.

2.3 Kinetic measurements

2.3.1 Experimental setup

Ethyl acetate transesterification with methanol and acetic acid esterification with methanol, was carried out in a three-necked glass flask of 180 mL capacity equipped with a reflux condenser, a thermocouple and a sampling port, see Figure 1. The temperature in the reactor was maintained within 0.5 K from the set point with a thermostat (Lauda Proline RP845) equipped with a PID-controller. The reaction mixture was stirred with a magnetic stirrer at a constant speed of 500 rpm throughout the experiment which sufficed to establish complete mixing of the reaction mixture, see Section 2.3.4.

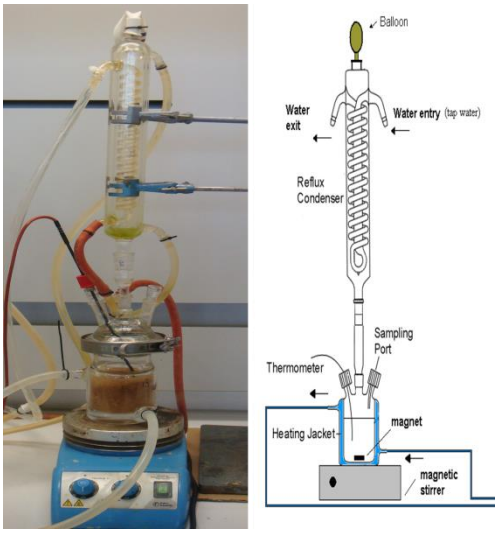

Figure 2-1 Experimental setup

The reactor was first loaded with methanol and catalyst and subsequently heated to the reaction temperature. The gas volume of the reactor was minimal and, hence, the amount of solvent lost to the vapour phase in the reactor was negligible. When the methanol and catalyst reached the desired temperature, preheated ethyl acetate or acetic acid and n-octane were added through the sampling port in order to have an as well determined starting point of the

(trans)esterification experiment as possible without disturbing the reactor temperature. *n*-Octane was used as internal standard for analytical purposes. At the same time, it allowed working with a constant total liquid volume throughout the experimentation when varying the initial methanol to ethyl acetate (acetic acid) molar ratio and keeping the initial ethyl acetate or acetic acid to resin ratio identical (3 %), without requiring the use of excessive amounts of resin. The *n*-octane content ranged from 56 to 3 mol-%, depending on the initial methanol to ethyl acetate or acetic acid molar ratio which ranged from 1:1 to 20:1. All experiments were performed at atmospheric pressure. Each experiment was performed at least double if not quadruple with an experimental error below 5%. The range of experimental conditions is given in Table 2-2.

Table 2-2 Range of experimental conditions for (trans)esterification

Temperature (K)	303.15 – 333.15
Pressure (MPa)	0.1
MeOH:EtOAc molar ratio (transesterification) MeOH:HOAc molar ratio (esterification)	1:1 – 20:1
Catalyst mass (10^{-3} kg)	0.5 -5.0
Experiment time (s)	0.0 – 25200.0
Batch time[a] (kg s)	12.6 – 126

[a] Defined as product of experiment time multiplied by the mass of catalyst

2.3.2 Sampling and analysis

Samples of the reaction mixture were withdrawn through the sampling port at regular times, mostly every 1800 s, to follow the evolution in concentration of reagents and products as a function of the batch time. By analysing the samples via gas chromatography, the concentrations of MeOAc, MeOAc and EtOH in transesterification and of HOAc and MeOAc in esterification were determined.

The 'Focus GC' gas chromatograph is equipped with an AS3000 auto sampler, a Stabilwax capillary column (30 m x 0.32 mm, 0.25 µm thickness) and a flame ionization detector (FID). The injector and detector temperatures were both set at 523 K. The oven temperature program started at 313 K for 300 s, then increased to 343 K at a rate of 6.0 Ks^{-1}, further increased to 473 K at a rate of 50.0 Ks^{-1} and was finally held constant at 473K for 120 s, see Figure 2-2. To avoid an excess of components on the column, the split flow was manipulated between 50 and 250. The H_2 flow over the column is 6.058 10^{-3} Nl/min and the

helium flow is 2.734 10^{-3} Nl/min. The Chromchard 2.3.2 software was used to analyze the gas chromatography data.

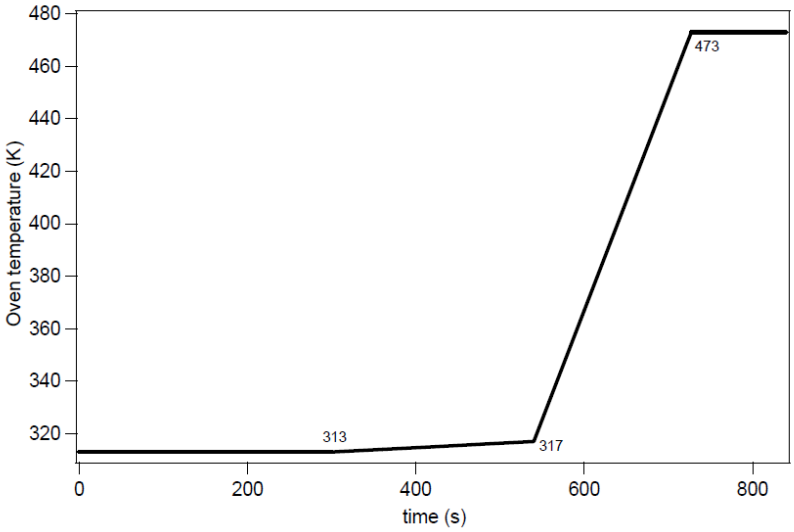

Figure 2-2 Oven temperature program for the gas chromatograph analysis

Quantification of the reaction components was performed by relating the peak surface areas to the mass of *n*-octane (m_{ref}), the internal standard:

$$\frac{A_{peak,ref}}{A_{peak,i}} = CF_i \frac{m_{ref}}{m_i} \tag{2-3}$$

where $A_{peak,i}$ and $A_{peak,ref,}$ are the peak surface area of component *i* and *n*-octane, m_i the mass of component *i* , and CF_i the calibration factor of component *i* with respect to *n*-octane. The calibration factor of component *i* was determined by the GC evaluation of 9 synthetic samples. The composition of these samples depends on the reaction and the initial molar ratio. E.g., for the calibration, when measuring the samples of a transesterification experiment with initial molar ratio MeOH:EtOAc of 10:1, 9 solutions, corresponding with EtOAc conversions between 0% and 90 % were prepared, see Appendix A2. Each solution was analysed at least in threefold.

The component peak surface areas as obtained in the 27 chromatograms were plotted against the component concentration, see Figure 2-3. The components' calibration factors were determined via linear regression, see equations in Figure 2-3, leading to the calibration factors for the components. For all investigated initial molar ratios, for transesterification as well as for esterification, no accurate measurement of MeOH could be achieved, due to its excess in the reaction mixture. For the transesterification the most accurate results were

obtained based on the EtOAc area. For the is, because the acetic acid peak area of the chromatogram shows tailing, the product methyl acetate area is used instead of the acetic acid. Hence, the kinetic experiments are expressed in terms of methyl acetate yield instead of acetic acid conversion.

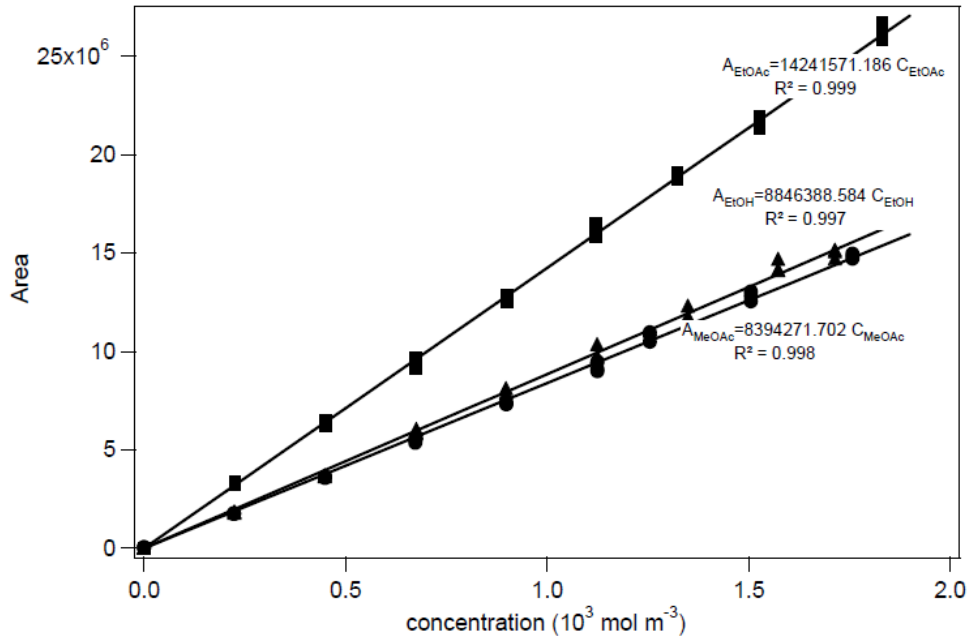

Figure 2-3 Calibration curve of EtOAc (■), EtOH (▲) and MeOAc (●) for the transesterification with an initial molar ratio MeOH:EtOAc of 10:1 .

Conversions were calculated as follows:

$$X_i = \frac{C_{i,0} - C_{i,t}}{C_{i,0}} \tag{2-4}$$

where X_i is the conversion of reactant i, $C_{i,0}$ the initial concentration of i and $C_{i,t}$ the concentration of i at time t [1].

Yields were calculated as follows:

$$Y_j = \frac{C_{j,t}}{C_{i,0}} \tag{2-5}$$

where Y_j is the yield of product j, $C_{i,0}$ the initial concentration of reagent i and $C_{j,t}$ the concentration of j at time t [1].

No additional peaks were observed in any of the chromatograms during the experiments. Only experiments with a mass balance deviation below 5% were used in the

kinetic modelling. The experimental data were scaled based on the acetate-balance, to obey a 100% mass balance.

2.3.3 Catalyst deactivation and leaching

Catalyst deactivation and leaching were investigated by reusing the spent catalyst from a previous experiment to assess the heterogeneous character of the catalysed reaction. After a transesterification experiment with a fresh catalyst batch, the catalyst was filtered from the reaction solution by a Buchner filter and dried overnight in an oven at 323 K. Subsequently, a transesterification experiment was performed with this used and dried catalyst. This sequence was repeated for 4 times and the catalytic activities obtained in these 5 runs were evaluated. It was observed that in at least 5 consecutive experiments, the same Lewatit K1221 sample exhibited transesterification behaviour which only differed from each other within the experimental error, see Figure 2-4. Similar results were obtained for Lewatit K2629. Yadav and Thathagar [2], by Lilja et al. [3] and López et al. [4] observed no deactivation up to four runs for their investigated (trans)esterification catalyzed by ion exchange resins.

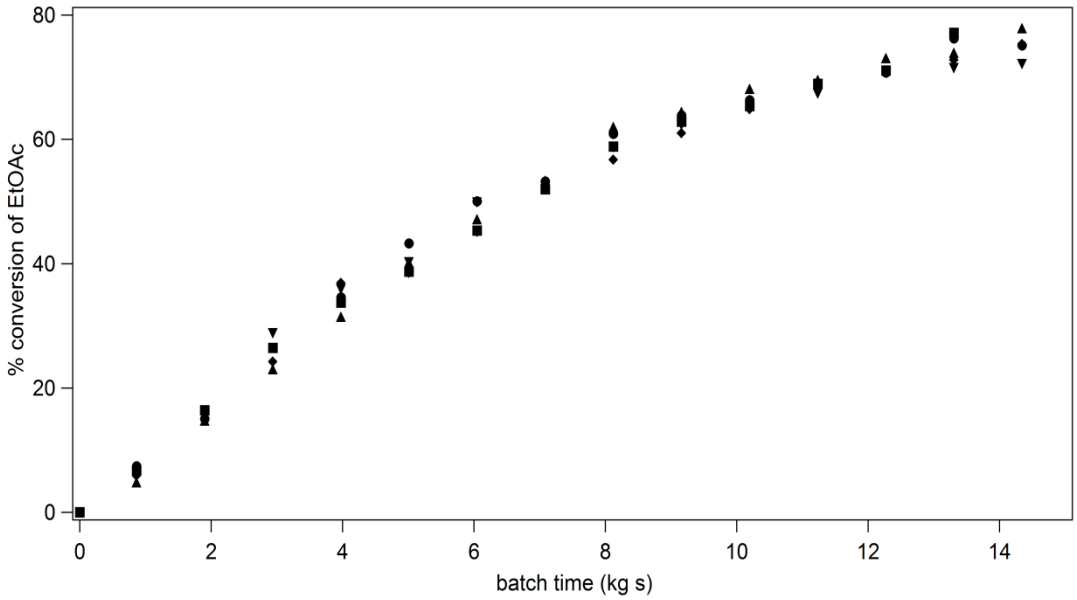

Figure 2-4 Effect of reusability on EtOAc conversion as a function of the batch time with Lewatit K1221 catalyst (▲ fresh; ● second run; ■ third run; ♦ forth run; ▼ fifth run) for the transesterification with an initial molar ratio MeOH:EtOAc of 10:1 at 333K and 0.578 g catalyst

2.3.4 Intrinsic kinetics

In order to ascertain that the experimental data represent intrinsic kinetics, they should be free from deviations due to non-ideal reactor behaviour and interference with transport phenomena. Two types of mass-transfer resistance have been verified, one at the solid-liquid interface occurring consecutively to the catalytic reaction and the other in the intraparticle space occurring in parallel with the reaction. Quantitative criteria to verify the absence of mass transfer limitations, such as the Carberry number C_a for external mass transfer and the Weisz modulus Φ for internal diffusion were calculated using the appropriate correlations, see Table 2-3 [1, 5]. The detailed calculation of the transport limitations is reported in Appendix A2.

Table 2-3 Criteria for the absence of transport limitations for a Lewatit K1221 catalyst particle under steady-state operation for the (trans)esterification.

Transport phenomenon	Criterion	Calculation Transesterification	Calculations Esterification
Extraparticle mass transport ('Carberry number')	$C_a = \frac{r_{obs}}{k_s a' c_{A,b}} < 0.05$	C_a = 7.7 10^{-3}	C_a = 1.3 10^{-2}
Intraparticle mass transport ('Wheeler-Weisz criterion')	$\Phi = \frac{r_{obs}}{a_v^2 D_{A,eff} c_{A,b}} \left(\frac{n+1}{2}\right) < 0.08$	Φ = 8.8 10^{-6}	Φ = 8.0 10^{-5}

In addition to these quantitative criteria, also some qualitative tests were performed to verify the importance of transfer phenomena and the complete mixing in the reactor. To evaluate the importance of external mass transport phenomena as well as the complete mixing in the reactor, transesterification experiments were performed at different agitation speeds. When external mass transport is not rate limiting, there is no effect of the agitation speed [1]. Figure 2-5 clearly shows that the external mass-transfer resistance is negligible between 200 and 1000 rpm. Hence, all experiments were conducted at a stirrer speed of 500 rpm to ensure that the reaction rate was not limited by external diffusion. This was also observed by Sanz et al. [6]. Several authors [7-10] indicate that external diffusion does not usually control the overall reaction rate in the ion exchange catalyzed (trans)esterification reaction catalyzed by Amberlyst 15 unless the agitation speed is very low or the reaction mixture is very viscous.

The possible effect of internal mass-transfer was verified by using different catalyst particle sizes [1]. The commercial Lewatit K1221 resin was screened into four different size ranges. As shown in Figure 2-6, no significant differences were found in the ethyl acetate

conversion with the batch time for the different catalyst sizes, i.e., the effect of internal mass transfer on the reaction kinetics could be considered negligible. Hence, all experiments were conducted with the ion-exchange resin as supplied by the manufacturer without any size screening.

Similar results were obtained for Lewatit K2629. Due to the chemical and structural similarity and their similar initial reaction rate, it can reasonably be assumed that no diffusion limitations occurred on Lewatit K2640 and Amberlyst 15 either.

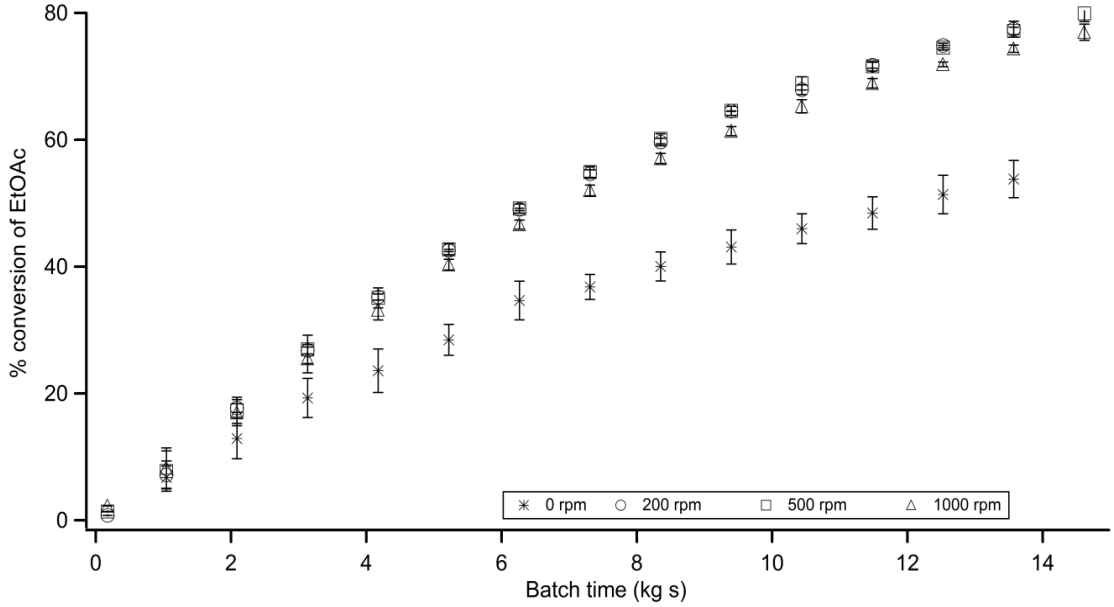

Figure 2-5 Effect of the agitation speed (legend) on the conversion of EtOAc catalyzed by Lewatit K1221. (T = 333 K, W = 0.58 10^{-3} kg, initial molar ratio of MeOH:EtOAc = 10:1)

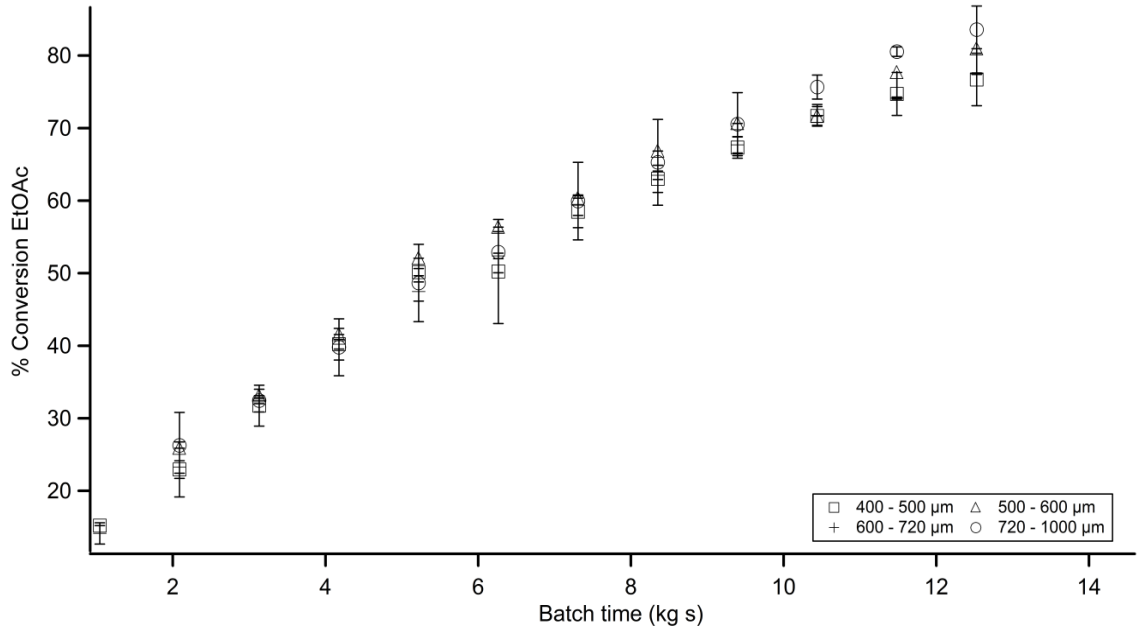

Figure 2-6 Effect of the particle size (legend) on the conversion of EtOAc catalyzed by Lewatit K1221. (T = 333K, W = 0.58 10^{-3} kg, initial molar ratio of MeOH:EtOAc = 10:1)

2.4 Thermodynamic properties and activity coefficients

2.4.1 Thermodynamic properties

Transesterification

The Gibbs reaction enthalpy was calculated based on thermodynamic data obtained from values tabulated in the ASPEN engineering suite™ 11.1, and was found to vary from -4.20 at 303 K to -0.50 kJ/mol at 333K, showing a slightly exothermic reaction. The corresponding entropy varies from -10.0 to 2.02 J/mol K. The corresponding equilibrium coefficient K_{eq},

$$K_{eq} = K_C K_\gamma = \frac{C_{MeOAc} C_{EtOH}}{C_{MeOH} C_{EtOAc}} \frac{\gamma_{MeOAc} \gamma_{EtOH}}{\gamma_{MeOH} \gamma_{EtOAc}} = \exp\left(\frac{-\Delta G^\circ_{R,T}}{RT} \right) \tag{2-6}$$

ranges from 1.59 at 303 K to 1.46 at 333 K, which is similar to values reported in previous transesterification studies [11]. In Equation 2-6, K_c represents the equilibrium coefficient expressed in concentrations, K_γ the ratio of the activity coefficients of the products to those of the reactants , C_i the concentration of component *i* and γ_i the activity coefficient of component *i*. $\Delta G^\circ_{R,T}$ is the standard Gibbs energy, *T* the temperature and *R* the universal gas constant.

Esterification

The Gibbs reaction enthalpy was found to be -4.39 kJ mol^{-1} on the NIST Chemistry WebBook, showing a slightly exothermic reaction. The corresponding equilibrium coefficient K_{eq}:

$$K_{eq} = K_C K_\gamma = \frac{C_{MeOAc} C_{water}}{C_{MeOH} C_{HOAc}} \frac{\gamma_{MeOAc} \gamma_{water}}{\gamma_{MeOH} \gamma_{HOAc}} = \exp\left(\frac{-\Delta G^\circ_{R,T}}{RT} \right) \tag{2-7}$$

is calculated using tabulated values of the standard Gibbs free energy of formation $\mathbf{\Delta G_f^\circ}$ of methanol, acetic acid, methyl acetate and water at different temperatures in the ASPEN engineering suite™ 11.1 and ranges from 261.52 at 293 K to 121.99 at 333 K. At 298 K values for the equilibrium coefficient ranging from 612.51 to 30.16 were published [8, 12-17]. Hence, in contrast to transesterification, where the equilibrium coefficient approximately equals unity and, hence, the equilibrium composition of an equimolar ethyl acetate and methanol mixture is practically equimolar, the equilibrium composition of an equimolar

acetic acid and methanol mixture after esterification is more to the side of the products, i.e., methyl acetate and water.

2.4.2 Thermodynamic non-ideality in liquid phase

Given the presence of organic compounds with varying polarity as well as water in the investigated reaction media, their thermodynamically non-ideal behaviour has to be assessed [12, 18]. Previously published work has been successful in accounting for the non-idealities involved in the transesterification of butanol with methyl acetate using the UNIQUAC [19, 20] and UNIFAC [21] methods. For the esterification of acetic acid with methanol several authors used UNIQUAC [13] or UNIFAC [22, 23]. For the esterification of acetic acid with propanol Bart et al. [24] used the UNIQUAC method while Ali et al. [25] opted for the UNIFAC method. Hence, some further considerations are required for selecting the proper method for both reactions that are investigated in this work [26].

While the UNIQUAC (UNIversal QUAsi Chemical) method is a molecular model, the UNIFAC (UNIQUAC Functional-group Activity Coefficients) method predicts the activity coefficients using group contribution. The fundamental assumption of a group contribution method is additivity: the contribution made by one group within a molecule is assumed to be independent of that made by any other group in that molecule. This assumption is valid only when the ‘effect’ of any group in a molecule on the other groups within that molecule is negligible [27].

The generic form of the UNIQUAC equation can be given as:

$$\ln \gamma_i\big|_{UNIQUAC} = f\left(\underline{x}, \mathrm{T}, \underline{A}, \underline{r}, \underline{q}\right), \text{ for } i = 1, \mathrm{N} \tag{2-8}$$

where $\underline{x}$ contains the molar fractions of the each component, T is the temperature, the parameters $\underline{A}$ are molecular interactions whose values are obtained by regression, $\underline{r}$ and $\underline{q}$ are measures of the molecular van der Waals volume and surface area of each compound, and N is the number of components in the mixture [28].

The generic form of the UNIFAC method is similar to the UNIQUAC equation (Equation 2-8) wherein the parameters $\underline{A}$, $\underline{r}$, $\underline{q}$ respectively replaced are by: $\underline{a}$ the group interaction parameters obtained through regression and $\underline{R}_k$ and $\underline{Q}_k$ are the group van der Waals volumes and group surface areas, respectively [28].

In both methods the calculation of the activity coefficient, see Equation 2-9, is separated into two parts, a combinatorial and a residual part.

$$\ln \gamma_i = \underset{combinatorial}{\ln \gamma_i^C} + \underset{residual}{\ln \gamma_i^R} \tag{2-9}$$

The combinatorial part accounts for the differences in molecular size and shape of the molecules present in the mixture and is the same for both methods. The combinatorial part is calculated using Equation 2-10:

$$\ln \gamma_i^C = \ln \frac{\Phi_i}{x_i} + \frac{z}{2} q_i \ln \frac{\theta_i}{\Phi_i} + l_i - \frac{\Phi_i}{x_i} \sum_j x_j l_j \tag{2-10}$$

with l_i a typical parameter is function of the pure component parameters: r_i and q_i, respectively, the molecular van der Waals volume and the molecular surface area, z is equal to 10, x_i the mole fraction of component i, θ_i the area fraction, Φ_i the segment fraction (similar to area fraction).

The residual part takes into account the interactions among the molecules in the mixture. In the UNIQUAC method this is achieved via tabulated molecular interaction parameters. In the UNIFAC method a group contribution method is used. [18, 29]. The residual part of the UNIQUAC activity coefficient is calculated using Equation 2-11.

$$\ln \gamma_i^R = q_i \left[1 - \ln \left(\sum_j \theta_j \tau_{ji} \right) - \sum_j \frac{\theta_j \tau_{ij}}{\sum_k \theta_k \tau_{kj}} \right] \tag{2-11}$$

with τ_{ij} and τ_{ji} as the tabulated molecular interaction parameters. No ternary (or higher) parameters are required for a multicomponent system.

The residual part of the UNIFAC activity coefficient is calculated using Equation 2-12, including a solution-of-group concept:

$$\ln \gamma_i^R = \sum_{\substack{k \\ all\ groups}} \nu_k^{(i)} \left[\ln \Gamma_k - \ln \Gamma_k^{(i)} \right] \tag{2-12}$$

where $\nu_k^{(i)}$ is the number of groups of type k in molecule i, Γ_k is the group residual activity coefficient and $\Gamma_k^{(i)}$ the residual activity coefficient of group k in a reference solution containing only molecules of type i. The group residual activity coefficient Γ_k is calculated using Equation 2-13, with Θ_m the ratio of the area fraction of group m and the sum over all

the different groups, X_m is the mole fraction of group *m* in the mixture, and Ψ_{mn} the group-interaction parameter between groups *m* and *n*.

$$\ln \Gamma_k = Q_k \left[1 - \ln\left(\sum_m \Theta_m \Psi_{mk} \right) - \sum_m \frac{\Theta_m \Psi_{km}}{\sum_n \Theta_n \Psi_{nm}} \right] \qquad (2\text{-}13)$$

The residual group activity coefficient Γ_k depends on the molecule *i* in which the group *k* is contained. To calculate the group-interaction parameter, Ψ_{mn}, the interaction energy between the two groups *m* and *n* must be known. These must be evaluated from experimental phase equilibrium data [29]. These data can be found in available literature. or in databases of the ASPEN engineering suite (Aspen Technology). The UNIFAC model contains two adjustable parameters, Ψ_{mn} per pair of functional groups [27, 29].

The UNIQUAC method often gives good representation of vapor-liquid and liquid-liquid equilibria for multicomponent mixtures containing a variety of nonelectrolytes such as hydrocarbons, ketones, esters, water, amines, alcohols, nitriles, …. [27, 29]. Moreover, UNIQUAC gives a more precise calculation of the liquid-liquid equilibrium data for the (trans)esterification component than UNIFAC [14, 30]. This can be attributed to the fitting of the UNIQUAC parameters to the available experimental data while the tabulated UNIFAC parameters did not use that experimental data for regression, because they employ a predefined, fixed set of model parameters, defined as a group parameters [28].

Carlson [26] suggests that the UNIFAC activity coefficient model is a good predictive approach that can be used when there are no experimental data or binary parameters available or when an approximate value suffices, e.g., for a component with low priority. As a result, UNIFAC is popular in the chemical industry and is widely used to estimate physicochemical properties [9, 21, 29, 31, 32]. Nevertheless, one of the main drawbacks of the UNIFAC model is the need for group-interaction parameters, c.q., nearly 50 % of the parameters are missing in the parameter table [17]. Revisions of UNIFAC parameters have been done many times in the past but there are still missing parameters in the UNIFAC parameter table because of the lack of experimental data [28].

Transesterification

Both methods, UNIFAC and UNIQUAC, are used in literature to calculate the non-idealities in the transesterification [19-21]. Nevertheless, in about half of the kinetic studies on short chain transesterification UNIFAC is used to describe the liquid phase non-ideality. As mentioned above UNIQUAC gives a more precise calculation of the liquid-liquid equilibrium data for the transesterification. At the start of the transesterification kinetic modelling work, however, the UNIQUAC interaction parameters were not available yet and, hence, UNIFAC was used to calculate the required liquid phase activity coefficients with interaction parameters as reported by Poling et al. [17]. At present, the necessary UNIQUAC parameters have become available to calculate liquid phase activity coefficients for all components involved in liquid phase ethyl acetate transesterification with methanol. Modelling results using the UNIQUAC method instead of the UNIFAC method lead to parameter values that are numerically slightly different but preserve the physical interpretation that has been made.

The UNIFAC group contribution method was implemented in the Athena Visual Studio code, see Appendix C. Detailed information about the calculation of the activity coefficients can be found in Appendix A3.

Table 2-4 shows the activity coefficients of each component for all the experimental conditions, at the start of the reaction and at thermodynamic equilibrium. Since the activity coefficients were different from 1.0, the reaction mixture clearly exhibits non-ideal behaviour. Deviations from ideality were most pronounced in the experiments with a high initial molar ratio.

Table 2-4 Activity coefficients of MeOH, EtOH, MeOAc, EtOAc and n-octane at different temperatures and different initial molar MeOH:EtOAc ratios, at the start of the reaction and at equilibrium ($C_{EtOAc,0}$ = 1,79 M; *: $C_{EtOAc,0}$ = 5.79 M)

Temperature (K)	303				313		323		333					
MeOH:EtOAc ratio	1:1*		10:1		10:1		10:1		1:1*		5:1		10:1	
Conversion (%)	0	56	0	94	0	94	0	94	0	56	0	89	0	94
MeOH	1.47	1.52	1.02	1.02	1.02	1.02	1.02	1.02	1.45	1.51	1.29	1.31	1.02	1.02
EtOH	-	1.41	-	1.19	-	1.18	-	1.18	-	1.39	-	1.28	-	1.17
MeOAc	-	1.27	-	2.12	-	2.08	-	2.05	-	1.25	-	1.62	-	2.02
EtOAc	1.25	1.25	2.27	2.27	2.24	2.24	2.21	2.20	1.23	1.23	1.59	1.57	2.17	2.17
n-octane	4.84	4.57	17.39	17.22	16.58	16.42	15.82	15.67	4.51	4.29	4.02	4.01	15.10	14.96

Esterification

In literature, examples can be found for the calculation of liquid phase activity coefficients in acetic acid esterification with *n*-butanol using both UNIFAC and UNIQUAC [24, 25]. Lee et al. [33] clearly showed that the UNIQUAC method, allowed a more reliable simulation of free fatty acid esterification than the UNIFAC method. This was confirmed by Coelho et al. [34] and Basso et al. [30]. Moreover, Coelho et al. [34] concluded that the binary system composed of water and glycerol could be quantitatively described by the UNIQUAC, but not by the UNIFAC method. The latter was assigned to the complex interactions between primary and secondary alcohol functions in glycerol on the one hand and water on the other hand. Therefore, the UNIQUAC method was used in this work for the calculation of the activity coefficients for the components involved in esterification. The values of the two adjustable binary parameters (τ_{ij} and τ_{ji}) of the residual part (Equation 2-11) were evaluated from experimental phase equilibrium data, published by Horstman et al .[35] and Alvarez et al. [36], and available in the commercial simulation software Aspen Plus. The UNIQUAC method was implemented in the Athena Visual Studio code, with the values of the binary parameters from the Aspen Engineering suite (Aspen Technology Inc.), see Appendix D. A detailed calculation of the activity coefficients by the UNIQUAC method is given in Appendix A3.

Table 2-5 shows the activity coefficients of each component for all experimental conditions, at the start of the reaction and at thermodynamic equilibrium. Strong deviations from ideality were found, during any experiment.

Table 2-5 Activity coefficients of MeOH, HOAc, MeOAc, water and n-octane at different temperatures and different initial molar MeOH:HOAc ratios, at the start of the reaction and at equilibrium ($C_{HOAc,0}$ = 1,97 M; *: $C_{HOAc,0}$ = 9.27 M)

Temperature (K)	303				333					
MeOH:HOAc ratio	1:1*		10:1		1:1*		5:1		10:1	
Conversion (%)	0	93.5	0	99.9	0	91.7	0	99.8	0	99.9
MeOH	0.7257	0.2432	0.9670	0.9672	0.9195	1.3185	1.0386	1.0162	1.0361	1.0036
HOAc	0.9424	0.2650	0.6776	0.5537	0.7899	0.1582	0.4906	0.1935	0.3962	0.2211
MeOAc	-	1.6346	-	2.7656	-	1.4064	-	1.9588	-	2.1683
water	-	2.2650	-	1.8217	-	2.2007	-	1.9389	-	1.9222
n-octane	3.493E-4	0.9966	1.283E-5	1.596E-5	0.03833	4.2995	0.3989	6.8386	1.0519	6.2428

2.5 Modeling and regression analysis

2.5.1 Reactor models

The mass balance for species *i* in a batch reactor, which is considered to be spatially uniform in composition and temperature, is given by:

$$\frac{1}{W}\frac{dn_i}{dt} = R_i = \nu_i r \tag{2-14}$$

with R_i the specific net production rate of component *i*, W the catalyst mass in the reactor, ν_i the stoichiometric coefficient of component i, n_i the number of moles of component i in the reaction mixture, and *t* the time. The net production rate is calculated according to equations derived from the various mechanisms that are proposed, i.e., pseudo-homogeneous (PH), Langmuir-Hinshelwood (LH) and Eley-Rideal (ER), see Chapter 3.

The net production rate is a function of the rate coefficient (*k*), temperature, activities and adsorption or exchange equilibrium coefficients of component *i* (K_i). Within the limited temperature interval, no temperature dependence of the adsorption or exchange equilibrium coefficients is considered. The rate coefficient is described by the Arrhenius law, which is reparameterized according to Kittrell [37] in order to avoid strong binary correlation between the Arrhenius parameters:

$$k = k_{T_{ref}} \exp\left[-\frac{E_A}{R}\left(\frac{1}{T} - \frac{1}{T_{ref}}\right)\right] \tag{2-15}$$

with E_A the activation energy, R the universal gas constant and $k_{T_{ref}}$ the reaction rate coefficient at the reference temperature. The activation energy and the rate coefficient at the reference temperature as well as the adsorption or exchange equilibrium coefficient for the adsorption- or exchange-based mechanisms have been determined by regression.

2.5.2 Parameter estimations

Parameter estimates are determined by minimizing the following objective function S, which is the sum of squared residuals between the observed and the calculated concentrations of component *i*:

$$S = \sum_{k=1}^{N} \left(C_{i,k} - \hat{C}_{i,k} \right)^2 \xrightarrow{b} \text{minimum} \tag{2-16}$$

with $C_{i,k}$ the observed concentration of component i in the k^{th} experiment and $\hat{C}_{i,k}$ the corresponding model calculated value, N the total number of experimental measurements and $\underline{b}$ the parameter vector, which is expected to approach the real parameter vector $\underline{\beta}$ when the optimum is reached [1, 19]. As mentioned in 2.32, for the transesterification ethyl acetate was used as response, while in esterification methyl acetate was used as response. In the present work, parameters were estimated using the nonlinear least-squares technique and the Bayesian estimation technique applying a single response Levenberg-Marquardt algorithm, available in Athena Visual Studio [38]. The residual sum of squares (RSSQ) equals the final value of S of Equation 2-16. The regression sum of squares (REG) is given by:

$$REG = \sum_{k=1}^{N} \hat{C}^2 \tag{2-17}$$

Several statistical tests were performed to evaluate the parameter estimation results. These tests include the *F* test for the global significance of the regression and the Student's *t* test for the significance of the individual parameters. The tabulated values for the 95% confidence level are typically used when evaluating the test results.

In the *F test*, *F* is the ratio of the regression sum of squares and the residual sum of squares divided by their respective degrees of freedom:

$$F = \frac{REG / p}{RSSQ / (N - p)} > F_{tab}(p, N - p, 95\%) \tag{2-18}$$

with *p* the number of model parameters [1, 39]. An *F* value higher than the tabulated *F* value at the 95 % probability level corresponds to a high significance of the global regression.

The square of the multiple correlation coefficient, R^2, is the ratio between the regression sum of squares and the total sum of squares, and is a measure of the quality of the regression. Naturally, R^2, lies between 0 and 1.

The Student *t* test is related to the sensitivity of the model calculations on the values of the individual parameters:

$$t = \frac{b_i - \beta_i}{s(b_i)} > t_{tab}(N - p, 95\%) \tag{2-19}$$

with b_i the estimated parameter value, β_i, the proposed value, c.q., zero, for parameter *i*, and $s(b_i)$ an estimate of the standard deviation [1, 40]. A parameter is estimated significantly different from zero when its *t* value is higher than the corresponding tabulated *t* value. A high *t* value is representative of a high sensitivity of the objective function and, hence, the model simulations, to the corresponding parameter. Hence, high t values are also equivalent with narrow 95% approximate individual confidence intervals.

The binary linear correlation between the estimated parameter values is assessed via the following correlation coefficients:

$$\rho_{i,j} = \frac{V(b)_{i,j}}{\sqrt{V(b)_{i,i}V(b)_{j,j}}} \tag{2-20}$$

with $V(b)_{i,j}$ the diagonal element on row j of the covariance matrix $V(b)$ of the parameter values b_i. Absolute values for $\rho_{i,j}$ close to 1, i.e., above 0.95, indicate a strong linear relationship between the estimated values of the corresponding parameters i and j.

The estimated parameters were also evaluated based on their physicochemical significance. The rate coefficients have to increase with temperature, i.e., the activation energy and the rate coefficient at the reference temperature have to be positive.

2.5.3 Model discrimination

Apart from the statistical and physical significance of the regression and the corresponding model parameters, discrimination between rival models can also be performed based on the so-called likelihood ratio. The likelihood ratio Λ is the ratio of the maximum in the likelihood function, L_{max} obtained for the rival models A, with p_A parameters and $RSSQ_A$, and B, with p_B parameters and $RSSQ_B$:

$$L_{\max} = \frac{(N-p)^{N/2}}{\left(\sqrt{2\pi RSSQ}\right)^{N}} \exp\left(-\frac{N-p}{2}\right) \tag{2-21}$$

$$\Lambda = \frac{(L_A)_{\max}}{(L_B)_{\max}} = \left[\frac{N-p_A}{N-p_B}\right]^{\frac{N}{2}} \exp\left(\frac{p_A-p_B}{2}\right)\left[\frac{RSSQ_B}{RSSQ_A}\right]^{\frac{N}{2}} \tag{2-22}$$

For a high ratio, model A has a higher probability to adequately describe the experimental data than model B and vice versa for a small ratio.

Of course, on top of this statistical discrimination between rival models also their physical significance was assessed when selecting the most adequate model.

2.5.4 Experimental design

In case the likelihood ratio or the physicochemical interpretation of the rival models, does not lead to a decisive discrimination, a design of experiments (DOE) can be performed to obtain more precise parameter estimates and, hence, to allow a better discrimination. In this work, a D-optimal experimental design is used, which minimizes the joint confidence interval of the model parameters and, hence, maximizes the determinant of the parameter estimation covariance matrix [1, 41, 42].

2.6 References

1. Froment, G.F. and K.B. Bischoff, *Chemical Reactor Analysis and Design*. second edition ed. 1990: Wiley. 664.
2. Yadav, G.D. and M.B. Thathagar, *Esterification of maleic acid with ethanol over cation-exchange resin catalysts.* Reactive & Functional Polymers, 2002. **52**(2): p. 99-110.
3. Lilja, J., D.Y. Murzin, T. Salmi, J. Aumo, P.M. Arvela, and M. Sundell, *Esterification of different acids over heterogeneous and homogeneous catalysts and correlation with the Taft equation.* Journal of Molecular Catalysis a-Chemical, 2002. **182**(1): p. 555-563.
4. Lopez, D.E., J.G. Goodwin, and D.A. Bruce, *Transesterification of triacetin with methanol on Nafion (R) acid resins.* Journal of Catalysis, 2007. **245**(2): p. 381-391.
5. Berger, R.J., F. Kapteijn, J.A. Moulijn, G.B. Marin, J. De Wilde, M. Olea, D. Chen, A. Holmen, L. Lietti, E. Tronconi, and Y. Schuurman, *Dynamic methods for catalytic kinetics.* Applied Catalysis a-General, 2008. **342**(1-2): p. 3-28.
6. Sanz, M.T., R. Murga, S. Beltran, J.L. Cabezas, and J. Coca, *Autocatalyzed and ion-exchange-resin-catalyzed esterification kinetics of lactic acid with methanol.* Industrial & Engineering Chemistry Research, 2002. **41**(3): p. 512-517.
7. Sert, E. and F.S. Atalay, *Determination of Adsorption and Kinetic Parameters for Transesterification of Methyl Acetate with Hexanol Catalyzed by Ion Exchange Resin.* Industrial & Engineering Chemistry Research, 2012. **51**(18): p. 6350-6355.
8. JagadeeshBabu, P.E., K. Sandesh, and M.B. Saidutta, *Kinetics of Esterification of Acetic Acid with Methanol in the Presence of Ion Exchange Resin Catalysts.* Industrial & Engineering Chemistry Research, 2011. **50**(12): p. 7155-7160.
9. Saha, B. and M. Streat, *Transesterification of cyclohexyl acrylate with n-butanol and 2-ethylhexanol: acid-treated clay, ion exchange resins and tetrabutyl titanate as catalysts.* Reactive & Functional Polymers, 1999. **40**(1): p. 13-27.
10. Ali, S.H., *Kinetics of Catalytic Esterification of Propionic Acid with Different Alcohols over Amberlyst 15.* International Journal of Chemical Kinetics, 2009. **41**(6): p. 432-448.
11. Dossin, T.F., M.F. Reyniers, R.J. Berger, and G.B. Marin, *Simulation of heterogeneously MgO-catalyzed transesterification for fine-chemical and biodiesel industrial production.* Applied Catalysis B-Environmental, 2006. **67**(1-2): p. 136-148.
12. Tsai, Y.T., H.M. Lin, and M.J. Lee, *Kinetics behavior of esterification of acetic acid with methanol over Amberlyst 36.* Chemical Engineering Journal, 2011. **171**(3): p. 1367-1372.
13. Popken, T., L. Gotze, and J. Gmehling, *Reaction kinetics and chemical equilibrium of homogeneously and heterogeneously catalyzed acetic acid esterification with methanol and methyl acetate hydrolysis.* Industrial & Engineering Chemistry Research, 2000. **39**(7): p. 2601-2611.
14. Wyczesany, A., *Chemical Equilibrium Constants in Esterification of Acetic Acid with C(1) - C(5) Alcohols in the Liquid phase.* Chemical and Process Engineering-Inzynieria Chemiczna I Procesowa, 2009. **30**(2): p. 243-265.
15. Wyczesany, A., *Modeling of simultaneous chemical and phase equilibria in esterification of acetic acid with ethanol in high-pressure carbon dioxide.* Industrial & Engineering Chemistry Research, 2007. **46**(16): p. 5437-5445.
16. Bematova, S., K. Aim, and I. Wichterle, *Isothermal vapour-liquid equilibrium with chemical reaction in the quaternary water plus methanol plus acetic acid plus methyl*

acetate system, and in five binary sub-systems. Fluid Phase Equilibria, 2006. **247**(1-2): p. 96-101.
17. Poling, B.E., J.M. Prausnitz, and J.O. Connell, *The Properties of Gases and Liquids*. 2000: McGraw-Hill.
18. Kikic, I., P. Alessi, P. Rasmussen, and A. Fredenslund, *On the combinatorial part of the UNIFAC and UNIQUAC models.* The Canadian Journal of Chemical Engineering, 1980. **58**(2): p. 253-258.
19. Bozek-Winkler, E. and J. Gmehling, *Transesterification of methyl acetate and n-butanol catalyzed by Amberlyst 15.* Industrial & Engineering Chemistry Research, 2006. **45**(20): p. 6648-6654.
20. Steinigeweg, S. and J. Gmehling, *Transesterification processes by combination of reactive distillation and pervaporation.* Chemical Engineering and Processing, 2004. **43**(3): p. 447-456.
21. Xu, B.Y., W.J. Zhang, X.M. Zhang, and C.F. Zhou, *Kinetic Study of Transesterification of Methyl Acetate with n-Butanol Catalyzed by NKC-9.* International Journal of Chemical Kinetics, 2009. **41**(2): p. 101-106.
22. Miao, S.J. and B.H. Shanks, *Mechanism of acetic acid esterification over sulfonic acid-functionalized mesoporous silica.* Journal of Catalysis, 2011. **279**(1): p. 136-143.
23. Song, W., G. Venimadhavan, J.M. Manning, M.F. Malone, and M.F. Doherty, *Measurement of residue curve maps and heterogeneous kinetics in methyl acetate synthesis.* Industrial & Engineering Chemistry Research, 1998. **37**(5): p. 1917-1928.
24. Bart, H.J., W. Kaltenbrunner, and H. Landschutzer, *Kinetics of esterification of acetic acid with propyl alcohol by heterogeneous catalysis.* International Journal of Chemical Kinetics, 1996. **28**(9): p. 649-656.
25. Ali, S.H. and S.Q. Merchant, *Kinetics of the esterification of acetic acid with 2-propanol: Impact of different acidic cation exchange resins on reaction mechanism.* International Journal of Chemical Kinetics, 2006. **38**(10): p. 593-612.
26. Carlson, E.C., *Don't gamble with physical properties for simulations.* Chemical Engineering Progress, 1996. **92**(10): p. 35-46.
27. Fredenslund, A., R.L. Jones, and J.M. Prausnitz, *Group-Contribution Estimation of Activity-Coefficients in Nonideal Liquid-Liquid mixtures.* Aiche Journal, 1975. **21**(6): p. 1086-1099.
28. Cunico, L.P., A.S. Hukkerikar, R. Ceriani, B. Sarup, and R. Gani, *Molecular structure-based methods of property prediction in application to lipids: A review and refinement.* Fluid Phase Equilibria, 2013. **357**: p. 2-18.
29. Poling, B.E., J.M. Prausnitz, and J.P. O'Connell, *The properties of gases and liquids*. 2001: McGraw-Hill.
30. Basso, R.C., F.H. Miyake, A.J.D. Meirelles, and E.A.C. Batista, *Liquid-liquid equilibrium data and thermodynamic modeling, at T/K=298.2, in the washing step of ethyl biodiesel production from crambe, fodder radish and macauba pulp oils.* Fuel, 2014. **117**: p. 590-597.
31. Ali, S.H., O. Al-Rashed, F.A. Azeez, and S.Q. Merchant, *Potential biofuel additive from renewable sources - Kinetic study of formation of butyl acetate by heterogeneously catalyzed transesterification of ethyl acetate with butanol.* Bioresource Technology, 2011. **102**(21): p. 10094-10103.
32. Pappu, V.K.S., A.J. Yanez, L. Peereboom, E. Muller, C.T. Lira, and D.J. Miller, *A kinetic model of the Amberlyst-15 catalyzed transesterification of methyl stearate with n-butanol.* Bioresource Technology, 2011. **102**(5): p. 4270-4272.

33. Lee, M.J., Y.C. Lo, and H.M. Lin, *Liquid-liquid equilibria for mixtures containing water, methanol, fatty acid methyl esters, and glycerol.* Fluid Phase Equilibria, 2010. **299**(2): p. 180-190.
34. Coelho, R., P.G. dos Santos, M.R. Mafra, L. Cardozo, and M.L. Corazza, *(Vapor plus liquid) equilibrium for the binary systems {water plus glycerol} and {ethanol plus glycerol, ethyl stearate, and ethyl palmitate} at low pressures.* Journal of Chemical Thermodynamics, 2011. **43**(12): p. 1870-1876.
35. Horstmann, S., T. Popken, and J. Gmehling, *Phase equilibria and excess properties for binary systems in reactive distillation processes Part I. Methyl acetate synthesis.* Fluid Phase Equilibria, 2001. **180**(1-2): p. 221-234.
36. Alvarez, V.H., S. Mattedi, M. Iglesias, R. Gonzalez-Olmos, and J.M. Resa, *Phase equilibria of binary mixtures containing methyl acetate, water, methanol or ethanol at 101.3 kPa.* Physics and Chemistry of Liquids, 2011. **49**(1): p. 52-71.
37. Schwaab, M. and J.C. Pinto, *Optimum reference temperature for reparameterization of the Arrhenius equation. Part 1: Problems involving one kinetic constant.* Chemical Engineering Science, 2007. **62**(10): p. 2750-2764.
38. Stewart, W.E. and M. Caracotsios, *Computer-aided modeling of reactive systems*. 2008: Wiley-Interscience.
39. Himmelblau, D.M., *Basic principles and calculations in chemical engineering*. 1989: Prentice Hall.
40. Draper, N.R. and H. Smith, *Applied regression analysis*. 1981: Wiley.
41. Atkinson, A.C., B. Bogacka, and M.B. Bogacki, *D- and T-optimum designs for the kinetics of a reversible chemical reaction.* Chemometrics and Intelligent Laboratory Systems, 1998. **43**(1-2): p. 185-198.
42. Zhang, Y. and T.F. Edgar, *PCA Combined Model-Based Design of Experiments (DOE) Criteria for Differential and Algebraic System Parameter Estimation.* Industrial & Engineering Chemistry Research, 2008. **47**(20): p. 7772-7783.

3

ADSORPTION AND REACTION IN THE TRANSESTERIFICATION OF ETHYL ACETATE WITH METHANOL ON LEWATIT K1221

This chapter is based on "Adsorption and Reaction in the Transesterification of Ethyl acetate with methanol on Lewatit K1221" by E. Van de Steene, J. De Clercq, J.W. Thybaut, Journal of Molecular Catalysis A: Chemical 359 (2012) 57-68

Abstract - *The reaction kinetics of the liquid-phase transesterification of ethyl acetate with methanol to methyl acetate and ethanol have been investigated as a model reaction for the transesterification of triglycerides in the production of biodiesel. The reaction has been catalyzed by the acid ion exchange resin Lewatit K1221. The effect of the initial reactant molar ratio and the temperature on the reaction kinetics was investigated and kinetic models, based on pseudo-homogeneous (PH), Eley-Rideal (ER) and Langmuir-Hinshelwood (LH) mechanisms, were used to describe the reaction rate. Because of the pronounced non-ideality of the reaction mixture, the kinetics were expressed in terms of activities Additional experiments, based on a D-optimum design of experiments, were performed to obtain more precise parameter estimates as required for final model discrimination. The kinetic model with the surface reaction of adsorbed methanol with ethyl acetate from the bulk as the rate-determining step according to an Eley-Rideal mechanism was found to best describe the observed kinetics. The corresponding rate equation agrees with a reaction mechanism in which physically adsorbed methanol reacts with protonated ethyl acetate.*

3.1. Introduction

As mentioned in the introductory chapter, transesterification of alkyl esters plays an important industrial role with numerous applications such as the production of biodiesel [1]. Nowadays most of these industrial processes are homogeneous base catalyzed. The disadvantages of this process are given in the introductory chapter. Sulfonic acid ion exchange resins are promising candidates for catalyzing the (trans)esterification. Kinetic models such as PH, ER and LH were used to describe the transesterification kinetics catalyzed with ion exchange resins.

The objective of this chapter is to investigate the transesterification kinetics of ethyl acetate (EtOAc) with methanol (MeOH) to form methyl acetate (MeOAc) and ethanol (EtOH) catalyzed by Lewatit K1221. Experiments in a perfectly mixed batch reactor have been performed and have been modeled to gain more insight into the reaction mechanism and the rate-determining step. Therefore, pseudo-homogeneous and adsorption-based models, such as Eley-Rideal and Langmuir-Hinshelwood, have been discriminated.

Lewatit K1221, a gel type resin, undergoes swelling in polar liquid media. As mentioned in Section 1.4.2, this swelling affects the reaction kinetics. However, because the discussion in this chapter is limited to a single catalyst, swelling was not explicitly taken into account in the model. When the scope is broadened to a wider range of catalysts, c.q., resins, in Chapter 4, their swelling behavior will be discussed in more detail.

3.2. Procedures

Transesterification reactions of ethyl acetate and methanol were experimentally investigated in a Lenz type liquid phase batch reactor. The catalyst properties and the reactor setup are described in more detail in Section 2.1 and 2.3 respectively. A reference experimental data set consisting of 1012 points from 68 experiments has been used for initial model regression. Subsequently, this data set was extended with 270 data points, from 17 experiments, according to a D-optimal design, see Section 2.5, for more precise parameter estimations and conclusive model discrimination.

To ascertain that the data represent intrinsic kinetics, the absence of mass-transfer resistance was evaluated as described in Section 2.3.4. The parameter estimation and model discrimination procedure has been described in detail in Section 2.5.

3.3 Kinetic model

The kinetic model for the ethyl acetate transesterification with methanol can be expressed according to either a pseudo-homogeneous or an adsorption reaction based reaction mechanism such as Langmuir-Hinshelwood (LH) or Eley-Rideal (ER) [2-5].

The pseudo-homogeneous kinetic equation is given by:

$$r = k_{PH}\left(a_{MeOH}a_{EtOAc} - \frac{1}{K_{eq}}a_{EtOH}a_{MeOAc}\right) \tag{3-1}$$

with k_{PH} the reaction rate coefficient, a_i the activity of component i and K_{eq} the equilibrium coefficient of the overall reaction.

For the adsorption-based models, the various LH mechanisms consist of five elementary steps, while the ER mechanisms consist of three elementary steps. The steps considered according to the rival mechanisms are summarized in Table 3-1. For the LH mechanisms, both reactants are adsorbed on a catalytically active site. Adsorbed ethyl acetate reacts with adsorbed methanol to form adsorbed methyl acetate and adsorbed ethanol. Methyl acetate and ethanol finally desorb from the active sites.

For the ER mechanisms, ethyl acetate or methanol first adsorbs on a catalytically active site. Then the adsorbed reactant reacts with the other reactant from the bulk phase to form methyl acetate and ethanol. One of these products is adsorbed. In the third step, the adsorbed product, methyl acetate or ethanol, desorbs.

Table 3-1 Elementary steps and reaction mechanism for the kinetic modeling of transesterification of ethyl acetate with methanol (* = active site).

Elementary reactions	Reaction mechanism			
	PH	LH	ER	
			alcohol adsorption	ester adsorption
$CH_3OH + * \rightleftarrows CH_3OH*$		1	1	
$CH_3CH_2COOCH_3 + * \rightleftarrows CH_3CH_2COOCH_3*$		1		1
$CH_3OH + CH_3CH_2COOCH_3 \rightleftarrows CH_3COOCH_3 + CH_3CH_2OH$	1			
$CH_3OH* + CH_3CH_2COOCH_3* \rightleftarrows CH_3COOCH_3* + CH_3CH_2OH*$		1		
$CH_3OH + CH_3CH_2COOCH_3* \rightleftarrows CH_3COOCH_3* + CH_3CH_2OH$				1
$CH_3OH* + CH_3CH_2COOCH_3 \rightleftarrows CH_3COOCH_3 + CH_3CH_2OH*$			1	
$CH_3CH_2OH* \rightleftarrows CH_3CH_2OH + *$		1	1	
$CH_3COOCH_3* \rightleftarrows CH_3COOCH_3 + *$		1		1

The determination of the rate equation for the ER-MeOH[1] model is described in detail now. The first step in the mechanism, i.e., methanol adsorption, is considered to be rate determining for the overall kinetics, see Table 3-1. By applying the law of mass action the rate expression becomes:

$$r = k_{MeOH}\left(a_{MeOH}a_{*} - \frac{1}{K_{MeOH}}a_{MeOH*}\right) \tag{3-2}$$

with k_{MeOH} the methanol adsorption rate coefficient, a_i the activity of component *i* in the bulk, a_{i*} the activity of adsorbed component *i* and a_* the activity of the free active sites, K_i the adsorption equilibrium coefficient of component *i*.

Since the overall reaction comprises a sequence of individual, elementary steps, the thermodynamic equilibrium coefficient for the overall reaction can be written as:

$$K_{eq} = \frac{K_{MeOH}K_{SR}}{K_{EtOH}} \tag{3-3}$$

with, K_{eq} the equilibrium coefficient of the overall reaction and K_{SR} the surface reaction equilibrium coefficient. Equation 3-3 is used to eliminate the unknown adsorption equilibrium coefficient K_{MeOH} in Equation 3-2.

Since the total concentration of 'available' active sites (C_{tot}) is constant, the following site balance can be made:

$$C_{tot} = C_{*} + C_{MeOH*} + C_{EtOH*} \tag{3-4}$$

with C_* the free active sites concentration and C_{i*} the concentration of the adsorbed component *i*.

Using the steady-state approximation for the surface intermediates and combining Equations 3-2, 3-3 and 3-4, the unobservable species concentrations C_{MeOH*}, C_{EtOH*} and C_* can be eliminated in terms of the bulk liquid concentrations C_{MeOH}, C_{EtOH}, C_{MeOAc}, C_{EtOAc} multiplied with their respective UNIFAC activity coefficients:

[1] The following convention has been adhered to in determining the short model names:

- the first two letters refer to the mechanism, i.e., Eley-Rideal (ER) or Langmuir-Hinshelwood (LH),
- in what follows, the rate-determining step is identified by referring (1) for ER to the component (MeOH, EtOAc, MeOAc or EtOH) of which the adsorption is rate-determining or if the surface reaction (SR) is rate determining, the letters refer to the adsorbing reagent (MeOH or EtOAc) followed by SR, and (2) for LH to the component (MeOH, EtOAc, MeOAc or EtOH) of which the adsorption is rate-determining or the rate-determining surface reaction (SR)

$$r = \frac{k_{MeOH}\left(a_{MeOH} - \frac{1}{K_{eq}}\frac{a_{MeOAc}a_{EtOH}}{a_{EtOAc}}\right)}{1 + \frac{K_{MeOH}}{K_{eq}}\frac{a_{MeOAc}a_{EtOH}}{a_{EtOAc}} + K_{EtOH}a_{EtOH}} \tag{3-5}$$

Similar expressions are obtained for the rate equations for the other models, see Table 3-2.

3.4 Experimental Results

3.4.1 Temperature effect on the transesterification

The temperature effect on the transesterification reaction rate was investigated by performing experiments between 303 and 333 K. In accordance with the Arrhenius law, a higher temperature results in a higher transesterification rate and a correspondingly higher ethyl acetate conversion at the same batch time, see Figure 3-1. The final equilibrium conversion is practically temperature independent, which is a logic consequence of the limited reaction enthalpy of the investigated transesterification reaction (Chapter 2) [5].

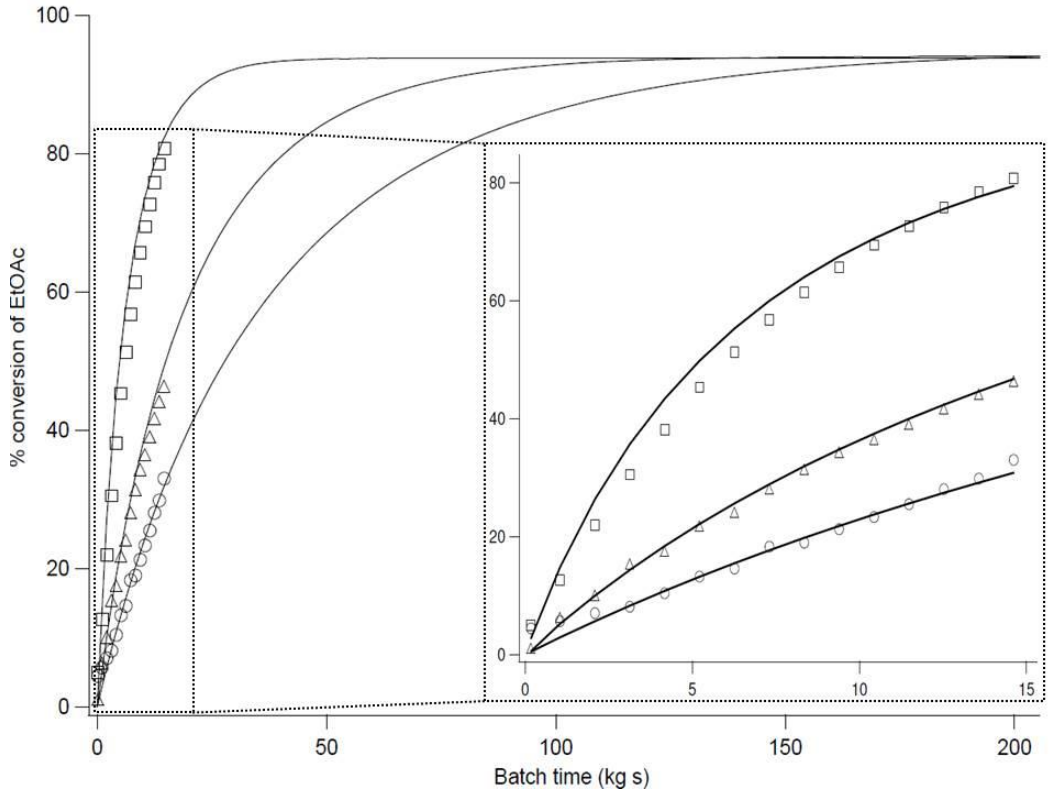

Figure 3-1 Simulated (lines) and experimental (symbols) conversion of ethyl acetate versus batch time at different temperatures (○ 303 K; Δ 313 K; □ 333 K). (Initial molar ratio of MeOH:EtOAc = 1:1, $C_{EtOAc,0}$= 1.79M, simulation model = ER-MeOH-SR)

Table 3-2 Reaction rates based on the mechanism and rate-determining step (with $K_i^{'} = K_i a_i$) for the transesterification of ethyl acetate and methanol.

Abbreviation	Rate-determining step	Corresponding reaction rate
	LH mechanism	
LH-MeOH	$CH_3COOH + * \rightleftarrows CH_3COOH*$	$r = \frac{k_{MeOH}\left(a_{MeOH} - \frac{1}{K_{eq}}\frac{a_{MeOAc}a_{EtOH}}{a_{EtOAc}}\right)}{1 + \frac{K_{MeOH}}{K_{eq}}\frac{a_{MeOAc}a_{EtOH}}{a_{EtOAc}} + K_{EtOAc}^{'} + K_{MeOAc}^{'} + K_{EtOH}^{'}}$
LH-EtOAc	$CH_3CH_2COOCH_3 + * \rightleftarrows CH_3CH_2COOCH_3*$	$r = \frac{k_{EtOAc}\left(a_{EtOAc} - \frac{1}{K_{eq}}\frac{a_{MeOAc}a_{EtOH}}{a_{MeOH}}\right)}{1 + K_{MeOH}^{'} + \frac{K_{EtOAc}}{K_{eq}}\frac{a_{MeOAc}a_{EtOH}}{a_{MeOH}} + K_{MeOAc}^{'} + K_{EtOH}^{'}}$
LH-SR	$CH_3COOH* + CH_3CH_2COOCH_3* \rightleftarrows CH_3COOCH_3* + CH_3CH_2OH*$	$r = \frac{k_{SR}K_{MeOH}K_{EtOAc}\left(a_{MeOH}a_{EtOAc} - \frac{1}{K_{eq}}a_{MeOAc}a_{EtOH}\right)}{\left(1 + K_{MeOH}^{'} + K_{EtOAc}^{'} + K_{MeOAc}^{'} + K_{EtOH}^{'}\right)^2}$
LH-EtOH	$CH_3CH_2OH* \rightleftarrows CH_3CH_2OH + *$	$r = \frac{k_{EtOH}K_{eq}\left(\frac{a_{MeOH}a_{EtOAc}}{a_{MeOAc}} - \frac{1}{K_{eq}}a_{EtOH}\right)}{1 + K_{MeOH}^{'} + K_{EtOAc}^{'} + K_{MeOAc}^{'} + K_{EtOH}K_{eq}\frac{a_{MeOH}a_{EtOAc}}{a_{MeOAc}}}$
LH-MeOAc	$CH_3COOCH_3* \rightleftarrows CH_3COOCH_3 + *$	$r = \frac{k_{MeOAc}K_{eq}\left(\frac{a_{MeOH}a_{EtOAc}}{a_{EtOH}} - \frac{1}{K_{eq}}a_{MeOAc}\right)}{1 + K_{MeOH}^{'} + K_{EtOAc}^{'} + K_{EtOH}^{'} + K_{MeOAc}K_{eq}\frac{a_{MeOH}a_{EtOAc}}{a_{EtOH}}}$
	ER mechanism with acetate adsorption	
ER-EtOAc	$CH_3CH_2COOCH_3 + * \rightleftarrows CH_3CH_2COOCH_3*$	$r = \frac{k_{EtOAc}\left(a_{EtOAc} - \frac{1}{K_{eq}}\frac{a_{MeOAc}a_{EtOH}}{a_{MeOH}}\right)}{1 + \frac{K_{EtOAc}}{K_{eq}}\frac{a_{MeOAc}a_{EtOH}}{a_{MeOH}} + K_{MeOAc}^{'}}$
ER-EtOAc-SR	$CH_3CH_2COOCH_3* + CH_3OH \rightleftarrows CH_3CH_2OH + CH_3COOCH_3*$	$r = \frac{k_{SR}K_{EtOAc}\left(a_{MeOH}a_{EtOAc} - \frac{1}{K_{eq}}a_{MeOAc}a_{EtOH}\right)}{1 + K_{EtOAc}^{'} + K_{MeOAc}^{'}}$
ER-MeOAc	$CH_3COOCH_3* \rightleftarrows CH_3COOCH_3 + *$	$r = \frac{k_{MeOAc}K_{eq}\left(\frac{a_{MeOH}a_{EtOAc}}{a_{EtOH}} - \frac{1}{K_{eq}}a_{MeOAc}\right)}{1 + K_{EtOAc}^{'} + K_{MeOAc}K_{eq}\frac{a_{MeOH}a_{EtOAc}}{a_{EtOH}}}$
	ER mechanism with alcohol adsorption	
ER-MeOH	$CH_3COOH + * \rightleftarrows CH_3COOH*$	$r = \frac{k_{MeOH}\left(a_{MeOH} - \frac{1}{K_{eq}}\frac{a_{MeOAc}a_{EtOH}}{a_{EtOAc}}\right)}{1 + \frac{K_{MeOH}}{K_{eq}}\frac{a_{MeOAc}a_{EtOH}}{a_{EtOAc}} + K_{EtOH}^{'}}$
ER-MeOH-SR	$CH_3COOH* + CH_3CH_2COOCH_3 \rightleftarrows CH_3CH_2OH* + CH_3COOCH_3$	$r = \frac{k_{SR}K_{MeOH}\left(a_{MeOH}a_{EtOAc} - \frac{1}{K_{eq}}a_{MeOAc}a_{EtOH}\right)}{1 + K_{MeOH}^{'} + K_{EtOH}^{'}}$
ER-EtOH	$CH_3CH_2OH* \rightleftarrows CH_3CH_2OH + *$	$r = \frac{k_{EtOH}K_{eq}\left(\frac{a_{MeOH}a_{EtOAc}}{a_{MeOAc}} - \frac{1}{K_{eq}}a_{EtOH}\right)}{1 + K_{MeOH}^{'} + K_{EtOH}K_{eq}\frac{a_{MeOH}a_{EtOAc}}{a_{MeOAc}}}$

3.4.2 Initial reactant molar ratio effect on the transesterification

The effect of the initial molar methanol to ethyl acetate ratio in the range of 1:1 to 10:1 is shown in Figure 3-2. Higher initial molar ratios result in higher ethyl acetate conversions. Because the initial EtOAc/catalyst amount ratio was kept constant in these experiments, this also corresponds to higher reaction rates. Also, the equilibrium conversion increases with increasing initial reactant molar ratio, see Figure 3-2. For lower initial MeOH:EtOAc ratios, longer batch times are needed to reach thermodynamic equilibrium.

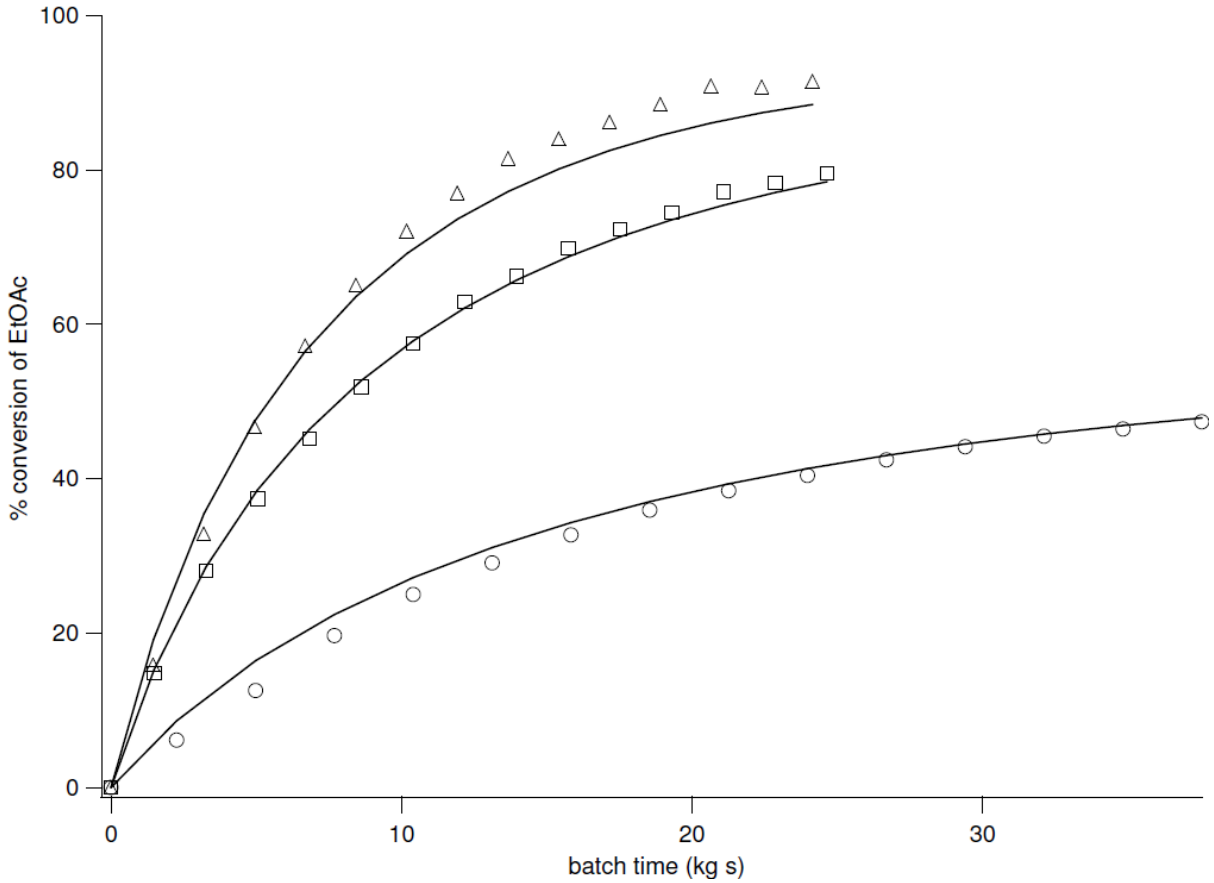

Figure 3-2 **Simulated (lines) and experimental (symbols) conversion of ethyl acetate versus batch time at different initial molar ratios (○ 1:1; □ 5:1; Δ 10:1). (Temperature = 333 K, $C_{EtOAc,0}$= 1.79 M, simulation model = ER-MeOH-SR)**

3.5 Model discrimination

The model parameters of the rival models reported in Table 3-2 have been estimated by regression as explained in Section 2.5. The corresponding Athena Visual Studio [6] code is included in Appendix C. Model discrimination is performed in order to determine the best performing model and, correspondingly, the most likely reaction mechanism, including the rate-determining step. Prior to regression and discrimination, initial parameter estimates have been determined.

3.5.1 Initial parameter estimates

Rate coefficients have first been determined via isothermal regressions using the PH model, see Figure 3-3. A linear regression of the obtained values to the Arrhenius relationship resulted in initial guesses for the activation energy E_A amounting to 50.3 kJ mol^{-1} and the rate coefficient at the reference temperature of 328 K amounting to 2.62 10^{-6} m^3 kg_{cat}^{-1} mol^{-1} s^{-1}.

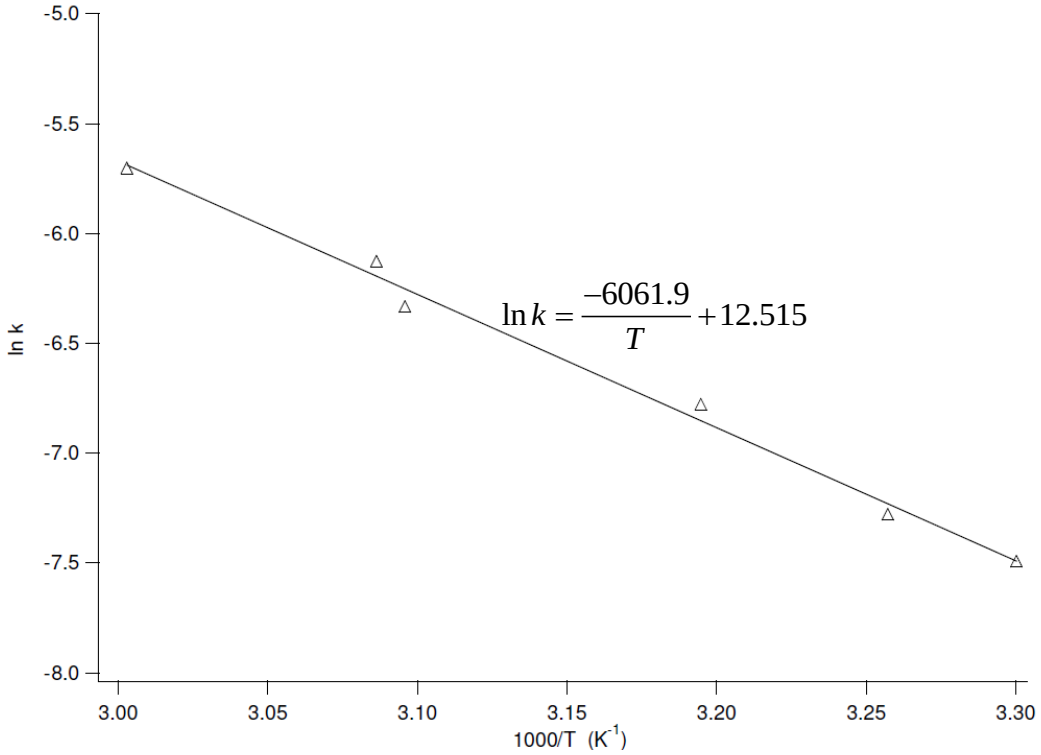

Figure 3-3 Arrhenius diagram for the transesterification rate coefficient of methanol and ethyl acetate using Lewatit K1221 catalyst (symbols obtained by isothermal regression with the PH model, line linear regression)

Initial values for the different adsorption equilibrium coefficients were taken from the literature and set equal to 0.1 m^3 mol^{-1} [7]. From initial regression efforts, it was clear that, in the rather narrow temperature range that has been investigated, the temperature dependence of the adsorption coefficients K_i would be practically impossible to estimate significantly. Hence, in an effort to reduce the number of adjustable parameters, the determination of adsorption coefficient values, K_i, has been limited to an average value over the investigated temperature range.

3.5.2 Performance evaluation between all rival models

The model regression and discrimination results are shown in Table 3-3. The obtained F values for the global significance of the regression range from 1 000 to 41 000. Typically,

only one or two of the adsorption equilibrium coefficients could be estimated significantly different from zero. As a result, various ER and LH models, such as ER-EtOAc and LH-EtOAc, LH-EtOH and ER-EtOH, and ER-MeOH and LH-MeOH, became mathematically equivalent to each other.

Table 3-3 Statistical evaluation of all models (1012 experimental points, experimental conditions Table 2-2)

Model	Number of statistically significantly estimated (total) parameters	RSSQ	F
ER-EtOAc / LH-EtOAc	3 (4) / 3 (7)	5	31 000
ER-MeOH-SR	4 (4)	5	21 000
ER-EtOAc-SR	4 (4)	7	15 000
PH	2 (2)	8	41 000
ER-EtOH / LH-EtOH	3 (4) / 3 (7)	9	20 000
ER-MeOAc / LH-MeOAc	3 (4) / 3 (7)	9	18 000
ER-MeOH / LH-MeOH	3 (4) / 3 (7)	25	8 000
LH-SR	4 (6)	59	1 000

The best performing models, i.e., those with the lowest residual sum of squares and the higher F value (31 000), correspond to an Eley-Rideal or a Langmuir-Hinshelwood mechanism with ethyl acetate adsorption as the rate-determining step (ER-EtOAc/LH-EtOAc). Model ER-MeOH-SR, corresponding to an Eley-Rideal mechanism with methanol adsorption and with the reaction of ethyl acetate from the bulk with adsorbed methanol on the catalyst surface as rate-determining step, has also a good performance in terms of the residual sum of squares. Because it contains an additional, significantly estimated parameter compared to the two previously discussed models, the corresponding F value for the global significance of the regression is limited to about 20 000, however. Similarly, the ER-EtOAc-SR model has a lower F value for the global significance of the regression, and moreover, the corresponding residual sum of squares is about 50% higher than that obtained with the above discussed models. The PH-model has an even higher residual sum of squares, but because this model has only two adjustable parameters, it has the highest F value for the global significance of the regression. The next four models that still perform reasonably well, i.e., ER-EtOH/LH-EtOH, ER-MeOAc/LH-MeOAc, all contain three significantly estimated parameters and correspond to Eley-Rideal mechanisms with ethanol desorption (LH-EtOH is mathematically equivalent to ER-EtOH), resp. methyl acetate desorption as rate-determining step (LH-MeOAc is mathematically equivalent to ER-MeOAc). However, the combination of (1) F values for the global significance of the regression below 20 000 and (2) RSSQ exceeding 8, is considered clearly inferior compared to the first described models. The

likelihood ratios of the best performing models compared to these 4 models exceed 18 and, hence, the latter can be rejected with a probability of 90 %. The other models, i.e., ER-MeOH/LH-MeOH, LH-SR, all have significantly higher residual sum of squares and corresponding F values below 10 000 and, hence, will not be further considered either.

The physical meaning of the remaining models (ER-EtOAc/LH-EtOAc, ER-MeOH-SR, ER-EtOAc-SR and PH) is explained below. ER-EtOAc corresponds to an Eley-Rideal mechanism with ethyl acetate adsorption as rate-determining step. Ethyl acetate adsorption is then followed by reaction with methanol from the bulk, see Table 3-1. The four adjustable parameters in this model are the activation energy and the rate coefficient $k_{EtOAc_{T_{ref}}}$ at the reference temperature, the adsorption equilibrium coefficient of respectively ethyl acetate and methyl acetate, K_{EtOAc} and K_{MeOAc}. The first three model parameters are estimated statistically significantly different from zero, while the adsorption equilibrium coefficient of methyl acetate is not. The final rate expression, hence, becomes:

$$r = \frac{k_{EtOAc}\left(a_{EtOAc}a_{MeOH} - \frac{1}{K_{eq}}\frac{a_{MeOAc}a_{EtOH}}{a_{MeOH}}\right)}{1+\frac{K_{EtOAc}}{K_{eq}}\frac{a_{MeOAc}a_{EtOH}}{a_{MeOH}}} \tag{3-6}$$

ER-MeOH-SR also corresponds to an Eley-Rideal mechanism but with the reaction of ethyl acetate from the bulk with adsorbed methanol on the catalyst surface as rate-determining step, see Table 3-2. The four adjustable parameters are the activation energy and the rate coefficient k_{sr} at reference temperature, the adsorption equilibrium coefficients of respectively ethanol and methanol, K_{EtOH} and K_{MeOH}. All these model parameters are estimated significantly different from zero. The corresponding rate expression is given in Table 3-2. ER-EtOAc-SR also corresponds to an Eley-Rideal mechanism with the reaction of adsorbed ethyl acetate with methanol from the bulk as rate-determining step, see Table 3-2. The four adjustable parameters are the activation energy and the rate coefficient k_{sr} at the reference temperature, the adsorption equilibrium coefficients of respectively ethyl acetate and methyl acetate K_{EtOAc} and K_{MeOAc} and are all estimated significantly different from zero. The corresponding rate expression is given in Table 3-2.

The PH model does not take into account any adsorption. Ethyl acetate and methanol react from the bulk to form ethanol and methyl acetate in the bulk. The corresponding rate expression and the explanation of the parameters is given in Equation 3.1 in Section 3.3.

3.5.3 Discrimination between best performing models using an experimental design

A D-optimum design of experiments has been performed aiming at a more precise parameter estimation in the remaining four rival models. This design is expected to simultaneously allow further model discrimination. It proposes experiments in the outer range of the operating conditions, in particular at an initial molar ratio of 1:1, a temperature of 303 K and a catalyst amount of 4.0 10^{-3} kg. These experiments have effectively been performed and the data points (270) were subsequently included in the data set used for regression and discrimination between the rival models. The statistical performance of the models is shown in Table 3-4, while the corresponding parameter estimates are reported in Table 3-5. The obtained F values range from 62 000 to 149 000.

Table 3-4 Statistical evaluation of the 4 rival models (1282 experimental points, experimental conditions: Table 2-2)

Model	Number of statistically significantly estimated (total) parameters	RSSQ	F
ER-MeOH-SR	4 (4)	27	62 000
ER-EtOAc-SR	3 (4)	35	78 000
PH	2 (2)	36	149 000
ER-EtOAc / LH-EtOAc	3 (4) / 3 (7)	48	47 000

ER-MeOH-SR has the lowest residual sum of squares (27) with all four adjustable parameters being estimated significantly. With one parameter less, ER-EtOAc-SR has a higher F value but also a significantly higher RSSQ (35). The PH-model only has 2 adjustable parameters which are both estimated significantly. This results in the highest F value among the considered models, despite the RSSQ which exceeds the smallest one, obtained with ER-MeOH-SR, by about one third. Due to the absence of any adsorption related terms in the PH-model, it cannot account for any surface coverage effects, however. ER-EtOAc/LH-EtOAc, with only three parameters that are estimated significantly different from zero, has an even higher RSSQ. Hence, this model is considered to describe the experimental data set not adequately.

The likelihood ratio of ER-MeOH-SR and ER-EtOAc-SR (Equation 2-12) is higher than 18, showing that there is a higher probability that the ER-MeOH-SR-model describes the data set better than the ER-EtOAc-SR-model.

Table 3-5 Parameter estimates with their 95% confidence interval, obtained by regression of 1282 experimental points. (T_{ref} = 328.38 K)

	ER-EtOAc LH-EtOAc	ER-MeOH-SR	ER-EtOAc-SR	PH
$k_{T_{ref}}$ (10^{-3} m^3 kg_{cat}^{-1} mol^{-1} s^{-1})	0.053 ± 0.002	0.259 ± 0.052	67.130 ± 0.719	0.003 ± 0.00003
E_A (kJ mol^{-1})	52.538 ± 1.542	50.190 ± 0.940	49.328 ± 0.995	49.405 ± 0.967
K_{EtOAc}	2.643 ± 0.194	a	a	a
K_{EtOH}	a	0.233 ± 0.040	a	a
K_{MeOH}	a	0.015 ± 0.004	a	a
K_{MeOAc}	a	a	0.052 ± 0.019	a

a not present in the model

Activation energies of about 50 kJ mol^{-1} are obtained, irrespective of the model used. These activation energies are in fact a composite activation energy, comprising the elementary steps involved in the reaction mechanism. This will be discussed in detail in section 4.5. For a transesterification reaction catalyzed by an acid ion exchange resin similar results were published in literature [4, 5, 7, 8]. E.g. López et al. [7] found for the transesterification of triacetin to diacetin an activation energy of 48.5 kJ mol^{-1} on a Nafion® SAC-13 ion exchange resin and an activation energy of 46.1 kJ mol^{-1} for sulphuric acid, as a homogeneous catalyst. An activation energy of 20 kJ mol^{-1} was determined by Dossin et al. [9] for the transesterification of ethyl acetate with methanol on a base MgO catalyst.

The $k_{T_{ref}}$ at 328.38 K varies between 0.003 10^{-3} and 67.130 10^{-3} m^3 kg_{cat}^{-1} mol^{-1} s^{-1}, depending on the model used. This value is similar to the one published by Bożek-Winkler and Gmehling [5] for the transesterification of methyl acetate and n-butanol catalyzed by Amberlyst 15.

The estimated values of the adsorption equilibrium coefficients for the transesterification with acid ion exchange resins, are quite similar with the published ones [5, 7, 8]. Based on the structural similarity and on the acid dissociation coefficient of MeOH and EtOH, which are rather close to each other, Dossin et al. [10] decided to estimate a single adsorption equilibrium coefficient for both alcohols. Data published by Bożek-Winkler and Gmehling [5] and Tesser et al. [11] indicate that the alcohol adsorption equilibrium coefficient values are indeed relatively close to each other, but that the one corresponding to methanol has the lowest value. The ratio of the adsorption coefficients as determined from the ER-MeOH-SR model amounts to 15. In particular the value obtained for K_{EtOH} significantly exceeds the one reported in literature, i.e., 0.233 versus 0.0289 [5]. As a result, a refined version of this model has been tested, in which this ratio has been fixed to 2. The

remaining three adjustable parameters have been determined by regression. With an RSSQ of 31 and an F value amounting to 80 000 with only three adjustable parameters, this refined version performs statistically better than the original ER-MeOH-SR model but is still inferior to the PH model. Hence, an ultimate model refinement consisted of fixing the adsorption coefficients for methanol and ethanol at their literature determined values, i.e., 0.0140 and 0.0289, respectively [5]. With an RSSQ amounting to 36 and a corresponding F value of 142 000, this ultimate version of the ER-MeOH-SR model is statistically practically identical to the PH model.

Besides the statistical significance of the models, the models are also evaluated on their physicochemical significance. Sulfonic acid ion exchange resins show a higher affinity for alcohols than for esters [5, 12-16]. This indicates that methanol will adsorb more strongly than ethyl acetate, which is in line with the assumptions made in ER-MeOH-SR but in clear contrast with the assumptions made in ER-EtOAc/LH-EtOAc and ER-EtOAc-SR. These physicochemical considerations, combined with the higher RSSQ of the latter models, see Table 3-5, lead to the elimination of ER-EtOAc/LH-EtOAc and ER-EtOAc-SR from the list of rival models. The PH-model lacks any adsorption effect. The good statistical performance of the PH-model, in terms of F value for the significance of the regression is an indication that the partial replacement of adsorbed methanol reactant by adsorbed ethanol product has only a limited effect on the simulated ethyl acetate concentration at the investigated operating conditions. Fixing the adsorption coefficient values K_{MeOH}, K_{EtOH} in ER-MeOH-SR at literature reported values, the corresponding F value and RSSQ of ER-MeOH-SR become comparable with the statistical results of the PH model. Hence, because of the additional physicochemical phenomena accounted for in the former model based on literature reported parameter values, ER-MeOH-SR is selected from the rival models as the most adequate model.

Figure 3-4 shows the residual diagram of the experimental and calculated ethyl acetate concentration using ER-MeOH-SR. The diagram shows a good agreement between experimental and simulated values and is not indicative of any systematic deviation. The agreement between ER-MeOH-SR model calculations and the experimental data is also evident from Figure 3-1 and Figure 3-2.

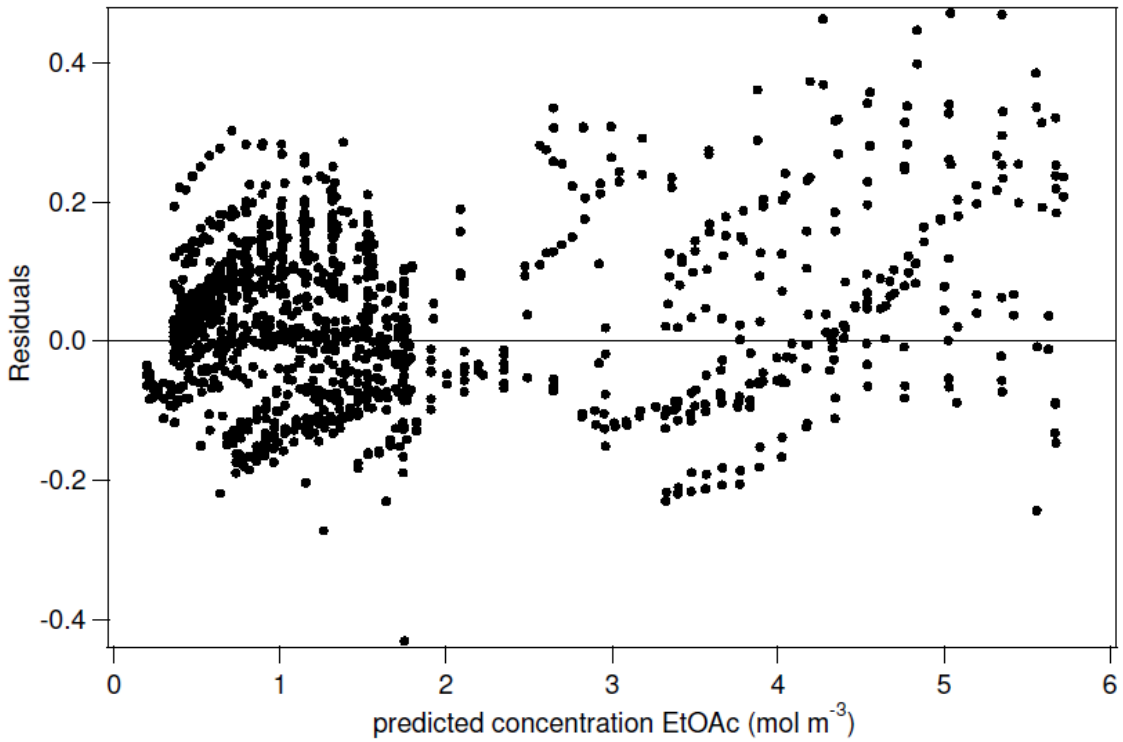

Figure 3-4 **Residual diagram for the concentration of ethyl acetate for the complete set of 1282 data points. The calculated values are obtained using Eq. 3-6) with the estimated model parameters of ER-MeOH-SR (Table 3-5). Range of experimental conditions (Table 2-2).**

3.6 Selected model assessment

3.6.1 Further considerations on the actual reaction mechanism

Homogeneous, acid catalyzed transesterification occurs via a mechanism that is equivalent to hydrolysis [17], see Figure 3-5. It starts with the protonation of the carboxyl group of the ester, c.q., ethyl acetate, step 1, followed by a nucleophilic attack of the alcohol, c.q., methanol, on this protonated ester, step 2, yielding a tetrahedral intermediate. The overall results of step 3 is that a proton is removed from the reacting methanol oxygen atom and that one proton is added to the product ethanol oxygen atom after which the tetrahedral intermediate decomposes into a protonated methyl acetate and ethanol, step 4. The fifth and last step in the reaction mechanism is the regeneration of the acid site [7, 17-23].

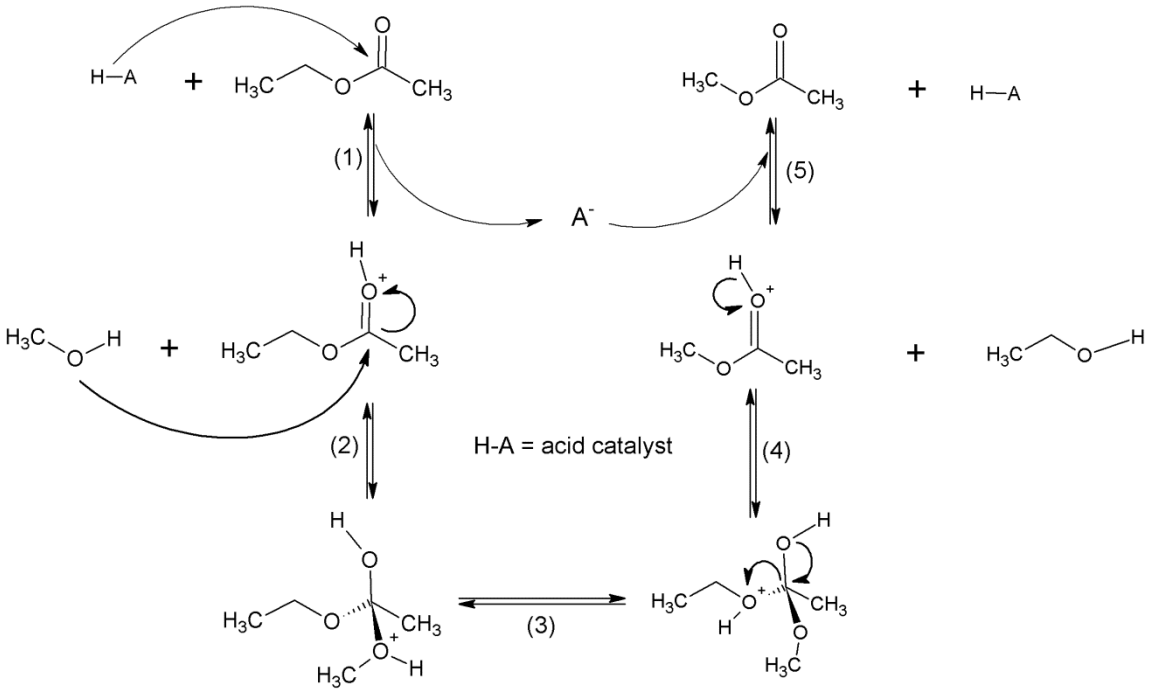

Figure 3-5 Homogeneous acid-catalyzed reaction mechanism for the transesterification of ethyl acetate with methanol

According to the selected ER-MeOH-SR model, the transesterification mechanism on Lewatit K1221, would be clearly distinct from the mechanism presented in Figure 3-5. Methanol should be adsorbed on the catalyst's active site with ethyl acetate reacting from the bulk, see Table 3-1 and section 3.5.3, while, according to the homogeneously catalyzed mechanism, it should be ethyl acetate which is adsorbed, c.q., protonated on the acid sites with methanol reacting from the bulk. This apparent contradiction can be explained by invoking a physical adsorption step in the mechanism, which is preceding any chemical elementary step on the acid sites. In this mechanism including reactant physical adsorption, both methanol and ethyl acetate are physisorbed in the pores of the resin. The physisorption of methanol being more pronounced than that of ethyl acetate, the physisorption of methanol is more likely to experience saturation effects, while that of ethyl acetate is situated in the Henry regime. Starting from these physically adsorbed reactants, the homogeneous, acid catalyzed mechanism can occur within the resin's pores, i.e., ethyl acetate protonation followed by reaction with methanol. As a result, an overall rate equation for transesterification on Lewatit K1221 will require an adsorption term for methanol but not for ethyl acetate, if in addition to the physisorption in the Henry regime, also the chemisorption/protonation of ethyl acetate is not suffering from saturation effects. Given the pK_a values of methanol and ethyl acetate, i.e., 16 vs. 21, it is indeed the protonation of ethyl acetate which can be expected to be more pronounced than that of methanol.

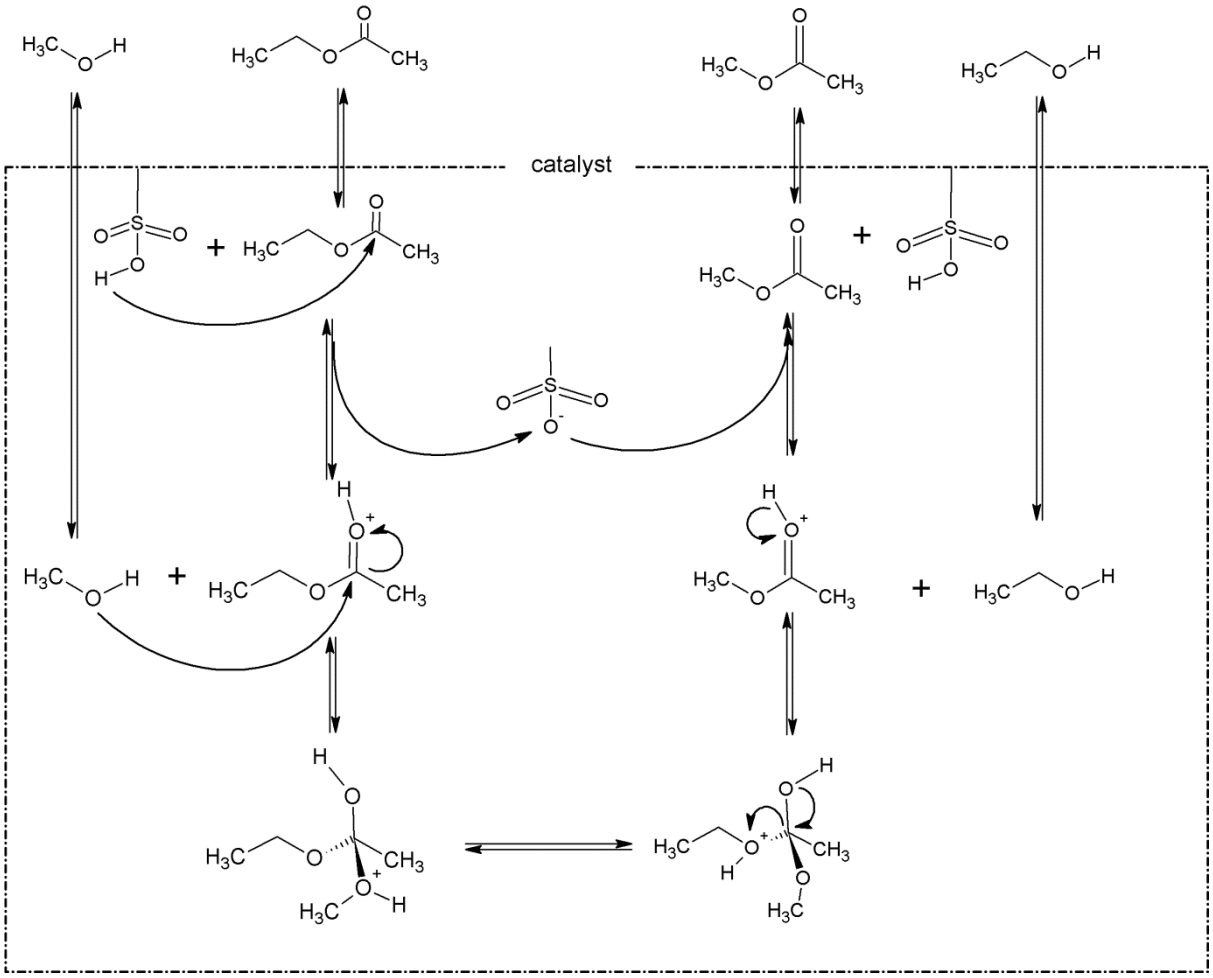

Figure 3-6 Heterogeneous acid ion exchange resin catalyzed reaction mechanism for the transesterification of ethyl acetate with methanol.

The above considerations about the reaction mechanism are in agreement with the results obtained by López et. al. [7]. These authors identified a methanol partial reaction order which tends to zero at high methanol concentrations [24]. It indicates the importance of accounting for methanol adsorption in the reaction mechanism, even if methanol is unlikely to interact directly with the acid sites. As a result, López et al. [7] ultimately derived a rate equation starting from a classical Eley-Rideal mechanism with ester adsorption on the active sites and reaction with methanol from the bulk, that was extended with a methanol adsorption term, $K_{MeOH}C_{MeOH}$. An adsorption term corresponding to the product ester was not included. The adsorption coefficients for methanol and the reacting ester, K_{MeOH} and K_{TG}, were small and similar. However, due to the significantly higher methanol concentration than ester concentration, only the methanol adsorption term was mathematically significant, as it is the case in the model developed as part of the present work.

The view on the acid catalyzed transesterification by ion exchange resins developed in this work also agrees with the interpretation by Alonso et al. [18]. The principal peculiarities in heterogeneous versus homogeneous transesterification observed by these authors were as follows: first, the activation of the carbonyl group of the ester comes with the chemisorption of the ester molecule on the Brønsted active site. Second, methanol is involved in the rate-determining step in the Eley-Rideal model. Methanol is not chemisorbed in this rate-determining elementary step, although it can be chemisorbed on the Brønsted acid sites. The methanol involved in the rate-determining step comes from the liquid medium present in the pores of the solid catalyst [18] (Figure 3-6).

3.6.2 Evolution of the physisorbed fractions in the catalyst pores

The evolution of the physisorbed methanol and ethanol fractions, i.e., θ_{MeOH*} and θ_{EtOH*}, as well as the fraction of free adsorption sites, θ_*, as a function of batch time at different experimental conditions has been calculated using the site balance and the quasi-equilibrium assumption for methanol and ethanol adsorption and are shown in Figure 3-7:

$$1 = \theta_* + \theta_{MeOH*} + \theta_{EtOH*} \tag{3-7}$$

$$\theta_* = \frac{1}{1 + K_{MeOH} a_{MeOH} + K_{EtOH} a_{EtOH}} \tag{3-8}$$

$$\theta_{MeOH*} = \frac{K_{MeOH} a_{MeOH}}{1 + K_{MeOH} a_{MeOH} + K_{EtOH} a_{EtOH}} \tag{3-9}$$

$$\theta_{EtOH*} = \frac{K_{EtOH} a_{EtOH}}{1 + K_{MeOH} a_{MeOH} + K_{EtOH} a_{EtOH}} \tag{3-10}$$

At 333K and an initial molar methanol to ethyl acetate ratio of 10:1, about 80 % of the physisorption sites is free while 20 % is occupied by methanol at the start of the experiment. Near completion of the experiment, the fraction of free sites is reduced to about 60 %, while 25% is occupied by ethanol and 15 % by methanol. The fraction of free physisorption sites on the catalyst decreases with increasing batch time, because ethanol physisorbs more strongly in the catalyst's pores than methanol. As a result, rather than saturation effects by methanol physisorption, some product inhibition effect will occur, because the product ethanol is occupying about one fourth of the available pore volume of the catalyst. At lower initial molar methanol to ethyl acetate ratios, this product inhibition effect will, accordingly, be more pronounced, because of the higher ester and, hence, product ethanol concentration.

Given the dominance of the fraction of free sites, the above described inhibition effects are only having a moderate effect on the calculated reaction rates. This is in agreement with the model discrimination on a statistical basis, in which the PH model was considered equivalent to the ER-MeOH-SR model.

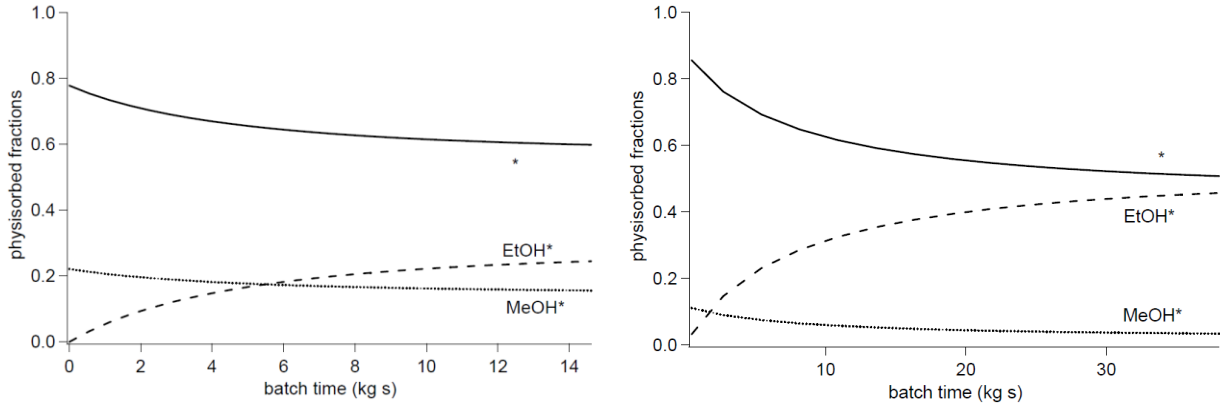

Figure 3-7 **Calculated physisorbed fractions as a function of batch time at 333 K, and with MeOH:EtOAc = 10:1 (left) and 1:1 (right). (MeOH* and EtOH* physisorbed fractions of methanol and ethanol, respectively; (*) fraction of free physisorption sites).**

3.7 Conclusions

Acid catalyzed transesterification reactions occur via a mechanism involving ester protonation followed by reaction with the alcohol. The use of sulfonic acid ion exchange resins such as Lewatit K1221, induces a physisorption step prior to the chemical elementary steps of the reaction mechanism. Because the physisorption of alcohols is more pronounced than that of esters, a model discrimination between a pseudo-homogeneous model and Langmuir-Hinshelwood and Eley-Rideal models with varying assumptions related to the rate-determining step and reactant and product adsorption, resulted in the selection of an Eley Rideal mechanism considering methanol adsorption with subsequent reaction with ethyl acetate from the bulk as rate-determining step as the most adequate model. No adsorption term related to ethyl acetate protonation had to be incorporated, indicating that the resin's acid sites were mainly unoccupied at the investigated operating conditions.

The model discrimination demonstrates the need of an assessment of the physical significance of the model and the corresponding parameters. This can be achieved by comparison with literature reported information on the various elementary steps in the reaction mechanism. The combined information about the homogeneously acid catalyzed

transesterification reaction mechanism and physical adsorption measurements of alcohols and esters on resins has allowed an advanced interpretation of the selected model based on typical discrimination activities.

In Chapter 4, the proposed model and reaction mechanism are evaluated to describe the kinetics of the transesterification catalyzed by macroporous ion exchange resins such as Lewatit K2640, Lewatit K2629 and Amberlyst 15. The ability of the proposed model to describe the swelling will also be addressed.

3.8 References

1. Ma, F. and M.A. Hanna, *Biodiesel production: a review.* Bioresource Technology, 1999. **70**(1): p. 1-15.
2. Teo, H.T.R. and B. Saha, *Heterogeneous catalysed esterification of acetic acid with isoamyl alcohol: kinetic studies.* Journal of Catalysis, 2004. **228**(1): p. 174-182.
3. Saha, B. and M.M. Sharma, *Reaction of dicyclopentadiene with formic acid and chloroacetic acid with and without cation-exchange resins as catalysts.* Reactive & Functional Polymers, 1997. **34**(2-3): p. 161-173.
4. Xu, B.Y., W.J. Zhang, X.M. Zhang, and C.F. Zhou, *Kinetic Study of Transesterification of Methyl Acetate with n-Butanol Catalyzed by NKC-9.* International Journal of Chemical Kinetics, 2009. **41**(2): p. 101-106.
5. Bozek-Winkler, E. and J. Gmehling, *Transesterification of methyl acetate and n-butanol catalyzed by Amberlyst 15.* Industrial & Engineering Chemistry Research, 2006. **45**(20): p. 6648-6654.
6. Stewart, W.E. and M. Caracotsios, *Computer-aided modeling of reactive systems*. 2008: Wiley-Interscience.
7. Lopez, D.E., J.G. Goodwin, and D.A. Bruce, *Transesterification of triacetin with methanol on Nafion (R) acid resins.* Journal of Catalysis, 2007. **245**(2): p. 381-391.
8. Ali, S.H., O. Al-Rashed, F.A. Azeez, and S.Q. Merchant, *Potential biofuel additive from renewable sources - Kinetic study of formation of butyl acetate by heterogeneously catalyzed transesterification of ethyl acetate with butanol.* Bioresource Technology, 2011. **102**(21): p. 10094-10103.
9. Dossin, T.F., M.F. Reyniers, and G.B. Marin, *Kinetics of heterogeneously MgO-catalyzed transesterification.* Applied Catalysis B-Environmental, 2006. **62**(1-2): p. 35-45.
10. Dossin, T.F., M.F. Reyniers, R.J. Berger, and G.B. Marin, *Simulation of heterogeneously MgO-catalyzed transesterification for fine-chemical and biodiesel industrial production.* Applied Catalysis B-Environmental, 2006. **67**(1-2): p. 136-148.
11. Tesser, R., L. Casale, D. Verde, M. Di Serio, and E. Santacesaria, *Kinetics and modeling of fatty acids esterification on acid exchange resins.* Chemical Engineering Journal, 2010. **157**(2-3): p. 539-550.
12. Qu, Y.X., S.J. Peng, S. Wang, Z.Q. Zhang, and J.D. Wang, *Kinetic Study of Esterification of Lactic Acid with Isobutanol and n-Butanol Catalyzed by Ion-exchange Resins.* Chinese Journal of Chemical Engineering, 2009. **17**(5): p. 773-780.
13. Sanz, M.T., R. Murga, S. Beltran, J.L. Cabezas, and J. Coca, *Kinetic study for the reactive system of lactic acid esterification with methanol: Methyl lactate hydrolysis reaction.* Industrial & Engineering Chemistry Research, 2004. **43**(9): p. 2049-2053.
14. Sanz, M.T., R. Murga, S. Beltran, J.L. Cabezas, and J. Coca, *Autocatalyzed and ion-exchange-resin-catalyzed esterification kinetics of lactic acid with methanol.* Industrial & Engineering Chemistry Research, 2002. **41**(3): p. 512-517.
15. Zhang, Y., L. Ma, and J.C. Yang, *Kinetics of esterification of lactic acid with ethanol catalyzed by cation-exchange resins.* Reactive & Functional Polymers, 2004. **61**(1): p. 101-114.
16. Delgado, P., M.T. Sanz, and S. Beltran, *Kinetic study for esterification of lactic acid with ethanol and hydrolysis of ethyl lactate using an ion-exchange resin catalyst.* Chemical Engineering Journal, 2007. **126**(2-3): p. 111-118.
17. Smith, M. and J. March, *March's advanced organic chemistry: reactions, mechanisms, and structure*. 2007: Wiley-Interscience.

18. Alonso, D.M., M.L. Granados, R. Mariscal, and A. Douhal, *Polarity of the acid chain of esters and transesterification activity of acid catalysts.* Journal of Catalysis, 2009. **262**(1): p. 18-26.
19. Lotero, E., Y.J. Liu, D.E. Lopez, K. Suwannakarn, D.A. Bruce, and J.G. Goodwin, *Synthesis of biodiesel via acid catalysis.* Industrial & Engineering Chemistry Research, 2005. **44**(14): p. 5353-5363.
20. Di Serio, M., R. Tesser, M. Dimiccoli, F. Cammarota, M. Nastasi, and E. Santacesaria, *Synthesis of biodiesel via homogeneous Lewis acid catalyst.* Journal of Molecular Catalysis a-Chemical, 2005. **239**(1-2): p. 111-115.
21. Di Serio, M., R. Tesser, L. Pengmei, and E. Santacesaria, *Heterogeneous catalysts for biodiesel production.* Energy & Fuels, 2008. **22**(1): p. 207-217.
22. Lotero, E., J.G. Goodwin, D.A. Bruce, K. Suwannakarn, Y.J. Liu, and D.E. Lopez, *The Catalysis of Biodiesel Synthesis*, in *Catalysis, Vol 19*, J.J. Spivey and K.M. Dooley, Editors. 2006, Royal Soc Chemistry: Cambridge. p. 41-83.
23. Schuchardt, U., R. Sercheli, and R.M. Vargas, *Transesterification of vegetable oils: a review.* Journal of the Brazilian Chemical Society, 1998. **9**(3): p. 199-210.
24. Mazzotti, M., B. Neri, D. Gelosa, A. Kruglov, and M. Morbidelli, *Kinetics of liquid-phase esterification catalyzed by acidic resins.* Industrial & Engineering Chemistry Research, 1997. **36**(1): p. 3-10.

4

ION-EXCHANGE RESIN CATALYZED ETHYL ACETATE TRANSESTERIFICATION WITH METHANOL: GEL VERSUS MACROPOROUS RESINS

This chapter is based on "Ion Exchange resin catalyzed transesterification of Ethyl Acetate with Methanol: Gel versus Macroporous resins" by E. Van de Steene, J. De Clercq, J.W. Thybaut, Chemical Engineering Journal 242 (2014) 170-179

Abstract - *The liquid-phase ethyl acetate transesterification kinetics with methanol to methyl acetate and ethanol catalyzed by gel (Lewatit K1221) and macroporous (Lewatit K2640, Lewatit K2629 and Amberlyst 15) ion-exchange resins have been investigated. The effects of the resins' swelling, the initial reactant molar ratio (1:1 – 10:1) and the temperature (303.15K - 333.15K) on the reaction kinetics were assessed. Macroporous Lewatit K2629, Lewatit K2640 and Amberlyst 15 exhibit a clearly inferior catalytic activity compared to the gel type Lewatit K1221, despite the similar number of sulfonic acid active sites. This trend in catalytic activity can be explained by the differences in acid site accessibility, which are related to the resins' swelling behavior and, hence, the amount of divinylbenzene cross-linking in the polymeric structure. A fundamental kinetic model, accounting for the chemical elementary steps as well as for the physical swelling due to solvent sorption, was constructed. According to this model (1) all active sites are initially occupied by protonated methanol, (2)*

the esters are activated by a proton exchange with protonated methanol and (3) the reaction occurs through an Eley-Rideal mechanism with the surface reaction of protonated ethyl acetate with methanol from the bulk as the rate-determining step. The kinetic model adequately described the experimental data as a function of temperature, initial molar ratio and catalyst resin type. A value of 49 kJ mol^{-1} was obtained for the activation energy, irrespective of the resin used. Differences in catalytic activity caused by the accessibility of the active sites are reflected by the values obtained for the reaction rate coefficient, which is 3- to 4-fold higher for a gel type resin compared to the macroporous ones.

4.1 Introduction

As explained in Chapter I is swelling due to solvent sorption is of particular importance in the use of ion-exchange resins as catalysts for the liquid phase transesterification reaction [1, 2]. Studies on the kinetics of the acetic acid and amyl alcohol esterification catalyzed by gel and macroporous resins [3, 4] typically observed a higher activity of the gel type resin versus the macroporous one, e.g. Amberlyst 15. However, a comprehensive theory for describing sorption and swelling behaviour of various components on a wide range of resins, related to resin catalyzed kinetics is not available yet [5]. Nevertheless, for the esterification of free fatty acids with methanol, Tesser et al. [1] accounted already for swelling phenomena in their kinetic model, by the use of a physical phase equilibrium relationship between the resin-absorbed and the external liquid phase.

The aim of this chapter is to enhance the kinetic model for ethyl acetate transesterification with methanol on a gel type resin as developed in Chapter 3 and extend its applicability to macroporous type ion exchange resins, c.q., Lewatit K2640, Lewatit K2629, and Amberlyst 15. The model should adequately capture the effect of the reaction temperature and initial molar alcohol to ester ratio on ethyl acetate transesterification with methanol. The model is based on an ion-exchange rather than an adsorption mechanism that also takes the swelling into account. The enhanced model performance will be compared with respect to the ER-MeOH-SR model proposed in Chapter 3. To gain more insight into the reaction occurring on the active sites of the catalyst, the surface fractions at different temperatures or different initial molar ratios are calculated.

4.2 Procedures

Ethyl acetate transesterification with methanol was experimentally investigated in a batch reactor. The catalyst properties and the reactor setup are described in more detail in Sections 2.1 and 2.3.1 respectively. The experiments for the four resins, c.q., Lewatit K1221, Lewatit K2629, Lewatit K2640 and Amberlyst 15, were performed within the range of experimental conditions of Table 2-2. The experimental data consist for the respective resins of 1282 points from 85 experiments (experimental data described and used in Chapter 3), 702 points from 47 experiments, 233 points from 18 experiments and 129 points from 11 experiments. Similar to transesterification on the gel type resin, the data sets on the macroporous resins were constructed starting from a factorial design followed by D-optimal

sequential design for more precise parameter estimations and conclusive model discrimination. To ascertain that the data represent intrinsic kinetics, the absence of mass-transfer resistance was evaluated as described in Section 2.3.4. The parameter estimation and model discrimination procedure has been described in detail in Section 2.5. The Athena Visual Studio [6] code is included in Appendix C.

4.3 Experimental results

4.3.1 Volumetric swelling tests

The volumetric swelling tests, see Table 4-1, indicate that resins' swelling is more pronounced when it is in contact with an alcohol compared to an ester. For the gel type resin, K1221, the swelling ratio nicely follows the dielectric constant of the considered components. This overall trend is preserved for the macroporous resins, however, due to their more rigid structure, the corresponding swelling is less pronounced, compared to a gel type resin, especially in solvents with a high dielectric constant.

The swelling ratio of the gel type resin, Lewatit K1221, increases with the initial molar ratio (Table 4-2). This can be explained by the higher polarity of the mixture. For the macroporous resin Lewatit K2640, the swelling ratio is independent of the initial molar ratio (Table 4-2). This can be explained by its higher degree of crosslinking, even with a less polar reaction mixture the maximum swelling ratio is already reached.

Table 4-1 Swelling ratio (S) of different resins in different pure solvents and the dielectric constant of the pure solvents

Swelling ratio	MeOH	EtOH	EtOAc	MeOAc
K1221	2.45 ± 0.07	2.34 ± 0.04	1.23 ± 0.04	1.24 ± 0.05
K2640	1.55± 0.05	1.56 ± 0.01	1.33 ± 0.03	1.32 ± 0.03
K2629	1.49 ± 0.08	1.50 ± 0.02	1.30 ± 0.03	1.32 ± 0.03
Amberlyst 15	1.43 ± 0.06	1.50 ± 0.03	1.35 ± 0.02	1.33 ± 0.07
Dielectric constant	32.7	24.5	6.02	6.70

Table 4-2 Swelling ratio (S) of resins K1221 and K2640 in reaction mixtures with different initial molar ratios MeOH:EtOAc (conversion 0%)

Swelling ratio	MR 10:1	MR 5:1	MR 1:1
K1221	2.5	2.1	1.8
K2640	1.5	1.5	1.5

Several factors potentially determine the swelling phenomenon [1], i.e., (1) the nature of the solvent: polar or apolar; (2) the degree of cross-linking of the resin; (3) the nature of the functional groups in the resin and (4) the resins' exchange capacity. For the resins considered in this chapter, factors (1) and (2) can be invoked to explain the observations. The more polar the solvent and, hence, the higher the dielectric constant, the higher the swelling ratio. A more pronounced cross-linking results in a decrease of the swelling ratio and a limitation of the volume increase due to swelling of 50 %. Various authors reported similar results for the effect of the solvent polarity and the degree of cross-linking [3, 7-15].

4.3.2 Catalytic activity

The catalytic activity of the four ion-exchange resins for transesterification is shown in Figure 4-1. Lewatit K1221 exhibits a noticeably higher activity than the other resins, despite the comparable active site concentration, see Table 2-2. The catalytic activity of K2629 and K2640 is rather similar while the lowest transesterification rates are observed with Amberlyst 15.

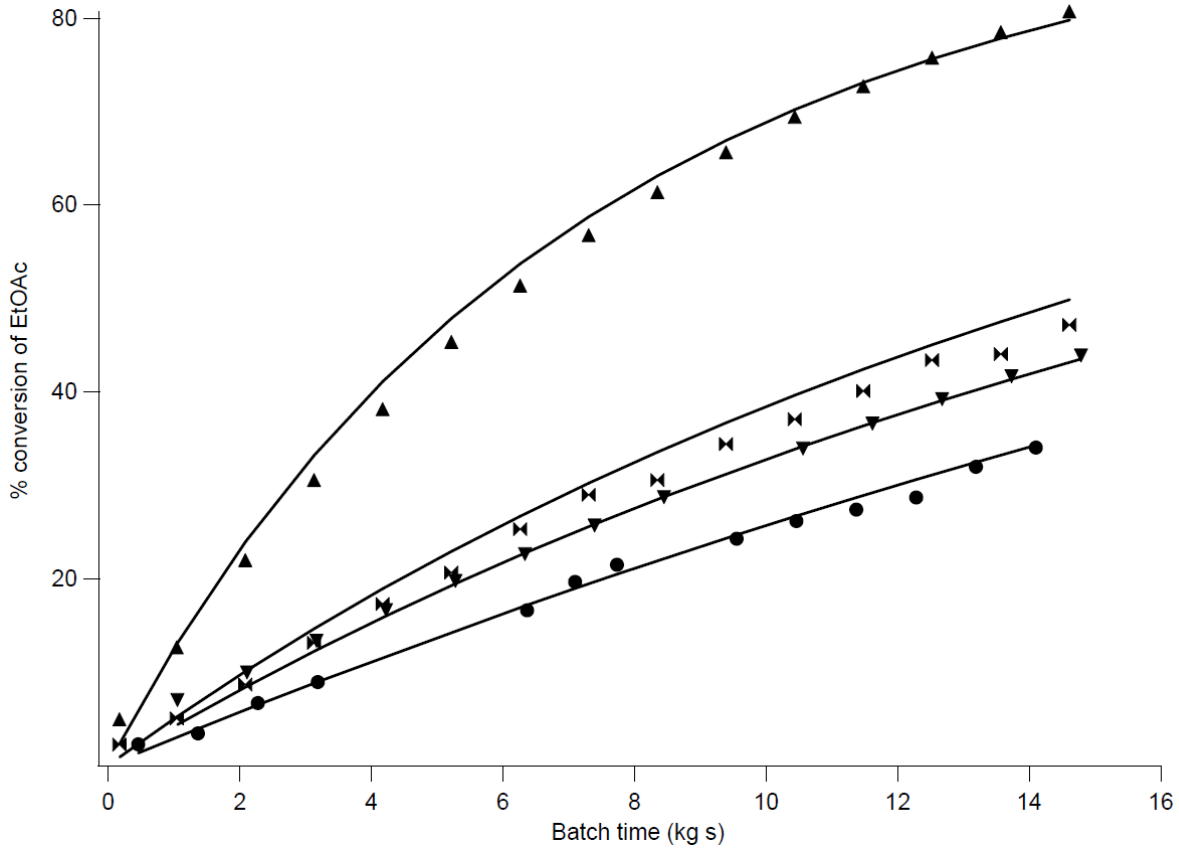

Figure 4-1 **Simulated (ER-exchange model, Eq. 4-4 with parameters as reported in Table 4-3) (lines) and experimental (symbols) conversion of ethyl acetate versus batch time catalyzed by different ion-exchange resins (▲K1221, ▼ K2629, ⋈ K2640, ● Amberlyst 15). (Initial molar ratio of MeOH:EtOAc = 10:1, Temperature = 333 K, $C_{EtOAc,0}$ = 1.79M)**

The reaction rate depends on the number of active sites, their acid strength and their accessibility. Because no proportionality is observed between the initial reaction rate, i.e., the slope of the concentration profile at time zero, and the number of active sites, particularly their accessibility, as affected by differences in swelling behavior, and, to a minor extent, their strength are considered to be the determining factors in the observed activity.

From the above mentioned factors the accessibility is indeed significantly affected by the swelling behavior. The latter can easily be related to the cross-linking degree. When dry Lewatit K1221 gel beads are placed in a polar reaction medium such as methanol, swelling with ca. 145 % of its initial volume occurs and, hence, all the active sites in the body of the bead and on the beads' surface are available for reaction [16]. When, on the other hand, dry macroporous resins, such as Lewatit K2640, K2629 or Amberlyst 15, are placed in a polar reaction medium, swelling with only ca. 55 % occurs. The reactants have easy access to the macropores of the bead, c.q., the external active sites of the gel particles [17], but experience severe constraints for entering the small gel particles, and accessing the internal active sites, see Figure 4-2. Hence, only the active sites on the surface, in the macropores and in the swollen part of the small gel particles are considered to be available for reaction. The catalytic activity exhibited by the resins is inversely related to their crosslinking with DVB: the gel type resin with 4% DVB has the highest catalytic activity, followed by the macroporous resins with 18 % DVB, while the macroporous type with 20 % DVB has the lowest catalytic activity. Gusler et al. [18] and Coutinho et al. [9] also found that the exchange capacity is directly proportional to resins' swelling.

Although the DVB content of K2640 and K2629 is identical and amounts to 18 %, K2640 is slightly more catalytically active. This can be attributed to the slight differences in acid strength between both resins due to the polysulfonation of Lewatit K2640. Siril et al. [19] observed that the acid strength of sulfonic groups on a polysulfonated resin, which has more than one sulfonic group per styrene unit, is slightly higher than stoichiometrically sulfonated resins such as Amberlyst 15, Lewatit K1221, and Lewatit K2629. A possible explanation lies in the formation of clustered sulfonic acid groups, in which hydrogen bonding between neighboring groups enhances the acid strength [19-21].

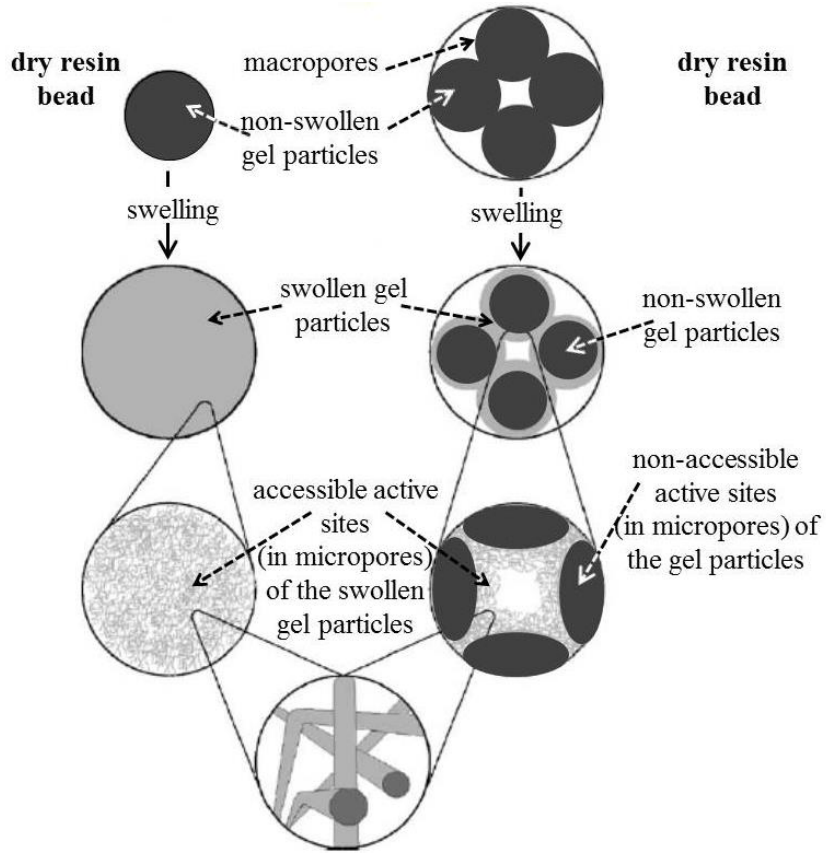

Figure 4-2 **Schematic representation of the micro- and nanoscale morphology of resins [16]**

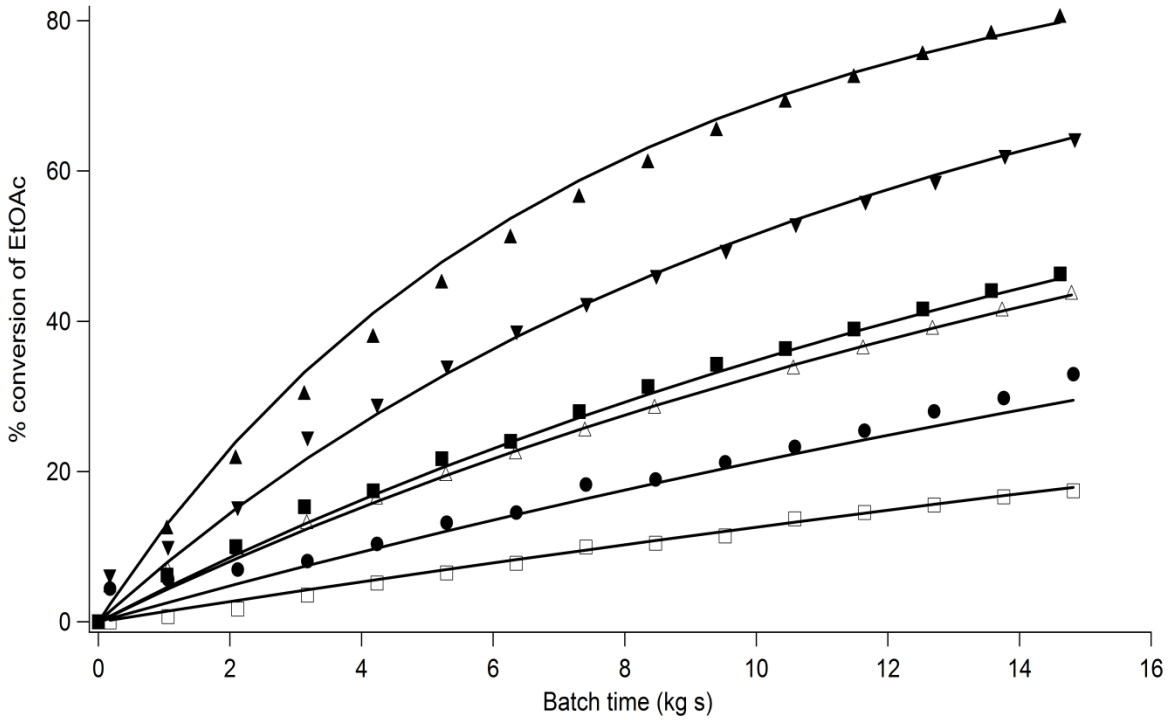

Figure 4-3 **Simulated (ER-exchange model, Eq. 4-4 with parameters as reported in Table 4-3) (lines) and experimental (symbols) conversion of ethyl acetate as function of the batch time catalyzed by gel (K1221) (filled symbols) and macroporous (K2629) (open symbols) ion-exchange resins at different temperatures (○ 303 K; □ 313 K; ▽ 323 K; △ 333 K) (initial molar ratio MeOH:EtOAc = 10:1; $C_{EtOAc,0}$ = 1.79 M)**

The temperature effect was investigated for both gel and macroporous resins in the range from 303 to 333 K. No peculiar adsorption/swelling effects were observed with the temperature and, hence, as expected a higher ethyl acetate conversion was observed at higher temperatures at the same batch time, see Figure 4-3.

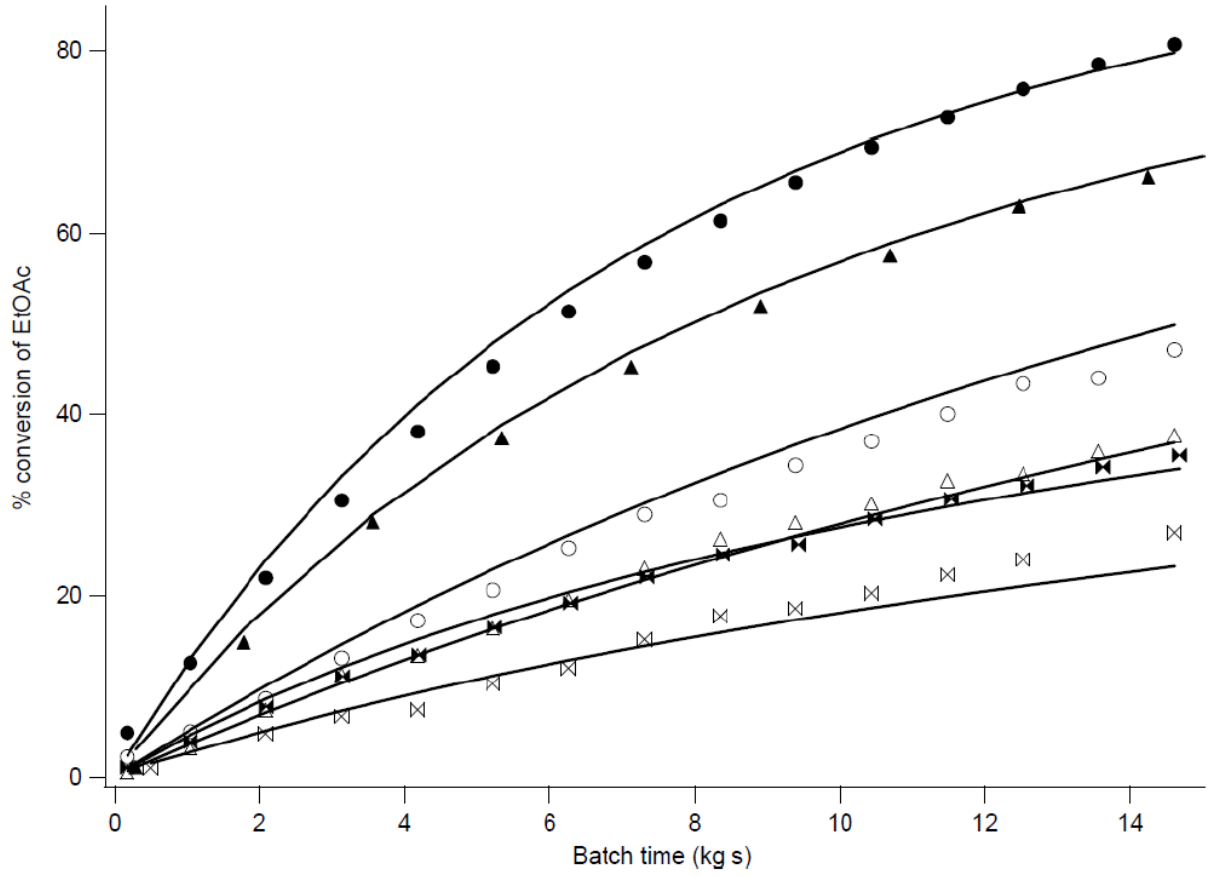

Figure 4-4 **Simulated (ER-exchange model, Eq. 4-4 with parameters as reported in Table 4-3) (lines) and experimental (symbols) conversion of ethyl acetate as function of the batch time catalyzed by gel (K1221) (filled symbols) and macroporous (K2640) ion-exchange resins (open symbols) at different molar ratios MeOH:EtOAc (● 10:1, ▲5:1, ⋈ 1:1) (Temperature = 333 K, $C_{EtOAc,0}$ = 1.79 M (10:1); $C_{EtOAc,0}$ = 3.03 M (5:1); $C_{EtOAc,0}$ = 5.79 M (1:1))**

The effect of the initial methanol to ethyl acetate ratio (1:1 – 10:1) was also investigated. An increase in the reactant methanol, expressed by a higher initial molar ratio, results in a higher ethyl acetate conversion, see Figure 4-4. Because the ethyl acetate/catalyst amount ratio was kept constant in the experiments, this also corresponds to higher specific reaction rates. If the initial molar ratio increases from 1:1 to 5:1, an increase in the initial reaction rate for K1221 and K2640 of respectively a factor 2.0 and 1.5 is obtained. For an increase in the initial molar ratio from 5:1 to 10:1, the initial reaction rate increases for both resins with a factor 1.4.

These differences can be explained by the combination of a different swelling ratio and reactant excess, c.q., methanol. At an initial molar ratio of 1:1 the reaction medium is, due to the small amount of methanol, less polar than at higher molar ratios. A more polar medium increases the resins' swelling and, hence, the accessibility of the active sites [22]. The swelling ratio of the gel type resin K1221 (Table 4-2), increases from 1.6 to 2.5 if the initial molar ratio increases from 1:1 to 10:1. The swelling ratio of the macroporous resin Lewatit K2640, on the other hand, is limited to a maximum value of 1.5, see Table 4-1 and 4-2. Hence, for Lewatit K2640 the increase in initial reaction rate, with an increase in initial molar ratio, can be entirely attributed to the excess of methanol.

4.4 Kinetic modeling of gel and macroporous resin catalyzed transesterification

The actual transesterification reaction mechanism compromises first the protonation of the carboxyl group of the ethyl acetate by the acid site. Subsequently, the formed protonated methyl acetate undergoes a deprotonation to regenerate this acid site [23-31]. TAs found in Chapter 3 and in the publication of Alonso et al. [24], these protonation and deprotonation steps must be taken into account in the kinetic model for an adequate, physically reasonable representation of the occurring phenomena,. In the pseudo-homogeneous model, the interaction, c.q., protonation and deprotonation, between component and resin is only implicitly included in the reaction rate coefficient.

4.4.1 Mathematical representation of the resins' swelling behavior in the rate equation

Two alternative ways for representing the adsorption/swelling phenomena are assessed. First conventional adsorption mechanisms are elaborated, while subsequently a more specific exchange based model is handled in which it is assumed, in accordance with the swelling phenomenon, that all accessible active sites are always occupied.

Adsorption-based model

In Chapter 3 the Eley-Rideal based model for transesterification on K1221 with the reaction of physisorbed methanol on the catalyst's active site with ethyl acetate reacting from the bulk as rate-determining step, to form physisorbed ethanol and methyl acetate released to

the bulk, was identified as the best performing one amongst a set of 12 competitive equations (Equation ER-MeOH-SR in Table 3-2).

Although adsorption-based models are commonly used to describe the transesterification reaction kinetics with ion-exchange resins, they do not explicitly account for the swelling behavior of these resins. Therefore, an enhanced version of the rate equation of the ER-MeOH-SR model is developed for the assessment of the experimental data for both gel and macroporous resins. The performance of the novel reaction rate equation will be compared with that of the ER-MeOH-SR model (Table 3-2).

Exchange based model

The Flory-Huggins theory of polymer swelling is the most advanced methodology for rationalizing the partitioning of components between the bulk liquid of a multicomponent mixture and the resins' internal volume [32]. In the framework of this theory, the uptake of solvent species is considered as a phase equilibrium requiring suitable expressions for the thermodynamic activities as a function of the phase composition in the resin. Given the typically high molar methanol excess in the experiments performed in this work, the benefits of using the Flory-Huggins theory are expected to be limited, and hence, so called exchange coefficients are employed to account for the resins' swelling and describe the reaction kinetics of the transesterification catalyzed by different resin types.

When adsorption-based models are applied to account for catalysis by macroporous and gel type resins, the adsorption equilibrium coefficient accounts both for adsorption on the active sites and resin swelling. The first step in an adsorption-based model is the adsorption of a component on the free active site of the resin [31], whereas in the exchange based model it is assumed that all active sites are always occupied and, hence, the first step is an exchange between 2 components on the active sites of the resin, see Figure 4-5. The exchange based kinetic model for the transesterification catalyzed by gel and macroporous resins is built on the schematic representation of the swelling of the two types of resins given in Figure 4-2. The adsorption-based kinetic model, as originally proposed in Chapter 3 [31] (Eq. in Table 3-2), is hence, extended with the following hypotheses:

(i) The swelling of the resin is attributed to the strong sorption of the solvent, i.e., methanol. All active sites of the resin are occupied, (initially) by protonated methanol. (Figure 4-5).

(ii) The esters, i.e. ethyl and methyl acetate, undergo a proton exchange with the protonated methanol on the active sites, equilibrium is assumed for this exchange see Figure 4-5 steps (1) and (5).

These hypotheses lead to the reaction mechanism shown in Figure 4-5.

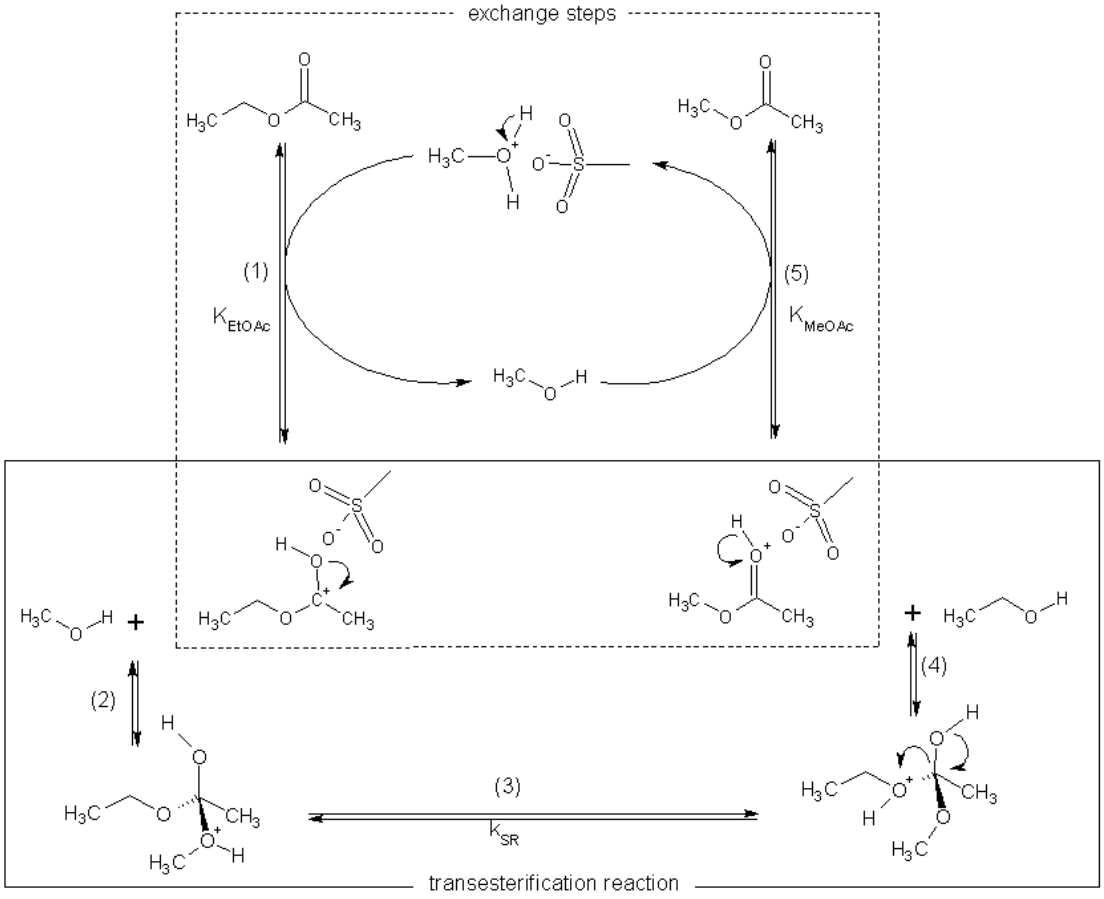

Figure 4-5 Heterogeneous acid ion-exchange resin catalyzed reaction mechanism for the transesterification of ethyl acetate with methanol.

The derivation of the corresponding rate equation starts with the law of mass action applied on step (3), which is assumed to be rate-determining step (RDS) for the overall kinetics. The rate expression becomes:

$$r = k_{SR}\left(a_{EtOAc^*}a_{MeOH} - \frac{1}{K_{SR}}a_{MeOAc^*}a_{EtOH}\right) \tag{4-1}$$

with k_{SR} the surface reaction rate coefficient, K_{SR} the surface reaction equilibrium coefficient, a_i the activity of a component in the bulk and the a_{i^*} the activity of the protonated component.

Since the overall reaction is the sum of the individual steps, the thermodynamic equilibrium coefficient for the overall reaction is

$$K_{eq} = \frac{K_{EtOAc} K_{SR}}{K_{MeOAc}} \tag{4-2}$$

with K_{EtOAc} and K_{MeOAc} the exchange equilibrium coefficient of ethyl and methyl acetate, corresponding to steps (1) and (5), see Figure 4-5. Equation 4-2 is used to eliminate the unknown surface reaction equilibrium coefficient K_{SR} in Equation 4-1.

The total concentration of available active sites is constant and all sites are occupied. Hence, the following equation can be written:

$$C_{tot} = C_{MeOH*} + C_{EtOAc*} + C_{MeOAc*} \tag{4-3}$$

Using the steady-state approximation for the surface intermediates and combining Equations 4-1, 4-2 and 4-3, the unobservable variables C_{MeOH*}, C_{EtOAc*} and C_{MeOAc*} can be eliminated in terms of the bulk liquid concentrations C_{MeOH}, C_{EtOAc}, C_{MeOAc} multiplied with their respective UNIFAC activity coefficients:

$$r = \frac{k_{SR} K_{EtOAc} \left(a_{EtOAc} - \frac{1}{K_{eq}} \frac{a_{EtOH} a_{MeOAc}}{a_{MeOH}} \right)}{1 + \frac{K_{EtOAc} a_{EtOAc}}{a_{MeOH}} + \frac{K_{MeOAc} a_{MeOAc}}{a_{MeOH}}} \tag{4-4}$$

The model parameters in the above kinetic equation are the surface reaction rate coefficient, k_{SR}, the activation energy, E_A, and the exchange equilibrium coefficients of ethyl and methyl acetate, K_{EtOAc} and K_{MeOAc}.

The exchange between ethanol and methanol on an active site is not considered in the model. Since ethanol is less polar due to the longer alkyl chain compared to methanol, the driving force for this exchange is limited. A potential exchange with ethanol would not contribute significantly to the calculated reaction rate and, hence, ethanol is assumed to be instantaneously released in the bulk liquid.

4.4.2 Model discrimination between exchange and adsorption-based model for the transesterification reaction catalyzed by Lewatit K1221

The adsorption (Equation ER-MeOH-SR in Table 3-2) and the exchange based model (Eq. 4-4), are mathematically quite similar. Both models consider the same driving force and have an adsorption term that comprises three terms. Where the latter correspond to the adsorption of the alcohols in the adsorption model, in the exchange based model they correspond to protonated methanol, methyl and ethyl acetate. The exchange coefficients in the denominator of rate equation (Eq. 4-4) correspond to the ratio of the adsorption coefficient of the concerned component to the adsorption coefficient of methanol. Comparing the two denominators, the term 1 of the adsorption-based model is replaced by a_{MeOH} in (Eq. 4-4) and the activity and the adsorption of the alcohols are replaced by the activity and the exchange of the esters.

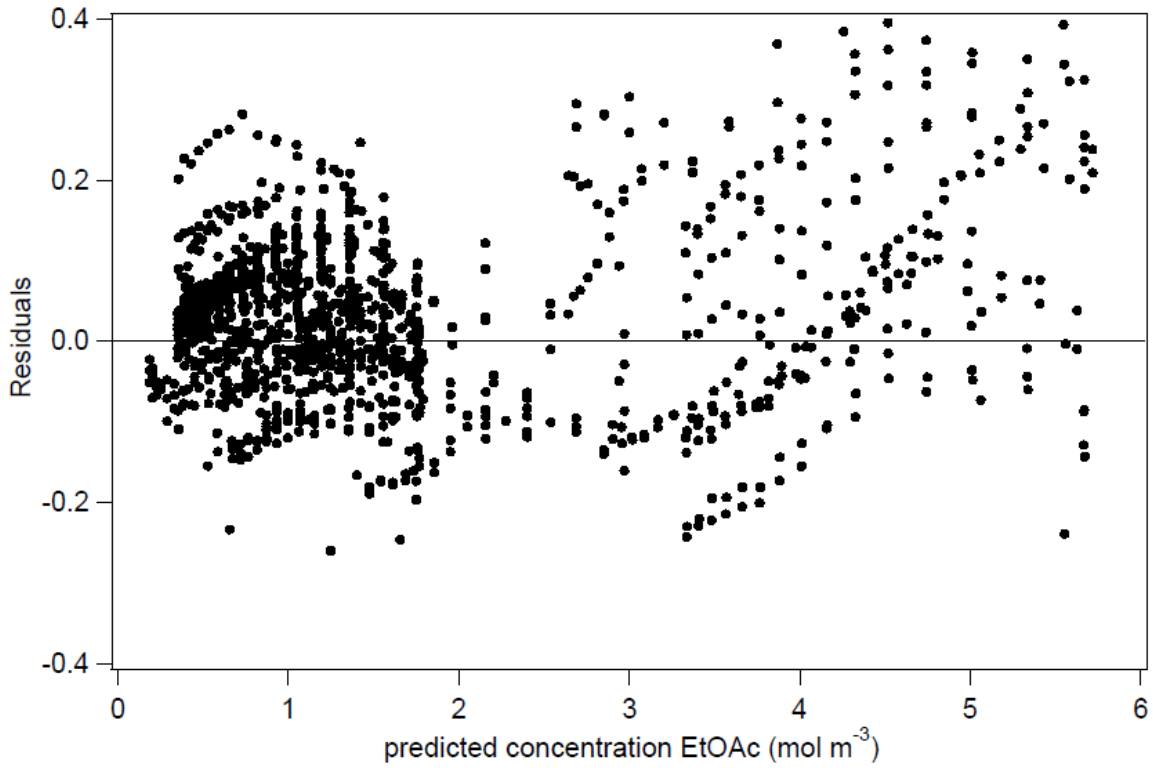

Figure 4-6 **Residual diagram for the concentration of ethyl acetate for the complete set of 1282 data points of the transesterification catalyzed by Lewatit K1221. The simulated values are obtained using Eq. 4-4 with the estimated model parameters of the exchange based model (Table 4-3). Range of experimental conditions (Table 2-2)**

All parameters in both versions of the model were estimated significantly different from zero. The obtained F values for the global significance of the regression range from 62 000 for the adsorption-based model (Table 3-4) to 71 000 for the exchange based model (Eq. 4-4), and exceed the tabulated F value by far. The best performing model in simulating experimentally observed kinetics is the exchange based model which has the lowest residual sum of squares (23.7) and the highest F-value (71 000). Although it does not outperform the adsorption-based model on the reference resin, the good statistics combined with the physicochemical meaning of the model, as explained in section 4.4.1, make the exchange based model the preferred one for further assessment of the transesterification kinetics on the various resins considered. A corresponding residual diagram for the exchange based model, see Figure 4-6, indicates the overall adequacy of the model. Comparing Figure 4-6 with Figure 3-4, the residual plot, especially for the predicted ethyl acetate concentrations less than 2.0 mol m^{-3} is slightly better.

A similar model discrimination for the macroporous resins, which also results in the selection of the exchange based mechanism as the most adequate one, is included in Appendix B (section B-1).

4.5 Quantitative assessment of the differences observed between Lewatit K1221, Lewatit K2640, Lewatit K2629 and Amberlyst 15

Model regression to the experimental data reported in section 4.3 by minimizing the objective function (Eq. 2-12) resulted in estimates for the four adjustable parameters in Equation 4-4 ($k_{SR_{Tref}}$, E_A, K_{EtOAc} and K_{MeOAc}). The obtained parameter estimates and the statistical performance of the model for the gel and macroporous resins are shown in Table 4-3. Within the limited temperature range of 303 K to 333K, the temperature dependence of the exchange equilibrium coefficients is not considered, in analogy with the temperature dependence of the adsorption equilibrium coefficients (see section 3.5.1).

The model adequately describes the experimental data on all resins. The global significance of the regression which is assessed by the F value, ranges from 18 000 to 125 000. This value clearly exceeds the tabulated F value and, hence, the regression is

globally significant for all four resins. Figure 4-1, Figure 4-3 and Figure 4-4 illustrate the good agreement between the model simulations and the experimental data.

Table 4-3 Statistical information and parameter estimation of the ER-exchange model for the ethyl acetate transesterification with methanol catalyzed by Lewatit K1221, Lewatit K2629 and Amberlyst 15

Resin	Kinetic parameters		Exchange equilibrium coefficients		Statistical evaluation		
	$k_{SR_{Tref}}$ (10^{-3}mol $kg_{cat}^{-1}s^{-1}$)	E_A (kJ mol^{-1})	K_{EtOAc}	K_{MeOAc}	N	RSSQ	F
K1221	52.7 ± 0.3	48.7 ± 0.9	1.15 ± 0.14	4.87 ± 0.38	1282	24	71 000
K2629	9.2 ± 1.0	49.7 ± 2.0	2.54 ± 0.35	9.04 ± 2.03	702	2	125 000
K2640	14.5 ± 4.1	42.9 ± 5.6	1.86 ± 0.67	6.26 ± 1.90	233	2	18 000
Amberlyst 15	10.3 ± 7.5	52.3 ± 6.6	1.36 ± 0.99	0.90 ± 6.04	129	6	35 000

Considering the individual confidence intervals, all activation energies are approximately equal to 49 kJ mol^{-1}, irrespective of the resin used. These activation energies are, de facto, a composite activation energy, E_A^{comp}, comprising the two elementary steps involved in the reaction mechanism, i.e., the proton exchange between ethyl acetate and protonated methanol, $\Delta H_{exchange}$, and the actual surface reaction, E_A, [33]:

$$E_A^{comp} = E_A + \Delta H_{exchange} \tag{4-3}$$

The true activation energy and the standard exchange enthalpy can, hence, not be estimated as separate parameters. The similar values obtained for the composite activation energies indicate that the energy barriers to be surmounted by the reacting components are comparable for all the catalysts. This can be explained by the formation of similar interactions on the same functional groups for all four catalysts. The composite activation energy obtained on Lewatit K2640 being on the lower side of this range may be attributed to the polysulfonated character of this resin and a corresponding, small effect on the exchange enthalpy. For a transesterification catalyzed with an acid ion-exchange resin similar (composite) activation energy values were published in literature [3, 11, 23, 34, 35].

The gel type catalyst, Lewatit K1221, has a combined reaction rate, $k_{SR_{Tref}} K_{HOAc}$, at 328.38 K that is 3- to 4-fold higher than that of the macroporous catalysts, Lewatit K2640, K2629 or Amberlyst 15, as could be expected from the experimental data and the similar composite activation energies. The pre-exponential factor of the rate coefficient accounts for the entropy difference between the reactants and the transition state species, as well as for the

number of active/accessible sites. Since macroporous resins swell less than gel type ones, the number of accessible active sites will typically be lower for the former compared to the latter, see Figure 4-2. It, hence, makes sense that the pre-exponential factor obtained for the macroporous resins is lower than that for the gel type resins. For Amberlyst 15 and Lewatit K2629, both with a total number of active sites of 4.8 meq kg^{-1}_{resin}, the same pre-exponential factor is obtained. Nevertheless, the confidence interval of $k_{SR_{Tref}}$ for Amberlyst 15 is quite wide. Because of the higher DVB content of the latter, i.e., 20% compared to 18% for Lewatit K2629, less swelling has been observed on Amberlyst 15, see Section 4.3.1, and, hence, the true value for the pre-exponential factor on Lewatit K2629 is expected to be higher than the true one on Amberlyst 15. For Lewatit K2629 and Lewatit K2640, both with a crosslinking degree of 18%, the true value of the pre-exponential factor on Lewatit K2629 will rather be lower than on Lewatit K2640, because of the higher total number of active sites of the latter, i.e. 5.2 meq kg^{-1}_{resin}, due to the polysulfonation.

The exchange equilibrium coefficients, K_{MeOAc} and K_{EtOAc} have the same order of magnitude for all catalysts. The value of K_{MeOAc} for Amberlyst 15 is not significantly different from zero, see Table 4-3, which is attributed to the limited number of experimental data, the correspondingly limited range of operating conditions as well as to the relatively low conversions obtained on Amberlyst 15 and, hence, the less significant presence of methyl acetate in the reaction mixture. The exchange equilibrium coefficients are slightly higher for the macroporous resins compared to the gel type resin, suggesting that the sorption of methanol on the gel type resin is more pronounced than on the macroporous resins as confirmed by the volumetric swelling experiments, see section 4.3.1. The ratio between the methyl and ethyl acetate exchange coefficient is identical for all resins and amounts to 4 approximately. This reflects the chemical similarity of the resins. The additional methylene group in ethyl acetate results in a lower exchange equilibrium coefficient, which is in agreement with the results obtained by Ali et al. [3] for butyl acetate versus ethyl acetate.

4.6 Assessment of molar fractions within the resin

In order to gain more insight in how the model quantifies the phenomena occurring at the active sites of the resin, the ethyl and methyl acetate fractions in the resin, i.e., θ_{EtOAc^*} and θ_{MeOAc^*}, as well as the methanol fraction in the resin, θ_{MeOH^*}, can be calculated employing

the exchange based kinetic model, making use of the site balance and the quasi-equilibrium assumption, see equations 4-5 to 4-8, in analogy with section 3.6.2.

$$1 = \theta_{MeOH*} + \theta_{EtOAc*} + \theta_{MeOAc*} \tag{4-5}$$

$$\theta_{MeOH*} = \frac{1}{1 + \frac{K_{EtOAc} a_{EtOAc}}{a_{MeOH}} + \frac{K_{MeOAc} a_{MeOAc}}{a_{MeOH}}} \tag{4-6}$$

$$\theta_{EtOAc*} = \frac{\frac{K_{EtOAc} a_{EtOAc}}{a_{MeOH}}}{1 + \frac{K_{EtOAc} a_{EtOAc}}{a_{MeOH}} + \frac{K_{MeOAc} a_{MeOAc}}{a_{MeOH}}} \tag{4-7}$$

$$\theta_{MeOAc*} = \frac{\frac{K_{MeOAc} a_{MeOAc}}{a_{MeOH}}}{1 + \frac{K_{EtOAc} a_{EtOAc}}{a_{MeOH}} + \frac{K_{MeOAc} a_{MeOAc}}{a_{MeOH}}} \tag{4-8}$$

The molar fractions in the resin as a function of conversion at different temperatures and different initial molar methanol to ethyl acetate ratios are shown in Figure 4-7 and Figure 4-8 for gel and macroporous resins, respectively.

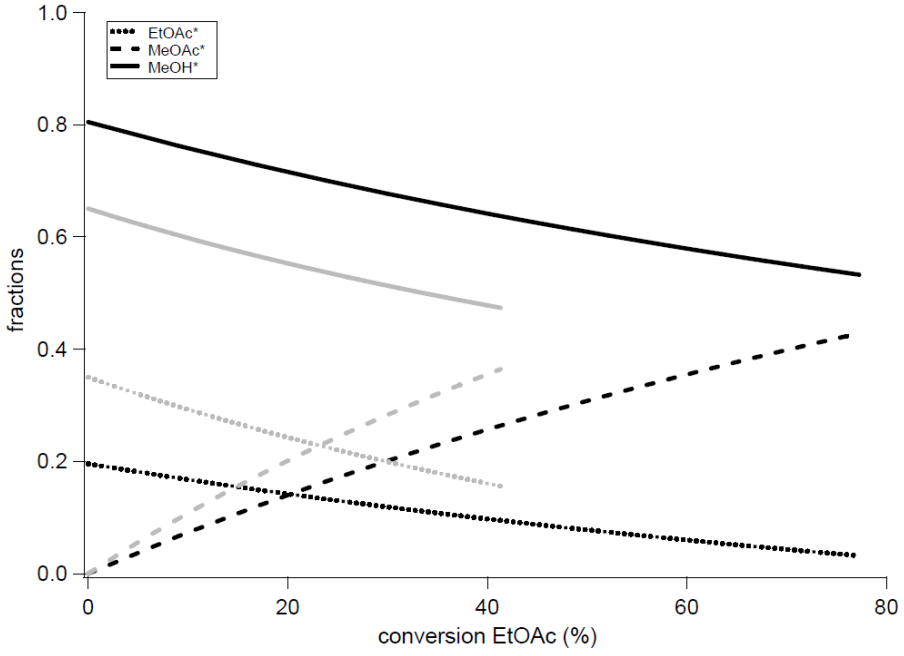

Figure 4-7 **Simulated (ER-exchange model, Eq. 4-4, with parameters as reported in Table 4-3) fractions as a function of the conversion at all temperatures and initial molar MeOH:EtOAc ratio = 10:1, catalyzed by Lewatit K1221 (black) and by Lewatit K2629 (grey). (EtOAc* and MeOAc* molar fractions of ethyl acetate and methyl acetate in the resin, respectively; (MeOH*) molar fraction of methanol in the resin).**

At the start of an experiment catalyzed by K1221 with an initial methanol to ethyl acetate molar ratio of 10:1, 80 % and 20 % of the sites is covered with methanol and ethyl acetate, independently of the temperature, see Figure 4-7. At 44 % ethyl acetate conversion, the methanol, ethyl acetate and methyl acetate fractions amount to 64 %, 10 % and 26 %. Given the absence of a temperature effect on the exchange coefficients, also at higher conversions the molar fractions within the resin are independent of the temperature. Of course, at higher temperatures, the same conversion is reached at a shorted batch time, see Figure 4-3. A similar evolution of the molar fractions within the resin as a function of the conversion is obtained for the macroporous resins, see Figure 4-7 for Lewatit K2629 as an example. Due to the higher exchange equilibrium coefficients for the esters on K2629, the initial methanol fraction is lower than that on the gel type resin. The same effect is still visible at 44 % ethyl acetate conversion, with methanol, ethyl acetate and methyl acetate fractions amounting to 48 %, 16 % and 36 %.

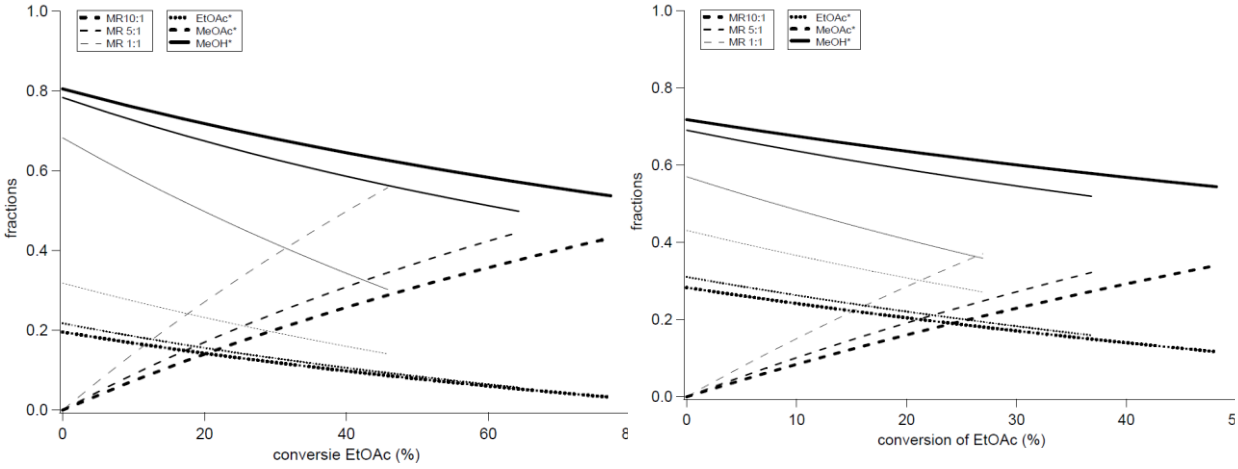

Figure 4-8 **Simulated (ER-exchange model, Eq. 4-4, with parameters as reported in Table 4-3) fractions as a function of conversion of ethyl acetate at 333 K with varying initial molar MeOH:EtOAc ratios (legend), catalyzed by Lewatit K1221 (left) and by Lewatit K2640 (right). (EtOAc* and MeOAc* molar fractions of ethyl acetate and methyl acetate in the resin, respectively; (MeOH*) molar fraction of methanol in the resin).**

The effect of the initial molar methanol to ethyl acetate ratio is investigated at 333K. The fractions obtained at an initial molar ratio of 10:1 and at an ethyl acetate conversion of 77 %, are 54 %, 3 % and 43 % for methanol, ethyl acetate and methyl acetate. At a molar ratio of 5:1, the results are comparable. An increase of initial molar ratio from 5:1 to 10:1, does not lead to appreciably different fractions. At an initial molar ratio of 1:1, the methanol fraction in the resin is lower, due to its lower liquid bulk concentration, i.e., 68% at the start and 30% at 46 % ethyl acetate conversion. The ethyl and methyl acetate fractions are

correspondingly higher, i.e., 32% and 0 % at the start and 14% and 56% at 46 % ethyl acetate conversion. Nevertheless, methanol remains the most abundant species within the resin, except at higher batch times with the lowest initial molar ratios. The different fractions obtained with initial molar ratio 1:1 and 5:1 or 10:1 are also due to differences in the activity coefficients of methanol, methyl and ethyl acetate. Similar trends are observed for the macroporous resins, see Figure 4-8 (right), which are in line with the experimental observations discussed in section 4.3.2.

4.7 Conclusions

Gel and macroporous acid ion-exchange resins can be used as catalysts for ethyl acetate transesterification with methanol to methyl acetate and ethanol. Due to the chemical similarity between the considered resins, differences in observed reaction rates were mainly related to the accessibility of the active sites. The latter is inversely proportional with the amount of cross-linking by divinylbenzene due to the corresponding swelling behavior of the resins. Gel type resins are subject to more pronounced swelling compared to macroporous resins due to the rigidity induced by the higher divinylbenzene cross linking in the latter. Resin swelling is also more pronounced when it is in contact with more polar solvents. The number of accessible active sites as well as their strength can, to a lesser extent, also be enhanced by polysulfonation.

A novel kinetic model, implicitly accounting for resin swelling, was developed with the following assumptions

(1) all active sites are occupied by either methanol, ethyl or methyl acetate
(2) the exchange between protonated methanol and the esters is quasi equilibrated, and
(3) an Eley-Rideal type surface reaction between protonated ethyl acetate with methanol from the bulk occurs as the rate-determining step.

and allowed interpreting the observed differences between the various resins. The latter were mainly reflected in the estimated rate coefficients. Just like the transesterification rates, the reaction rate coefficients were found to be proportional to the accessibility of the active sites and, hence, inversely proportional to the cross-linking degree. The activation energy amounts to 49 kJ/mol independent of the considered resin and is an indication of their chemical similarity. Methanol is the most abundant surface intermediate, followed by methyl and ethyl acetate respectively. Due to the additional methylene group, the ethyl acetate exchange equilibrium coefficient is a factor 3 to 4 smaller than that of methyl acetate. The presented

modelling methodology has resulted in an accurate simulation of the kinetic behavior of different types of resins and allowed developing a physically sound interpretation of the reaction kinetics and mechanism.

4.8 References

1. Tesser, R., L. Casale, D. Verde, M. Di Serio, and E. Santacesaria, *Kinetics and modeling of fatty acids esterification on acid exchange resins.* Chemical Engineering Journal, 2010. **157**(2-3): p. 539-550.
2. Tesser, R., M. Di Serio, L. Casale, L. Sannino, M. Ledda, and E. Santacesaria, *Acid exchange resins deactivation in the esterification of free fatty acids.* Chemical Engineering Journal, 2010. **161**(1-2): p. 212-222.
3. Ali, S.H., O. Al-Rashed, F.A. Azeez, and S.Q. Merchant, *Potential biofuel additive from renewable sources - Kinetic study of formation of butyl acetate by heterogeneously catalyzed transesterification of ethyl acetate with butanol.* Bioresource Technology, 2011. **102**(21): p. 10094-10103.
4. Lee, M.J., H.T. Wu, and H.M. Lin, *Kinetics of catalytic esterification of acetic acid and amyl alcohol over Dowex.* Industrial & Engineering Chemistry Research, 2000. **39**(11): p. 4094-4099.
5. Helfferich, F.G., *Ion Exchange*. 1995: Dover Publications.
6. Stewart, W.E. and M. Caracotsios, *Computer-aided modeling of reactive systems*. 2008: Wiley-Interscience.
7. Rehfinger, A. and U. Hoffmann, *Kinetics of methyl tertairy butyl ether liquid-phase synthesis cataalyzed by ion-exchange resin. 1. Intrinsic rate expression in liquid-phase activities* Chemical Engineering Science, 1990. **45**(6): p. 1605-1617.
8. Corain, B., M. Zecca, P. Canton, and P. Centomo, *Synthesis and catalytic activity of metal nanoclusters inside functional resins: an endeavour lasting 15 years.* Philosophical Transactions of the Royal Society a-Mathematical Physical and Engineering Sciences, 2010. **368**(1915): p. 1495-1507.
9. Coutinho, F.M.B., S.M. Rezende, and B.G. Soares, *Characterization of sulfonated poly(styrene-divinylbenzene) and poly(divinylbenzene) and its application as catalysts in esterification reaction.* Journal of Applied Polymer Science, 2006. **102**(4): p. 3616-3627.
10. Sainio, T., M. Laatikainen, and E. Paatero, *Phase equilibria in solvent mixture-ion exchange resin catalyst systems.* Fluid Phase Equilibria, 2004. **218**(2): p. 269-283.
11. Bozek-Winkler, E. and J. Gmehling, *Transesterification of methyl acetate and n-butanol catalyzed by Amberlyst 15.* Industrial & Engineering Chemistry Research, 2006. **45**(20): p. 6648-6654.
12. Mazzotti, M., A. Kruglov, B. Neri, D. Gelosa, and M. Morbidelli, *A continuous chromatographic reactor: SMBR.* Chemical Engineering Science, 1996. **51**(10): p. 1827-1836.
13. Mazzotti, M., B. Neri, D. Gelosa, A. Kruglov, and M. Morbidelli, *Kinetics of liquid-phase esterification catalyzed by acidic resins.* Industrial & Engineering Chemistry Research, 1997. **36**(1): p. 3-10.
14. Zimehl, R., *Flow microcalorimetry and competitive liquid sorption - II. Liquid sorption and wetting on macroreticular hydrophilic/hydrophobic networks.* Thermochimica Acta, 1998. **310**(1-2): p. 207-215.
15. Tsai, Y.T., H.M. Lin, and M.J. Lee, *Kinetics behavior of esterification of acetic acid with methanol over Amberlyst 36.* Chemical Engineering Journal, 2011. **171**(3): p. 1367-1372.
16. Corain, B., P. Centomo, S. Lora, and M. Kralik, *Functional resins as innovative supports for catalytically active metal nanoclusters.* Journal of Molecular Catalysis a-Chemical, 2003. **204**: p. 755-762.

17. Ihm, S.K., J.H. Ahn, and Y.D. Jo, *Interaction of reaction and mass transfer in ion-exchange resin catalysts.* Industrial & Engineering Chemistry Research, 1996. **35**(9): p. 2946-2954.
18. Gusler, G.M., T.E. Browne, and Y. Cohen, *Sorption of Organics from Aqueous-solution onto Polymeric Resins.* Industrial & Engineering Chemistry Research, 1993. **32**(11): p. 2727-2735.
19. Siril, P.F., A.D. Davison, J.K. Randhawa, and D.R. Brown, *Acid strengths and catalytic activities of sulfonic acid on polymeric and silica supports.* Journal of Molecular Catalysis a-Chemical, 2007. **267**(1-2): p. 72-78.
20. Siril, P.F. and D.R. Brown, *Acid site accessibility in sulfonated polystyrene acid catalysts: Calorimetric study of NH3 adsorption from flowing gas stream.* Journal of Molecular Catalysis a-Chemical, 2006. **252**(1-2): p. 125-131.
21. Siril, P.R., H.E. Cross, and D.R. Brown, *New polystyrene sulfonic acid resin catalysts with enhanced acidic and catalytic properties.* Journal of Molecular Catalysis a-Chemical, 2008. **279**(1): p. 63-68.
22. Chakrabarti, A. and M.M. Sharma, *Cationic Ion-Exchange Resins as Catalyst.* Reactive Polymers, 1993. **20**(1-2): p. 1-45.
23. Lopez, D.E., J.G. Goodwin, and D.A. Bruce, *Transesterification of triacetin with methanol on Nafion (R) acid resins.* Journal of Catalysis, 2007. **245**(2): p. 381-391.
24. Alonso, D.M., M.L. Granados, R. Mariscal, and A. Douhal, *Polarity of the acid chain of esters and transesterification activity of acid catalysts.* Journal of Catalysis, 2009. **262**(1): p. 18-26.
25. Lotero, E., Y.J. Liu, D.E. Lopez, K. Suwannakarn, D.A. Bruce, and J.G. Goodwin, *Synthesis of biodiesel via acid catalysis.* Industrial & Engineering Chemistry Research, 2005. **44**(14): p. 5353-5363.
26. Di Serio, M., R. Tesser, M. Dimiccoli, F. Cammarota, M. Nastasi, and E. Santacesaria, *Synthesis of biodiesel via homogeneous Lewis acid catalyst.* Journal of Molecular Catalysis a-Chemical, 2005. **239**(1-2): p. 111-115.
27. Di Serio, M., R. Tesser, L. Pengmei, and E. Santacesaria, *Heterogeneous catalysts for biodiesel production.* Energy & Fuels, 2008. **22**(1): p. 207-217.
28. Lotero, E., J.G. Goodwin, D.A. Bruce, K. Suwannakarn, Y.J. Liu, and D.E. Lopez, *The Catalysis of Biodiesel Synthesis*, in *Catalysis, Vol 19*, J.J. Spivey and K.M. Dooley, Editors. 2006, Royal Soc Chemistry: Cambridge. p. 41-83.
29. Schuchardt, U., R. Sercheli, and R.M. Vargas, *Transesterification of vegetable oils: a review.* Journal of the Brazilian Chemical Society, 1998. **9**(3): p. 199-210.
30. Smith, M. and J. March, *March's advanced organic chemistry: reactions, mechanisms, and structure*. 2007: Wiley-Interscience.
31. Van de Steene, E., J. De Clercq, and J.W. Thybaut, *Adsorption and reaction in the transesterification of ethyl acetate with methanol on Lewatit K1221.* Journal of Molecular Catalysis A: Chemical, 2012. **359**(0): p. 57-68.
32. Polyanskii, N.G. and V.K. Sapozhnikov, *New Advances in Catalysis by Ion-exchange Resins.* Russian Chemical Reviews, 1977. **46**(3): p. 445-476.
33. Thybaut, J.W., C.S.L. Narasimhan, G.B. Marin, J.F.M. Denayer, G.V. Baron, P.A. Jacobs, and J.A. Martens, *Alkylcarbenium ion concentrations in zeolite pores during octane hydrocracking on Pt/H-USY zeolite.* Catalysis Letters, 2004. **94**(1-2): p. 81-88.
34. Xu, B.Y., W.J. Zhang, X.M. Zhang, and C.F. Zhou, *Kinetic Study of Transesterification of Methyl Acetate with n-Butanol Catalyzed by NKC-9.* International Journal of Chemical Kinetics, 2009. **41**(2): p. 101-106.

35. Ali, S.H. and S.Q. Merchant, *Kinetics of the esterification of acetic acid with 2-propanol: Impact of different acidic cation exchange resins on reaction mechanism.* International Journal of Chemical Kinetics, 2006. **38**(10): p. 593-612.

5

KINETIC STUDY OF ACETIC ACID ESTERIFICATION WITH METHANOL CATALYZED BY LEWATIT K1221

This chapter is based on "Kinetic Study of the Esterification Catalyzed by Lewatit K1221" by E. Van de Steene, J. De Clercq, J.W. Thybaut, American Institute of Chemical Engineers Annual Meeting (AIChE), San Francisco, United States, November 2013

Abstract - *The reaction kinetics of the liquid-phase acetic acid esterification with methanol to methyl acetate and water have been investigated using the acid ion-exchange resin Lewatit K1221 as catalyst. This gel-type polystyrene-based resin, crosslinked with divinylbenzene, exhibits a remarkable swelling phenomenon when contacted with polar solvents, such as water and methanol. The effects of the resin swelling, the initial molar methanol to acetic acid ratio (1:1 – 10:1) and the temperature (303– 333 K) on the reaction kinetics were investigated. The exchange based Eley-Rideal model, as developed for transesterification, served as a basis for the esterification kinetics model. It was assumed that: (1) all active sites are occupied by methanol in protonated form, (2) acetic acid undergoes a proton exchange with protonated methanol,(3) the reaction occurs through an Eley-Rideal mechanism with the surface reaction of protonated acetic acid with methanol from the bulk as the rate-determining step and (4) water competes with methanol for the active sites. This exchange based kinetic model best described the observed kinetics. The composite esterification rate coefficient exceeds that of transesterification by a factor of 4. The activation energy was estimated at 46 kJ mol^{-1}. The ion exchange equilibrium coefficients for acetic acid and the reaction products amounted to 4.6 and 3.6, respectively.*

5.1 Introduction

Acetic acid esterification with methanol kinetics have mainly been described in the literature by adsorption-based models [1-9]. It concerns two Eley-Rideal models and one Langmuir-Hinshelwood model, in which for Langmuir-Hinshelwood both adsorbed reagents react, where in the case of an Eley-Rideal mechanism only one reagent is adsorbed and react with the other from the bulk. The surface reaction is assumed to be rate determining. The products formed in the Langmuir-Hinshelwood model are both adsorbed, while in the Eley-Rideal only one product is adsorbed. For the Eley-Rideal model, several possible combinations are possible, depending on which reagent or product is adsorbed, whereas for the Langmuir-Hinshelwood only one combination exist. Of course, as it was the case for transesterification, also the more simple pseudo-homogeneous model is frequently proposed [1, 7, 10-12]. More particularly for the use of resins as catalyst, an exchange based ER model has been developed as part of Chapter 4 for ethyl acetate transesterification.

In this chapter, acetic acid esterification with methanol to methyl acetate and water, catalyzed by Lewatit K1221 has been investigated using a similar methodology as for transesterification, see Chapter 3 and Chapter 4. Kinetic measurements were performed to evaluate the effect of the temperature and initial molar methanol to acetic acid ratio on the esterification rates. Resin swelling tests with pure reactants and products have been performed as well to quantify the swelling of Lewatit K1221.

5.2 Procedures

Acetic acid esterification with methanol was experimentally investigated in a batch reactor. The catalyst properties and the reactor setup are described in more detail in Sections 2.1 and 2.3.1 respectively. The experimental data set consists of 749 experimental points stemming from 58 experiments, within the range of conditions reported in Table 2-2. Similarly to Chapter 3 the data set is constructed from an initial data set based on a factorial design which was extended making use of a D-optimal sequential experimental design for more precise parameter estimations and conclusive model discrimination.

To ascertain that the data represent intrinsic kinetics, the absence of mass-transfer resistance was evaluated as described in Section 2.3.4. The parameter estimation and model discrimination procedure has been described in detail in Section 2.5.

5.3 Experimental results

5.2.1. Volumetric swelling tests

Table 5-1 shows that the resin Lewatit K1221, in analogy with what is reported in Table 4-1 and in the literature [4, 13, 14], undergoes a more pronounced swelling in polar solvents compared to less or apolar solvents. Resin swelling is found to increase with the dielectric constant of the solvents and, hence, is proportional to the polarization of the mixture [4, 15]. Although water has a very high dielectric constant, the swelling ratio is lower than expected based on the trend exhibited by the swelling ratio when going from acetic acid and methyl acetate towards methanol. This can be related to a full stretching of the polystyrene chains in the resin and, hence, to reaching the corresponding, upper limit in the resins' swelling.

Table 5-1 Swelling ratio (S) of Lewatit K1221 in different solvents and dielectric constant of the different solvents

Swelling ratio	water	methanol MeOH	methyl acetate MeOAc	acetic acid HOAc
K1221	2.56 ± 0.09	2.45 ± 0.07	1.24 ± 0.05	1.18 ± 0.08
Dielectric constant	80.1	32.7	6.70	6.15

5.2.2. Intrinsic kinetic measurements

The temperature effect and the effect of the initial molar methanol to acetic acid ratio were investigated by performing experiments between 303.15 and 333.15 K and 1:1 and 10:1 mol mol^{-1} respectively. As expected, a higher temperature results in a higher esterification rate and a correspondingly higher methyl acetate yield at the same batch time, see Figure 5-1. The equilibrium conversion is practically temperature independent, which is a logic consequence of the limited reaction enthalpy, i.e., -4.39 kJ mol^{-1}, of the investigated reaction [3, 5, 16], see also Chapter 2. Higher initial molar ratios result in a higher methyl acetate yield, see Figure 5-2. Increasing the initial molar ratio from 1:1 to 5:1, results in a pronounced increase in the esterification rate. Nevertheless, an increase of the initial molar ratio from 5:1 to 10:1, only slightly increases the reaction rate, indicating that an alcohol excess only slightly further enhances the esterification rate.

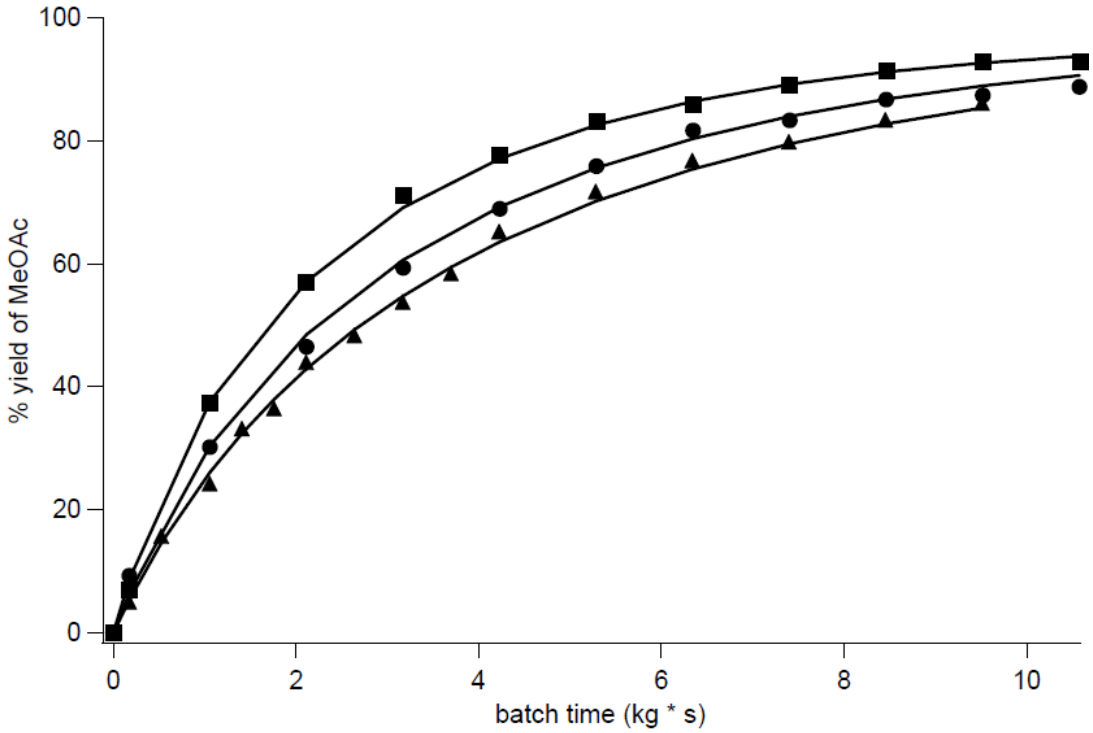

Figure 5-1 **Simulated (lines; ER-exchange model, Eq. 5-1 with parameters as reported in Table 5-4) and experimental (symbols) methyl acetate yield versus batch time catalyzed by Lewatit K1221 ion exchange resin at different temperatures (▲ 316 K, ● 323 K, ■ 333 K). (Initial molar ratio of MeOH:HOAc = 10:1; $C_{HOAc,0}$ = 1.90 M)**

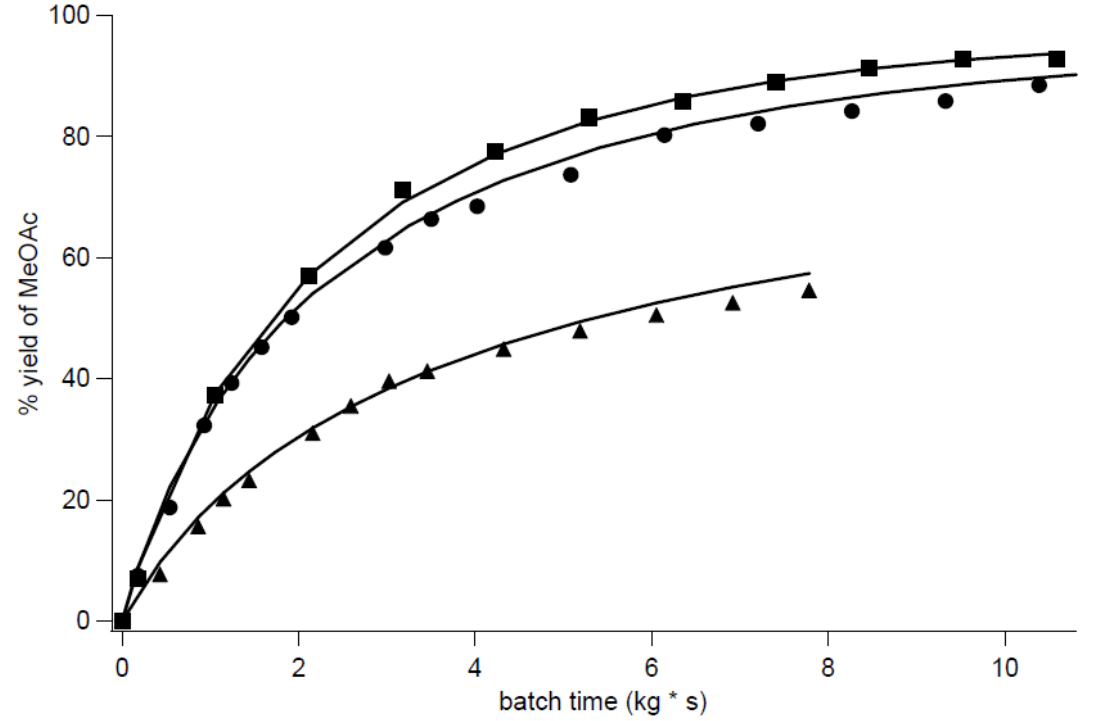

Figure 5-2 **Simulated (lines; ER-exchange model, Eq. 5-1 with parameters as reported in Table 5-4) and experimental (symbols) methyl acetate yield versus batch time catalyzed by Lewatit K1221 ion exchange resin at different initial molar ratios of methanol to acetic acid (▲ 1:1, ● 5:1, ■ 10:1). (Temperature = 333 K; $C_{HOAc,0}$ = 1.90 M (10:1); $C_{HOAc,0}$ = 3.50 M (5:1); $C_{HOAc,0}$ = 9.50 M (1:1))**

5.4 Kinetic modelling of the esterification catalyzed by Lewatit K1221

The acetic acid esterification with methanol has been simulated in literature using kinetic models based on several mechanisms, such as Eley-Rideal and Langmuir-Hinshelwood [1-6, 10, 12, 16-31]. Similar to Table 3-1 for transesterification, a table with all the elementary steps and reaction mechanism can be written down for the esterification. Only the most frequently used mechanisms and corresponding models with the best physical and statistical performance are further considered in this chapter, namely: ER-HOAc-water[1], ER-MeOH-water[1], ER-exchange, LH and PH, see Table 5-2. In the corresponding mechanisms the surface reaction is always considered rate determining.

The pseudo-homogeneous model (PH) considers the heterogeneous esterification as a (quasi) homogeneous reaction, i.e., implicitly assuming that no sorption related effects dominate the observations. The ER-HOAc-water model corresponds with an Eley-Rideal mechanism with adsorbed acetic acid reacting with methanol from the bulk. The ER-MeOH-water model is similar to the ER-HOAc-water model, however, instead of acetic acid, methanol is the adsorbed reagent. The LH model corresponds with a mechanism where both reactants and products are adsorbed.

An acetic acid esterification kinetic model is constructed based on the exchange-based model as proposed for transesterification in Chapter 4. Because methanol and water strongly sorb in the resin, see Table 5-1, all the active sites of the resin are assumed to be occupied. Acetic acid and methyl acetate undergo a proton exchange with protonated methanol on the active sites, see Figure 5-3. The surface reaction between protonated acetic acid and methanol from the bulk to form protonated methyl acetate and water is considered to be rate determining. In contrast to transesterification the second reaction product in esterification, i.e. water, has a high affinity towards the sulfonic acid groups. Hence, in the present esterification model the produced water is also allowed to exchange with protonated methanol in contrast to the ethanol produced in transesterification, see also Chapter 3 and Chapter 4. Water therefore competes with methanol for the active sites and may lead to (significant) product inhibition [32].

[1] ER_i_j is an abbreviation of an Eley-Rideal reaction mechanism where reactant *i* is absorbed and product *j* will be desorbed. The surface reaction is the rate-determining step.

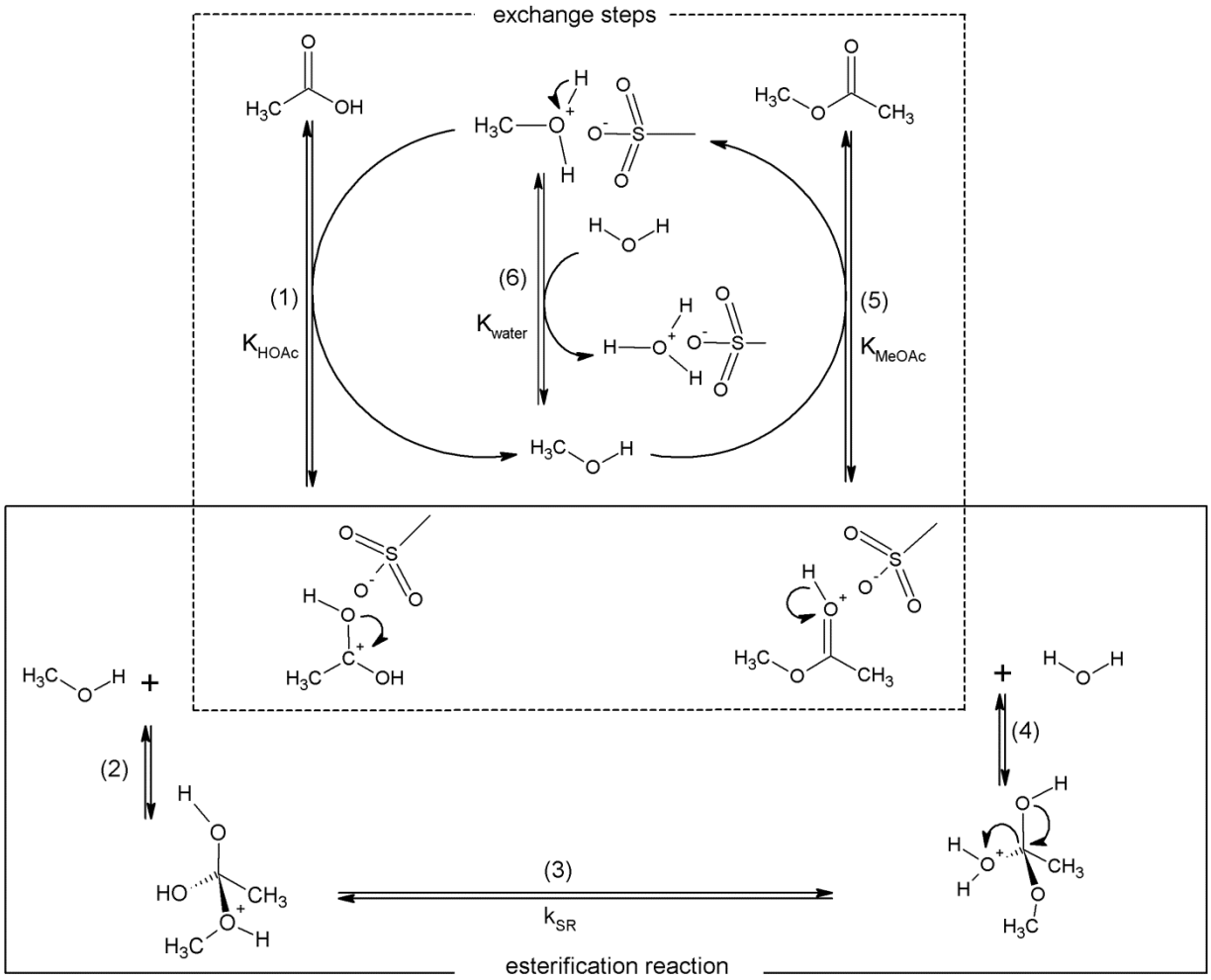

Figure 5-3 Heterogeneous acid ion exchange resin catalyzed reaction mechanism for the acetic acid esterification with methanol.

Because of the identical evolution of the water and methyl acetate concentration throughout the experimentation, it was impossible to determine separate values for the adsorption or exchange coefficients for water and methyl acetate [6, 8, 33, 34]. Independent adsorption/exchange coefficient determination or incorporation of experimental measurements into the data set in which a specific amount of reaction product, i.e., water or methyl acetate was added to the initial mixture may have allowed a separate determination of the adsorption/exchange coefficients for methyl acetate and water [34]. Because such information is not contained in the kinetic data set acquired in the present work, i.e., all experiments were performed in such conditions that only equal methyl acetate and water concentrations are part of the dataset, a single value was estimated for the methyl acetate and the water adsorption/exchange coefficient, as indicated in Table 5-2 with K_l.

Table 5-2 Reaction rates for different mechanisms and rate-determining steps for the esterification of acetic acid and methanol.

Abbreviation	Rate-determining step	Corresponding reaction rate
	PH	
PH	HOAc + MeOH $\rightleftarrows$ MeOAc + H_2O	$r = k_{SR}\left(a_{MeOH}a_{HOAc} - \frac{1}{K_{eq}}a_{MeOAc}a_{H_2O}\right)$
	ER mechanism	
ER-HOAc-water	HOAc* + MeOH $\rightleftarrows$ H_2O* + MeOAc	$r = \frac{k_{SR}K_{HOAc}\left(a_{MeOH}a_{HOAc} - \frac{1}{K_{eq}}a_{MeOAc}a_{H_2O}\right)}{1 + a_{HOAc}K_{HOAc} + a_{H_2O}K_{H_2O}}$
ER-MeOH-water	HOAc + MeOH* $\rightleftarrows$ H_2O* + MeOAc	$r = \frac{k_{SR}K_{MeOH}\left(a_{MeOH}a_{HOAc} - \frac{1}{K_{eq}}a_{MeOAc}a_{H_2O}\right)}{1 + a_{MeOH}K_{MeOH} + a_{H_2O}K_{H_2O}}$
ER-exchange	HOAc* + MeOH $\rightleftarrows$ MeOAc* + H_2O	$r = \frac{k_{SR}K_{HOAc}\left(a_{HOAc} - \frac{1}{K_{eq}}\frac{a_{MeOAc}a_{H_2O}}{a_{MeOH}}\right)}{1 + K_{HOAc}\frac{a_{HOAc}}{a_{MeOH}} + K_l\left(\frac{a_{MeOAc} + a_{H_2O}}{a_{MeOH}}\right)}$
	LH mechanism	
LH	HOAc* + MeOH* $\rightleftarrows$ MeOAc* + H_2O*	$r = \frac{k_{SR}K_{MeOH}K_{HOAc}\left(a_{MeOH}a_{HOAc} - \frac{1}{K_{eq}}a_{MeOAc}a_{H_2O}\right)}{\left(1 + a_{MeOH}K_{MeOH} + a_{HOAc}K_{HOAc} + K_l\left(a_{MeOAc} + a_{H_2O}\right)\right)^2}$

5.5 Model discrimination between PH, adsorption and exchange based models

Prior to the model regression and discrimination, initial parameter estimates have been determined in a similar way as described in section 3.5.1. Values for the rate coefficient at each investigated temperature were estimated by isothermal regression using the PH model. Initial values for the different adsorption equilibrium coefficients and exchange equilibrium coefficients were taken from literature [5, 6, 23, 32].

The regression and discrimination results are shown in Table 5-3. The obtained F values for the global significance of the regression are all situated in a narrow range from 21 000 to 32 700. The best performing models, i.e., the ones with the lowest residual sum of squares, i.e., between 13 and 14, and an F value between 21 000 and 29 000 are the ER-exchange, the ER-HOAc-water and the LH model.

Table 5-3 Statistical evaluation of the 5 rival models (Table 5-2) for the esterification catalyzed by Lewatit K1221 (748 experimental points, experimental conditions Table 6-1)

Model	Number of statistically significantly estimated (total) parameters	Residual sum of squares	R^2	F
ER-exchange	4 (4)	13.13	0.991	29 000
LH	5 (5)	13.48	0.991	21 000
ER-HOAc-water	4 (4)	13.76	0.991	27 400
ER-MeOH-water	3 (4)	20.74	0.986	27 600
PH	2 (2)	43.17	0.971	32 700

The ER-MeOH-water model has a higher residual sum of squares and a lower multiple correlation coefficient compared with these best performing models, indicating that it is, albeit only slightly, inferior to the three first models. Nevertheless, because only 3 model parameters were estimated significantly, the ER-MeOH-water model has a practically identical F value for the global significance of the regression as the ER-HOAc-water model. The residual sum of squares obtained with the PH model amounts to more than the double of those obtained with the other models. The PH model also has the lowest multiple correlation coefficient. Nevertheless, it leads to the highest F value for the global significance of the regression, i.e., 32 700, because it has the lowest number of adjustable parameters, i.e., 2. The correspondingly calculated likelihood ratios are inconclusive. As a result, on a purely statistical basis, see Table 5-3, none of the models can be selected nor rejected, such that physical grounds have to be invoked for a proper model discrimination.

As already indicated in Chapter 3 for transesterification, the PH model is mathematically much simpler than the other models, however, it is inadequate for the interpretation of a more complex reaction mechanism. In particular, it does not explicitly, nor implicitly, take into account the resin swelling and/or reactant and product adsorption and is, hence, discarded.

The parameter estimates for the four remaining models are reported in Table 5-4. Whereas the composite activation energy appears to be independent of the exact model formulation [1,2], as it was the case in transesterification, see Chapter 3, major differences are observed between the composite rate coefficient at the average temperature and the adsorption/exchange coefficients. Although these differences may partly stem from correlation between the parameter estimates, e.g., binary correlation coefficients amounting

to 0.999 between k_{Tref} and K_i and to 0.997 between various K_i's, some generic features are observed that allows a preliminary discrimination.

Table 5-4 Parameter estimates with their 95 % confidence interval, obtained by regression of 748 experimental points. (T_{ref} = 323.15 K)

Model	ER-exchange	LH	ER-HOAc-water	ER-MeOH-water	PH
k_{Tref} (mol $kg_{cat}^{-1}s^{-1}$)	0.215 ± 0.012	8.138 ± 0.701	0.386 ± 0.040	385.9 ± 22.4	0.020 ± 0.001
E_A (kJ mol^{-1})	46.00 ± 1.86	46.66 ± 1.94	45.72 ± 1.87	46.81 ± 2.38	51.07 ± 3.14
K_{HOAc}	4.580 ± 0.314	1.624 ± 0.980	0.110 ± 0.013	a	a
K_{MeOH}	a	0.559 ± 0.345	a	0.000001	a
K_{MeOAc}	a	a	a	a	a
K_{water}	a	a	0.266 ± 0.033	0.327 ± 0.042	a
K_l	3.611 ± 0.338	1.102 ± 0.606	a	a	a

[a] not present in the model

Both adsorption-based Eley Rideal models, i.e., ER-HOAc-water and ER-MeOH-water, exhibit low values for the adsorption coefficients of water and acetic acid or methanol respectively. The correspondingly simulated molar fractions within the resin are shown in Figure 5-4. The fraction of free active sites that is simulated with both models always exceeds always 33%, independently of the initial molar methanol to acetic acid ratio. According to the LH model the maximum fraction of free sites amounts to 10 %, whereas a full coverage of active sites is assumed in the exchange model.

Such high values for the fraction of free active sites obtained with ER-HOAc-water and ER-MeOH-water seem rather unlikely in view of the pronounced resin swelling and the correspondingly assumed full occupation of the active sites [23], see also Chapter 4. The low adsorption coefficients, see Table 5-4, especially for ER-MeOH-water, are compensated by high composite rate coefficients which exceeds what is typically reported for these reactions [16, 22, 31]. As a result, both adsorption-based Eley Rideal are considered not to physically represent the occurring phenomena and, hence, are discarded.

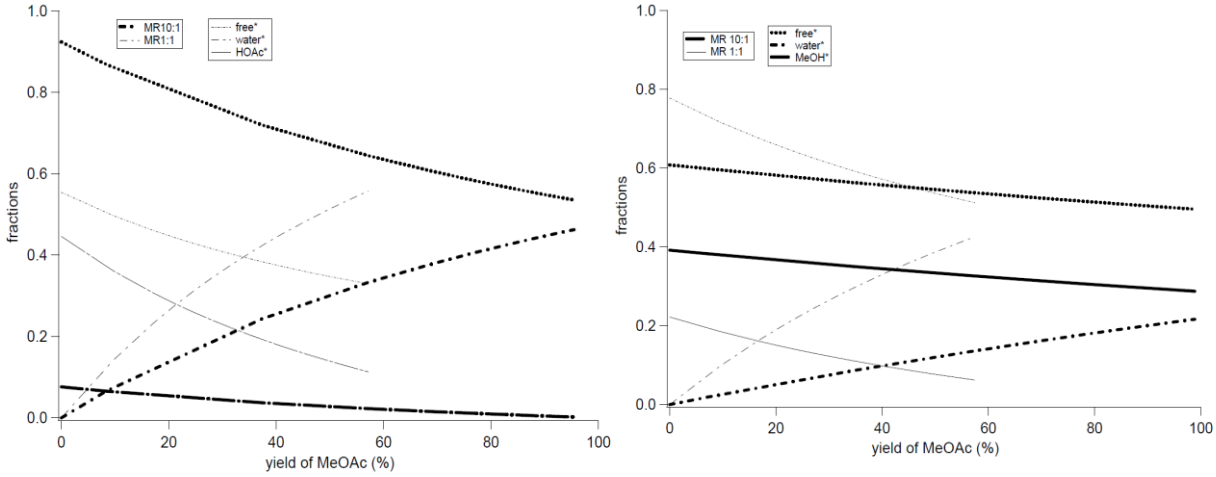

Figure 5-4 Simulated (ER-HOAc-water model (left), ER-MeOH-water model (right) Equation in Table 5-2, with parameters as reported in Table 5-4) surface fractions as a function of methyl acetate yield at 333 K with various initial molar MeOH:HOAc ratios (legend), catalyzed by Lewatit K1221.

The parameter estimates in the LH model are highly correlated, while no pronounced correlation is observed between the estimates obtained for the ER-exchange model. Because the LH model has one adjustable parameter more than the ER-exchange model the acetic acid and products adsorption coefficients were constrained to obey the ratio as obtained for the corresponding exchange coefficients in the ER-exchange model. Despite this adjustable parameter reduction to an equal number as in the ER-exchange model, the correlations between the surface reaction rate coefficient and the adsorption coefficients remained high, suggesting that further constraints would need to be imposed to reduce the correlation between the remaining parameters. As a result, it seems that the ER-exchange model is better able to capture the dominant phenomena in acetic acid esterification on Lewatit K1221.

The acetic acid exchange coefficient being higher than the one obtained for the products, i.e., $K_{HOAc} > K_l$, is unexpected based on the swelling ratios obtained when using them as solvent and on their dielectric constants, see Table 5-1. Reconsidering the (implicit) assumptions made in the derivation of the rate equations, see section 4.4.1, a distinction has only been made between the liquid bulk and the protonated species inside the resin. In reality, the resin sorbs more molecules than the stoichiometrically equivalent of the number of accessible sulfonic acid groups, particularly when it concerns small and strongly polar molecules [32]. As a result, it may be more appropriate to consider an additional phase in the model that could be denoted as ‘polymer phase’ which is clearly distinct from the bulk liquid and from the protonated species on the sulfonic acid functional groups. The presence of sulfonic acid groups in the resin can logically be expected to differentiate the

thermodynamics within the polymer phase from those in the liquid bulk, such that complex theories as the one by Flory Huggins, specifically developed for simulating solvent uptake by a swelling polymer, would be most appropriate [4, 35]. The latter theory allows calculating polymer phase activities which can be clearly distinct from the bulk liquid ones [14, 36] and not identical as it is implicitly assumed in the present version of the ER-exchange model. Hence, an adequate combination of a thermodynamic model and a kinetic model is expected to allow to better describe the entire evolutions of the reaction mixture as a function of the methyl acetate yield[37]. Summarizing, the unexpected trend in exchange coefficients points towards the need of considering a separate phase within the resin. However, for the purpose of reaction mechanism interpretation in the present work, a qualitative, preliminary assessment was made with the present ER-exchange model. The higher value than expected for the acetic acid exchange coefficient is attributed to the low activity coefficient for acetic acid. Despite this low activity coefficient, the correspondingly calculated acetic acid molar fraction in the resin remains rather high, indicating the need of more advanced theories to quantitatively assess the molar fractions in the resin during esterification.

Figure 5-1 and Figure 5-2 visualize the performance of the ER-exchange model in the simulation of the collected acetic acid esterification data and provides a quantified interpretation of temperature and initial molar methanol to acetic acid ratio effects on the observed reaction rate.

The evolution of the product, acetic acid and methanol fractions within the resin, as a function of the methyl acetate yield at 333 K, at an initial molar ratio of methanol to acetic acid of 10:1 and 1:1, is given in Figure 5-5. The product fraction increases with conversion, which can be explained by simultaneous production of water and methyl acetate. The increase of the product fraction for an initial molar ratio of 1:1 is more pronounced compared to an initial molar ratio of 10:1. At an initial molar ratio of methanol to acetic acid of 10:1 at the beginning of the experiment 85 % of the active sites are covered by methanol. At 95 % yield, 73% of the active sites are covered by methanol and 27 % by the products. At the start of an esterification reaction with an initial molar ratio of 1:1 almost 80 % of the active sites are covered by acetic acid. At 57 % conversion, almost 52 % of the active sites are covered by the products, 10 % by methanol and 38 % by acetic acid. A reaction mixture with an initial ratio of 1:1 is, due to the lower amount of the polar methanol, less polar than a reaction mixture with an initial molar ratio of 10:1, and, hence, the swelling is more pronounced with an increase of initial molar ratio (similar to transesterification discussed in Chapter 4), and, hence, leads to an increase of the methanol fraction in the resin.

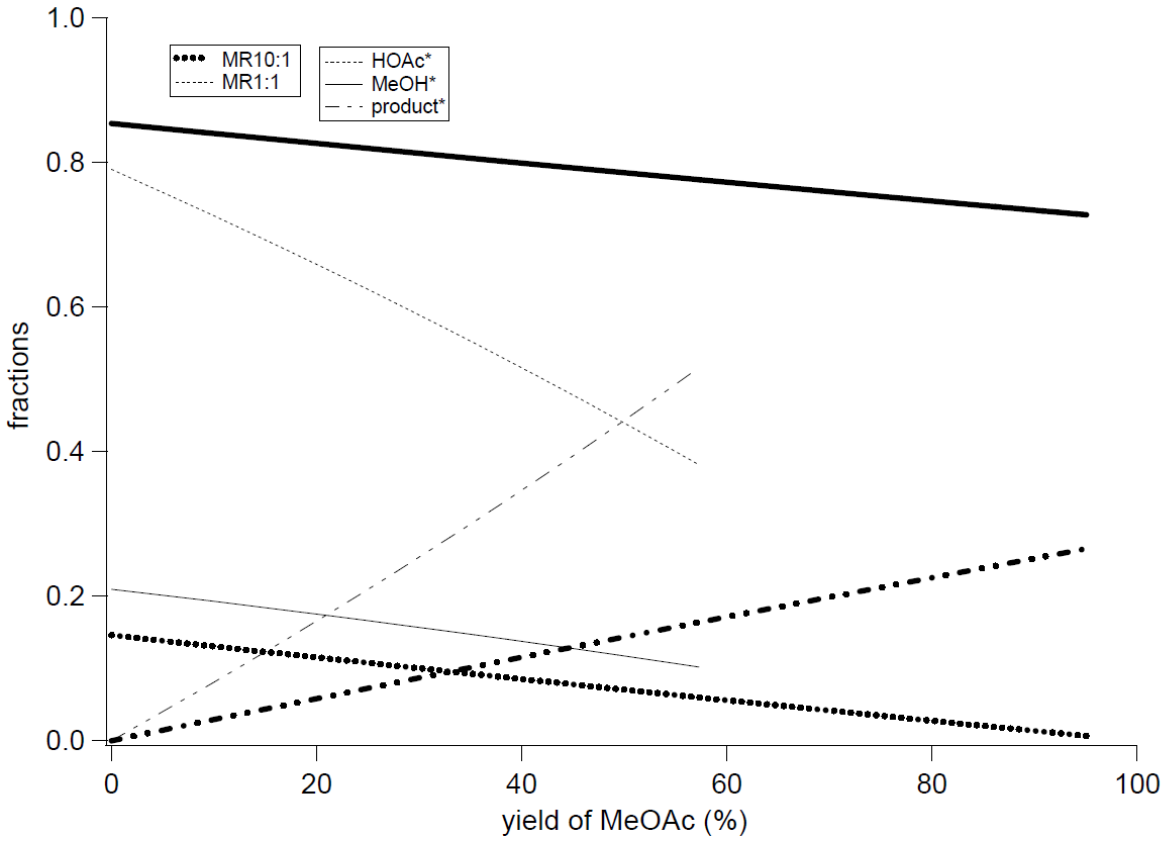

Figure 5-5 Simulated (ER-exchange model, with parameters as reported in Table 5-4) fractions as a function of methyl acetate yield at 333 K with various initial molar MeOH:HOAc ratios (legend), catalyzed by Lewatit K1221 (The fraction of MeOH at an initial molar ratio of 1:1 is behind the fraction of HOAc at an initial molar ratio of 10:1).

5.6 Conclusions

The acetic acid esterification kinetics with methanol have been investigated on a gel-type resin, i.e., Lewatit K1221. Increasing the temperature or initial molar methanol to acetic acid ratio enhances the esterification rate. Four frequently reported literature based models such as a pseudo-homogeneous model and adsorption-based Langmuir-Hinshelwood or Eley-Rideal reaction mechanisms as well as an exchange based model developed as part of this work were used to simulate the kinetic data. A single adsorption or exchange coefficient was estimated for the reaction products, i.e., methyl acetate and water. Whereas the statistical performance of the investigated models was practically identical, a discrimination based on physical grounds resulted in the exchange based Eley-Rideal model as the preferred one. It most closely follows the physical interpretation that swelling results in a complete occupation of all active sites in the resin, initially by the solvent, i.e., methanol, but upon injection of the reactant acid also by this acid and, more importantly, by the reaction product water. The

exchange based ER model performs well in simulating the observed esterification behavior at different temperatures and initial methanol to acetic acid molar ratios.

The estimated composite activation energy amounts to 46 kJ mol^{-1}. A particularly high exchange coefficient is obtained for acetic acid, exceeding the one of the products, which indicates the need for considering a separate, so-called 'polymer phase' which is situated in between the liquid bulk and the protonated species. Despite the low activity coefficient for acetic acid, a surprisingly high acetic acid fraction was simulated within the resin, particularly for an initial molar methanol to acetic acid fraction of 1:1, which further indicates the need for more advanced theories such as Flory-Huggins' to describe the thermodynamics within the resin.

Similar to the transesterification, the proposed reaction mechanism and kinetic model will be evaluated to describe the experimental data performed with macroporous resins (Chapter 6).

5.7 References

1. Sanz, M.T., R. Murga, S. Beltran, J.L. Cabezas, and J. Coca, *Autocatalyzed and ion-exchange-resin-catalyzed esterification kinetics of lactic acid with methanol.* Industrial & Engineering Chemistry Research, 2002. **41**(3): p. 512-517.
2. Ali, S.H., *Kinetics of Catalytic Esterification of Propionic Acid with Different Alcohols over Amberlyst 15.* International Journal of Chemical Kinetics, 2009. **41**(6): p. 432-448.
3. Ali, S.H. and S.Q. Merchant, *Kinetics of the esterification of acetic acid with 2-propanol: Impact of different acidic cation exchange resins on reaction mechanism.* International Journal of Chemical Kinetics, 2006. **38**(10): p. 593-612.
4. Mazzotti, M., B. Neri, D. Gelosa, A. Kruglov, and M. Morbidelli, *Kinetics of liquid-phase esterification catalyzed by acidic resins.* Industrial & Engineering Chemistry Research, 1997. **36**(1): p. 3-10.
5. Popken, T., L. Gotze, and J. Gmehling, *Reaction kinetics and chemical equilibrium of homogeneously and heterogeneously catalyzed acetic acid esterification with methanol and methyl acetate hydrolysis.* Industrial & Engineering Chemistry Research, 2000. **39**(7): p. 2601-2611.
6. Song, W., G. Venimadhavan, J.M. Manning, M.F. Malone, and M.F. Doherty, *Measurement of residue curve maps and heterogeneous kinetics in methyl acetate synthesis.* Industrial & Engineering Chemistry Research, 1998. **37**(5): p. 1917-1928.
7. Sanz, M.T., R. Murga, S. Beltran, J.L. Cabezas, and J. Coca, *Kinetic study for the reactive system of lactic acid esterification with methanol: Methyl lactate hydrolysis reaction.* Industrial & Engineering Chemistry Research, 2004. **43**(9): p. 2049-2053.
8. Gangadwala, J., S. Mankar, S. Mahajani, A. Kienle, and E. Stein, *Esterification of acetic acid with butanol in the presence of ion-exchange resins as catalysts.* Industrial & Engineering Chemistry Research, 2003. **42**(10): p. 2146-2155.
9. Russbueldt, B.M.E. and W.F. Hoelderich, *New sulfonic acid ion-exchange resins for the preesterification of different oils and fats with high content of free fatty acids.* Applied Catalysis a-General, 2009. **362**(1-2): p. 47-57.
10. Qu, Y.X., S.J. Peng, S. Wang, Z.Q. Zhang, and J.D. Wang, *Kinetic Study of Esterification of Lactic Acid with Isobutanol and n-Butanol Catalyzed by Ion-exchange Resins.* Chinese Journal of Chemical Engineering, 2009. **17**(5): p. 773-780.
11. Pappu, V.K.S., A.J. Yanez, L. Peereboom, E. Muller, C.T. Lira, and D.J. Miller, *A kinetic model of the Amberlyst-15 catalyzed transesterification of methyl stearate with n-butanol.* Bioresource Technology, 2011. **102**(5): p. 4270-4272.
12. Delgado, P., M.T. Sanz, and S. Beltran, *Kinetic study for esterification of lactic acid with ethanol and hydrolysis of ethyl lactate using an ion-exchange resin catalyst.* Chemical Engineering Journal, 2007. **126**(2-3): p. 111-118.
13. Lilja, J., E. Murzina, H. Grenman, H. Vainio, T. Salmi, and D.Y. Murzin, *The selective sorption of solvents on sulphonic acid polymer catalyst in binary mixtures.* Reactive & Functional Polymers, 2005. **64**(2): p. 111-118.
14. Sainio, T., M. Laatikainen, and E. Paatero, *Phase equilibria in solvent mixture-ion exchange resin catalyst systems.* Fluid Phase Equilibria, 2004. **218**(2): p. 269-283.
15. Helfferich, F.G., *Ion Exchange*. 1995: Dover Publications.
16. Tsai, Y.T., H.M. Lin, and M.J. Lee, *Kinetics behavior of esterification of acetic acid with methanol over Amberlyst 36.* Chemical Engineering Journal, 2011. **171**(3): p. 1367-1372.

17. Altiokka, M.R. and A. Citak, *Kinetics study of esterification of acetic acid with isobutanol in the presence of amberlite catalyst.* Applied Catalysis a-General, 2003. **239**(1-2): p. 141-148.
18. Lilja, J., D.Y. Murzin, T. Salmi, J. Aumo, P.M. Arvela, and M. Sundell, *Esterification of different acids over heterogeneous and homogeneous catalysts and correlation with the Taft equation.* Journal of Molecular Catalysis a-Chemical, 2002. **182**(1): p. 555-563.
19. Bart, H.J., W. Kaltenbrunner, and H. Landschutzer, *Kinetics of esterification of acetic acid with propyl alcohol by heterogeneous catalysis.* International Journal of Chemical Kinetics, 1996. **28**(9): p. 649-656.
20. Zhang, Y., L. Ma, and J.C. Yang, *Kinetics of esterification of lactic acid with ethanol catalyzed by cation-exchange resins.* Reactive & Functional Polymers, 2004. **61**(1): p. 101-114.
21. Teo, H.T.R. and B. Saha, *Heterogeneous catalysed esterification of acetic acid with isoamyl alcohol: kinetic studies.* Journal of Catalysis, 2004. **228**(1): p. 174-182.
22. JagadeeshBabu, P.E., K. Sandesh, and M.B. Saidutta, *Kinetics of Esterification of Acetic Acid with Methanol in the Presence of Ion Exchange Resin Catalysts.* Industrial & Engineering Chemistry Research, 2011. **50**(12): p. 7155-7160.
23. Tesser, R., L. Casale, D. Verde, M. Di Serio, and E. Santacesaria, *Kinetics and modeling of fatty acids esterification on acid exchange resins.* Chemical Engineering Journal, 2010. **157**(2-3): p. 539-550.
24. Santacesaria, E., R. Tesser, M. Di Serio, M. Guida, D. Gaetano, and A.G. Agreda, *Kinetics and mass transfer of free fatty acids esterification with methanol in a tubular packed bed reactor: A key pretreatment in biodiesel production.* Industrial & Engineering Chemistry Research, 2007. **46**(15): p. 5113-5121.
25. Pasias, S., N. Barakos, C. Alexopoulos, and N. Papayannakos, *Heterogeneously catalyzed esterification of FFAs in vegetable oils.* Chemical Engineering & Technology, 2006. **29**(11): p. 1365-1371.
26. Pasias, S.A., N.K. Barakos, and N.G. Papayannakos, *Catalytic Effect of Free Fatty Acids on Cotton Seed Oil Thermal Transesterification.* Industrial & Engineering Chemistry Research, 2009. **48**(9): p. 4266-4273.
27. Ali, S.H., O. Al-Rashed, F.A. Azeez, and S.Q. Merchant, *Potential biofuel additive from renewable sources - Kinetic study of formation of butyl acetate by heterogeneously catalyzed transesterification of ethyl acetate with butanol.* Bioresource Technology, 2011. **102**(21): p. 10094-10103.
28. Yadav, G.D. and M. Rahuman, *Cation-exchange resin-catalysed acylations and esterifications in fine chemical and perfumery industries.* Organic Process Research & Development, 2002. **6**(5): p. 706-713.
29. Yadav, G.D. and M.B. Thathagar, *Esterification of maleic acid with ethanol over cation-exchange resin catalysts.* Reactive & Functional Polymers, 2002. **52**(2): p. 99-110.
30. Xu, Y., W.J. Dou, Y.J. Zhao, G.X. Huang, and X.B. Ma, *Kinetics Study for Ion-Exchange-Resin Catalyzed Hydrolysis of Methyl Glycolate.* Industrial & Engineering Chemistry Research, 2012. **51**(36): p. 11653-11658.
31. Yu, W.F., K. Hidajat, and A.K. Ray, *Determination of adsorption and kinetic parameters for methyl acetate esterification and hydrolysis reaction catalyzed by Amberlyst 15.* Applied Catalysis a-General, 2004. **260**(2): p. 191-205.
32. Tesser, R., M. Di Serio, L. Casale, G. Carotenuto, and E. Santacesaria, *Absorption of water/methanol binary system on ion-exchange resins.* Canadian Journal of Chemical Engineering, 2010. **88**(6): p. 1044-1053.

33. Parra, D., J. Tejero, F. Cunill, M. Iborra, and J.F. Izquierdo, *Kinetic-study of MTBE liquid-phase synthesis using C-4 olefinic cut.* Chemical Engineering Science, 1994. **49**(24A): p. 4563-4578.
34. Huang, Y.S. and K. Sundmacher, *Kinetics study of propyl acetate synthesis reaction catalyzed by Amberlyst 15.* International Journal of Chemical Kinetics, 2007. **39**(5): p. 245-253.
35. Lode, F., S. Freitas, M. Mazzotti, and M. Morbidelli, *Sorptive and catalytic properties of partially sulfonated resins.* Industrial & Engineering Chemistry Research, 2004. **43**(11): p. 2658-2668.
36. Tiihonen, J., I. Markkanen, A. Karki, P. Aanismaa, M. Laatikainen, and E. Paatero, *Modelling the sorption of water-ethanol mixtures in cross-linked ionic and neutral polymers.* Chemical Engineering Science, 2002. **57**(11): p. 1885-1897.
37. Mazzotti, M., A. Kruglov, B. Neri, D. Gelosa, and M. Morbidelli, *A continuous chromatographic reactor: SMBR.* Chemical Engineering Science, 1996. **51**(10): p. 1827-1836.

6

KINETIC STUDY OF ACETIC ACID ESTERIFICATION WITH METHANOL CATALYZED BY GEL AND MACROPOROUS RESINS

Abstract - *The liquid-phase esterification kinetics of acetic acid with methanol to methyl acetate and water catalyzed by gel (Lewatit K1221) and macroporous (Lewatit K2629) ion exchange resins have been investigated and compared with literature reported data acquired on Amberlyst 15. The effects of the resin swelling, the initial molar methanol to acetic acid ratio (1:1 – 10:1) and the temperature (303 – 333 K) on the reaction kinetics were investigated. Similar to ethyl acetate transesterification, the gel type resin exhibits a remarkably higher catalytic activity compared to the macroporous resins, despite the similar number of sulfonic acid groups. This can be attributed to the differences in the accessibility of active sites during reaction, which are related to the resins' swelling, especially when these resins are in contact with polar components, such as water and methanol. The differences in catalytic behavior between the considered resins have been assessed using an exchange based Eley-Rideal model in which it is assumed that (1) all the active sites are occupied, (2) the acid undergoes a proton exchange with the protonated methanol and (3) the reaction occurs according to an Eley-Rideal mechanism with the surface reaction between protonated acetic acid and methanol from the bulk as rate-determining step. The activation energy was determined at 47 kJ mol^{-1}, irrespective of the resin used.*

6.1 Introduction

The kinetics and thermodynamics of a wide variety of esterification reactions have been investigated throughout the history of physical chemistry, dating back to pioneering efforts of Berthelot and Gilles in 1863 [1]. The nature and the type of ion exchange resins used as catalyst, in combination with more conventional reaction parameters such as the reaction temperature and the initial molar acid to alcohol ratio, strongly affect the kinetics and, hence, the time required to establish target conversions and yields as determined by thermodynamics [2].

In the present chapter, acetic acid esterification kinetics have been assessed on a gel type and macroporous resins making use of a kinetic model according to an exchange based Eley-Rideal mechanism. The latter model performs well in the simulation of the kinetics data acquired on a gel type resin Lewatit K1221, see Chapter 5. Apart from the data set on this reference resin, intrinsic acetic acid esterification kinetics have also been measured on a macroporous resin, i.e., Lewatit K2629. Moreover, a literature data set acquired on Amberlyst 15 [3] has been included in the comparison.

6.2 Procedures

Ion exchange catalyzed liquid phase esterification reactions of acetic acid with methanol catalyzed by Lewatit K1221, Lewatit K2629 and Amberlyst 15 were considered. The measurements on Lewatit K1221 and Lewatit K2629 have been acquired as part of the present work, whereas the data on Amberlyst 15 were taken from the literature [3]. The catalyst properties are described in more detail in Section 2.1. All experiments have been performed in a batch reactor.

The pretreatment of Lewatit K1221 and Lewatit K2629, consisted of 24 h freeze drying under vacuum at 233K, see also Section 2.1. The pretreatment of Amberlyst 15, consisted of a wash step with methanol followed by several wash steps with water to remove impurities. Wash steps with water were repeated until the supernatant liquid became colorless. Afterwards the washed Amberlyst 15 was dried under vacuum at 363 K until the mass remained constant, which usually took about 2 days [3].

The reactor setup for the experiments catalyzed by Lewatit K1221 or Lewatit K2629 and the kinetic experimental procedure are described in more detail in Section 2.3.1. For Amberlyst 15, Pöpken et al. [3] used an isothermal glass reactor with a volume of 500 mL. A constant stirring at a speed of 250 rpm was imposed by a plate-type stirrer. The kinetic

experimental procedure was similar to the one described in in Section 2.3.1. During each experiment between 15 and 45 samples were taken. The acetic acid concentration of each sample was analyzed by potentiometric titration with sodium hydroxide [3].

Similar to Chapter 3 an intrinsic kinetics dataset for gel and macroporous resins was acquired. The number of experimental points, the number of experiments and also the experimental conditions of the experiments are given in Table 6-1. Particular attention should be paid to the limited information obtained with respect to the temperature dependence of the acetic acid esterification kinetics on Lewatit K2629, i.e., experiments are only available at 323.15 and 333.15 K, and to the amount of catalyst used in the experiments with Amberlyst 15. The latter exceeds that used in the case of Lewatit K1221 or Lewatit K2629 by at least a factor of 10.

Table 6-1 Range of experimental conditions for acetic acid esterification with methanol

Catalyst	Lewatit K1221	Lewatit K2629	Amberlyst 15 [3]
Number of experimental points	748	164	61
Number of experiments	58	12	10
Temperature (K)	303.15 – 333.15	323.15 & 333.15	303.45 – 323.15
Pressure (MPa)	0.1	0.1	0.1
MeOH:HOAc molar ratio	0.7:1 – 10:1	1:1 – 10:1	1:1 – 20:1
Mass of catalyst (10^{-3} kg)	0.5 – 2.1	0.5 – 2.9	5.0 – 55.4
Experiment time (s)	0.0 – 25200.0	0.0 – 14400.0	0.0 – 7260.0
Batch time* (kg s)	0.0 – 37.8	0.0 – 37.0	0.0 – 39.7

*Defined as product of experiment time multiplied by the mass of catalyst

To ascertain that the data represent intrinsic kinetics, the absence of internal as well as external mass-transfer resistances in the kinetics observed on Lewatit K1221 and Lewatit K2629, was evaluated as described in Section 2.3.4. Pöpken et al. [3] have evaluated the mass transfer resistance experimentally for Amberlyst 15 and proved absence of internal and external mass transfer resistances. The parameter estimation and model discrimination procedure has been described in detail in Section 2.5.

6.3 Experimental results

6.3.1 Volumetric swelling tests

The swelling ratios of the investigated resins in contact with the pure reactants and products are reported in Table 6-2. Similarly to gel type resins, see Chapter 5, macroporous resins swell more in polar than in less or apolar solvents. Swelling in water is more pronounced than in any of the solvents with a lower dielectric constant [4, 5]. It is also evident from Table 6-2 that a macroporous resin, c.q., Lewatit K2629 or Amberlyst 15, swells to a lesser extent than a gel type resin. Similar observations have been made when investigating the swelling with the components involved in ethyl acetate transesterification with methanol, see Table 4-2, and can be explained by the different crosslinking degrees, see Table 2-1 and section 4.3.1.

Table 6-2 Swelling ratio (S) of Lewatit K1221, Lewatit K2629 and Amberlyst 15 in water, methanol, methyl acetate and acetic acid, and dielectric constant of these components.

Swelling ratio	water	methanol MeOH	methyl acetate MeOAc	acetic acid HOAc
K1221	2.56 ± 0.09	2.45 ± 0.07	1.24 ± 0.05	1.18 ± 0.08
K2629	1.66 ± 0.07	1.49 ± 0.14	1.32 ± 0.03	1.42 ± 0.03
Amberlyst 15	1.59 ± 0.04	1.43 ± 0.06	1.33 ± 0.07	1.40 ± 0.01
Dielectric constant	80.1	32.7	6.70	6.15

6.3.2 Catalytic activity

The catalytic activity of the considered resins is shown in Figure 6-1. Similar to transesterification, Lewatit K1221 exhibits a higher activity than the macroporous resins, despite the comparable active site concentration, see Table 2-2. The difference in catalytic activity between gel type and macroporous resins can be attributed to the accessibility of the active sites, which is related to the swelling capacity of the resin, see Section 4.3.2 and Section 6.3.1. The importance of resin swelling in esterification kinetics has also been demonstrated by Lotero et al. [6]. Resin swelling guarantees substrate accessibility to the active sites and, hence, affects its overall reactivity. Upon swelling, the resins' gel beads expand their polystyrene chains such that new/additional porous space and, hence, active sites become available.

The evolution of the methyl acetate yield on both macroporous resins deserves some further, more specific attention. Although the reaction with Amberlyst 15 has been performed

at 323 K, compared to 333 K for Lewatit K2629, at short batch times, Amberlyst 15 exhibits higher methyl acetate yields and, hence, a higher initial reaction rate, compared to Lewatit K2629. With increasing batch time, however, the methyl acetate yield on Amberlyst 15 increases more slowly than on Lewatit K2629 such that, ultimately, the highest methyl acetate yields are obtained over the latter resin. Hence, whereas Amberlyst 15 initially, apparently, swells more than Lewatit K2629, the former exhibits more pronounced product adsorption and, hence, inhibition, than the latter. Note that the swelling ratios for K2629 and Amberlyst 15 as reported in Table 6-2 are within each other's confidence interval and, hence, do not confirm of/nor form a contra-indication against the suggested interpretation. It should also be kept in mind that Amberlyst 15 underwent a different pretreatment procedure, see Section 6.2.

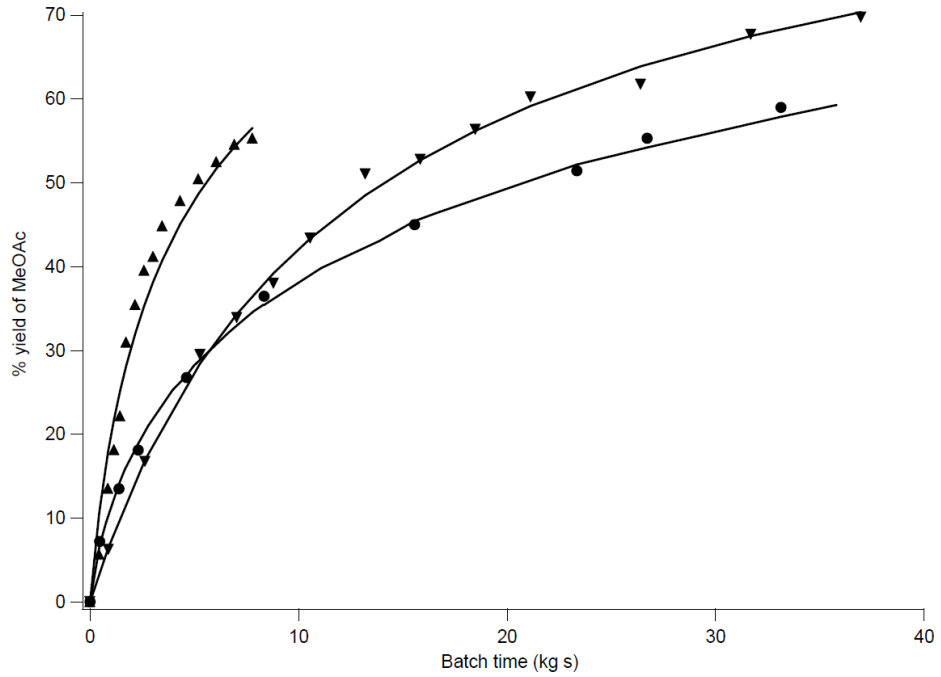

Figure 6-1 **Simulated (lines; ER_exchange model, Eq 5-1 with parameters as reported in Table 6-3) and experimental (symbols) methyl acetate yield versus batch time catalyzed by different ion exchange resins (▲ Lewatit K1221, ▼ Lewatit K2629 and ● Amberlyst 15). (Temperature = 333 K and $C_{HOAc,0}$ = 9.50 M for Lewatit K1221 and Lewatit K2629; 323 K and $C_{HOAc,0}$ = 4.02 M for Amberlyst 15; Initial molar ratio of MeOH:HOAc = 1:1)**

Figure 6-2 shows that, under the investigated operating conditions, the reaction kinetics can be enhanced by using a methanol excess. The esterification rate, however, will not keep on increasing linearly with initial molar methanol to acetic acid ratio. It has already been demonstrated in the literature [4, 7, 8] that the initial acetic acid esterification rate with methanol first increases with the initial molar methanol to acetic acid ratio before reaching a

maximum and that it subsequently decreases. The latter evolution can be relatively easily rationalized in terms of establishing optimum molar fractions within the resin for obtaining a maximum rate for a bimolecular reaction. The higher methyl acetate yield as a function of the batch time at high initial molar methanol to acetic acid ratios for Amberlyst 15 and Lewatit K2629 are in line with what is obtained for acetic acid esterification on Lewatit K1221, see Figure 5-2, as well as for transesterification on all investigated resins, see Section 4.3.2.

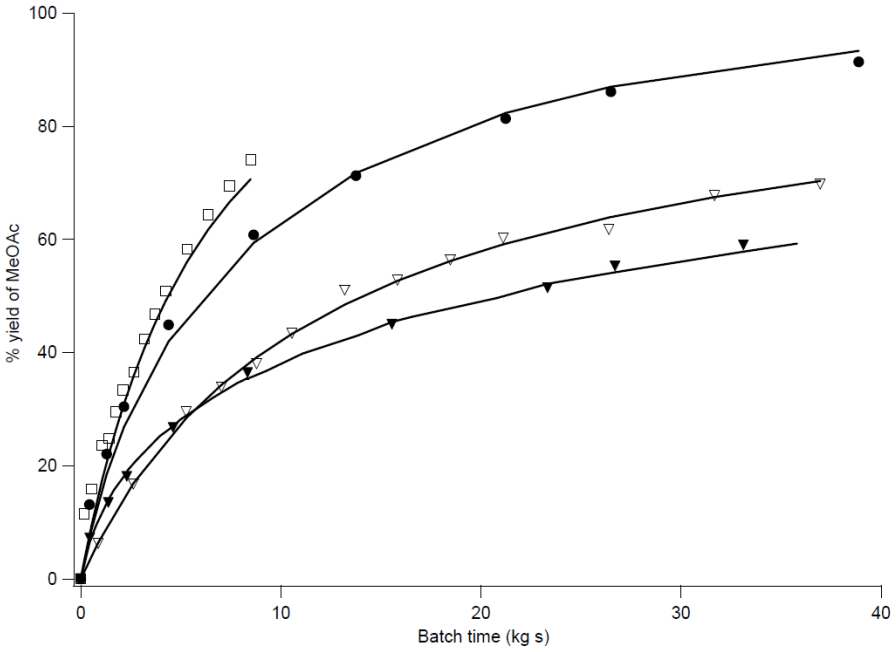

Figure 6-2 **Simulated (lines; ER_exchange model, Eq 5-1 with parameters as reported in Table 6-3) and experimental (symbols) methyl acetate yield versus batch time catalyzed by Amberlyst 15 (filled symbols) and Lewatit K2629 (empty symbols) at different initial MeOH:HOAc molar ratios (■ 10:1; ● 8.3:1; ▼ 1:1) (Temperature = 323 K and $C_{HOAc,0}$ = 0.86 M (8.3:1); $C_{HOAc,0}$ = 4.02 M (1:1) for Amberlyst 15) (Temperature = 333 K and $C_{HOAc,0}$ = 1.90 M (10:1); $C_{HOAc,0}$ = 9.50 M (1:1) for Lewatit K2629)**

6.4 Kinetic modeling of gel and macroporous resin catalyzed esterification

The ability of the ER-exchange model, see Chapter 5, to adequately describe the reaction kinetics catalyzed by macroporous resins is evaluated first. The reaction mechanism and corresponding rate equation are described in detail in section 5.3 and 5.4. Similar to Chapter 4, a model regression to the experimental kinetics data measured on the alternative resins has been performed for the model selected on the reference resin, i.e., ER-exchange. Moreover, amongst the models considered in Chapter 5 for acetic acid esterification on Lewatit K1221, the same ER-exchange model was found to be best performing on the macroporous resins considered here, see Appendix B (Section B-2).

6.4.1 Parameter estimation

The parameter estimates and corresponding statistics for the three considered resins are reported in Table 6-3. All multiple correlation coefficients exceed 0.990. All regressions are globally significant with F values above 1000 if not 10 000. The comparatively lower F value obtained for Amberlyst 15 most probably stems from the lower number of data points. In conclusion, these values indicate an appropriate representation of the experimental data by the ER-exchange model for all three catalysts such that the model provides a sound basis for the comparison of their behavior.

Table 6-3 Statistical information and parameter estimation of the ER-exchange model for the esterification catalyzed by Lewatit K1221, Lewatit K2629 and Amberlyst 15.

Catalyst	K1221	K2629	Amberlyst 15
N	748	164	61
RSSQ	13.13	1.446	0.305
R^2	0.991	0.996	0.990
F value	29 000	19 300	1 900
$k_{SR\,Tref}$ (mol $kg_{cat}^{-1}s^{-1}$)	0.215 ± 0.012	0.057 ± 0.004	0.300 ± 0.124
E_A (kJ mol^{-1})	46.00 ± 1.86	47.00[b]	47.58 ± 0.44
K_{HOAc}	4.580 ± 0.314	5.812 ± 0.479	1.1026 ± 0.657
K_l	3.611 ± 0.338	1.983 ± 0.318	4.805 ± 1.478

[b] This parameter was fixed, as there was not enough temperature variation in the experimental dataset (Table 6-1).

The regressions resulted in a comparable composite activation energies for acetic acid esterification catalyzed by Amberlyst 15 and K1221, as could be expected based on the results obtained for transesterification, see section 4.5. Because the experimental data set acquired on Lewatit K2629 only contains experiments at 323.15 and 333.15 K, the estimation of a composite activation energy resulted in an unacceptably wide confidence interval. Hence, an average value from those obtained for Lewatit K1221 and Amberlyst 15 was used, i.e., 47 kJ mol^{-1} for this resin. Several authors published similar values ranging from 38.13 to 51.88 kJ mol^{-1} for the acetic acid esterification with methanol catalyzed with Amberlyst 15 [1, 9, 10].

In section 6.3.2, the difference in catalytic activity was attributed to the accessibility of the active sites, which is related to the swelling of the resin in the reaction mixture. The swelling ratio depends on the crosslinking degree and, hence, the surface reaction rate coefficient for K1221 is expected to be higher than the ones for Lewatit K2629 and Amberlyst 15. A similar surface reaction rate coefficient is expected for Lewatit K2629 and Amberlyst 15. It is evident from Table 6-3 that the expected order in surface reaction rate coefficients is not respected by the obtained parameter estimates. This may be the result of

correlation between this surface reaction rate coefficient and the acetic acid exchange coefficient. When looking at the product of both also denoted as the composite rate coefficient, as it occurs in the in the numerator of the rate expression, see Table 5-2, the expected order is indeed found: 0.985 (K1221) > 0.331 (K2629) ≈ 0.330 (Amberlyst 15). The ratio between the composite rate coefficient on gel-type versus macroporous resins amounts to about three, which is in to the range of 3- to 4-fold as reported for transesterification, see Section 4.5.

The surface reaction rate of the esterification is 4 to 6 times bigger compared to the surface reaction rate of the transesterification, as could be expected from the experimental results.

Whereas the products exchange coefficients, K_l, are relatively similar in a range from 2 (K2629) to 5 (Amberlyst 15), slightly more pronounced differences are obtained for the acetic acid exchange coefficients, K_{HOAc}, that range from 1 (Amberlyst 15) to 6 (K2629). Particularly noteworthy is that the ratio of the acetic acid and products exchange coefficients exceeds one for Lewatit K1221 and Lewatit K2629 while it is lower than one for Amberlyst 15. Whereas the higher than expected acetic acid exchange coefficient compared to that of the products has been attributed to the lack of distinction between the bulk liquid and resin phase in addition to the protonated species, see Section 5.5, apparently, additional phenomena are at stake on Amberlyst 15. It was already evident from Figure 6-1, see Section 6.3.2, that, at higher batch times, the methyl acetate yield evolves less steep on Amberlyst 15 than on Lewatit K2629 at higher batch times, which can be interpreted in terms of more pronounced product inhibition. The latter can, indeed, become evident via a comparatively higher product exchange coefficient. It should also, again, be pointed out that the acetic acid esterification data on Amberlyst 15 were taken from the literature, while those on Lewatit K1221 and Lewatit K2629 have been measured as part of the present work. As a result, the differences observed in the estimates for the exchange coefficients may also be related to procedural issues. Firstly the Amberlyst 15 resin was washed with methanol and water to remove the impurities, and afterwards dried under vacuum for 2 days at 363 K. This pretreatment is distinct from the 24h freeze drying at 233 K, which has been performed for Lewatit K1221 and Lewatit K2629. Another difference in the experimental data obtained on Lewatit K1221 and Lewatit K2629, compared to Amberlyst 15 is that the ratio of the reactant concentration to that of the active sites is 20 to 60 times higher on the former than on the latter.

It is evident from the above discussion that, whereas no objections based on physical grounds could be made against the exchange-based Eley-Rideal mechanism for ethyl acetate

transesterification, the results obtained so far for acetic acid esterification indicate the need for some further refinement, in particular with respect to the thermodynamics within the resin. The polarities or dielectric constants of the components involved in esterification vary in a much wider range than those of the components involved in transesterification. More specifically the presence of water as reaction product in acetic acid esterification results in much more pronounced variations in polarization of the reaction mixture compared to transesterification. As a result, the resin swelling and component sorption in an esterification mixture, with changing polarization with methyl acetate yield, is much more complex than expected from what was observed with ethyl acetate transesterification. Mazzotti et al. [4] found that the esterification equilibrium that could be obtained in a batch reactor depended on the amount of Amberlyst 15 used. By increasing the resin to reactants ratio, not only the esterification rate was enhanced but also the equilibrium composition shifted towards the side of the reaction products. This effect could be attributed to the significant swelling of the resin due to solvent sorption and, hence, due to the non-negligible volume of the sorbed phase compared to the bulk phase. Such effects are less likely or will even not occur in non-swelling solid catalysts [4]. Similar conclusions were reached by Sainio et al. [11] and Tesser et al. [12]. They attributed the effect of the amount of resin used in a batch reactor on the equilibrium composition to the simultaneous chemical and phase equilibrium between liquid bulk and resin. Sainio et al. [11] also mentioned that a significant solvent uptake by the resins occurred in a batch reactor when using a low reactants to resin ratio, such as for the Amberlyst 15. Given the above described indications that a further model enhancement is required with respect to the description of the thermodynamics within the resin, it can be understood that kinetics measurements performed at significantly different reagent to catalyst/resin ratio lead to different estimates for the exchange coefficients and/or different trends in these values.

In summary, several potential causes have been identified for the apparent discrepancies between the exchange coefficients obtained based on the literature reported Amberlyst 15 data on the one hand and the data measured on Lewatit K1221 and Lewatit K2629 on the other hand. Mainly differences in pretreatment may have resulted in a more pronounced product inhibition, which became evident via a higher product to acetic acid exchange coefficient ratio. On the other hand, the reactant concentration to active sites ratio in the Amberlyst 15 data was 20 up to 60 times smaller compared to the other data. This range of reactant concentration to active sites ratio may be wider than can be adequately described by the model for the exchange of components between the bulk and the resin with a

unique set of parameter values, indicating, again, that an enhanced model, e.g., based on Flory-Huggins theory will be required.

6.5 Assessment of molar fractions within the resin

Despite the identified need for further model enhancement, a qualitative assessment of the evolution of the molar fractions in the resin as a function of the methyl acetate yield may provide further insight in the model behavior and give indications how enhancements may be implemented. The evolution of the molar fractions in the resin as a function of the methyl acetate yield is simulated for varying initial molar methanol to acetic acid ratios and is given in Figure 6-3 for Lewatit K2629 and Amberlyst 15. A qualitatively similar evolution is obtained for the gel type resin Lewatit K1221, see Figure 5-6. Such a similarity was also found for ethyl acetate transesterification, see Chapter 4.

Particularly at an initial molar methanol to acetic acid ratio of 1:1 the evolution of the molar fractions in the resin for Amberlyst 15 is entirely different from that simulated for Lewatit K1221 or Lewatit K2629. Initially, i.e., at short batch times, methanol is much more abundant on Amberlyst 15 than on the other resins, where acetic acid is the most abundant component. When the reaction proceeds, the products fraction rather rapidly becomes the most abundant one, especially for Amberlyst 15. It represents the acknowledge of several researchers about the adverse effect of water on the reaction rate on a cation exchange resin catalysis system. [13-17].

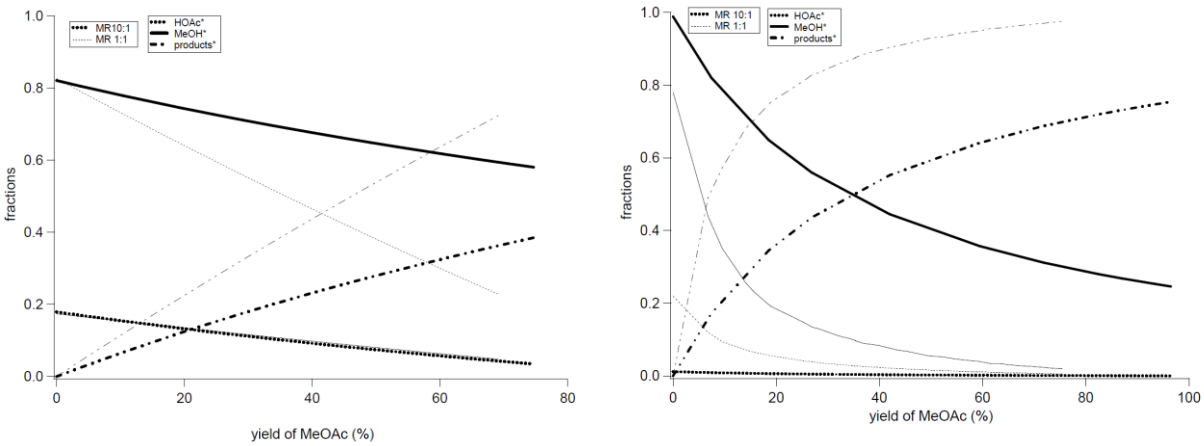

Figure 6-3 **Simulated (ER_exchange model, Eq. 5-1, with parameters as reported in Table 6-3) fractions as a function of the methyl acetate yield at 333 K (left) at 323 K (right) with various MeOH:EtOAc ratios (1:1 = fine lines, 10:1 = bold lines), catalyzed by Lewatit K2629 (left) and Amberlyst 15 (right). (HOAc* and products* chemisorbed fractions of acetic acid and products (methyl acetate and water), respectively; (MeOH*) fraction of sites covered by methanol).**

6.6 Conclusions

A wide range of acid ion exchange resins can be used as catalysts for acetic acid esterification with methanol to methyl acetate and water. Due to the chemical similarity between the considered resins, differences in observed reaction rates were mainly related to the accessibility of the active sites, which are inversely proportional with the amount of crosslinking by divinylbenzene due to the corresponding swelling behavior of the resins. An exchange based kinetic model, which implicitly accounts for resin swelling, allowed interpreting the observed differences between the various resins, although the estimates obtained for the acetic acid and products exchange coefficients indicated the need for a more elaborate description of the thermodynamics in the resin. The composite rate coefficient, defined as the product of the surface reaction rate coefficient and the acetic acid exchange coefficient, was found to be proportional to the accessibility of the active sites and, hence, inversely proportional to the crosslinking degree. Similar as for transesterification, the composite rate coefficient on the gel type resin, Lewatit K1221, was 3-fold higher than on the macroporous resins. The composite activation energy amounts to 46 kJ/mol independently of the considered resin, which is an indication of their chemical similarity.

6.7 References

1. JagadeeshBabu, P.E., K. Sandesh, and M.B. Saidutta, *Kinetics of Esterification of Acetic Acid with Methanol in the Presence of Ion Exchange Resin Catalysts.* Industrial & Engineering Chemistry Research, 2011. **50**(12): p. 7155-7160.
2. Polyanskii, N.G. and V.K. Sapozhnikov, *New Advances in Catalysis by Ion-exchange Resins.* Russian Chemical Reviews, 1977. **46**(3): p. 445-476.
3. Popken, T., L. Gotze, and J. Gmehling, *Reaction kinetics and chemical equilibrium of homogeneously and heterogeneously catalyzed acetic acid esterification with methanol and methyl acetate hydrolysis.* Industrial & Engineering Chemistry Research, 2000. **39**(7): p. 2601-2611.
4. Mazzotti, M., B. Neri, D. Gelosa, A. Kruglov, and M. Morbidelli, *Kinetics of liquid-phase esterification catalyzed by acidic resins.* Industrial & Engineering Chemistry Research, 1997. **36**(1): p. 3-10.
5. Helfferich, F.G., *Ion Exchange*. 1995: Dover Publications.
6. Lotero, E., Y.J. Liu, D.E. Lopez, K. Suwannakarn, D.A. Bruce, and J.G. Goodwin, *Synthesis of biodiesel via acid catalysis.* Industrial & Engineering Chemistry Research, 2005. **44**(14): p. 5353-5363.
7. Ali, S.H. and S.Q. Merchant, *Kinetics of the esterification of acetic acid with 2-propanol: Impact of different acidic cation exchange resins on reaction mechanism.* International Journal of Chemical Kinetics, 2006. **38**(10): p. 593-612.
8. Mazzotti, M., A. Kruglov, B. Neri, D. Gelosa, and M. Morbidelli, *A continuous chromatographic reactor: SMBR.* Chemical Engineering Science, 1996. **51**(10): p. 1827-1836.
9. Yu, W.F., K. Hidajat, and A.K. Ray, *Determination of adsorption and kinetic parameters for methyl acetate esterification and hydrolysis reaction catalyzed by Amberlyst 15.* Applied Catalysis a-General, 2004. **260**(2): p. 191-205.
10. Tsai, Y.T., H.M. Lin, and M.J. Lee, *Kinetics behavior of esterification of acetic acid with methanol over Amberlyst 36.* Chemical Engineering Journal, 2011. **171**(3): p. 1367-1372.
11. Sainio, T., M. Laatikainen, and E. Paatero, *Phase equilibria in solvent mixture-ion exchange resin catalyst systems.* Fluid Phase Equilibria, 2004. **218**(2): p. 269-283.
12. Tesser, R., L. Casale, D. Verde, M. Di Serio, and E. Santacesaria, *Kinetics and modeling of fatty acids esterification on acid exchange resins.* Chemical Engineering Journal, 2010. **157**(2-3): p. 539-550.
13. du Toit, E. and W. Nicol, *The rate inhibiting effect of water as a product on reactions catalysed by cation exchange resins: formation of mesityl oxide from acetone as case study.* Applied Catalysis a-General, 2004. **277**(1-2): p. 219-225.
14. Chakrabarti, A. and M.M. Sharma, *Cationic Ion-Exchange Resins as Catalyst.* Reactive Polymers, 1993. **20**(1-2): p. 1-45.
15. Limbeck, U., C. Altwicker, U. Kunz, and U. Hoffmann, *Rate expression for THF synthesis on acidic ion exchange resin.* Chemical Engineering Science, 2001. **56**(6): p. 2171-2178.
16. Yang, B.L., S.B. Yang, and R.Q. Yao, *Synthesis of ethyl tert-butyl ether from tert-butyl alcohol and ethanol on strong acid cation-exchange resins.* Reactive & Functional Polymers, 2000. **44**(2): p. 167-175.
17. Kawase, M., Y. Inoue, T. Araki, and K. Hashimoto, *The simulated moving-bed reactor for production of bisphenol A.* Catalysis Today, 1999. **48**(1-4): p. 199-209.

7

CONCLUSIONS AND FUTURE WORK

This work has explored the potential of ion exchange resins in the heterogeneously catalyzed (trans)esterification of ethyl acetate and acetic acid with methanol. A wide range of resins, including gel-type, Lewatit K1221, and macroporous acid ion exchange resins, Lewatit K2640, Lewatit K2629 and Amberlyst 15 has been investigated in a batch reactor set-up to determine intrinsic kinetics.

The effect of temperature and initial molar methanol to ester/acid ratio was investigated for both reactions, with both types of resins and resulted in behavior as could be expected, i.e., (i) higher reaction rates at higher temperatures and correspondingly higher conversions at the same batch time and (ii) higher initial molar methanol to ester/acid ratios resulting in a higher ester/acid conversion and, hence, higher reaction rates, because the (ethyl acetate)acetic acid/catalyst amount ratio was kept constant. Thanks to the pronounced polarity of the reaction mixtures involved, the highest (trans)esterification rates were obtained on the gel type resin.

Due to their particular structure, the studied ion exchange resins are subjected to a remarkable swelling phenomenon when contacted with polar solvents. Gel type resins swell more than macroporous resins due to the rigidity induced by the higher divinylbenzene cross linking in the latter. Swelling is also more pronounced in more polar solvents.

The (trans)esterification kinetic data showed that Lewatit K1221, the gel type and reference catalyst, exhibits a noticeably higher catalytic activity than the other resins, despite the comparable active site concentration. The catalytic activity for transesterification of Lewatit K2629 and Lewatit K2640 is quite similar, while Amberlyst 15 shows the lowest catalytic activity for transesterification. For esterification, the catalytic activities of Amberlyst 15 and Lewatit K2629 were comparable. These observations show that resin-catalyzed (trans)esterification rates do not only depend on the number of active sites but also on their

accessibility. The latter is determined by the divinylbenzene content of the resin, i.e., a higher content reduces the resins' swelling and, hence, also the accessibility of the active sites, leading to a lower catalytic activity.

The resins' swelling, hence plays a fundamental role in the observed (trans)esterification kinetics. Although the pseudo-homogeneous or the adsorption-based models are frequently used in literature to conceptualize and quantify the (trans)esterification [1-13], the kinetics observed with such a resin require a different approach than the conventional, heterogeneous catalysts. In this thesis, a novel exchange based kinetic model, that implicitly accounts for resin swelling, has been developed with the following assumptions: (1) all active sites are occupied, (2) the exchange reactions between protonated reagents or protonated products are quasi-equilibrated and (3) an Eley-Rideal type surface reaction between protonated ester/acid with methanol from the bulk is the rate-determining step. The non-ideal behavior of the reaction mixture was assessed. Results showed that activity coefficients are quite different from 1, indicating pronounced non-ideality. Therefore activities instead of concentrations were used in the kinetic models.

First, a model discrimination between adsorption-based models has been performed for ethyl acetate transesterification with methanol catalyzed by Lewatit K1221. The best performing model was that based on an Eley-Rideal mechanism, with the surface reaction of adsorbed methanol with ethyl acetate from the bulk as the rate-determining step. It indicates that pronounced sorption saturation effects occurred for methanol whereas, according to the homogeneous transesterification reaction mechanism, such effects would rather have been expected for ethyl acetate. This apparent contradiction has been the onset of a model refinement in which resin swelling was implicitly accounted for via an assumed full occupation of the resins' active sites and component exchange between these sites and the liquid bulk.

Second, model discrimination between this exchange and adsorption-based models for the (trans)esterification reaction catalyzed by the reference catalyst, Lewatit K1221, identified the exchange based model as the preferred one. Although the exchange based model does not outperform the adsorption-based models, the good statistics combined with the physicochemical meaning of the model were the decisive factors in its selection for the further assessment of the (trans)esterification kinetics on the alternative resins.

The exchange based model describes all experimental (trans)esterification data accurately. Activation energies equal to 49 kJ mol^{-1} and 47 kJ mol^{-1}, for respectively transesterification and esterification, irrespective the resin used, are obtained. For both

reactions, the composite rate coefficient, defined as the product of the surface reaction rate coefficient and the reactant ester/acid at the reference temperature, is three to four times higher for the gel type catalyst than for the macroporous catalysts. This could be expected from the experimental data and the similar activation energies. The esterification rate coefficient exceeds that for transesterification by a factor of 4.

The exchange equilibrium coefficients all have the same order of magnitude for all catalysts. For transesterification, the ratio between the methyl and ethyl acetate exchange coefficient is identical for all four resins, Lewatit K1221, Lewatit K2629, Lewatit K2640 and Amberlyst 15, and amounts to approximately 4. This reflects the similarity of the resins. The additional methylene group in ethyl acetate results in a lower exchange equilibrium coefficient. For esterification the exchange coefficients of the products and acetic acid exhibit some apparent discrepancies. The more pronounced variation of the polarity of the reaction mixture in esterification compared to in transesterification, in addition to the 20 to 60 times higher resin to reactant ratio in the literature reported data set on Amberlyst 15 compared to the data sets acquired on Lewatit K1221 and Lewatit K2629 acquired in the present work, apparently resulted in exchange behavior that can only be captured by an enhanced version of the model for describing the thermodynamics in the resin, e.g., by the Flory Huggins theory.

The presented modelling methodology has resulted in an accurate simulation of the kinetic behavior of the (trans)esterification catalyzed by different types of resins and allowed developing a physically sound interpretation of the reaction kinetics and mechanism. Hence, the proposed model is able to simulate the (trans)esterification, of low-molecular weight components, catalyzed by ion exchange resins.

The present work can be further extended in several directions. The experimental knowledge about the catalytic activity of ion exchange resins can be used to evaluate of the catalytic activity of new synthesized or commercial available catalysts. For the modeling part: first some more thorough, additional experimental investigation of the (trans)esterification, e.g. on an additional resin, within a wide range of experimental conditions, e.g. with higher-molecular weight reactants, and with (synthetic) feedstocks containing mixtures of esters and acids, to provide more insight, validate and refine the kinetic model with respect to accounting for a distinct ‘polymer phase’ in between the liquid bulk and the protonated species. Second, the ability of the kinetic model to describe other reactions, such as etherification, condensation, alkylation, catalyzed by ion-exchange resins could be evaluated. Third, this kinetic model may be helpful as a tool for resin selection. While resin selection and design frequently occurs on a trial and error basis, the insight

gained by models such as the one developed in this work may provide clear guidelines about the desired resin properties, such as divinylbenzene percentage, sulfonation degree, macroporosity,… . Similar knowledge can also be exploited for industrial reactor design and optimization.

1. Saha, B. and M. Streat, *Transesterification of cyclohexyl acrylate with n-butanol and 2-ethylhexanol: acid-treated clay, ion exchange resins and tetrabutyl titanate as catalysts.* Reactive & Functional Polymers, 1999. **40**(1): p. 13-27.
2. Jimenez, L., A. Garvin, and J. Costa-Lopez, *The production of butyl acetate and methanol via reactive and extractive distillation. I. Chemical equilibrium, kinetics, and mass-transfer issues.* Industrial & Engineering Chemistry Research, 2002. **41**(26): p. 6663-6669.
3. Pappu, V.K.S., A.J. Yanez, L. Peereboom, E. Muller, C.T. Lira, and D.J. Miller, *A kinetic model of the Amberlyst-15 catalyzed transesterification of methyl stearate with n-butanol.* Bioresource Technology, 2011. **102**(5): p. 4270-4272.
4. Bozek-Winkler, E. and J. Gmehling, *Transesterification of methyl acetate and n-butanol catalyzed by Amberlyst 15.* Industrial & Engineering Chemistry Research, 2006. **45**(20): p. 6648-6654.
5. Steinigeweg, S. and J. Gmehling, *Transesterification processes by combination of reactive distillation and pervaporation.* Chemical Engineering and Processing, 2004. **43**(3): p. 447-456.
6. Ali, S.H., *Kinetics of Catalytic Esterification of Propionic Acid with Different Alcohols over Amberlyst 15.* International Journal of Chemical Kinetics, 2009. **41**(6): p. 432-448.
7. Ali, S.H. and S.Q. Merchant, *Kinetic Study of Dowex 50 Wx8-Catalyzed Esterification and Hydrolysis of Benzyl Acetate.* Industrial & Engineering Chemistry Research, 2009. **48**(5): p. 2519-2532.
8. Popken, T., L. Gotze, and J. Gmehling, *Reaction kinetics and chemical equilibrium of homogeneously and heterogeneously catalyzed acetic acid esterification with methanol and methyl acetate hydrolysis.* Industrial & Engineering Chemistry Research, 2000. **39**(7): p. 2601-2611.
9. Mazzotti, M., B. Neri, D. Gelosa, A. Kruglov, and M. Morbidelli, *Kinetics of liquid-phase esterification catalyzed by acidic resins.* Industrial & Engineering Chemistry Research, 1997. **36**(1): p. 3-10.
10. Sanz, M.T., R. Murga, S. Beltran, J.L. Cabezas, and J. Coca, *Autocatalyzed and ion-exchange-resin-catalyzed esterification kinetics of lactic acid with methanol.* Industrial & Engineering Chemistry Research, 2002. **41**(3): p. 512-517.
11. Sanz, M.T., R. Murga, S. Beltran, J.L. Cabezas, and J. Coca, *Kinetic study for the reactive system of lactic acid esterification with methanol: Methyl lactate hydrolysis reaction.* Industrial & Engineering Chemistry Research, 2004. **43**(9): p. 2049-2053.
12. Qu, Y.X., S.J. Peng, S. Wang, Z.Q. Zhang, and J.D. Wang, *Kinetic Study of Esterification of Lactic Acid with Isobutanol and n-Butanol Catalyzed by Ion-exchange Resins.* Chinese Journal of Chemical Engineering, 2009. **17**(5): p. 773-780.
13. Delgado, P., M.T. Sanz, and S. Beltran, *Kinetic study for esterification of lactic acid with ethanol and hydrolysis of ethyl lactate using an ion-exchange resin catalyst.* Chemical Engineering Journal, 2007. **126**(2-3): p. 111-118.

APPENDIX A1

CALIBRATION FACTOR CURVES AND VOLUMES

The calibration factor of component i was determined by the GC evaluation of 9 synthetic calibration samples. The composition of the calibration samples depends on the reaction and the initial molar ratio, and are given in Table A1-1 to A1-5 for the transesterification, and Table A1-6 to A1-8. The 9 solutions were prepared according to conversions of 0% to 100% of ethyl acetate (transesterification) or acetic acid (esterification). When the component was added, the exact value of the added volume was written down in order to know the exact concentration of each component in the solution. Subsequently, the real concentration of each component was calculated and linked with the corrected peak area (Eq A1-1) of that component in the chromatogram.

$$A_i = \frac{A_{i,\text{uncorrected}}\,\overline{A_{n-oct}}}{A_{n-oct}} \qquad \text{(A1-1)}$$

with A_i the corrected peak area of component i, $A_{i,uncorrected}$ is the uncorrected peak area of component i and $\overline{A}_{n-oct}$ is the average value of the peak area of n-octane. Linear regression of the corrected peak area in function of the concentration of component i give the CF_i of that component. Linear regression of this plot gave values for the calibration factor of each component, see equations in Figure A1-1. The values for the calibration factors are given in Table A1-6.

A1.1 Calibration volumes for transesterification experiments

Table A1-1 Volumes for the preparation of 9 calibration samples for transesterification experiments with initial molar ratio of MeOH:EtOAc of 1:1

Sample nummer	X_{EtOAc} (%)	V_{MeOAc} (10^{-3} L)	V_{EtOH} (10^{-3} L)	V_{EtOAc} (10^{-3} L)	V_{MeOH} (10^{-3} L)	$V_{n\text{-octane}}$ (10^{-3} L)
1	0.0	0.000	0.000	1.800	7.244	0.956
2	12.5	0.178	0.131	1.500	7.235	0.956
3	25.0	0.358	0.262	1.300	7.124	0.956
4	37.5	0.536	0.394	1.100	7.014	0.956
5	50.0	0.716	0.524	0.884	6.920	0.956
6	62.5	0.896	0.656	0.662	6.830	0.956
7	75.0	1.000	0.787	0.442	6.815	0.956
8	87.5	1.200	0.918	0.222	6.704	0.956
9	100.0	1.400	1.000	0.000	6.644	0.956

Table A1-2 Volumes for the preparation of 9 calibration samples for transesterification experiments with initial molar ratio of MeOH:EtOAc of 5:1

Sample nummer	X_{EtOAc} (%)	V_{MeOAc} (10^{-3} L)	V_{EtOH} (10^{-3} L)	V_{EtOAc} (10^{-3} L)	V_{MeOH} (10^{-3} L)	$V_{n\text{-octane}}$ (10^{-3} L)
1	0.0	0.000	0.000	1.800	7.244	0.956
2	12.5	0.178	0.131	1.500	7.235	0.956
3	25.0	0.358	0.262	1.300	7.124	0.956
4	37.5	0.536	0.394	1.100	7.014	0.956
5	50.0	0.716	0.524	0.884	6.920	0.956
6	62.5	0.896	0.656	0.662	6.830	0.956
7	75.0	1.000	0.787	0.442	6.815	0.956
8	87.5	1.200	0.918	0.222	6.704	0.956
9	100.0	1.400	1.000	0.000	6.644	0.956

Table A1-3 Volumes for the preparation of 9 calibration samples for transesterification experiments with initial molar ratio of MeOH:EtOAc of 10:1

Sample number	X_{EtOAc} (%)	V_{MeOAc} (10^{-3} L)	V_{EtOH} (10^{-3} L)	V_{EtOAc} (10^{-3} L)	V_{MeOH} (10^{-3} L)	$V_{n\text{-octane}}$ (10^{-3} L)
1	0.0	0.000	0.000	1.800	7.244	0.956
2	12.5	0.178	0.131	1.500	7.235	0.956
3	25.0	0.358	0.262	1.300	7.124	0.956
4	37.5	0.536	0.394	1.100	7.014	0.956
5	50.0	0.716	0.524	0.884	6.920	0.956
6	62.5	0.896	0.656	0.662	6.830	0.956
7	75.0	1.000	0.787	0.442	6.815	0.956
8	87.5	1.200	0.918	0.222	6.704	0.956
9	100.0	1.400	1.000	0.000	6.644	0.956

Table A1-4 Volumes for the preparation of 9 calibration samples for transesterification experiments with initial molar ratio of MeOH:EtOAc of 15:1

Sample number	X_{EtOAc} (%)	V_{MeOAc} (10^{-3} L)	V_{EtOH} (10^{-3} L)	V_{EtOAc} (10^{-3} L)	V_{MeOH} (10^{-3} L)	$V_{n\text{-octane}}$ (10^{-3} L)
1	0.0	0.000	0.000	1.255	7.757	0.988
2	12.5	0.127	0.093	1.099	7.693	0.988
3	25.0	0.255	0.186	0.942	7.629	0.988
4	37.5	0.382	0.280	0.785	7.566	0.988
5	50.0	0.509	0.373	0.628	7.502	0.988
6	62.5	0.637	0.466	0.471	7.438	0.988
7	75.0	0.764	0.559	0.314	7.374	0.988
8	87.5	0.891	0.653	0.157	7.310	0.988
9	100.0	1.019	0.746	0.000	7.246	0.988

Table A1-5 Volumes for the preparation of 9 calibration samples for transesterification experiments with initial molar ratio of MeOH:EtOAc of 20:1

Sample number	X_{EtOAc} (%)	V_{MeOAc} (10^{-3} L)	V_{EtOH} (10^{-3} L)	V_{EtOAc} (10^{-3} L)	V_{MeOH} (10^{-3} L)	$V_{n\text{-octane}}$ (10^{-3} L)
1	0.0	0.000	0.000	0.974	8.021	1.006
2	12.5	0.099	0.072	0.852	7.972	1.006
3	25.0	0.197	0.145	0.730	7.922	1.006
4	37.5	0.296	0.217	0.609	7.873	1.006
5	50.0	0.395	0.289	0.487	7.823	1.006
6	62.5	0.494	0.361	0.365	7.774	1.006
7	75.0	0.592	0.434	0.244	7.724	1.006
8	87.5	0.691	0.506	0.122	7.675	1.006
9	100.0	0.790	0.578	0.000	7.625	1.006

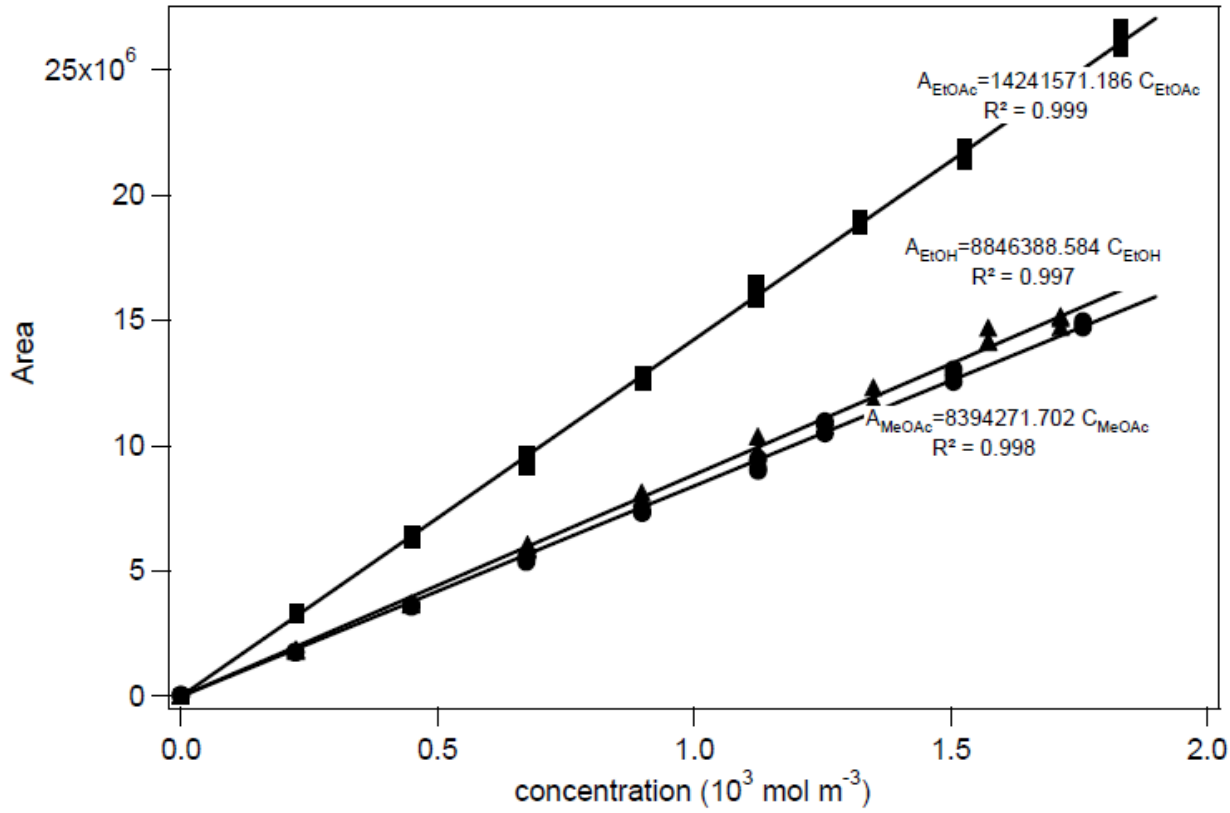

Figure A1-1 Calibration curve for the transestefication with an intial molar ratio MeOH:EtOAc of 10:1 (EtOAc ■, EtOH ▲ and MeOAc ●).

Table A1-6 Examples of calibration factors for the transesterification in function of the initial molar ratio

initial MeOH:EtOAc ratio	CF_{EtOAc}	CF_{MeOAc}	CF_{EtOH}
1:1	26 820 670	42 763 289	44 973 324
5:1	18 438 634	10 246 751	11 566 517
10:1	14 590 389	8 717 781	9 201 942
15:1	9 568 461	5 358 092	5 975 666
20:1	8 958 972	5 151 249	5 541 605

A1.2 Calibration volumes for transesterification experiments

Table A1-7 Volumes for the preparation of 9 calibration samples for esterification experiments with initial molar ratio of MeOH:HOAc of 1:1

Sample nummer	X_{HOAc} (%)	V_{HOAc} (10^{-3} L)	V_{MeOH} (10^{-3} L)	V_{MeOAc} (10^{-3} L)	V_{water} (10^{-3} L)	$V_{n\text{-octane}}$ (10^{-3} L)
1	0.0	5.329	3.771	0.000	0.000	0.900
2	10.0	4.663	3.299	0.928	0.210	0.900
3	20.0	3.997	2.828	1.856	0.420	0.900
4	40.0	3.331	2.356	2.783	0.629	0.900
5	50.0	2.664	1.885	3.711	0.839	0.900
6	60.0	1.998	1.414	4.639	1.049	0.900
7	70.0	1.332	0.943	5.566	1.259	0.900
8	80.0	0.666	0.471	6.494	1.469	0.900
9	90.0	0.000	0.000	7.421	1.678	0.900

Table A1-8 Volumes for the preparation of 9 calibration samples for esterification experiments with initial molar ratio of MeOH:HOAc of 5:1

Sample nummer	X_{HOAc} (%)	V_{HOAc} (10^{-3} L)	V_{MeOH} (10^{-3} L)	V_{MeOAc} (10^{-3} L)	V_{water} (10^{-3} L)	$V_{n\text{-octane}}$ (10^{-3} L)
1	0.0	1.982	7.013	0.000	0.000	1.005
2	12.5	1.735	6.838	0.345	0.078	1.005
3	25.0	1.487	6.662	0.690	0.156	1.005
4	37.5	1.239	6.487	1.035	0.234	1.005
5	50.0	0.991	6.312	1.380	0.312	1.005
6	62.5	0.743	6.136	1.726	0.390	1.005
7	75.0	0.496	5.961	2.071	0.468	1.005
8	87.5	0.248	5.785	2.416	0.546	1.005
9	100.0	0.000	5.610	2.761	0.624	1.005

Table A1-9 Volumes for the preparation of 9 calibration samples for esterification experiments with initial molar ratio of MeOH:HOAc of 10:1

Sample nummer	X_{HOAc} (%)	V_{HOAc} (10^{-3} L)	V_{MeOH} (10^{-3} L)	V_{MeOAc} (10^{-3} L)	V_{water} (10^{-3} L)	$V_{n\text{-octane}}$ (10^{-3} L)
1	0.0	1.111	7.858	0.000	0.000	1.032
2	12.5	0.972	7.759	0.193	0.044	1.032
3	25.0	0.833	7.661	0.387	0.087	1.032
4	37.5	0.694	7.563	0.580	0.131	1.032
5	50.0	0.555	7.465	0.773	0.175	1.032
6	62.5	0.416	7.366	0.967	0.219	1.032
7	75.0	0.278	7.268	1.160	0.262	1.032
8	87.5	0.139	7.170	1.353	0.306	1.032
9	100.0	0.000	7.072	1.547	0.350	1.032

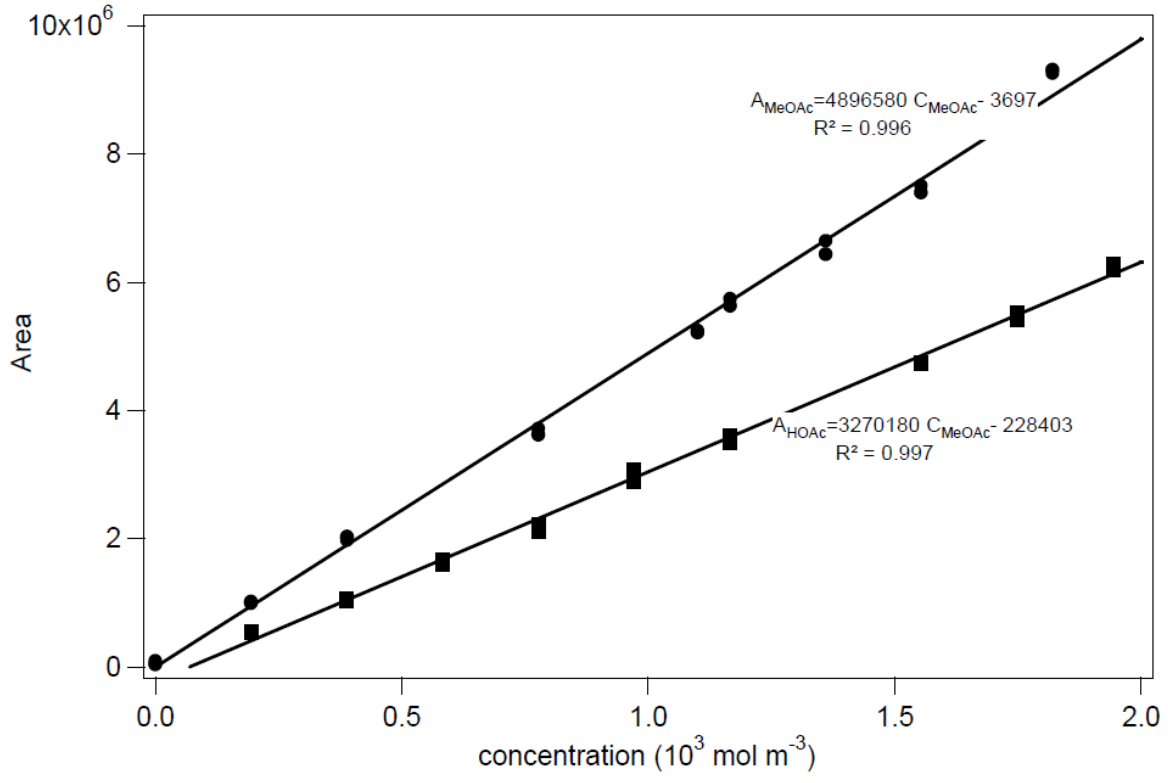

FigureA1 -2 Calibration curve for the estefication with an intial molar ratio MeOH:HOAc of 10:1 (HOAc ■ and MeOAc ●).

Table A1-10 Examples of calibration factors for the esterification in function of the initial molar ratio

initial MeOH:HOAc ratio	A_{HOAc}	A_{MeOAc}
1:1	10 634 822 C_{HOAc} – 758 537	10 699 886 C_{MeOAc} – 8 159 868
5:1	3 477 238 C_{HOAc} – 65 728	4 992 211 C_{MeOAc} – 469
10:1	3 270 180 C_{HOAc} – 228 403	4 896 580 C_{MeOAc} – 3 697

APPENDIX A2

CORRELATIONS TO CALCULATE TRANSPORT LIMITATIONS

Amongst the many processes taking place in the batch reactor, the surface reaction is certainly the most important. Intrinsic kinetics refers to the laws governing the rate of reaction when all other processes, specifically diffusional processes, are much faster than the rate of reaction so that the effect of diffusional limitation on the actual (or apparent) rates of reactions is negligible. The major advantage of using intrinsic reaction kinetics is that these are scale independent, in contrast with the often-used, so-called apparent kinetics, which still include the effects of transport phenomena. Experimental and computer test were determined to evaluate the intrinsic kinetics. The results are given in Chapter 2. A more detailed insight in the calculation of the computer tests is given underneath.

A2.1 External Mass Transfer Limitations

For a reaction of order *n*, diffusion limitations in the film around the particle can be assumed negligible if the deviation between the observed production rate $R_{v,L}^{obs}$ and the "real" reaction rate $R_{v,\mathrm{L}}$ is less than 5/n percent. This deviation is calculated by means of the Carberry number (Ca):

$$Ca = \frac{R_{v,L}^{obs}}{k_s a_{l,s} C_{i,b}} = \frac{C_{i,b} - C_{i,s}}{C_{i,b}} < \frac{0.05}{n} \qquad \text{(A2-1)}$$

with

$R_{v,L}^{obs}$	observed volumetric production rate per unit of liquid volume	$mol/m_l^3 s$
k_s	mass transfer coefficient between catalyst and bulk	$m_l^3/m_k^2 s$

$a_{l,s}$	external surface of catalyst per unit of liquid volume	m_k^2 / m_l^3
$C_{i,b}$	concentration of component *i* in bulk	mol / m_l^3
$C_{i,s}$	concentration of component *i* at the catalyst surface	mol / m_l^3
n	order of the reaction	–

The mass transfer coefficient k_s is calculated using equation A2-2.

$$k_s = \frac{Sh.D_{m,i}}{d_k} \tag{A2-2}$$

The Sherwood number is calculated using equation A2-3

$$Sh = 2 + 0.55\,\mathrm{Re}_K^{1/2}\,Sc^{1/3} \tag{A2-3}$$

$$\mathrm{Re}_K = \frac{\rho_l d_k^{4/3} \varepsilon^{1/3}}{\mu_l} \tag{A2-4}$$

$$\varepsilon = \frac{N_p N_i^3 d_r^5}{V_l} \tag{A2-5}$$

$$Sc = \frac{\mu_l}{\rho_l D_{m,i}} \tag{A2-6}$$

Sh	Sherwood number	
$D_{m,A}$	molecular diffusion coefficient of component A in the liquid phase	m_l^3 / ms
d_k	diameter of the catalyst	m
Re_K	Reynolds number (Kolmogoroff theory)	–
Sc	Schmidt number	–
ρ_l	density of the liquid	kg / m_l^3
ε	energy dissipation of the stirrer	W / kg
μ_l	viscosity of the liquid	cP
N_p	power number of the stirrer	–
N_i	stirrer speed	s^{-1}

d_r	reactor diameter	m
V_l	reaction mixture volume	m^3

$D_{m,i}$ is calculated using the correlation of Wilke and Chang (Coulson & Richardson, 1999)

$$D_{m,i} = \frac{3.71^{-15} T \sqrt{\phi M}}{\mu_l V_m^{0.6}} \tag{A2-7}$$

with

T	temperature	K
μ_l	dynamic viscosity of the liquid phase	kg/ms
V_m	molar volume of component *i* at its boiling point	$m^3/kmol$
M	molecular weight of component *i*	kg/mol

The external particle surface area per unit of reactor volume of equation A2-1 is calculated:

$$a_{l,s} = \frac{a_v W}{\rho_k V_l} \tag{A2-8}$$

with

a_v	external volumetric catalyst surface	m^2/m^3

Because of the spherical catalyst beat, a_v can be expressed as:

$$a_v = \frac{6}{d_k}$$

with d_k catalyst bead diameter m

W	catalyst weight	kg
ρ_k	density of the catalyst	kg/m_s^3
V_l	total liquid reaction volume	m^3

A2.2 Internal Diffusion Limitations

If the Weisz-modulus Φ is small enough, the internal diffusion rate inside the pellet is much higher than the reaction rate so that there are no internal concentration gradients. The Weisz-Prater criterion for a reaction of order *n* is given in equation A2-9.

$$\Phi = \frac{n+1}{2} \frac{R_{v,\mathrm{k}}^{obs}}{a_v^2 D_{i,\mathrm{eff}} C_{i,b}} < 0.08 \qquad \text{(A2-9)}$$

with

Φ	Weisz-modulus	–
$R_{v,\mathrm{k}}^{obs}$	observed reaction rate per mass of catalyst	$mol/kg_{cat}s$
a_v	external particle surface area per unit of catalyst volume	m^2/m^3
$D_{i,eff}$	effective diffusion coefficient of component *i* in the catalyst	m^2/s
$C_{i,b}$	concentration of component *i* in bulk	mol/m_l^3
n	order of the reaction	–

The effective diffusion coefficient of component A in the catalyst, $D_{A,eff}$ can be calculated:

$$D_{i,eff} = \frac{\varepsilon_k D_{m,i}}{\tau} \qquad \text{(A2-10)}$$

$$\tau = \frac{1}{\sqrt{\varepsilon_k}} \qquad \text{(A2-11)}$$

with

$D_{m,i}$	molecular diffusion coefficient of component *i* in solvent s	m^2/s
ε_{k}	the porosity of the catalyst	m_{pore}^3/m_c^3
τ	tortuosity of the catalyst	–

A2.3 Properties for the calculation of the limitations

In order to calculate these correlations, knowledge of the physical properties of the catalyst, the reactor and the reaction mixture is needed. These are given in Table A2-1. The calculation results are given in Table A2-2.

Table A2-1 Properties of the catalyst, the reactor and the reaction mixture to calculate the diffusion limitation criteria for (trans)esterification

Properties of the catalyst (Lewatit K1221)			
d_k	0.00056		m
ρ_k	760		kg/m_s^3
k_k	0.15		W/mK
m_k	0.00058		kg
ε_k	0.6		–
τ	1.3		–
Properties of the reactor			
V_l	0.000185		m^3
N_i	500		s^{-1}
T	60		$°C$
d_r	0.04		m
Properties of the reaction mixture			
	Transesterification	Esterification	
$D_{m,i}$	$2.59\ 10^{-9}$	$2.59\ 10^{-9}$	m^2/s
ρ_l	830	772.36	kg/m_l^3
k_l	0.1500	0.1718	W/mK
μ_l	0.6	0.3819	cP
$R_{v,L}^{obs}$	0.1960	0.4512	$mol/m_l^3 s$
$R_{v,k}^{obs}$	0.0216	0.1420	$mol/kg_{cat} s$

Table A2-2 Criteria for the absence of transport limitations for a Lewatit K1221 catalyst particle under steady-state operation for the (trans)esterification.

Mass transport phenomenon	Criterion	Calculation Transesterification	Calculations Esterification
Extraparticle	$C_a = \frac{r_{obs}}{k_s a' c_{i,b}} < 0.05$	$C_a = 7.7E-03$	$C_a = 1.3E-02$
Intraparticle	$\Phi = \frac{r_{obs}}{a_v^2 D_{i,eff} c_{i,b}} \left(\frac{n+1}{2}\right) < 0.08$	$\Phi = 7.5E-02$	$\Phi = 8.0E-05$

APPENDIX A3

CALCULATION OF THE ACTIVITY COEFFICIENTS

A3.3 Non ideality of the transesterification of methanol and ethyl acetate

Table A3-1 UNIFAC group contribution method, determination of the molecular subgroups for transesterification reaction mixture [1]

		Molecular subgroups	
Component number	Name	Description	amount
1	Methanol	CH_3OH	1
2	Ethanol	CH_3	1
		CH_2	1
		OH	1
3	EtOAc	CH_3	1
		CH_2	1
		CH_3COO	1
4	MeOAc	CH_3	1
		CH_3COO	1
5	n-octane	CH_3	2
		CH_2	6

Table A3-2 Van der Waals area and volume for the main groups in the transesterification reaction mixture [1]

Subgroup	Main group	Main group number	R_k	Q_k
CH_3OH	CH_3OH	6	1.4311	1.432
CH_3	CH_3	1	0.9011	0.848
CH_2	CH_2	1	0.6744	0.540
OH	OH	5	1.0000	1.200
CH_3COO	CCOO	11	1.9031	1.728

Table A3-3 UNIFAC group contribution method, binary interaction parameters a_{mn} for the main groups, with $\Psi_{mn} = \exp\frac{-a_{mn}}{T}$ [1]

Main group *m*	Main group *n*	a_{mn}
6	5	249.10
26	1	16.51
6	11	-10.72
5	6	-137.10
35	1	156.40
5	11	101.10
1	6	697.20
1	5	986.50
1	11	232.10
11	6	249.63
11	5	245.40
11	1	114.80

Table A3-4 Activity coefficients of MeOH, EtOH, MeOAc, EtOAc and n-octane at different temperatures and different MeOH:EtOAc ratios, at the start of the reaction and at equilibrium ($C_{EtOAc,0}$ = 1,79 M; *: $C_{EtOAc,0}$ = 5.79M)

Temperature	303 K				313 K		323 K		333 K					
MeOH:EtOAc atio	1:1*		10:1		10:1		10:1		1:1*		5:1		10:1	
Conversion (%)	0	56	0	94	0	94	0	94	0	56	0	89	0	94
MeOH	1.47	1.52	1.02	1.02	1.02	1.02	1.02	1.02	1.45	1.51	1.29	1.31	1.02	1.02
EtOH	-	1.41	-	1.19	-	1.18	-	1.18	-	1.39	-	1.28	-	1.17
MeOAc	-	1.27	-	2.12	-	2.08	-	2.05	-	1.25	-	1.62	-	2.02
EtOAc	1.25	1.25	2.27	2.27	2.24	2.24	2.21	2.20	1.23	1.23	1.59	1.57	2.17	2.17
n-octane	4.84	4.57	17.39	17.22	16.58	16.42	15.82	15.67	4.51	4.29	4.02	4.01	15.10	14.96

A3.4 Non ideality of the esterification of acetic acid and methanol

Table A3-5 Temperature-dependent UNIQUAC interaction parameters for the esterification of acetic acid with methanol

Component 1	Component 2	i	j	a_{ij} (K)	b_{ij}	c_{ij} (K^{-1})
MeOH	HOAc	1	2	65.245	-2.0346	$3.1570\ 10^{-3}$
		2	1	390.26	0.97039	$3.1570\ 10^{-3}$
MeOAc	HOAc	1	2	195.08	0.40148	-
		2	1	-76.614	-0.33388	-
MeOAc	MeOH	1	2	620.11	-0.96715	-
		2	1	-86.020	0.13943	-
MeOAc	Water	1	2	593.70	0.010143	$-2.1609\ 10^{-3}$
		2	1	-265.83	0.96295	$2.0113\ 10^{-4}$
MeOH	Water	1	2	-235.52	0.41274	$-1.5415\ 10^{-3}$
		2	1	-761.48	5.2418	$-4.3663\ 10^{-3}$
Water	HOAc	1	2	-98.120	-0.29355	$-7.6741\ 10^{-5}$
		2	1	422.38	-0.051007	$-2.4019\ 10^{-4}$

Table A3-6 Pure component parameters: relative van der Waas volumes, r_i, and surfaces, q_i for the esterification components

Component	r_i	q_i
MeOH	1.4311	1.432
HOAc	2.2024	2.072
MeOAc	2.8042	2.576
water	0.9200	1.400

Table A3-7 Activity coefficients of MeOH, HOAc, MeOAc, water and n-octane at different temperatures and different initial MeOH:HOAc ratios, at the start of the reaction and at equilibrium ($C_{HOAc,0}$ = 1.79 M; * : $C_{HOAc,0}$ = 9.27 M)

Temperature	303								333											
MeOH:HOAc ratio	1:1*				10:1				1:1*				5:1				10:1			
%Conversion	0	30	60	93.5	0	30	60	99.9	0	30	60	91.7	0	30	60	99.8	0	30	60	99.9
MeOH	0.7257	0.7682	0.6438	0.2162	0.9670	0.9698	0.9697	0.9672	0.9195	1.1124	1.2729	1.3185	1.0386	1.0487	1.0432	1.0162	1.0361	1.0306	1.0207	1.0036
HOAc	0.9424	0.7534	0.5112	0.2432	0.6776	0.6308	0.5933	0.5537	0.7899	0.5768	0.3560	0.1582	0.4906	0.3799	0.2892	0.1935	0.3962	0.3290	0.2760	0.2211
MeOAc	-	2.015	1.8702	1.6346	-	2.9065	2.8353	2.7656	-	1.8248	1.6410	1.4064	-	2.3318	2.1639	1.9588	-	2.4055	2.2941	2.1683
Water	-	1.4596	1.8625	2.2650	-	1.6960	1.7559	1.8217	-	1.5168	1.8665	2.2007	-	1.7308	1.8316	1.9389	-	1.8105	1.8654	1.9222
n-octane	3.49E-4	0.0017	0.0183	0.9966	1.28E-5	1.39 E-5	1.48 E-5	1.60E-5	0.03833	0.1199	0.5476	4.2995	0.3989	0.9504	2.2309	6.8386	1.0519	1.9334	3.3172	6.2428

APPENDIX B

INDIVIDUAL MODEL DISCRIMINATION FOR EACH RESIN

B.1 Transesterification of ethyl acetate and methanol

Table B-1 Statistical evaluation of the all models (Table 3-2 and Eq. 3-1) for the transesterification catalyzed by Lewatit K1221 (1282 experimental points, experimental conditions Table 2-2)

Model	Number of statistically significantly estimated (total) parameters	RSSQ	R^2	F
ER_swelling	4 (4)	23.7	0.994	71 000
ER_MeOH_SR	4 (4)	27.2	0.994	62 000
PH	2 (2)	36.2	0.992	149 000
ER_EtOH / LH_EtOH	4 (4) / 5 (6)	34.3	0.991	37 000 / 49 000
ER_MeOAc / LH_MeOAc	3 (4) / 4 (6)	35.3	0.991	73 000 / 48 000
ER_EtOAc / LH_EtOAc	3 (4) / 3 (6)	47.9	0.988	47 000
ER_MeOH / LH_MeOH	3 (4) / 3 (6)	111.1	0.972	27 000

Table B-2 Statistical evaluation of the all models (Table 3-2 and Eq. 3-1) for the transesterification catalyzed by Lewatit K2640 (233 experimental points, experimental conditions Table 2-2)

Model	Number of statistically significantly estimated (total) parameters	RSSQ	R^2	F
LH_SR	5 (6)	1.0	0.998	26 000
ER_EtOH	4 (4)	1.3	0.997	25 000
ER_MeOAc	4 (4)	1.3	0.997	24 500
ER_swelling	4 (4)	1.8	0.996	18 000
ER_EtOAc / LH_EtOAc	4 (4) / 4 (6)	2.3	0.995	13 500
ER_MeOH_SR	3 (4)	2.3	0.995	20 000
ER_MeOH / LH_MeOH	3 (4) / 3 (6)	4.3	0.990	12 500
PH	2 (2)	4.9	0.988	20 000

Table B-3 Statistical evaluation of the all models (Table 3-2 and Eq. 3-1) for the transesterification catalyzed by Lewatit K2629 (702 experimental points, experimental conditions Table 2-2)

Model	Number of statistically significantly estimated (total) parameters	RSSQ	R^2	F
ER_swelling	4 (4)	2.5	0.998	125 000
LH_SR	6 (6)	2.5	0.998	76 000
ER_MeOH_SR	3 (4)	2.7	0.998	171 000
PH	2 (2)	3.0	0.998	313 500
ER_EtOH / LH_EtOH	4 (4) / 4 (6)	3.4	0.997	91 000
ER_MeOAc / LH_MeOAc	3 (4) / 3 (6)	3.5	0.997	134 000
ER_EtOAc / LH_EtOAc	3 (4) / 3 (6)	5.6	0.996	78 000
ER_MeOH	3 (4)	8.9	0.993	57 500
LH_MeOH	2 (6)	10.0	0.993	103 000

Table B-4 Statistical evaluation of the all models (Table 3-2 and Eq. 3-1) for the transesterification catalyzed by Amberlyst 15 (129 experimental points, experimental conditions Table 2-2)

Model	Number of statistically significantly estimated (total) parameters	RSSQ	R^2	F
ER_swelling	4 (4)	6.4	0.999	35 000
ER_MeOAc / LH_MeOAc	3 (4) / 4 (6)	6.4	0.999	53 000 / 35 000
ER_EtOH / LH_EtOH	4 (4) / 4 (6)	6.5	0.999	35 000
ER_MeOH_SR	4 (4)	6.6	0.999	34 000
ER_EtOAc / LH_EtOAc	3 (4) / 3 (6)	7.4	0.999	46 000
PH	2 (2)	8.1	0.999	86 000
LH_SR	4 (6)	11.3	0.998	20 000
ER_MeOH / LH_MeOH	3 (4) / 3 (6)	13.1	0.998	27 000

B.2 Esterification of acetic acid and methanol

Table B-5 Statistical evaluation of the 5 rival models (Table 5-2 and Eq. 5-1) for the esterification catalyzed by Lewatit K1221 (748 experimental points, experimental conditions Table 6-1)

Model	Number of statistically significantly estimated (total) parameters	Residual sum of squares	R^2	F
ER-exchange-sum	4 (4)	13.13	0.991	29 000
LH_sum	5 (5)	13.48	0.991	21 000
ER-HOAc-water	4 (4)	13.76	0.991	27 400
ER-MeOH-water	3 (4)	20.74	0.986	27 600
PH	2 (2)	43.17	0.971	32 700

Table B-6 Statistical evaluation of the rival models (Table 5-2 and Eq. 5-1) for the esterification catalyzed by Lewatit K2629 (165 experimental points, experimental conditions Table 6-1)

Model	Number of statistically significantly estimated (total) parameters	Residual sum of squares	R^2	F
ER-HOAc-water	3 (5)	1.346	0.996	20 800
LH_sum	3 (5)	1.356	0.996	20 650
ER-exchange-sum	3 (4)	1.383	0.996	20 200
ER-MeOH-water	2 (5)	4.213	0.988	13 300
PH	1 (2)	10.01	0.971	6 800

Table B-7 Statistical evaluation of the rival models (Table 5-2 and Eq. 5-1) for the esterification catalyzed by Amberlyst 15 (61 experimental points, experimental conditions Table 6-1)

Model	Number of statistically significantly estimated (total) parameters	Residual sum of squares	R^2	F
LH-sum	5 (5)	0.303	0.990	1 400
ER-exchange-sum	4 (4)	0.305	0.990	1 900
ER-HOAc-water	3 (4)	0.396	0.987	2 200
ER-MeOH-water	4 (4)	0.427	0.986	1 300
PH	1 (2)	1.205	0.960	1 900

APPENDIX C

ATHENA VISUAL STUDIO CODE FOR MODEL DISCRIMIATION OF THE TRANSESTERIFICATION

```
Global kB, EB As Real
Global kq, kp, KEQ, Kae, kam, ikeq, kaea, kama, kqea As Real
Global k1, kB1, EB1, kq1, Kae1 As Real
Global k2, kB2, EB2, kp2, kam2 As Real
Global k3, ksam3, kB3, EB3, kae3, kam3 As Real
Global k4, kB4, EB4, kq4, Kae4, kam4, kaea4, kama4 As Real
Global k5, kB5, EB5, Kae5, kam5, kama5, kqea5 As Real
Global k6, ksam6, kB6, EB6, Kae6, kam6, kaea6, kama6 As Real
Global k7, kB7, EB7, Kae7, kp7, kam7, kaea7 As Real
Global k8, kB8, EB8, kp8, kam8, kaea8, kama8 As Real
Global k9, kB9, EB9, kq9, kama9 As Real
Global k10, kB10, EB10 As Real
Global k11, ksam11,  kB11, EB11, kaea11, kama11 As Real
Global k12, kB12, EB12, kp12, kaea12 As Real
Global k13, ksam13, kB13, EB13, kam13, kae13, kama13, kaea13 As Real
Global ksam14, EB14, kB14, kam14, kaea14, kama14, kae14, astot, kaeah14, kamah14 As Real
Global ksam15, EB15, kB15, kam15, kaea15, kama15, kae15, cst15, kaeah15, kamah15, cf15, cft15 As Real
Global ksam16, EB16, kB16, kam16, kaea16, kama16, kae16, cst16, kaeah16, kamah16 As Real
Global ksam17, EB17, kB17, kam17, kaea17, kama17, kae17, cft17, kaeah17, kamah17, kamh17, kaeh17 As
Real
Global ksam18, EB18, kB18, kam18, kaeah18, kamah18 As Real
Global ksam19, EB19, kB19, kaeah19, kamah19 As Real
Global WA, WB, WC, WD, cf151, cf152, ff1, ff2 As Real
Global Temp, EtOAc, MEOH, EtOH, MeOAc As Real
Global Tb, Rg, WW, bb, cc, a, Keqgam As Real
Global Rk(5), Qk(5), ri(5), qi(5), mo(5), xa, Ni(5), Xi(5), ntot As Real
Global xr(5), xq(5), xrtot, xqtot, Phii(5), theta(5), Z, L(5), Ltot As Real
Global LNGAMMAC(5), lngamr(5), amn(5,5), phi2(5,5), xn(5,5) As Real
Global allcomp(5,5), qnxn(5,5), phin(5,5),TERMA(5,5),TERMB(5,5) As Real
Global NOEMER, PSIN(5,5), GROEP(5), XGROEP(5), GROEPXTOT, XK(5) As Real
Global XKQK(5),THETAK(5), TERMA2(5), TERMB2(5), NOEMER2(5) As Real
Global PSIN2(5), gammai(5), lngamma(5) As Real
Global i,j,k,m As Integer
```

```
Tb=55.23+273.15
Rg=8.314
Keqgam=1.0
        Rk(1) = 0.6744
        Rk(2) = 0.9011
        Rk(3) = 1.0
        Rk(4) = 1.4311
        Rk(5) = 1.9031
        Qk(1) = 0.54
        Qk(2)= 0.848
        Qk(3) = 1.2
        Qk(4) = 1.432
        Qk(5) = 1.728
        amn(1,1)= 0.0
        amn(2,1) =0.0
        amn(3,1)= 156.4
        amn(4,1) = 16.51
        amn(5,1)=114.8
        amn(1,2)= 0.0
        amn(2,2) =0.0
        amn(3,2)= 156.4
        amn(4,2) = 16.51
        amn(5,2)=114.8
        amn(1,3) = 986.5
        amn(2,3) = 986.5
        amn(3,3) = 0.0
        amn(4,3) = 249.1
        amn(5,3) = 245.4
        amn(1,4) = 697.2
        amn(2,4) = 697.2
        amn(3,4) = -137.1
        amn(4,4) = 0.0
        amn(5,4) = 249.63
        amn(1,5) = 232.1
        amn(2,5) = 232.1
        amn(3,5)=101.1
        amn(4,5) = -10.72
        amn(5,5) = 0.0

    xa = 0.0
    ntot = 0.0
    xrtot = 0.0
    xqtot = 0.0
    Z = 10.0
    Ltot = 0.0
    NOEMER = 0.0
    GROEPXTOT = 0.0
    Do i = 1,5
    Ni(i) = 0.0
    Xi(i) = 0.0
    mo(i) = 0.0
    xr(i) = 0.0
    xq(i) = 0.0
    theta(i) = 0.0
    Phii(i) = 0.0
    L(i) = 0.0
    ri(i) = 0.0
    qi(i) = 0.0
    LNGAMMAC(i) = 0.0
    lngamr(i) = 0.0
    GROEP(i)=0.0
    XGROEP(i)=0.0
      XK(i)=0.0
      XKQK(i)=0.0
      THETAK(i)=0.0
      TERMA2(i) =0.0
      TERMB2(i) =0.0
      NOEMER2(i) = 0.0
      PSIN2(i)=0.0
      lngamma(i) = 0.0
      Do k = 1,5
        TERMA(i,k) =0.0
        TERMB(i,k) = 0.0
        PSIN(i,k) = 0.0
      EndDo
    EndDo

        allcomp(1,1:2)=1.0
    allcomp(1,5)=1.0
    allcomp(2,4)=1.0
    allcomp(3,1:3)=1.0
    allcomp(4,2)=1.0
    allcomp(4,5)=1.0
        allcomp(1,3:4)=0.0
        allcomp(2,1:3)=0.0
        allcomp(2,5)=0.0
        allcomp(3,4:5)=0.0
        allcomp(4,1)=0.0
        allcomp(4,3:4)=0.0
        allcomp(5,3:5)=0.0
        allcomp(5,1)=6.0
        allcomp(5,2)=2.0
    gammai(1)=1.019
    gammai(2)=1.2002
    gammai(3)=2.04895
    gammai(4)=2.2025
    gammai(5)=15.429

If(iModel==1)Then
CHMAX(5:109)=0.0
ElseIf(iModel==2)Then
CHMAX(1:4)=0.0
CHMAX(9:109)=0.0
ElseIf(iModel==3)Then
CHMAX(1:8)=0.0
CHMAX(13:109)=0.0
ElseIf(iModel==4)Then
CHMAX(1:12)=0.0
CHMAX(20:109)=0.0
ElseIf(iModel==5)Then
CHMAX(1:19)=0.0
CHMAX(26:109)=0.0
ElseIf(iModel==6)Then
CHMAX(1:25)=0.0
CHMAX(32:109)=0.0
ElseIf(iModel==7)Then
CHMAX(1:31)=0.0
CHMAX(38:109)=0.0
ElseIf(iModel==8)Then
CHMAX(1:37)=0.0
CHMAX(44:109)=0.0
ElseIf(iModel==9)Then
CHMAX(1:43)=0.0
CHMAX(48:109)=0.0
```

```
ElseIf(iModel==10)Then
CHMAX(1:47)=0.0
CHMAX(50:109)=0.0
ElseIf(iModel==11)Then
CHMAX(1:49)=0.0
CHMAX(54:109)=0.0
ElseIf(iModel==12)Then
CHMAX(1:53)=0.0
CHMAX(58:109)=0.0
ElseIf(iModel==13)Then
CHMAX(1:57)=0.0
CHMAX(64:109)=0.0
ElseIf(iModel==14)Then
CHMAX(1:63)=0.0
CHMAX(73:109)=0.0
ElseIf(iModel==15)Then
CHMAX(1:72)=0.0
CHMAX(83:109)=0.0
ElseIf(iModel==16)Then
CHMAX(1:82)=0.0
CHMAX(91:109)=0.0
ElseIf(iModel==17)Then
CHMAX(1:90)=0.0
CHMAX(101:109)=0.0
ElseIf(iModel==18)Then
CHMAX(1:100)=0.0
CHMAX(106:109)=0.0
ElseIf(iModel==19)Then
CHMAX(1:105)=0.0
EndIf

@Initial Conditions
U(1)=Xu(5)  ! mol/L
U(2)=Xu(6)
U(3)=0.000001
U(4)=0.000001
U(5)=Xu(7)
@Connect Variables
Temp=Xu(3)+273.15
KEQ=(-0.00528*Temp+3.42727)
ikeq=1.0/KEQ
WW=Xu(4)
a=((1/Temp)-(1/Tb))/Rg
bb=Xu(5)
cc=Xu(6)

k1=kB1*exp(-a*EB1)
kB1=Par(1)
EB1=Par(2)
kq1=Par(3)
Kae1=Par(4)
k2=kB2*exp(-a*EB2)
kB2=Par(5)
EB2=Par(6)
kp2=Par(7)
kam2=Par(8)
!k3=kB3*exp(-a*EB3)
ksam3=kB3*exp(-a*EB3)
kB3=Par(9)
EB3=Par(10)
kae3=Par(11)
kam3=Par(12)
k4=kB4*exp(-a*EB4)
kB4=Par(13)
EB4=Par(14)
kq4=Par(15)
Kae4=Par(16)
kam4=Par(17)
kaea4=Par(18)
kama4=Par(19)
k5=kB5*exp(-a*EB5)
kB5=Par(20)
EB5=Par(21)
Kae5=Par(22)
kam5=Par(23)
kama5=Par(24)
kqea5=Par(25)
!k6=kB6*exp(-a*EB6)
ksam6=kB6*exp(-a*EB6)
kB6=Par(26)
EB6=Par(27)
Kae6=Par(28)
kam6=Par(29)
kaea6=Par(30)
kama6=Par(31)
k7=kB7*exp(-a*EB7)
kB7=Par(32)
EB7=Par(33)
Kae7=Par(34)
kp7=Par(35)
kam7=Par(36)
kaea7=Par(37)
k8=kB8*exp(-a*EB8)
kB8=Par(38)
EB8=Par(39)
kp8=Par(40)
kam8=Par(41)
kaea8=Par(42)
kama8=Par(43)
k9=kB9*exp(-a*EB9)
kB9=Par(44)
EB9=Par(45)
kq9=Par(46)
kama9=Par(47)
k10=kB10*exp(-a*EB10)
kB10=Par(48)
EB10=Par(49)
!k11=kB11*exp(-a*EB11)
ksam11=kB11*exp(-a*EB11)
kB11=Par(50)
EB11=Par(51)
kaea11=Par(52)
kama11=Par(53)
k12=kB12*exp(-a*EB12)
kB12=Par(54)
EB12=Par(55)
kp12=Par(56)
kaea12=Par(57)
!k13=kB13*exp(-a*EB13)
ksam13=kB13*exp(-a*EB13)
kB13=Par(58)
EB13=Par(59)
kae13=Par(60)
kam13=Par(61)
```

```
kaea13=Par(62)
kama13=Par(63)
!k14=kB14*exp(-a*EB14)
ksam14=kB14*exp(-a*EB14)
kB14=Par(64)
EB14=Par(65)
kae14=Par(66)
kam14=Par(67)
kaea14=Par(68)
kama14=Par(69)
astot=Par(70)
kaeah14=Par(71)
kamah14=Par(72)
ksam15=kB15*exp(-a*EB15)
kB15=Par(73)
EB15=Par(74)
kae15=Par(75)
kam15=Par(76)
kaea15=Par(77)
kama15=Par(78)
kaeah15=Par(79)
kamah15=Par(80)
cst15=Par(81)*WW/0.185
cft15=Par(82)
ksam16=kB16*exp(-a*EB16)
kB16=Par(83)
EB16=Par(84)
kae16=Par(85)
kam16=Par(86)
kaea16=Par(87)
kama16=Par(88)
kaeah16=Par(89)
kamah16=Par(90)
ksam17=kB17*exp(-a*EB17)
kB17=Par(91)
EB17=Par(92)
kae17=Par(93)
kam17=Par(94)
kaea17=Par(95)
kama17=Par(96)
kaeh17=Par(97)
kamh17=Par(98)
kaeah17=Par(99)
kamah17=Par(100)
ksam18=kB18*exp(-a*EB18)
kB18=Par(101)
EB18=Par(102)
kam18=Par(103)
kaeah18=Par(104)
kamah18=Par(105)

ksam19=kB19*exp(-a*EB19)
kB19=Par(106)
EB19=Par(107)
kaeah19=Par(108)
kamah19=Par(109)

@Before Calling Solver
        Rk(1) = 0.6744
        Rk(2) = 0.9011
        Rk(3) = 1.0
        Rk(4) = 1.4311
        Rk(5) = 1.9031
        Qk(1) = 0.54
        Qk(2)= 0.848
        Qk(3) = 1.2
        Qk(4) = 1.432
        Qk(5) = 1.728
        amn(1,1)= 0.0
        amn(2,1) =0.0
        amn(3,1)= 156.4
        amn(4,1) = 16.51
        amn(5,1)=115.8
        amn(1,2)= 0.0
        amn(2,2) =0.0
        amn(3,2)= 156.4
        amn(4,2) = 16.51
        amn(5,2)=114.8
        amn(1,3) = 986.5
        amn(2,3) = 986.5
        amn(3,3) = 0.0
        amn(4,3) = 249.1
        amn(5,3) = 245.4
        amn(1,4) = 697.2
        amn(2,4) = 697.2
        amn(3,4) = -137.1
        amn(4,4) = 0.0
        amn(5,4) = 249.63
        amn(1,5) = 232.1
        amn(2,5) = 232.1
        amn(3,5)=101.1
        amn(4,5) = -10.72
        amn(5,5) = 0.0

xa = 0.0
ntot = 0.0
xrtot = 0.0
xqtot = 0.0
Z = 10.0
Ltot = 0.0
NOEMER = 0.0
GROEPXTOT = 0.0
Do i = 1,5
Ni(i) = 0.0
Xi(i) = 0.0
mo(i) = 0.0
xr(i) = 0.0
xq(i) = 0.0
theta(i) = 0.0
Phii(i) = 0.0
L(i) = 0.0
ri(i) = 0.0
qi(i) = 0.0
LNGAMMAC(i) = 0.0
lngamr(i) = 0.0
GROEP(i)=0.0
XGROEP(i)=0.0
XK(i)=0.0
XKQK(i)=0.0
THETAK(i)=0.0
TERMA2(i) =0.0
TERMB2(i) =0.0
NOEMER2(i) = 0.0
PSIN2(i)=0.0
```

```
      gammai(i) =0.0
      lngamma(i) = 0.0
      Do k = 1,5
        TERMA(i,k) =0.0
        TERMB(i,k) = 0.0
        PSIN(i,k) = 0.0
        allcomp(i,k)=0.0
      EndDo
   EndDo
         allcomp(1,4)=1.0
    allcomp(2,1:3)=1.0
    allcomp(3,2)=1.0
    allcomp(3,5)=1.0
    allcomp(4,1:2)=1.0
    allcomp(4,5)=1.0
         allcomp(5,1)=6.0
         allcomp(5,2)=2.0

! Calculate Ri and Qi

         Do i = 1, 5
                  Do j = 1,5
                           ri(i) =
ri(i)+allcomp(i,j)*Rk(j)
                           qi(i) =
qi(i)+allcomp(i,j)*Qk(j)
                  EndDo
         EndDo

! calculate xi
                  ntot = 0.0
                  Ni(1) = U(2)
                  Ni(2) = U(4)
                  Ni(3) = U(3)
                  Ni(4) = U(1)
                  Ni(5) = U(5)

         Do i = 1,5
                  ntot = ntot + Ni(i)*0.185
         EndDo
         Do i = 1,5
                  Xi(i) = Ni(i)/(ntot/0.185)
         EndDo
! calculate xi ri and xi qi
      Do i = 1,5
        xr(i) = Xi(i)*ri(i)
        xq(i) = Xi(i)*qi(i)
      EndDo

      Do i = 1,5
        xrtot = xrtot + xr(i)
        xqtot = xqtot + xq(i)
      EndDo

! calculate theta and phi
      Do i = 1,5
        Phii(i)= xr(i)/xrtot
        theta(i) = xq(i)/xqtot
      EndDo
! calculate Li
      Do i = 1,5
        L(i) = Z/2 * (ri(i) - qi(i)) - (ri(i) - 1)
      EndDo
      Do i = 1,5
        Ltot = Ltot + L(i)*Xi(i)
      EndDo

! combinatoreel deel
      Do i = 1,5
        LNGAMMAC(i)
=((log(Phii(i)/Xi(i))+(Z/2*qi(i)*log(theta(i)/Phii(i)))+
L(i) -(Phii(i)/Xi(i)*Ltot)))
      EndDo

! berekenren van residueel deel
      Do i = 1,5
        Do j = 1,5
          phi2(i,j) = exp(-amn(i,j) / Temp)
        EndDo
      EndDo
      Do i = 1,5
        Do j = 1,5
        xn(i,j)
=allcomp(i,j)/(allcomp(i,1)+allcomp(i,2)+allcomp(i,3)
+ allcomp(i,4)+allcomp(i,5))
        EndDo
      EndDo
      Do i = 1,5
        Do j = 1,5
        qnxn(i,j) =  xn(i,j) * Qk(j)
        EndDo
      EndDo
      Do i = 1,5
        Do j = 1,5
        phin(i,j) =
qnxn(i,j)/(qnxn(i,1)+qnxn(i,2)+qnxn(i,3)+qnxn(i,4)+qn
xn(i,5))
        EndDo
      EndDo
     Do i = 1,5
       Do j = 1,5
         If (phin(i,j).NE.0) Then
           Do k = 1,5
           If(phin(i,k).NE.0) Then
            TERMA(i,j) = TERMA(i,j) +
phin(i,k)*phi2(k,j)
            Else
              Continue
            EndIf
           EndDo
            TERMA(i,j) = log(TERMA(i,j))
         EndIf

       EndDo
     EndDo

     Do i = 1,5
       Do j = 1,5
        If (phin(i,j).NE.0) Then
         Do k = 1,5
           NOEMER = 0.0
           Do m = 1,5
             If (phin(i,m).NE.0) Then
```

```
              NOEMER = NOEMER +
phin(i,m)*phi2(m,k)
              Else
              Continue
              EndIf
           EndDo
            TERMB(i,j) = TERMB(i,j) +
phin(i,k)*phi2(j,k)/NOEMER
         EndDo
       EndIf

       EndDo
     EndDo

     Do i = 1,5
       Do j = 1,5
         If(TERMA(i,j).NE.0.0) Then
         PSIN(i,j) = Qk(j) * (1 - TERMA(i,j) -
TERMB(i,j))
          EndIf
       EndDo
     EndDo

     Do j = 1,5
       Do i = 1,5
         GROEP(i) = GROEP(i) + allcomp(i,j)
       EndDo
       EndDo
       Do i = 1,5
         GROEPXTOT = GROEPXTOT +
GROEP(i)*Xi(i)
       EndDo
      Do i = 1,5
        Do j = 1,5
          XK(i) = XK(i) + allcomp(j,i) *
Xi(j)/GROEPXTOT

       EndDo
      EndDo
     Do i = 1,5
       XKQK(i) = XKQK(i) + XK(i)*Qk(i)
      EndDo
      Do i = 1,5
        THETAK(i) = XKQK(i)/(XKQK(1) +
XKQK(2) +XKQK(3) +XKQK(4)+ XKQK(5))
     EndDo
     Do j = 1,5
     Do i = 1,5
       NOEMER2(j) =
NOEMER2(j)+THETAK(i)*phi2(i,j)
       EndDo
       EndDo
      Do i = 1,5
        TERMA2(i) = log(NOEMER2(i))
      EndDo
      Do i = 1,5
        Do j = 1,5
          TERMB2(i) = TERMB2(i) +
phi2(i,j)*THETAK(j)/NOEMER2(j)
      EndDo

      EndDo
      Do i = 1,5
        PSIN2(i) = Qk(i) * (1 - TERMA2(i) -
TERMB2(i))
     EndDo
     Do i = 1,5
       Do j = 1,5
      lngamr(i) = lngamr(i)+ allcomp(i,j)*(PSIN2(j) -
PSIN(i,j))
       EndDo
      EndDo
     Do i = 1,5
       lngamma(i) =(LNGAMMAC(i) + lngamr(i))
       gammai(i) = exp(lngamma(i))
      EndDo
```

```
@Model Equations

If(iModel==1)Then
F(1)= -WW*k1*(U(2)*gammai(1)-ikeq*((gammai(3)*U(4)*gammai(2)*U(3)))/(gammai(4)*U(1)))/
(1+kq1*((gammai(3)*U(4)*gammai(2)*U(3))/(U(1)*gammai(4)))+Kae1*U(3)*gammai(3))

ElseIf(iModel==2)Then
F(1)=-WW*k2*KEQ*(((U(2)*gammai(1)*U(1)*gammai(4))-(ikeq*gammai(3)*U(4)*gammai(2)*U(3)))/
(U(4)*gammai(2)+kam2*U(2)*gammai(1)*U(4)*gammai(2)+kp2*U(2)*gammai(1)*U(1)*gammai(4)))

ElseIf(iModel==3)Then
F(1)=-WW*ksam3*((U(2)*gammai(1)*U(1)*gammai(4)-ikeq*U(3)*gammai(3)*U(4)*gammai(2))/
(1+kam3*U(2)*gammai(1)+kae3*U(3)*gammai(3)))

ElseIf(iModel==4)Then
F(1)=-WW*k4*(U(2)*gammai(1)-ikeq*((U(4)*gammai(2)*U(3)*gammai(3))/(U(1)*gammai(4))))/
(1+kq4*((U(4)*gammai(2)*U(3)*gammai(3))/(U(1)*gammai(4)))+kaea4*U(1)*gammai(4)+kama4*U(4)
*gammai(2)+Kae4*U(3)*gammai(3))

ElseIf(iModel==5)Then
F(1)=-WW*k5*(U(1)*gammai(4)-ikeq*((U(4)*gammai(2)*U(3)*gammai(3))/(U(2)*gammai(1))))/
(1+kqea5*((U(4)*gammai(2)*U(3)*gammai(3))/(U(2)*gammai(1)))+kam5*U(2)*gammai(1)+kama5*U(4)
*gammai(2)+Kae5*U(3)*gammai(3))

ElseIf(iModel==6)Then
F(1)=-WW*ksam6*((U(1)*gammai(4)*U(2)*gammai(1)-ikeq*U(4)*gammai(2)*U(3)*gammai(3))/
(1+kam6*U(2)*gammai(1)+kaea6*U(1)*gammai(4)+kama6*U(4)*gammai(2)+Kae6*U(3)*gammai(3))^2)

ElseIf(iModel==7)Then
F(1)=-WW*k7*KEQ*((U(2)*gammai(1)*U(1)*gammai(4)-ikeq*U(4)*gammai(2)*U(3)*gammai(3))/
(U(3)*gammai(3)+kp7*U(2)*gammai(1)*U(1)*gammai(4)+kam7*U(2)*gammai(1)*U(3)*gammai(3)+kaea7*U(
1)*gammai(4)*U(3)*gammai(3)+Kae7*U(3)*gammai(3)*U(3)*gammai(3)))

ElseIf(iModel==8)Then
F(1)=-WW*k8*KEQ*((U(2)*gammai(1)*U(1)*gammai(4)-ikeq*U(3)*gammai(3)*U(4)*gammai(2))/
(U(4)*gammai(2)+kp8*U(2)*gammai(1)*U(1)*gammai(4)+kam8*U(2)*gammai(1)*U(4)*gammai(2)+kaea8*U(
1)*gammai(4)*U(4)*gammai(2)+kama8*U(4)*gammai(2)*U(4)*gammai(2)))

ElseIf(iModel==9)Then
F(1)=-WW*k9*(U(1)*gammai(4)-ikeq*((U(4)*gammai(2)*U(3)*gammai(3))/(U(2)*gammai(1))))/
(1+kq9*((U(4)*gammai(2)*U(3)*gammai(3))/(U(2)*gammai(1)))+kama9*U(4)*gammai(2))

ElseIf(iModel==10)Then
F(1)=-WW*k10*(U(2)*gammai(1)*U(1)*gammai(4)-ikeq*(U(3)*gammai(3)*U(4)*gammai(2)))

ElseIf(iModel==11)Then
F(1)=-WW*ksam11*((U(2)*gammai(1)*U(1)*gammai(4)-ikeq*U(3)*gammai(3)*U(4)*gammai(2))/
(1+kaea11*U(1)*gammai(4)+kama11*U(4)*gammai(2)))

ElseIf(iModel==12)Then
F(1)=-WW*k12*KEQ*(((U(2)*gammai(1)*U(1)*gammai(4))-(ikeq*gammai(3)*U(4)*gammai(2)*U(3)))/
(U(3)*gammai(3)+kaea12*U(1)*gammai(4)*U(3)*gammai(3)+kp12*U(2)*gammai(1)*U(1)*gammai(4)))

ElseIf(iModel==13)Then
F(1)=-WW*ksam13*((U(1)*gammai(4)*U(2)*gammai(1)-ikeq*U(4)*gammai(2)*U(3)*gammai(3))/
((1+kam13*U(2)*gammai(1)+kae13*U(3)*gammai(3))*
(1+kaea13*U(1)*gammai(4)+kama13*U(4)*gammai(2))))
```

```
ElseIf(iModel==14)Then
F(1)=-WW*ksam14*((U(1)*gammai(4)*U(2)*gammai(1)-ikeq*U(4)*gammai(1)*U(3)*gammai(3))/
((1+kam14*U(2)*gammai(1)+kaea14*U(1)*gammai(4)+kama14*U(4)*gammai(2)+kae14*U(3)*gammai(3))^2)*
(1+((astot*(kaeah14*kaea14*U(1)*gammai(4)+kamah14*kama14*U(4)*gammai(2)))/(1+kam14*U(2)*gammai(1
)+kaea14*U(1)*gammai(4)+kama14*U(4)*gammai(2)+kae14*U(3)*gammai(3)))))

ElseIf(iModel==16)Then
F(1)=-WW*ksam16*(U(1)*gammai(4)*U(2)*gammai(1)-ikeq*U(4)*gammai(2)*U(3)*gammai(3))/
((1+kaea16*U(1)*gammai(4)+kam16*U(2)*gammai(1)+kama16*U(4)*gammai(2)+kae16*U(3)*gammai(3)+U(1
)*gammai(4)*kaeah16+U(4)*gammai(2)*kamah16)^2)

ElseIf(iModel==17)Then
F(1)=-WW*ksam17*((U(1)*gammai(4)*U(2)*gammai(1)-ikeq*U(4)*gammai(2)*U(3)*gammai(3))/
(1+kam17*U(2)*gammai(1)+kaea17*U(1)*gammai(4)+kama17*U(4)*gammai(2)+kae17*U(3)*gammai(3)+(U(2
)*gammai(1)*kamh17+kaeh17*U(3)*gammai(3)+U(1)*gammai(4)*kaeah17+U(4)*gammai(2)*kamah17))^2)
ElseIf(iModel==18)Then
F(1)=-WW*ksam18*((U(1)*gammai(4)*U(2)*gammai(1)-ikeq*U(4)*gammai(2)*U(3)*gammai(3))/
(1+kam18*U(2)*gammai(1)+U(1)*gammai(4)*kaeah18+U(4)*gammai(2)*kamah18))

ElseIf(iModel==19)Then
F(1)=-WW*ksam19*((U(1)*gammai(4)-ikeq*((U(4)*gammai(2)*U(3)*gammai(3))/(U(2)*gammai(1))))/
(1+((U(1)*gammai(4))/(U(2)*gammai(1)))*kaeah19+((U(4)*gammai(2))/(U(2)*gammai(1)))*kamah19))
EndIf

F(2)= U(2)-U(1)-cc+bb
F(3)= U(3)+U(1)-bb
F(4)= U(4)+U(1)-bb

@Coefficient Matrix
E(1)=1.0
E(2)=0.0
E(3)=0.0
E(4)=0.0

@Response Model
Y(1)=U(1)

@Phi Functions
Phi(1)=Par(106)/Par(108)
```

APPENDIX D

ATHENA VISUAL STUDIO CODE FOR MODEL DISCRIMIATION OF THE ESTERIFICATION

```
Global kB, EB As Real
Global kq, kp, KEQ, Kae, kam, ikeq, kaea, kama, kaw, kaa As Real
Global k5, kB5, EB5, kaa5, kaw5, ksam5 As Real
Global k11, kB11, EB11, kam11, kaw11, ksam11 As Real
Global k15, ksam15, kB15, EB15, kaa15, kam15, kama15, kaw15, kasom15 As Real
Global k18, kB18, EB18 As Real
Global k19, ksam19, kB19, EB19, kaa19, kama19, kaw19, kasom19 As Real
Global k6, ksam6, kB6, EB6, kam6, kaa6, kama6, kaw6, kasom6 As Real
Global Temp, HAc, MEOH, MeOAc, H2O As Real
Global Tb, Rg, WW, bb, cc, a, ist, Keqgam As Real
Global som, ratio As Real
Global Rk(8), Qk(8), ri(8), qi(8), mo(8), xa, Ni(8), Xi(8), ntot As Real
Global xiri(8), xiqi(8), xiritot, xiqitot, Phii(8), theta(8), Z, L(8), Ltot As Real
Global LNGAMMAC(8), lngammar(8), amn(8,8), psii(8,8), xn(8,8) As Real
Global allcomp(8,8), qnxn(8,8), thetam(8,8),TERMA(8,8),TERMB(8,8) As Real
Global NOEMER, lngammak1(8,8), aij(8,8), tau(8,8), bij(8,8), GROEP(8), XGROEP(8), GROEPXTOT, XK(8)
As Real
Global XKQK(8),THETAK(8), TERMA2(8), TERMB2(8), NOEMER2(8) As Real
Global LNgammak2(8), gammai(5), lngamma(8) As Real
Global i,j,k,m As Integer
```

```
Tb=50.0+273.15  ! K
 Rg=8.314  ! J/(K.mol)

If(iModel==1)Then
CHMAX(5:27)=0.0
ElseIf(iModel==2)Then
CHMAX(1:4)=0.0
CHMAX(9:27)=0.0
ElseIf(iModel==3)Then
CHMAX(1:8)=0.0
CHMAX(15:27)=0.0
ElseIf(iModel==4)Then
CHMAX(1:14)=0.0
CHMAX(17:27)=0.0
ElseIf(iModel==5)Then
CHMAX(1:16)=0.0
CHMAX(19)=0.0
CHMAX(22:27)=0.0
ElseIf(iModel==6)Then
CHMAX(1:21)=0.0
ElseIf(iModel==7)Then
CHMAX(1:16)=0.0
CHMAX(22:27)=0.0
ElseIf(iModel==8)Then
CHMAX(1:21)=0.0
CHMAX(26)=0.0
ElseIf(iModel==9)Then
CHMAX(1:8)=0.0
CHMAX(13)=0.0
CHMAX(15:27)=0.0
EndIf

@Initial Conditions
U(1)=Xu(5)  ! mol/L
U(2)=Xu(6)
U(3)=0.000001
U(4)=0.000001

@Connect Variables
Temp=Xu(3)+273.15
KEQ=60.8203-0.10289*Temp
ikeq=1.0/KEQ
WW=Xu(4)*0.001
a=((1/Temp)-(1/Tb))/Rg
bb=Xu(5)
cc=Xu(6)
ist=Xu(8)

ksam5=kB5*exp(-a*EB5)
!ksam5=k5*kaa5
kB5=Par(1)
EB5=Par(2)
kaa5=Par(3)
kaw5=Par(4)

ksam11=kB11*exp(-a*EB11)
!ksam11=k11*kam11
kB11=Par(5)
EB11=Par(6)
kaw11=Par(8)
kam11=0.75*kaw11

ksam15=kB15*exp(-a*EB15)
!ksam15=k15*kaa15*kam15
kB15=Par(9)
EB15=Par(10)
kaa15=Par(11)
kam15=Par(12)
If(iModel==3)Then
kama15=Par(13)
kaw15=Par(14)
ElseIf(iModel==9)Then
kasom15=Par(14)
EndIf

k18=kB18*exp(-a*EB18)
kB18=Par(15)
EB18=Par(16)

If(iModel==5)Then
ksam19=kB19*exp(-a*EB19)
kB19=Par(17)
EB19=Par(18)
kaa19=Par(19)
kama19=Par(20)
kaw19=Par(21)

ElseIf(iModel==7)Then
ksam19=kB19*exp(-a*EB19)
kB19=Par(17)
EB19=Par(18)
kaa19=Par(19)
kasom19=Par(21)
EndIf

If(iModel==6)Then
ksam6=kB6*exp(-a*EB6)
kB6=Par(22)
EB6=Par(23)
kaa6=Par(24)
kam6=Par(25)
kama6=Par(26)
kaw6=Par(27)

ElseIf(iModel==8)Then
ksam6=kB6*exp(-a*EB6)
kB6=Par(22)
EB6=Par(23)
kaa6=Par(24)
kam6=Par(25)
kasom6=Par(27)
EndIf


Do i=1,6
        ri(i)=0.0
        qi(i)=0.0
        Do j=1,6
                aij(i,j)=0.0
```

```
                bij(i,j)=0.0
                tau(i,j)=0.0
        EndDo
EndDo

@Before Calling Solver
If(Xu(7)==1) Then
        stand = 6
        Rk(1) = 0.9011
        Rk(2) = 0.6744
        Rk(3) = 1.4311
        Rk(4) = 0.92
        Rk(5) = 1.9031
        Rk(6) = 1.3013
        Qk(1) = 0.848
        Qk(2) = 0.54
        Qk(3) = 1.432
        Qk(4) = 1.4
        Qk(5) = 1.728
        Qk(6) = 1.224
        amn(1,1) = 0.0
        amn(2,1) = 0.0
        amn(3,1) = 16.51
        amn(4,1) = 300.0
        amn(5,1) = 114.8
        amn(6,1) = 315.3
        amn(1,2) = 0.0
        amn(2,2) = 0.0
        amn(3,2) = 16.51
        amn(4,2) = 300.0
        amn(5,2) = 114.8
        amn(6,2) = 315.3
        amn(1,3) = 697.2
        amn(2,3) = 697.2
        amn(3,3) = 0.0
        amn(4,3) = 289.6
        amn(5,3) = 249.6
        amn(6,3) = 339.8
        amn(1,4) = 1318.0
        amn(2,4) = 1318.0
        amn(3,4) = -181.0
        amn(4,4) = 0.0
        amn(5,4) = 200.8
        amn(6,4) = -66.17
        amn(1,5) = 232.1
        amn(2,5) = 232.1
        amn(3,5) = -10.72
        amn(4,5) = 72.87
        amn(5,5) = 0.0
        amn(6,5) = -256.3
        amn(1,6) = 663.5
        amn(2,6) = 663.5
        amn(3,6) = -202.0
        amn(4,6) = -14.09
        amn(5,6) = 660.2
        amn(6,6) = 0.0


    xa = 0.0
    ntot = 0.0
    xiritot = 0.0
    xiqitot = 0.0
    Z = 10.0
    Ltot = 0.0
    NOEMER = 0.0
    GROEPXTOT = 0.0
    Do i = 1,8
        Ni(i) = 0.0
        Xi(i) = 0.0
        mo(i) = 0.0
        xiri(i) = 0.0
        xiqi(i) = 0.0
        theta(i) = 0.0
        Phii(i) = 0.0
        L(i) = 0.0
        ri(i) = 0.0
        qi(i) = 0.0
        LNGAMMAC(i) = 0.0
        lngammar(i) = 0.0
        GROEP(i)=0.0
        XGROEP(i)=0.0
        XK(i)=0.0
        XKQK(i)=0.0
        THETAK(i)=0.0
        TERMA2(i) =0.0
        TERMB2(i) =0.0
        NOEMER2(i) = 0.0
        LNgammak2(i)=0.0
        lngamma(i) = 0.0
        Do k = 1,8
        TERMA(i,k) =0.0
                TERMB(i,k) = 0.0
                lngammak1(i,k) = 0.0
                allcomp(i,k)=0.0
        EndDo
        EndDo

    allcomp(1,1)=1.0
    allcomp(1,6)=1.0
    allcomp(2,3)=1.0
    allcomp(3,1)=1.0
    allcomp(3,5)=1.0
    allcomp(4,4)=1.0
        allcomp(5,1)=2.0
        allcomp(5,2)=6.0

ElseIf (Xu(7)==2) Then
        stand = 7
        Rk(1) = 0.9011
        Rk(2) = 0.6744
        Rk(3) = 1.4311
        Rk(4) = 0.92
        Rk(5) = 1.9031
        Rk(6) = 0.9183
        Rk(7) = 1.3013
        Qk(1) = 0.848
        Qk(2) = 0.54
        Qk(3) = 1.432
        Qk(4) = 1.4
        Qk(5) = 1.728
```

```
        Qk(6) = 0.78
        Qk(7) = 1.224
        amn(1,1) = 0.0
        amn(2,1) = 0.0
        amn(3,1) = 16.51
        amn(4,1) = 300.0
        amn(5,1) = 114.8
        amn(6,1) = 83.36
        amn(7,1) = 315.3
        amn(1,2) = 0.0
        amn(2,2) = 0.0
        amn(3,2) = 16.51
        amn(4,2) = 300.0
        amn(5,2) = 114.8
        amn(6,2) = 83.36
        amn(7,2) = 315.3
        amn(1,3) = 697.2
        amn(2,3) = 697.2
        amn(3,3) = 0.0
        amn(4,3) = 289.6
        amn(5,3) = 249.6
        amn(6,3) = 238.4
        amn(7,3) = 339.8
        amn(1,4) = 1318.0
        amn(2,4) = 1318.0
        amn(3,4) = -181.0
        amn(4,4) = 0.0
        amn(5,4) = 200.8
        amn(6,4) = -314.7
        amn(7,4) = -66.17
        amn(1,5) = 232.1
        amn(2,5) = 232.1
        amn(3,5) = -10.72
        amn(4,5) = 72.87
        amn(5,5) = 0.0
        amn(6,5) = 461.3
        amn(7,5) = -256.3
        amn(1,6) = 251.5
        amn(2,6) = 251.5
        amn(3,6) = -128.6
        amn(4,6) = 540.5
        amn(5,6) = -235.7
        amn(6,6) = 0.0
        amn(7,6) = -338.5
        amn(1,7) = 663.5
        amn(2,7) = 663.5
        amn(3,7) = -202.0
        amn(4,7) = -14.09
        amn(5,7) = 660.2
        amn(6,7) = 664.6
        amn(7,7) = 0.0


    xa = 0.0
    ntot = 0.0
    xiritot = 0.0
    xiqitot = 0.0
    Z = 10.0
    Ltot = 0.0
    NOEMER = 0.0
    GROEPXTOT = 0.0
    Do i = 1,8
        Ni(i) = 0.0
        Xi(i) = 0.0
        mo(i) = 0.0
        xiri(i) = 0.0
        xiqi(i) = 0.0
        theta(i) = 0.0
        Phii(i) = 0.0
        L(i) = 0.0
        ri(i) = 0.0
        qi(i) = 0.0
        LNGAMMAC(i) = 0.0
        lngammar(i) = 0.0
        GROEP(i)=0.0
        XGROEP(i)=0.0
        XK(i)=0.0
        XKQK(i)=0.0
        THETAK(i)=0.0
        TERMA2(i) =0.0
        TERMB2(i) =0.0
        NOEMER2(i) = 0.0
        LNgammak2(i)=0.0
        lngamma(i) = 0.0
        Do k = 1,8
        TERMA(i,k) =0.0
                TERMB(i,k) = 0.0
                lngammak1(i,k) = 0.0
                allcomp(i,k)=0.0
        EndDo
        EndDo

    allcomp(1,1)=1.0
    allcomp(1,7)=1.0
    allcomp(2,3)=1.0
    allcomp(3,1)=1.0
    allcomp(3,5)=1.0
    allcomp(4,4)=1.0
        allcomp(5,2)=2.0
        allcomp(5,6)=2.0

ElseIf (Xu(7)==3) Then
        stand=8
        Rk(1) = 0.9011
        Rk(2) = 0.6744
        Rk(3) = 0.4469
        Rk(4) = 0.2195
        Rk(5) = 1.4311
        Rk(6) = 0.92
        Rk(7) = 1.9031
        Rk(8) = 1.3013
        Qk(1) = 0.848
        Qk(2) = 0.54
        Qk(3) = 0.228
        Qk(4) = 0.0
        Qk(5) = 1.432
        Qk(6) = 1.4
        Qk(7) = 1.728
        Qk(8) = 1.224
        amn(1,1) = 0.0
```

```
amn(2,1) = 0.0
amn(3,1) = 0.0
amn(4,1) = 0.0
amn(5,1) = 16.51
amn(6,1) = 300.0
amn(7,1) = 114.8
amn(8,1) = 315.3
amn(1,2) = 0.0
amn(2,2) = 0.0
amn(3,2) = 0.0
amn(4,2) = 0.0
amn(5,2) = 16.51
amn(6,2) = 300.0
amn(7,2) = 114.8
amn(8,2) = 315.3
amn(1,3) = 0.0
amn(2,3) = 0.0
amn(3,3) = 0.0
amn(4,3) = 0.0
amn(5,3) = 16.51
amn(6,3) = 300.0
amn(7,3) = 114.8
amn(8,3) = 315.3
amn(1,4) = 0.0
amn(2,4) = 0.0
amn(3,4) = 0.0
amn(4,4) = 0.0
amn(5,4) = 16.51
amn(6,4) = 300.0
amn(7,4) = 114.8
amn(8,4) = 315.3
amn(1,5) = 697.2
amn(2,5) = 697.2
amn(3,5) = 697.2
amn(4,5) = 697.2
amn(5,5) = 0.0
amn(6,5) = 289.6
amn(7,5) = 249.6
amn(8,5) = 339.8
amn(1,6) = 1318.0
amn(2,6) = 1318.0
amn(3,6) = 1318.0
amn(4,6) = 1318.0
amn(5,6) = -181.0
amn(6,6) = 0.0
amn(7,6) = 200.8
amn(8,6) = -66.17
amn(1,7) = 232.1
amn(2,7) = 232.1
amn(3,7) = 232.1
amn(4,7) = 232.1
amn(5,7) = -10.72
amn(6,7) = 72.87
amn(7,7) = 0.0
amn(8,7) = -256.3
amn(1,8) = 663.5
amn(2,8) = 663.5
amn(3,8) = 663.5
amn(4,8) = 663.5
amn(5,8) = -202.0
    amn(6,8) = -14.09
    amn(7,8) = 660.2
    amn(8,8) = 0.0

xa = 0.0
ntot = 0.0
xiritot = 0.0
xiqitot = 0.0
Z = 10.0
Ltot = 0.0
NOEMER = 0.0
GROEPXTOT = 0.0
Do i = 1,8
    Ni(i) = 0.0
    Xi(i) = 0.0
    mo(i) = 0.0
    xiri(i) = 0.0
    xiqi(i) = 0.0
    theta(i) = 0.0
    Phii(i) = 0.0
    L(i) = 0.0
    ri(i) = 0.0
    qi(i) = 0.0
    LNGAMMAC(i) = 0.0
    lngammar(i) = 0.0
    GROEP(i)=0.0
    XGROEP(i)=0.0
    XK(i)=0.0
    XKQK(i)=0.0
    THETAK(i)=0.0
    TERMA2(i) =0.0
    TERMB2(i) =0.0
    NOEMER2(i) = 0.0
    LNgammak2(i)=0.0
    lngamma(i) = 0.0
    Do k = 1,8
    TERMA(i,k) =0.0
        TERMB(i,k) = 0.0
        lngammak1(i,k) = 0.0
        allcomp(i,k)=0.0
    EndDo
    EndDo

allcomp(1,1)=1.0
allcomp(1,8)=1.0
allcomp(2,5)=1.0
allcomp(3,1)=1.0
allcomp(3,7)=1.0
allcomp(4,6)=1.0
    allcomp(5,1)=5.0
    allcomp(5,2)=1.0
    allcomp(5,3)=1.0
    allcomp(5,4)=1.0

    EndIf

    Do i = 1, 5
        Do j = 1,stand
            ri(i) = ri(i)+allcomp(i,j)*Rk(j)
            qi(i) = qi(i)+allcomp(i,j)*Qk(j)
```

```
                EndDo
        EndDo

! berekening xi
                ntot = 0.0
                Ni(1) = U(1)
                Ni(2) = U(2)
                Ni(3) = U(3)
                Ni(4) = U(4)
                Ni(5) = ist

        Do i = 1,5
                ntot = ntot + Ni(i)
        EndDo
        Do i = 1,5
                Xi(i) = Ni(i)/ntot
        EndDo



! berekening xi ri en xi qi
    Do i = 1,5
        xiri(i) = Xi(i)*ri(i)
        xiqi(i) = Xi(i)*qi(i)
    EndDo

    Do i = 1,5
        xiritot = xiritot + xiri(i)
        xiqitot = xiqitot + xiqi(i)
    EndDo

! berekening theta en phi
    Do i = 1,5
        Phii(i)= xiri(i)/xiritot
        theta(i) = xiqi(i)/xiqitot
    EndDo

! berekening Li
    Do i = 1,5
         L(i) = Z/2 * (ri(i) - qi(i)) - (ri(i) - 1)
    EndDo

    Do i = 1,5
         Ltot = Ltot + L(i)*Xi(i)
    EndDo

! combinatoreel deel
    Do i = 1,5
LNGAMMAC(i)=((log(Phii(i)/Xi(i))+(Z/2*qi(i)*log(thet
a(i)/Phii(i)))+ L(i) -(Phii(i)/Xi(i)*Ltot)))
    EndDo

! berekenen van residueel deel
     Do i = 1,stand
        Do j = 1,stand
        psii(i,j) = exp(-amn(i,j) / Temp)
        EndDo
     EndDo

     Do i = 1,5
        som = 0.0
        Do j = 1,stand
                som = som + allcomp(i,j)
        EndDo
        Do j = 1,stand
                xn(i,j) = allcomp(i,j)/som
        EndDo
    EndDo

    Do i = 1,5
        Do j = 1,stand
                qnxn(i,j) =  xn(i,j) * Qk(j)
        EndDo
    EndDo

    Do i = 1,5
        Do j = 1,stand
                If (stand==6) Then
thetam(i,j) = qnxn(i,j)/
(qnxn(i,1)+qnxn(i,2)+qnxn(i,3)+qnxn(i,4)+qnxn(i,5)+qnx
n(i,6))
                ElseIf (stand==7) Then
thetam(i,j) = qnxn(i,j)/
(qnxn(i,1)+qnxn(i,2)+qnxn(i,3)+qnxn(i,4)+qnxn(i,5)+qnx
n(i,6)+qnxn(i,7))
                ElseIf (stand==8) Then
 thetam(i,j) = qnxn(i,j)/
(qnxn(i,1)+qnxn(i,2)+qnxn(i,3)+qnxn(i,4)+qnxn(i,5)+qnx
n(i,6)+qnxn(i,7)+qnxn(i,8))
                EndIf
        EndDo
     EndDo

    Do i = 1,5
        Do j = 1,stand
                If (thetam(i,j).NE.0) Then
                        Do k = 1,stand
If(thetam(i,k).NE.0)
Then
TERMA(i,j) = TERMA(i,j) + thetam(i,k)*psii(k,j)
        Else
        Continue
        EndIf
        EndDo
        TERMA(i,j) = log(TERMA(i,j))
        EndIf
        EndDo
    EndDo

    Do i = 1,5
        Do j = 1,stand
                If (thetam(i,j).NE.0) Then
                Do k = 1,stand
                NOEMER = 0.0
                Do m = 1,stand
                If (thetam(i,m).NE.0)
Then
NOEMER = NOEMER + thetam(i,m)*psii(m,k)
                Else
                Continue
                EndIf
```

```
                    EndDo
TERMB(i,j) = TERMB(i,j) +thetam(i,k)*psii(j,k)/
NOEMER
                    EndDo
                    EndIf
          EndDo
    EndDo

    Do i = 1,5
          Do j = 1,stand
                    If(TERMA(i,j).NE.0.0) Then
lngammak1(i,j) = Qk(j) * (1 - TERMA(i,j) - TERMB(i,j))
          EndIf
          EndDo
    EndDo

    Do j = 1,stand
          Do i = 1,5
          GROEP(i) = GROEP(i) + allcomp(i,j)
          EndDo
    EndDo
    Do i = 1,5
GROEPXTOT = GROEPXTOT + GROEP(i)*Xi(i)
    EndDo
    Do i = 1,stand
          Do j = 1,5
XK(i) = XK(i) + allcomp(j,i) * Xi(j)/GROEPXTOT
          EndDo
    EndDo


    Do i = 1,stand
          XKQK(i) = XKQK(i) + XK(i)*Qk(i)
    EndDo

    Do i = 1,stand
          If (stand==6) Then
THETAK(i) = XKQK(i)/
(XKQK(1)+XKQK(2)+XKQK(3)+XKQK(4)+XKQK(5)
+XKQK(6))
          ElseIf (stand==7) Then
THETAK(i) = XKQK(i)/
(XKQK(1)+XKQK(2)+XKQK(3)+XKQK(4)+XKQK(5)
+XKQK(6)+XKQK(7))
          ElseIf (stand==8) Then
THETAK(i) = XKQK(i)/
(XKQK(1)+XKQK(2)+XKQK(3)+XKQK(4)+XKQK(5)
+XKQK(6)+XKQK(7)+XKQK(8))
          EndIf
    EndDo

    Do j = 1,stand
          Do i = 1,stand
NOEMER2(j) = NOEMER2(j)+THETAK(i)*psii(i,j)
          EndDo
    EndDo

    Do i = 1,stand
TERMA2(i) = log(NOEMER2(i))
    EndDo

    Do i = 1,stand
          Do j = 1,stand
TERMB2(i) = TERMB2(i) +
psii(i,j)*THETAK(j)/NOEMER2(j)
          EndDo
    EndDo

    Do i = 1,stand
        LNgammak2(i) = Qk(i) * (1 - TERMA2(i) -
TERMB2(i))
    EndDo

    Do i = 1,5
      Do j = 1,stand
      lngammar(i) = lngammar(i)+
allcomp(i,j)*(LNgammak2(j) - lngammak1(i,j))
      EndDo
    EndDo

    Do i = 1,5
       lngamma(i) = LNGAMMAC(i) + lngammar(i)
       gammai(i) = exp(lngamma(i))
       EndDo

ikeq=1.0/KEQ
```

```
@Model Equations

If(iModel==1)Then! ER HAc ads H2O des SR SBS (Model5)
F(1)= -WW*ksam5*(U(1)*gammai(1)*U(2)*gammai(2)-ikeq*U(3)*gammai(3)*U(4)*gammai(4))/
(1+kaa5*U(1)*gammai(1)+U(4)*gammai(4)*kaw5)

ElseIf(iModel==2)Then! ER MeOH ads H2O des SR SBS (Model11)
F(1)= -WW*ksam11*(U(2)*gammai(2)*U(1)*gammai(1)-ikeq*U(3)*gammai(3)*U(4)*gammai(4))/
(1+kam11*U(2)*gammai(2)+kaw11*U(4)*gammai(4))

ElseIf(iModel==3)Then! LHHW SR SBS (Model15)
F(1)= -WW*ksam15*(U(1)*gammai(1)*U(2)*gammai(2)-ikeq*U(3)*gammai(3)*U(4)*gammai(4))/
(((1+kaa15*U(1)*gammai(1)+kam15*U(2)*gammai(2)+kama15*U(3)*gammai(3)+kaw15*U(4)*gammai(4))^2

ElseIf(iModel==9)Then !LH som
F(1)= -WW*ksam15*(U(1)*gammai(1)*U(2)*gammai(2)-
ikeq*U(3)*gammai(3)*U(4)*gammai(4))/(((1+kaa15*U(1)*gammai(1)+kam15*U(2)*gammai(2)+kasom15*U(
3))^2))

ElseIf(iModel==4)Then! PH (Model18)
F(1)= -WW*k18*(U(1)*gammai(1)*U(2)*gammai(2)-ikeq*U(3)*gammai(3)*U(4)*gammai(4))

ElseIf(iModel==5)Then ! Zwelling (Model19)
F(1)=-WW*ksam19*(U(1)*gammai(1)-
ikeq*((U(3)*gammai(3)*U(4)*gammai(4))/(U(2)*gammai(2))))/(1+(kama19*((U(3)*gammai(3))/(U(2)*gamma
i(2))))+(kaa19*((U(1)*gammai(1))/(U(2)*gammai(2))))+(kaw19*((U(4)*gammai(4))/(U(2)*gammai(2)))))

ElseIf(iModel==7)Then!ER-zwelling_nSOM
F(1)=-WW*ksam19*(U(1)*gammai(1)-
ikeq*((U(3)*gammai(3)*U(4)*gammai(4))/(U(2)*gammai(2))))/(1+(kaa19*((U(1)*gammai(1))/(U(2)*gammai(
2))))+(kasom19*((U(3)*gammai(3)+U(4)*gammai(4))/(U(2)*gammai(2)))))

ElseIf(iModel==6)Then! ER_zwelling_uitgewerkt
F(1)= -WW*ksam6*(U(1)*gammai(1)*U(2)*gammai(2)-ikeq*U(3)*gammai(3)*U(4)*gammai(4))/
((kaa6*U(1)*gammai(1)+kam6*U(2)*gammai(2)+kama6*U(3)*gammai(3)+kaw6*U(4)*gammai(4)))

ElseIf(iModel==8)Then! ER_zwelling_uitgewerkt_SOM
F(1)= -WW*ksam6*(U(1)*gammai(1)*U(2)*gammai(2)-ikeq*U(3)*gammai(3)*U(4)*gammai(4))/
((kaa6*U(1)*gammai(1)+kam6*U(2)*gammai(2)+kasom6*U(3)))
EndIf

F(2)= U(2)-U(1)-cc+bb
F(3)= U(3)+U(1)-bb
F(4)= U(4)+U(1)-bb

@Coefficient Matrix
E(1)=1.0
E(2)=0.0
E(3)=0.0
E(4)=0.0

@Response Model
Y(1)=U(3)

@Phi Functions

If(iModel==1)Then
Phi(1)=Par(1)/Par(3)

ElseIf(iModel==2)Then
```

```
Phi(1)=Par(5)/Par(7)

ElseIf(iModel==3)Then
Phi(1)=Par(9)/(Par(11)*Par(12))

ElseIf(iModel==9)Then
Phi(1)=Par(9)/(Par(11)*Par(12))

ElseIf(iModel==5)Then
Phi(1)=Par(17)/Par(19)
Phi(2)=Par(17)/Par(20)

ElseIf(iModel==6)Then
Phi(1)=Par(22)/Par(24)
Phi(2)=Par(24)/Par(25)
Phi(3)=Par(26)/Par(25)
Phi(3)=Par(27)/Par(25)

ElseIf(iModel==7)Then
Phi(1)=Par(17)/Par(19)

ElseIf(iModel==8)Then
Phi(1)=Par(22)/Par(24)
Phi(5)=Par(24)/Par(25)
Phi(6)=Par(27)/Par(25)
EndIf
```